Investigating the role of lysosomes during mammalian cell division

Charlotte Nugues

Thesis submitted in accordance with the requirements of University of Liverpool for the degree of Doctor in Philosophy

December 2018

Abstract

Lysosomes are acidic, intracellular, membrane-bound organelles present in all eukaryotic cells. They are filled with more than 60 different hydrolases responsible for the degradation of a wide range of intracellular targets arising from autophagy and extracellular particles internalised through endocytic and phagocytic pathways. Their luminal acidity is achieved via the action of the Vacuolar-ATPase. This complex, multi-subunit, molecular proton pump generates the low pH essential for optimal catalytic activity of hydrolytic enzymes by actively pumping H^+ ions (protons) into the lysosome lumen. Historically, lysosomes have been predominantly considered cellular "waste bags" involved in the degradation and recycling of cellular and extracellular content, however new findings reveal that they are highly dynamic organelles tasked with a wide spectrum of unique biological functions. Lysosomes are equipped to sense and monitor the nutrient status of the cell and coordinate an appropriate response. Similar to the ER, they contain high levels of calcium (Ca^{2+}), therefore they might participate in calcium homeostasis by acting as Ca^{2+} stores, and are potentially involved in Ca^{2+} signalling. Ca^{2+} is also known to play a pivotal role in lysosome trafficking, recycling and fusion with the plasma membrane (PM). The latter process, known as exocytosis, enables membrane donation during PM wound repair, allows the cell to "rid itself" of unwanted content and participates in the release of hydrolases that perform important extracellular functions such as bone remodelling and extracellular matrix degradation. More recently, lysosomes have been suggested to play a role in cell division, more particularly, cytokinesis. Cytokinesis is the final stage of cell division. This highly orchestrated process involves the formation of an ingression furrow that progressively constricts forming a transient cytoplasmic intercellular bridge. Eventually, the bridge is severed at abscission allowing separation of daughter cells. Lysosomes were found to cluster at either side of the intercellular bridge that separates nascent daughter cells and disruption of lysosomal positioning through a PI4KIIIβ-dependent mechanism was associated with a significant increase in cytokinesis failure. This suggests a functional requirement for lysosomes in cytokinesis. Understanding the regulation of cytokinesis is of the utmost interest as failure in cell division can

lead to aneuploidy, genetic instability and malignant phenotypes. The purpose of this thesis was therefore to identify the specific lysosomal function(s) involved in cytokinesis. Using a combination of biochemical and pharmacological approaches coupled with confocal microscopy and TIRF imaging techniques, exocytosis of these organelles was shown to significantly increase during cell division, most specifically in cytokinesis. Finally, lysosome exocytosis during cytokinesis was linked to PI4KIIIβ activity. These findings demonstrate for the first time a role of lysosomal exocytosis in cytokinesis. Manipulation of cytokinesis through targeting a specific aspect of lysosomal physiology (exocytosis) opens up new avenues of investigation. This knowledge may permit novel future approaches to tackling a number of prevalent human diseases.

Acknowledgements

I would like to express my huge gratitude to my supervisor, Dr Lee Haynes. I know how much he will hate reading these complimentary words. His insightful guidance not only helped me throughout my research but also allowed me to become a more confident scientist. I have learned a great deal working with him and I have enjoyed every moment of my PhD thanks to his awesome teaching skills and razor-sharp sense of humour! So a big thank you Lee, I sincerely wish you all the best and I hope many more students/post-docs will benefit from your supervision. “Dr Lee Haynes is truly the greatest supervisor to have ever graced a laboratory” (Haynes et al., 2018). I think everyone who worked with him would agree on that!

A big thank you to my other supervisor, Prof. Bob Burgoyne, whose insightful comments helped me a lot at the beginning of my PhD. I wish him a happy retirement.

I also want to thank everyone in Red Block, past, present and honorary members. Thank you Paul for blasting your Christmas songs in the lab 4 months before Christmas and for your help during my Masters. Thank you to my hipster friend Shiquan for creating Charquan and Jean-Paul, my proudest progeny, and for being such a good friend throughout my PhD. A massive thank you to Ali who relentlessly accompanied me to the pub. Thank you for perpetuating the Friday drinks tradition, for making awkward jokes and of course for making me the best cups of tea. I also want to thank Rick for being such a great friend and for the constant smell of curry in the common room. Marie, thank you for baking delicious cakes and for your daily good mood. Thank you Iman, Bangfu and all other Red Block members. Special thanks to Hannah and Dayani, I cannot express how lucky I feel to have such wonderful friends. Your help, support and friendship are invaluable.

I would like to warmly thank Chuck Nordine for his incredible help throughout my PhD. He was always available to answer my questions, helped me improve/troubleshoot my experiments and I truly benefitted from his acute expertise in science. He has been a wonderful mentor. He has also become a

very good friend and I cannot be thankful enough for all the laugh we have had! Un grand merci Nordine!

Thank you also to Jeff Barclay for organising the best Canada day and making the lab a cheerful environment. And thank you Alan for your great help during the lab meetings.

I would like to heartily thank my amazing family, my parents, Margaux, Lili, Sof, Achille, Oscar and Matthieu for their unconditional love and support and for passing on to me the values of work, perseverance and optimism. I am truly thankful for having you in my life and I would not be the positive person I am without you.

Last but not least, I would like to thank the one and only Ewan MacDonald. I am grateful for your help throughout my PhD, your love and for all the happiness you bring into my life. Meeting you in the microscope room was truly the best thing that happened to me. I look forward to our life together as a pair of married scientists.

Table of Contents

Abbreviations

ADP: Adenosine Diphosphate

AP1: Adaptor Protein 1

Arf6: ADP-ribosylation factor 6

Arl8: Arf-like small GTPase 8

ASPM: Abnormal Spindle-like Microcephaly-associated protein

ATM: Ataxia Telangiectasia Mutated protein

ATR: Telangiectasia and RAD3-Related protein

Atg: autophagy gene

BAR: Bin-Amphiphysin-Rvs

BORC: BLOC-1-related complex

BSA: Bovine Serum Albumin

CaBP: Ca^{2+} Binding Protein

CAX: Calcium Hydrogen Exchanger

CCP: Clathrin-Coated Pit

CCV: Clathrin-Coated Vesicle

CHK: Checkpoint Kinase

CLASP: CLIP-Associated protein 1

CLEAR: Coordinated Lysosomal Expression and Regulation

CO_2: Carbon Dioxyde

ConA: Concanamycin A

CDK: Cyclin-dependent kinase

CIT-K: Citron Kinase

CMA: Chaperone-Mediated Autophagy

CPC: Chromosomal Passenger Complex

CTCF: Corrected Total Cell Fluorescence

DAG: Diacylglycerol

DMEM: Dulbecco's Modified Eagle Medium

DMSO: Dimethyl Sulfoxide

DNA: Deoxyribonucleic Acid

dNTP; deoxynucleotide trisphosphate

ECM: Extracellular Matrix

ECT2: Epithelial Cell Transforming protein 2

EDTA: Ethylenediaminetetraacetate

EE: Early Endosomes

EMEM: Eagle's Minimum Essential Medium

ER: Endoplasmic Reticulum

ERM: Ezrin Radixin Moesin

ESCRT: Endosomal Sorting Complex Required for Transport

FBS: Fetal Bovine Serum

FIP3: Family of Rab-Interacting Protein 3

Fwd: Forward

Fwd: Four Wheel Drive

FYCO1: FYVE- and coiled-coil-domain-containing protein

GaAsP-PMT: Gallium Arsenide Phosphide Photomultiplier Tube

GAP: GTPase Activating Protein

GEF: Guanine Exchange Factor

GFP: Green Fluorescent Protein

GGA: Golgi-localised, γ-ear-containing, ADP ribosylation factor binding proteins

GOLPH3: Golgi Phosphoprotein 3

GPN: glycyl-L-phenylalanine 2-naphthylamide

HEPES: 4-(2-hydroxyethyl)-1-piperazineethanesulfonic acid

HF: High Fidelity

HOPS: Homotypic fusion and vacuole Protein Sorting

HRP: Horseradish Peroxidase

hsc70: heat shock cognate protein of 70 kDa

IF: Immunofluorescence

Ig: Immunoglobulin

ILV: Intraluminal Vesicle

INCENP: Inner Centromere Protein

IP_3: Inositol 1,4,5-trisphosphate

kb: kilobase

KCl: Potassium Chloride

kDa: kiloDalton

KIF: Kinesin Family member

KLP: Kinesin-Like Protein

LAMP: Lysosome-Associated Membrane Protein

LB: Luria Broth

LE: Late Endosome

LED UV: Light-Emitting Diode Ultraviolet

LIMP: Lysosomal Integral Membrane Protein

LMP: Lysosomal Membrane Protein

LpH-mCh: LysopHluorin-mCherry

LSD: Lipid Storage Disorder

LYNUS: Lysosome Nutrient Sensing

M6P: Mannose 6-Phosphate

M6PR: Mannose 6-Phosphate Receptor

MA: Macroautophagy

MAP: Microtubule-Associated Protein

mCh: mCherry

$MgCl_2$: Magnesium Chloride

MICAL1: Molecules Interacting with CasL 1

MLC: Myosin Light Chain

MP-GAP: M Phase GTPase Activating Protein

MTM: Myotubularin

MTOC: Microtubule Organising Centre

mTORC1: mammalian Target Of Rapamycin Complex 1

MVB: Multivesicular Body

MYPT: Myosin Phosphatase Targeting subunit

Na_2PO_4: Disodium Phosphate

NAADP: Nicotinic Acid Adenine Dinucleotide Phosphate

NaCl: Sodium Chloride

NAG: N-Acetyl-β-D-Glucosaminidase

NaH_2PO_4: Sodium Dihydrogen Phosphate

NaOH: Sodium Hydroxide

NEM: N-Ethylmaleimide

NMHC IIA: Non-Muscle myosin Heavy Chain IIA

NRK: Normal Rat Kidney

NSF: N-ethylmaleimide-Sensitive Factor

OCRL: Oculocerebrorenal syndrome of Lowe

PBS: Phosphate Buffer Saline

PBST: Phosphate Buffer Saline Tween

PCR: Polymerase Chain Reaction

pH: power of Hydrogen

PH: Pleckstrin Homology

PI: Phosphoinositide

PI(3)P: Phosphatidyl inositol 3-phosphate

PI(3,4,5)P_3: Phosphatidyl inositol 3,4,5-trisphosphate

PI(4)P: Phosphatidyl inositol 4-phosphate

PI(4,5)P2: Phosphatidyl inositol 4,5-bisphosphate

PI4K: phosphatidylinositol 4-kinaseIIIβ

PIP: phosphatidylinositol phosphate

Plk1: Polo-Like Kinase 1

PLC: Phospholipase C

PM: Plasma Membrane

PMA: Phorbol 12-Myristate 13-Acetate

PRC1: Protein Required for Cytokinesis 1

P/S: Penicillin/Streptomycin

PtdIns: Phosphatidyl Inositol

PTEN: Phosphatase and Tensin homolog

RB1: retinoblastoma protein 1

RE: Recycling Endosome

Rev: Reverse

RFP: Red Fluorescent Protein

RILP: Rab7-interacting lysosomal protein

RIPA buffer: Radioimmunoprecipitation Assay buffer

ROCK: Rho-associated Kinase

ROI: Region of Interest

RPMI: Roswell Park Memorial Institute Medium

SDS: Sodium Dodecyl Sulfate

SDS-PAGE: Sodium Dodecyl Sulfate Polyacrylamide Gel Electrophoresis

S.E.M: Standard Error of the Mean

SKIP: SifA and kinesin-interacting protein

Slp-4a: Synaptotagmin-Like Protein 4-a

SNAP: Soluble N-ethylmaleimide Attachment Protein

SNARE: Soluble N-ethylmaleimide-sensitive factor-Attachment protein repeptor

SOC: Super Optimal broth with Catabolite repression

STX: Syntaxin

Syt: Synaptotagmin

TAE: Tris base, Acetic acid and EDTA

TE: Tris-EDTA

TFEB: Transcription Factor EB

TGM: THP1 growth Media

TGN: *Trans*-Golgi Network

TIRF: Total Internal Reflection Microscopy

T_m: Melting Temperature

TPC: Two-Pore Channel

TRP: transient Receptor Potential

TRPML: Transient Receptor Potential-Mucolipin

Tsg101: Tumour Susceptibility Gene 101

Vacuolin: Vacuolin-1

VAMP7: Vesicle-Associated Membrane Protein 7

V-ATPase: Vacuolar ATPase

VSDs: Variable Secondary Dichroics

v/v: Volume per Volume

WB: Western Blot

w/v: Weight per Volume

YFP: Yellow Fluorescent Protein

Diagrams, Figures and Tables List

Diagrams

Tables

Figures

Chapter 1: Introduction

1.1. The cell cycle

The cell cycle is a highly orchestrated and complex process responsible for the growth and proliferation of cells and the development, repair and ageing of all living organisms (Schafer 1998), ensuring the perennation of life across generations. It includes a series of regulated events that ultimately lead to the accurate duplication and equal partitioning of the DNA into two identical daughter cells (Alberts *et al.* 2002). The investigation of the cell cycle was initiated in the mid-nineteenth century with the exploration of cell division by Schwann and Schleiden, two supporters of the cell theory (Schwann 1847). However their idea, which proposed that cells derive from pre-existing cells by crystallisation was gradually replaced by a concept of cellular fission greatly influenced by Virchow and accurately summarised in his "*omnis cellula e cellula*" (where a cell arises, there a cell must have previously existed) (Virchow and Chance 1860). The emergence of more advanced microscopic techniques led to the discovery, by Fleming, of chromosomal 'threads' that elongate, split and thicken at the various stages of mitosis (Flemming 1965). Later studies helped to gain further insight into the description and regulation of the events characterising the cell cycle (Nurse 2000). Understanding the mechanisms governing this fundamental process is also essential to creating unique therapeutic opportunities and to tackling the aberrant cell proliferation underlying the development of cancers (Vermeulen *et al.* 2003).

1.1.1. Phases of the cell cycle

The eukaryotic cell cycle is commonly divided into 4 consecutive phases: G1, S, G2 and M. G1, S and G2 together form the interphase which lasts for approximately 23 hours in the 24-hour model human cell cycle; M phase occupies only one hour (Alberts *et al.* 2002) (**Diagram 1.1.**). G1 and G2, also termed gap phases, allow the growth of the cell and the inspection of the external environment, ensuring optimal conditions before the commitment of the cell into subsequent phases. The key steps of genetic duplication and segregation occur at S phase and M phase, respectively (Norbury and Nurse 1992). Cells in G1 can exit the cell cycle and enter a resting, non-proliferative

state called G0 (Vermeulen *et al.* 2003) and many checkpoints ensure the normal progression of the cell through the cell cycle (Chin and Yeong 2010).

1.1.2. Regulation of the cell cycle

The cell cycle is regulated by cyclin-dependent kinases (CDKs), which are members of the serine/threonine protein kinase family, their binding targets, the cyclins, and their inhibitors CDKIs (Bai *et al.* 2017) (**Diagram 1.2.**). CDKs operate as switch-like transition factors throughout the cell cycle by associating with specific cyclins expressed in a cell cycle-dependent manner (Hochegger *et al.* 2008). Cyclin-associated CDKs sense extracellular cues such as nutrient availability and growth factors and in turn direct cell cycle progression (Lapenna and Giordano 2009).

Mitogenic stimuli relieve CDK inhibition by p16 and induce association of D-type cyclins (D1, D2 and D3) with CDK4 and CDK6. This leads to the subsequent phosphorylation and inactivation of the transcriptional repressor retinoblastoma protein (RB1), sequestration of the CDK inhibitors p21 and p27 and entry of quiescent cells (G0) into the G1 phase (Weinberg 1995; Sherr and Roberts 2004; Bai *et al.* 2017).

The transition from G1 to S is ensured by the cyclin E-CDK2 complex, which further represses RB1 function and forms the restriction point, beyond which RB1 is maintained in a hyperphosphorylated state by CDK2-cyclin A, CDK1-cyclin A and cyclin B-CDK1 heterodimers in subsequent cell cycle phases (Lapenna and Giordano 2009) (**Diagram 1.2.**). Detection of DNA damage induces the rapid interruption of the cell cycle by activation of the related kinases ataxia telangiectasia mutated (ATM), ataxia telangiectasia and RAD3-related proteins (ATR) and their effectors checkpoint kinase 1 (CHK1) and checkpoint kinase 2 (CHK2). The ATM-ATR cascade of events gives the cell time to carry out the necessary DNA repairs during the DNA damage checkpoints, preserving genomic integrity (Hakem 2008). During all phases of the cell cycle many checkpoints are implemented to ensure precise orchestration of the process (Chin and Yeong 2010) (**Diagram 1.1.**).

During S phase, DNA replication is regulated by cyclin A and its binding partner CDK2; the cyclin A-CDK2 complex, in conjunction with cyclin A-CDK1 also controls S phase completion (Hochegger *et al.* 2008). Entry into M phase is subsequently driven by cyclin A association with CDK1, which also initiates chromosome decondensation (Barr and Gergely 2007). Finally mitosis is triggered by the CDK1-cyclin B heterodimer (Ito 2000), which ensures normal timing of mitotic entry in conjunction with Aurora and polo-like kinase proteins (Barr and Gergely 2007; Archambault and Glover 2009; Bai *et al.* 2017).

In parallel to cell-cycle dependent activation of cyclin-CDK complexes, cells operate additional layers of cell cycle control by CDKI-mediated repression and ubiquitination of unwanted cell cycle proteins (Fischer *et al.* 2018).

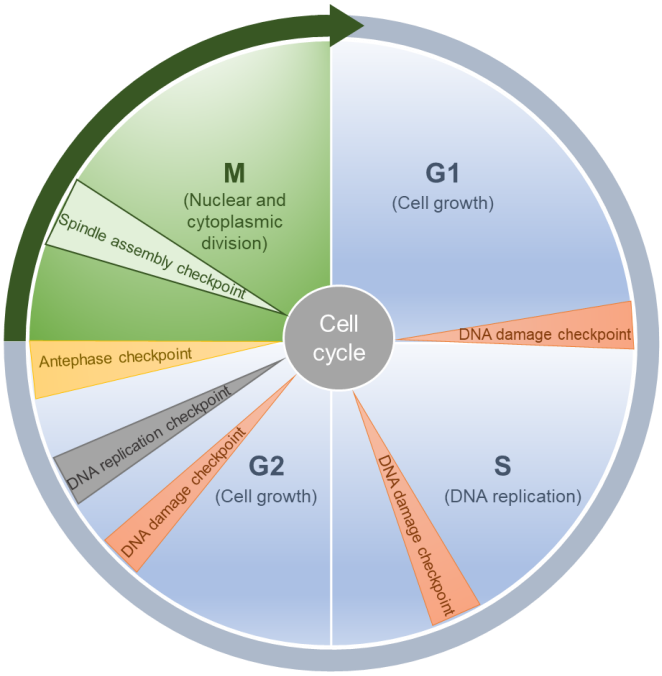

Diagram 1.1. The stages of the cell cycle and the checkpoints regulating it. Cell growth and DNA replication occur in interphase (blue). The gap phases G1 and G2 allow the monitoring of the environment and delay commitment to S phase or M phase if needed. The end of the cell cycle is reached at M phase (green) where nuclear (mitosis) and cytoplasmic (cytokinesis) divisions take place. The cell cycle is punctuated by many checkpoints which determine the readiness of the cell to enter subsequent phases. Adapted from (Chin and Yeong 2010).

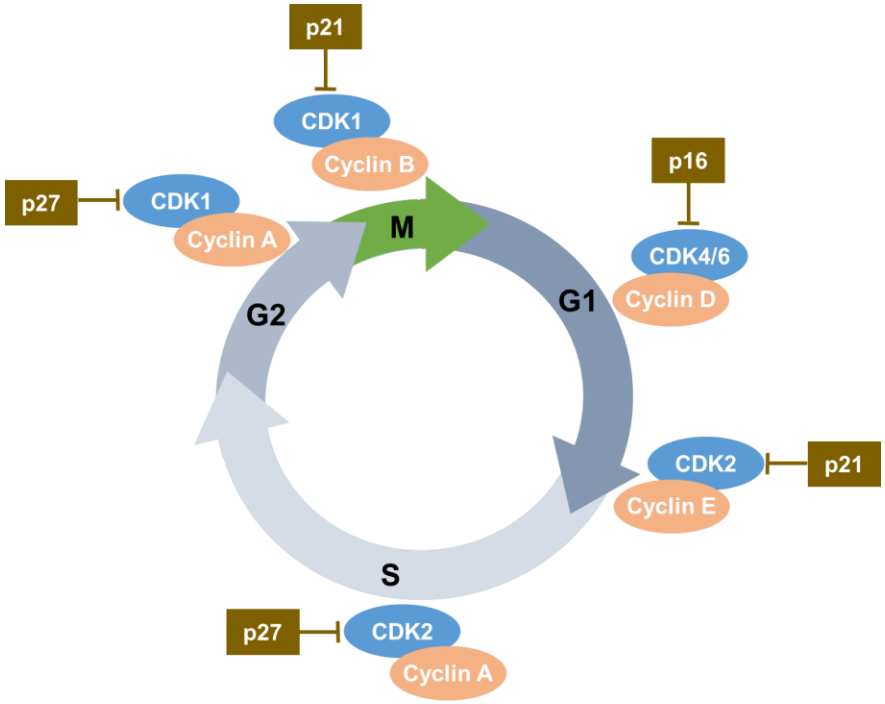

Diagram 1.2. Temporal regulation of the cell cycle by cyclin-dependent kinases (CDKs), their binding targets (cyclins) and their inhibitors. Adapted from (Bai *et al.* 2017).

1.1.3. Mitosis

The entry of cells in M phase marks their commitment to mitosis, the process by which duplicated chromosomes segregate equally between the two progeny cells. Mitosis can be further divided in 5 stages: prophase, prometaphase, metaphase, anaphase and telophase (**Diagram 1.3.**). At prophase, chromosomes condense, centrosomes separate and the nuclear envelope breaks down. Centrosomes form a mitotic spindle apparatus onto which sister chromatids attach during prometaphase. Chromosomes then align at the equatorial plane during metaphase and each sister chromatid migrates toward opposite poles at anaphase. Telophase is marked by the decondensation of chromosomes and reformation of the nuclear envelope (Fischer *et al.* 2018).

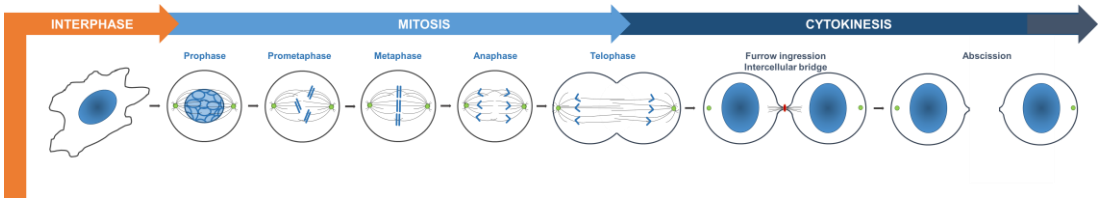

Diagram 1.3. The stages of cell division: mitosis (nuclear division) and cytokinesis (cytoplasmic division). The different stages of mitosis lead to the equal segregation of chromosomes, which become enclosed in two newly formed nuclei. At cytokinesis, the portion of cytoplasm between the nascent cells constricts forming a transient intercellular bridge and the midbody is generated (red circle). Cytokinesis is complete when the cytoplasm is severed during abscission. Adapted from (Alberts *et al.* 2002) and (Normand and King 2010).

Specific cyclin-CDK complexes promote major mitotic events such as chromosome condensation, breakdown of the nuclear envelope and mitotic spindle formation. Cyclins A, B and B3 play a particularly important role in mitotic progression up until metaphase (Sullivan and Morgan 2007) (**Diagram 1.4.**). Beyond metaphase, the anaphase-promoting complex (APC), as its name suggests, allows anaphase to take place by ubiquitylating securin, a protein that prevents chromatid separation by degrading cyclins and additional proteins such as Polo-like kinase-1. APC remains activated in telophase and initiates mitotic exit. (Gocheva *et al.* 2006).

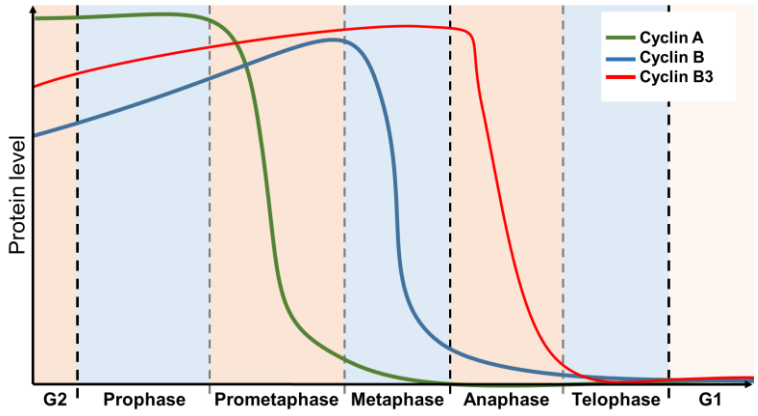

Diagram 1.4. Mitotic-specific degradation of cyclins. Cyclins A, B and B3 are sequentially degraded by the anaphase-promoting complex (APC). Cyclin A initiates

chromosome condensation and nuclear breakdown. Its levels decline early in mitosis, during prometaphase. Cyclin B, which further mediates chromosome condensation and spindle formation is degraded in metaphase. The levels of cyclin B3, whose function remains unclear decrease during anaphase. Adapted from (Sullivan and Morgan 2007).

1.1.4. Cytokinesis

During cell division, mitosis is followed by the physical separation of the two daughter cells, a process known as cytokinesis (**Diagram 1.5.**). It starts in anaphase with the specification of a cleavage plane at the equatorial cortex. Subsequently the cleavage furrow ingresses inward, pinching the portion of cytoplasm located between the two nascent cells, forming a transient tubulin-rich intercellular bridge. At the centre of the bridge sits an organelle, the midbody, which acts as a regulatory platform for abscission. Cytokinesis is complete when the cytoplasm between the progeny cells is severed at abscission (D'Avino *et al.* 2015).

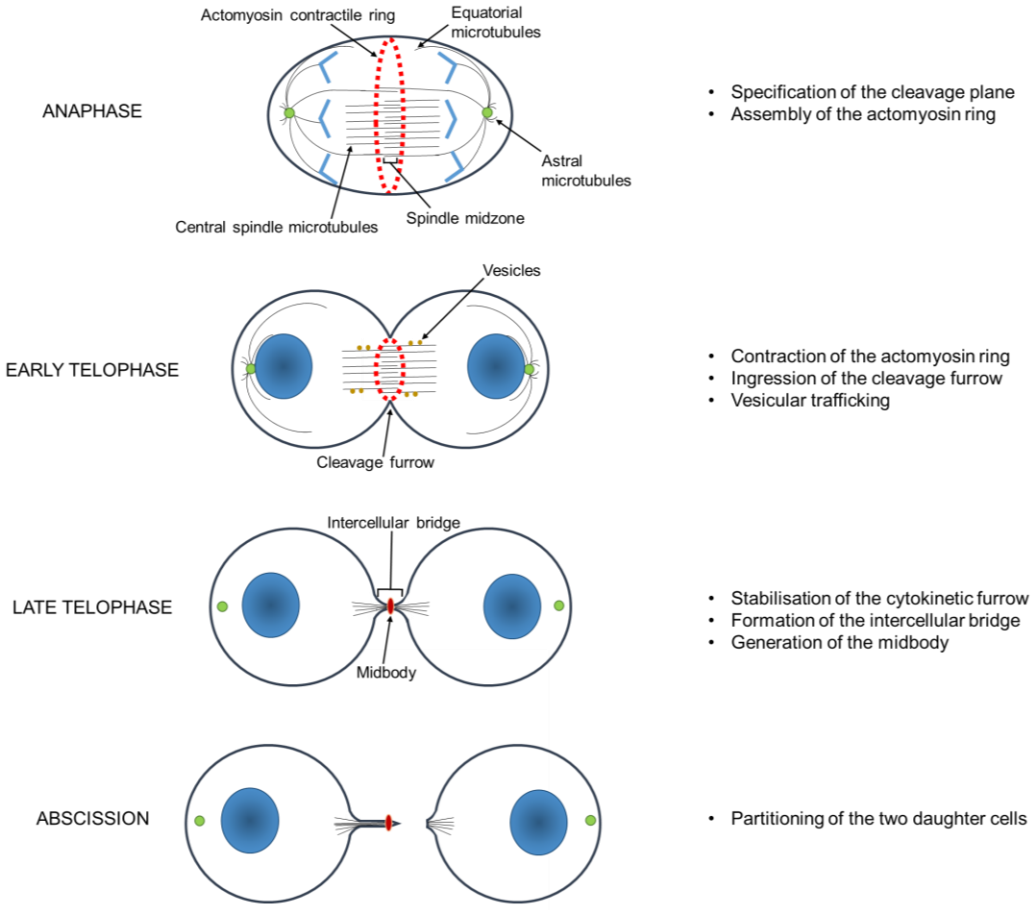

Diagram 1.5. Overview of the multiple stages of cytokinesis. Chromosomes and nuclei are represented in blue, centrosomes are depicted in green. Adapted from (Normand and King 2010) and (D'Avino *et al.* 2015).

1.1.5. Importance of cytokinesis in health and disease

Cytokinesis is a dynamic and highly regulated process involving an elaborate network of molecular factors (Li 2007). It is crucial for the correct partitioning of chromosomes and other cellular elements such as centrosomes (D'Avino *et al.* 2015). Defects in cytokinesis (illustrated in **Diagram 1.6.**) have been linked to chromosome instability (Rosario *et al.* 2010), supernumerary centrosomes and states of tetraploidy (duplicated genome) (Ganem *et al.* 2009). An excessive number of centrosomes was found in many cancer types including breast (Lingle *et al.* 1998; Lingle *et al.* 2002), prostate (Pihan *et al.* 2001), bladder (Yamamoto *et al.* 2009), pancreatic cancer (Sato *et al.* 1999) and in head and neck squamous cell carcinoma (Mark Gustafson *et al.* 2000). In mouse models, implantation of tetraploid cells resulted in malignant cancer formation (Fujiwara *et al.* 2005). Repeated cytokinesis failure can cause cells to become aneuploid, a characteristic of tumorigenic cells (Högnäs *et al.* 2012). Association between abnormal cytokinesis and oncogenic transformation is further demonstrated in several other studies indicating that mutations in tumour suppressor factors are intimately linked to cytokinesis failure (Whitaker 1997; Yang *et al.* 2004; Caldwell *et al.* 2007). Moreover overexpression of Aurora B, a protein involved in chromosome segregation and cytokinesis, has been strongly associated with lymph node metastasis in oral squamous cell carcinomas, suggesting a possible link between cytokinesis dysregulation and cancer migration and invasiveness (Qi *et al.* 2007). In addition to cancer, mutations in cytokinesis factors are involved in other human diseases including Fanconi anaemia (Vinciguerra *et al.* 2010) and Lowe syndrome (Dambournet *et al.* 2011). Overall, the normal completion of cytokinesis permits cellular growth whilst safeguarding the organism from potential pathological afflictions. Understanding the mechanisms governing cytokinesis is therefore of the utmost importance as it could open up opportunities into treating a number of prevalent diseases.

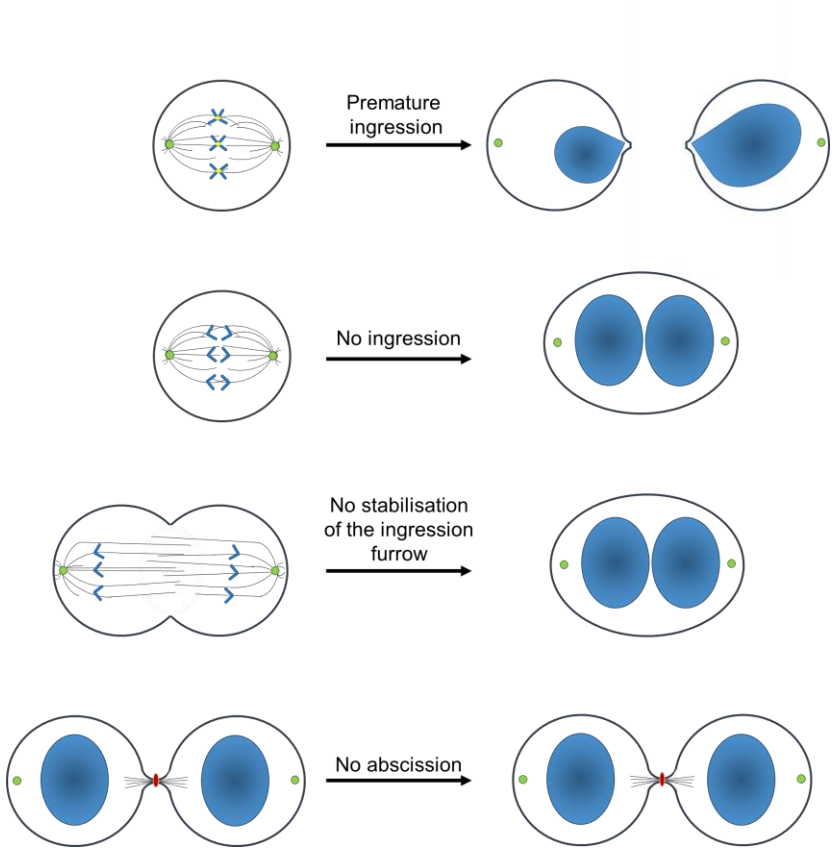

Diagram 1.6. Examples of cytokinesis defects and associated phenotypes. Dysregulation of cytokinesis components leads to various phenotypes: premature ingression of the cleavage furrow is associated with abnormal segregation of chromosomes and DNA alteration (aneuploidy), absence of ingression/regression of the cleavage furrow gives rise to binucleation and tetraploidy. Defects in the abscission process are reflected in the persistence of the intercellular bridge, which ultimately leads to the collapse of nascent cells back into one binucleate cell. Chromosome instability and states of polyploidy are both accepted drivers of tumorigenesis. Adapted from (Normand and King 2010) and (Kops *et al.* 2004).

1.1.6. The molecular players involved in the different stages of cytokinesis

1.1.6.1. Central spindle assembly, specification of the cleavage plane and contractile ring assembly.

The assembly of the central spindle precedes the onset of cytokinesis. The central spindle encompasses antiparallel bundles of microtubules that overlap in the midzone. They arise from the metaphase spindle but also *de novo* from augmin-stimulated nucleation during anaphase (Uehara and Goshima 2010). The decrease in CDK1 activity in anaphase stabilises microtubules and allows mitotic spindle reorganisation by activating factors required for central spindle formation (Fededa and Gerlich 2012). One essential component is the protein required for cytokinesis 1 (PRC1), a microtubule binding protein, which upon CDK1 decline forms homodimers that link overlapping plus ends of microtubules (Zhu *et al.* 2006; Subramanian *et al.* 2010) (**Diagram 1.7.**, top panel). PRC1 also interacts with the kinesin family member (KIF) 4A, which suppresses excessive microtubule polymerisation, thereby preventing microtubule instability (Bastos *et al.* 2013) (**Diagram 1.7.**, middle panel). Centralspindlin is another key element of the central spindle. It forms a tetrameric complex consisting of two MKLP1 kinesin motor proteins and two Rho GTPase activating proteins (GAP) also known as MgcRacGAPs (Pavicic-Kaltenbrunner *et al.* 2007). During anaphase, Aurora B induces accumulation and clustering of centralspindlin via phosphorylation of MKLP1, promoting further bundling of the central spindle microtubules (Guse *et al.* 2005). The third molecular component of the central spindle machinery is the chromosomal passenger complex (CPC) which includes Aurora B, survivin, borealin and the inner centromere protein (INCENP). Upon decrease in CDK1 activity, the CPC relocalises to the spindle midzone and to the equatorial cortex, the region of plasma membrane (PM) located in the midzone (Carmena *et al.* 2012) (**Diagram 1.7.**, top panel). The CPC phosphor-regulates essential molecules, including MKLP1 (Guse *et al.* 2005) and PRC1 (Ban *et al.* 2004). Many other molecules participate in the central spindle assembly (**Table 1.**) such as microtubule-associated proteins (MAPs) and the CLIP-associated protein 1 (CLASP) (D'Avino *et al.* 2015). The abnormal spindle-like microcephaly-associated protein (ASPM) promotes central spindle organisation by binding to the minus end of central microtubules (Higgins *et al.* 2010). Overall assembly of the spindle midzone results from multiple factors whose mutual interactions allow correct spatio-temporal formation of a delineated region of overlapping microtubules.

Factors	Function	Reference
Anillin	Stabilises the contractile ring	(Basant and Glotzer 2018)
Aurora B	Kinase (CPC component)	(Carmena *et al.* 2012)
ASPM	MAP, binds to the minus end of microtubules	(Riparbelli *et al.* 2002)
Borealin	CPC component	(Carmena *et al.* 2012)
CIT-K	Kinase (contractile ring protein)	(Bassi *et al.* 2011)
CLASP	MAP (central spindle assembly)	(Inoue *et al.* 2004)
ECT2	GEF, activates RhoA	(Somers and Saint 2003)
INCENP	CPC component	(Carmena *et al.* 2012)
KIF4A	KLP, limits microtubule growth	(Kurasawa *et al.* 2004)
KIF14	KLP, interacts with PRC1, allows CIT-K localisation to the central spindle	(Gruneberg *et al.* 2006)
KIF23	KLP (centralspindlin component)	(Mishima *et al.* 2002)
MgcRacGAP	GAP (centralspindlin component)	(Pavicic-Kaltenbrunner *et al.* 2007)
Plk1	Kinase, allows binding of MgcRacGAP with ECT2	(Wolfe *et al.* 2009)
PRC1	MAP, recruits KIF4A, associates with CIT-K.	(Zhu *et al.* 2006)
RhoA	GTPase, promotes contractile ring assembly	(Yüce *et al.* 2005)
ROCK	Kinase, myosin II activation	(Kosako *et al.* 2000)

Table 1. Proteins regulating the central spindle and actomyosin ring assembly in mammalian cytokinesis. ASPM: abnormal spindle-like microcephaly-associated protein; CIT-K: citron kinase; CLASP: CLIP-associated protein 1; CPC: chromosome passenger complex; ECT2: epithelial cell transforming protein 2;GAP: GTPase activating protein; GEF: guanine exchange factor; INCENP: inner centromere protein; KIF: kinesin family member; KLP: kinesin-like protein; MAP: ;Plk1: Polo-like kinase 1; PRC1: protein required for cytokinesis 1; ROCK: Rho-associated kinase.

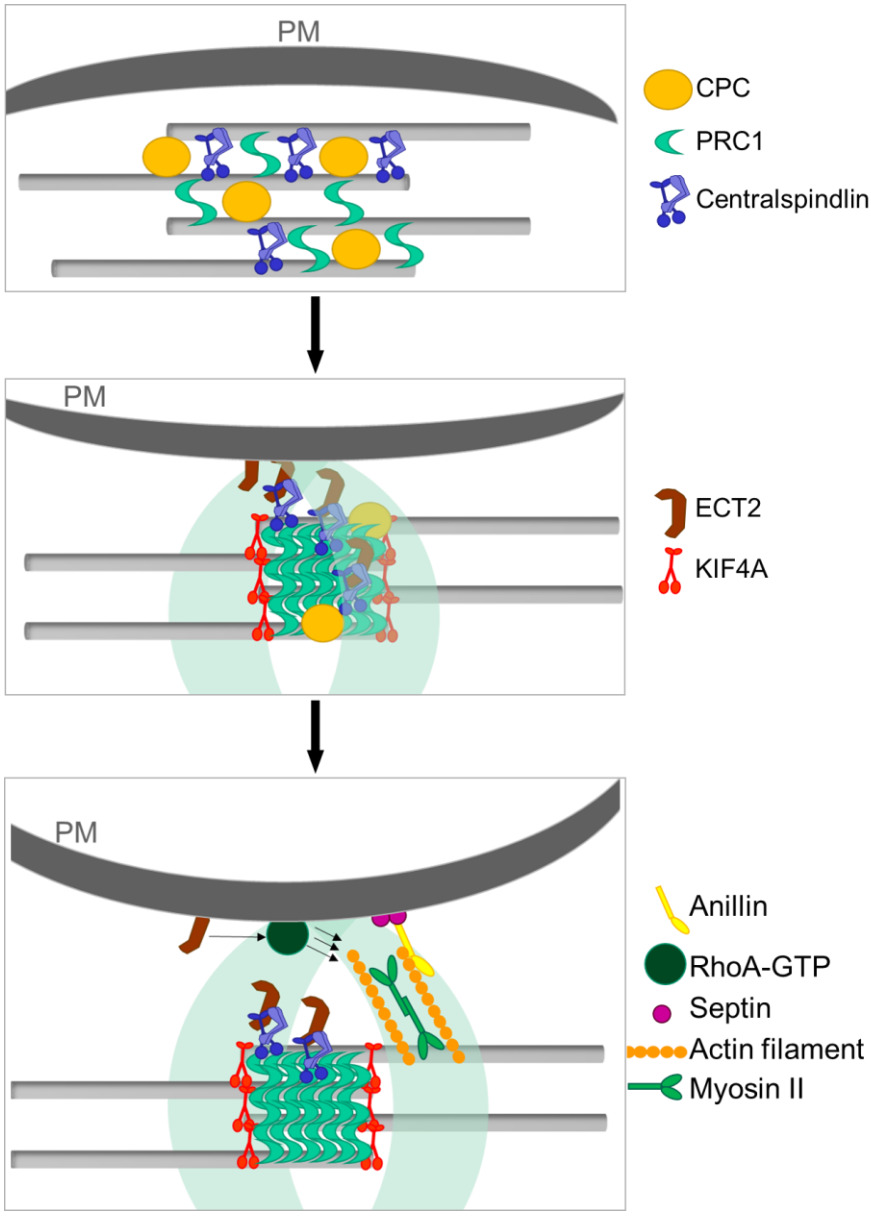

Diagram 1.7. Molecular players involved in central spindle assembly, cleavage site specification and contractile ring assembly. Top panel: during early anaphase, antiparallel microtubules bundle at the midzone to form the central spindle with the help of the CPC, PRC1 and centralspindlin. Middle panel: PRC1 recruits KIF4A to the zone of microtubule overlap later in anaphase. KIF4A prevents excessive microtubule polymerisation and delineates the overlap region. ECT2 associates with MgcRacGAP of centralspindlin and also locates to the PM. Bottom panel: On reaching the cortex, ECT2 promotes RhoA-GTP formation which subsequently activates contractile ring assembly. Note that the CPC and centralspindlin oligomers are also present at the PM (not depicted here for more clarity). Adapted from (Green *et al.* 2012).

An early study on echinoderm eggs demonstrated that the central spindle dictates the position of the cleavage site (Rappaport and Rappaport 1974). The mechanisms by which the central spindle specifies the cleavage site have been highly debated (von Dassow 2009). The process of division site specification is known to rely on at least four processes: 1) It depends on local RhoA GTPase activation by the guanine exchange factor (GEF) epithelial cell transforming protein 2 (ECT2) at the cell equator during anaphase (Yüce *et al.* 2005). RhoA stimulation at the equatorial cortex triggers formin-mediated actin filament generation and activates the Rho-associated kinase ROCK that allows myosin filament formation, promoting actomyosin ring assembly (Kosako *et al.* 2000; Wagner and Glotzer 2016; Pollard 2017) (**Diagram 1.8.**). ECT2 is released from the nucleus upon nuclear envelope breakdown but its autoinhibitory function keeps it inactive (Kim *et al.* 2005). The MgcRacGAP of centralspindlin targets it at the equatorial cortex (Kotýnková *et al.* 2016) and activates its GEF function (Zhang and Glotzer 2015). In turn ECT2 locally stimulates RhoA in the narrow equatorial region (Normand and King 2010) (**Diagram 1.7.**, bottom panel). Polo-like kinase 1 (Plk1) indirectly promotes RhoA activation by activating the ECT2 binding site on MgcRacGAP (Kim *et al.* 2014). How ECT2 and RhoA are directed to the future cleavage plane remains unclear. A study on echinoderm embryos suggests that they are transferred to the equatorial region by travelling along astral microtubules, independently of the spindle or chromosome position (Su *et al.* 2014); 2), the GAP component of centralspindlin inhibits Rac GTPase activity, resulting in decrease in the cortical stiffness due to branched actin filaments and loss of cell adhesion (D'Avino *et al.* 2015); 3), the component of the CPC Aurora B counteracts the inhibition of centralspindlin oligomerisation by PAR-5/14-3-3 at the PM to allow local interaction of MgcRacGAP with ECT2 and subsequent RhoA activation at the equatorial cortex (Basant *et al.* 2015) and 4), although not fully elucidated, a potential GAP-mediated mechanism of RhoA repression at astral microtubules is likely to occur in parallel to RhoA activation at equatorial regions, preventing mislocalisation of RhoA signals in the polar regions (Basant and Glotzer 2018). These mechanisms collectively explain how the cleavage site is defined, positioned and how the actomyosin ring is

assembled, however the process by which RhoA targets the equatorial cortex is yet to be fully investigated.

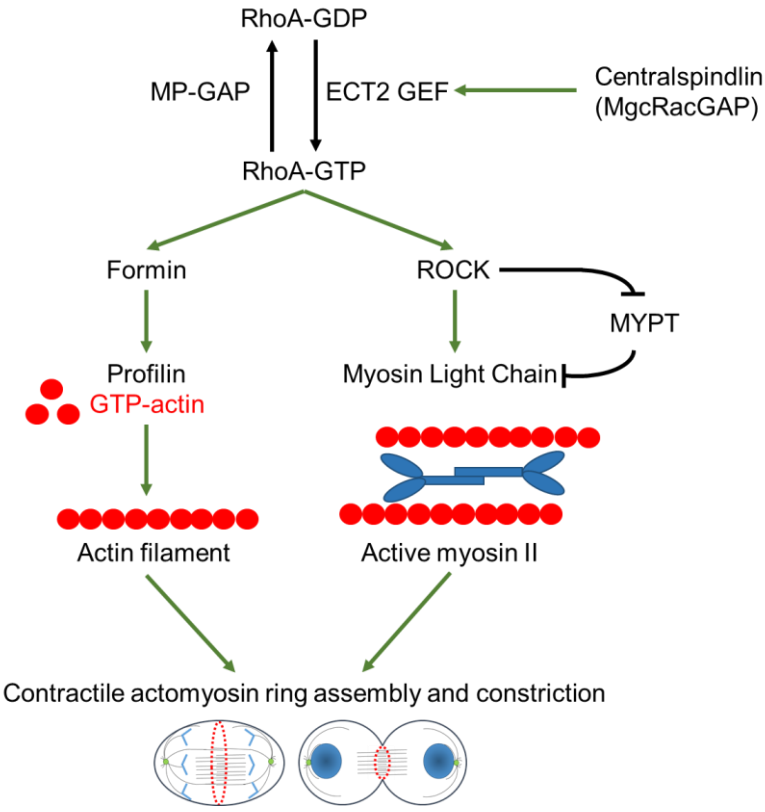

Diagram 1.8. Regulation of the RhoA pathway during division plane specification and actomyosin contractile ring assembly. Green arrows indicate positive regulations and black lines with bars depict inhibitory effects. As for any conventional GAP, the M phase GAP (MP-GAP) promotes RhoA inactivation, potentially to prevent RhoA function at the polar cortical regions. ECT2 is the primary activator of RhoA. Loss of the ECT2 autoinhibitory conformation and targeting of ECT2 to the central spindle is mediated by interaction with the centralspindlin component MgcRacGAP. Thus, counterintuitively, MgcRacGAP stimulates the formation of GTP-bound RhoA. In turn active RhoA induces polymerisation of actin filament via stimulation of formin. ROCK kinase, another active RhoA effector, activates myosin II by phosphorylating the myosin light chain (MLC). In parallel, it also suppresses the inhibitory effect of the phosphatase-targeting subunit MYPT on MLC. Assembly of actin and activation of myosin motors promote the formation of a functional contractile ring. Adapted from (Fededa and Gerlich 2012), (D'Avino *et al.* 2015) and (Basant and Glotzer 2018).

In addition to actin and myosin, the contractile ring requires scaffold and linker proteins which stabilise and anchor it to the PM and central spindle (**Table1.**). Such proteins include citron kinase (CIT-K), which maintains correct localisation of RhoA and central spindle components such as MAPs, PRC1 and KIF23; CIT-K also associates with actin and myosin (Bassi *et al.* 2011; Bassi *et al.* 2013). The actomyosin ring is connected to the equatorial cortex via anillin which recruits the cytoskeletal protein septin to the division furrow (Field *et al.* 2005a) (**Diagram 1.7.**, bottom panel) and binds to RhoA and MgcRacGAP, linking central spindle components to the PM (D'Avino *et al.* 2008; Gregory *et al.* 2008; Piekny and Glotzer 2008). Additional mechanisms of actomyosin attachment to the cell cortex are involved such as lipid- (see section 1.1.7.) and transmembrane protein-mediated anchorage (Pollard 2017).

Once the contractile ring is fully functional, it forms a tightening 'purse string' that triggers ingression of the cleavage furrow (Wang 2005). The issue with this model is that many actin filaments form a randomly distributed network, and are not aligned with the division plane, suggesting that the mechanism of furrow ingression is not fully understood (Fishkind and Wang 1993). In addition the force-generating process underlying furrow ingression remains elusive (Pollard 2017). Myosin II is a well-known motor protein responsible for contraction (Matsumura 2005) however mammalian COS-7 cells are able to divide with inactive myosin II (Pollard 2017), suggesting its loss of function might be compensated by other myosins. Identifying all the molecular players activated during ring constriction and the upstream pathways regulating them, would therefore be highly beneficial.

1.1.6.2. Abscission

The furrow ingresses until it forms a thin intercellular bridge of 1-2 μm diameter that connects the two nascent cells for up to several hours into G1. As the bridge matures and compacts the central spindle, the contractile ring disassembles and an electron-dense structure termed the midbody forms at its centre that constitutes an anchorage platform for the abscission machinery which eventually severs the PM (Mierzwa and Gerlich 2014). Proteins such as

Aurora B flank the midbody (Gruneberg *et al.* 2004), components including RhoA, anillin, septins, centralspindlin and CIT-K surround it, whilst the CPC is removed (D'Avino *et al.* 2015). CIT-K is particularly important in midbody structure and localisation, through its interaction with contractile ring components and MAPs (Bassi *et al.* 2013). Connection of the midbody and the PM has been shown to depend on anillin (Kechad *et al.* 2012) and MgcRacGAP (Lekomtsev *et al.* 2012). The process by which the cytoplasm is severed is mediated by the endosomal sorting complex required for transport (ESCRT), a multi-subunit structure responsible for PM remodelling and scission events, such as those observed in the formation of multivesicular body and retroviral budding (Carmena 2012; Schmidt and Teis 2012). The component of the abscission machinery are sequentially recruited to the midbody (**Diagram 1.9.**). The initial recruiter protein is Cep55, which is targeted to the midbody by MKLP1. It interacts with the tumour susceptibility gene 101 (Tsg101, ESCRT-I component) and ALIX, which in turn recruit ESCRT-III at the midbody (D'Avino *et al.* 2015). A putative model postulates that the ESCRT-III subunit CHMP4 assembles as filaments surrounding the future abscission site and induces membrane curvature. This spiral structure gives rise to a secondary constriction zone that eventually undergoes fission (Carmena 2012; Fededa and Gerlich 2012) (**Diagram 1.9.**). However the secondary ingression was found to form prior to ESCRT-III recruitment and often away from the midbody (Schiel *et al.* 2012). In addition, a distinct CHMP4 pool was observed at the site of abscission (Schiel *et al.* 2013). This suggests that the ESCRT-III component CHMP4 is solely responsible for membrane splitting and other mechanisms are required to generate a secondary ingression (see section 1.1.7.). Complete abscission requires the clearance of microtubules by ESCRT-III-mediated recruitment of spastin (Fededa and Gerlich 2012) or minus-end retraction (Schiel *et al.* 2012). Removal of actin filaments is also needed (Frémont and Echard 2018) (see section 1.1.7.).

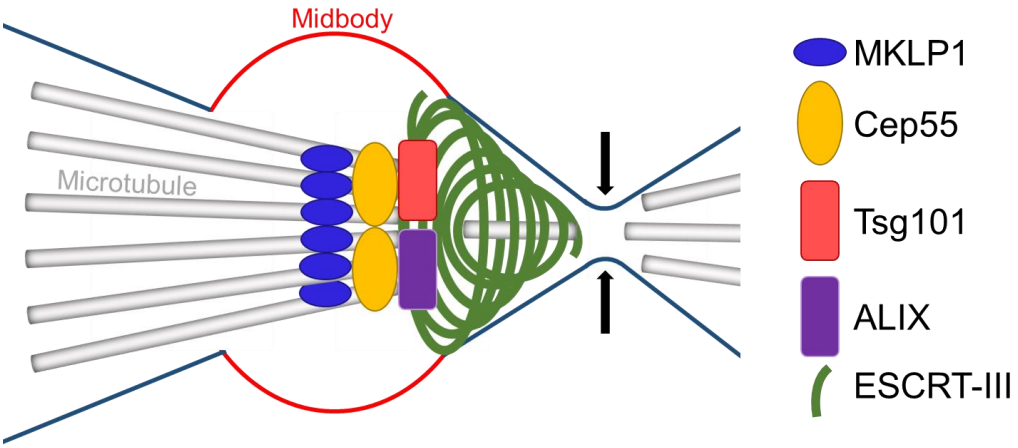

Diagram 1.9. Mechanisms of ESCRT-III recruitment to the midbody and hypothetical model for abscission. Cep55 is recruited to the midbody by the centralspindlin component MKLP1 and targets ALIX and the ESCRT-I component Tsg101 at the midbody. Subsequently ALIX interacts with the CHMP4 component of ESCRT-III. CHMP4 was alluded to form filaments that constrict the membrane (arrows) and allow abscission. The abscission site also requires microtubule (depicted in grey) disassembly and actin clearance (not shown). Adapted from (Carmena 2012), (Fededa and Gerlich 2012) and (Schiel *et al.* 2011).

1.1.7. Membrane trafficking and lipid dynamics in cytokinesis

1.1.7.1. Vesicle trafficking: a requirement for successful cytokinesis

In addition to the molecular players described above, cytokinesis involves membrane trafficking thought to be responsible for total membrane surface increase and for spatio-temporal delivery of key cytokinesis regulators (D'Avino *et al.* 2015). Transport vesicles of Golgi origin were shown to traffic to the furrow and accumulate at the midbody (Goss and Toomre 2008). In addition, recycling endosomes (REs) were found to cluster outside, and to later move inside, the intercellular bridge near the abscission site (Schiel *et al.* 2011). In accordance with a role of post-Golgi secretory vesicles in cytokinesis, treatment of HeLa cells with brefeldin A, a compound that inhibits Golgi trafficking, leads to cytokinesis defects (Gromley *et al.* 2005). Likewise disruption of endosomal proteins causes cytokinesis failure (Baluška *et al.* 2006). Adenosine-diphosphate-ribosylation factors (Arfs) and monomeric Rab GTPases are regulators of endosome trafficking and several endosome

Rabs/Arfs and their effectors have been found to localise at the ingression furrow or intercellular bridge. The most extensively studied are recycling endosome Rab11 and Rab35, that have documented functions in cytokinesis (Schiel *et al.* 2011; Frémont and Echard 2018). The potential roles of vesicle trafficking in cytokinesis are discussed next.

A study on GFP-tagged endosomes decorated with Rab11 and its effector, Family of Rab-Interacting Protein 3 (FIP3), demonstrated the presence of these organelles at the intercellular bridge. Additionally, during secondary ingression, the GFP fluorescence was lost, suggesting that fusion of endosomes is potentially implicated in secondary ingression formation. FIP3 positive endosomes were also shown to co-localise with SCAMP-3, a protein that interacts with Tsg101 responsible for ESCRT-III recruitment, further suggesting a link between the Rab effector, ESCRT-III assembly and abscission (Schiel *et al.* 2012). Rab11-FIP3 endosomes might also restrict actin filament formation near the future abscission site. They transport p50RhoGAP, which negatively regulates RhoA responsible for actin polymerisation (D'Avino *et al.* 2015). Consistent with this, accumulation of F-actin in the intercellular bridge and delays in abscission were associated with p50RhoGAP depletion (Frémont and Echard 2018). Actin clearance at the future abscission site is also mediated by Rab35-endosomes and its associated effectors interacting with CasL 1 (MICAL1), an enzyme that catalyses local actin depolymerisation. MICAL1 is targeted to the abscission site and activated by Rab35 to promote actin clearance via its oxidoreductase function (Frémont *et al.* 2017). Another effector of Rab35, the phosphoinositide 5-phosphatase OCRL, the product of a gene involved in the oculocerebrorenal syndrome of Lowe, hydrolyses $PI(4,5)P_2$, an activator of actin polymerisation at the late bridge, further participating in actin removal prior to abscission (Dambournet *et al.* 2011). Finally Rab35 was also found to play a role earlier in cytokinesis by stabilising the ingressed furrow via interaction with septins (Kouranti *et al.* 2006).

In addition to their accumulation at the ingression furrow, vesicles undergo localised fusion. Accordingly, some of the molecules involved in vesicular transport to, docking at and fusion with the PM have been identified (Frémont

and Echard 2018) (**Diagram 1.10**). Rab11-FIP3 endosomes are transported to the bridge by plus-end directed movement with the help of the motor protein kinesin-1 (Montagnac *et al.* 2009). Docking and tethering of the organelle can occur via interaction with the exocyst. The exocyst is an octameric structure that organises in a ring-like structure at the midbody rim (Neto *et al.* 2013). Rab11-FIP3 endosomes are linked to Sec15 and Sec10 components of the exocyst by Arf6 (Simon *et al.* 2008). In addition, Arf6 links centralspindlin to Rab11-FIP3-positive endosomes at the midbody (Simon *et al.* 2008). Accumulation and tethering at the exocyst of Rab11-FIP3 endosomes is also thought to be mediated by the target soluble N-ethylmaleimide-sensitive factor-attachment protein receptor (SNARE) Syntaxin 16 (Neto *et al.* 2013). Subsequent fusion of Rab11 endosomes with the PM might also be controlled by SCAMP-2-3, which are known to participate in exocytosis (Liu *et al.* 2005).

The role of Golgi-derived vesicles in cytokinesis is less clear. The fusion of secretory vesicles with the PM is thought to participate in surface area expansion required for furrow ingression and daughter cell formation, as membrane insertion and ingression occur concomitantly (Bluemink and De Laat 1973; Shuster and Burgess 2002). To date the Rab8 cargo has not been identified but Rab8-vesicles were shown to be transported to the intercellular bridge by dynein and to maintain intercellular bridge stability before abscission (Kaplan and Reiner 2011). Tethering of Rab8 vesicles to the midbody might occur via MICAL3 which interacts with MKLP1, a centralspindlin component (Liu *et al.* 2016) (**Diagram 1. 10**).

Finally vesicle trafficking is thought to participate in phosphoinositide enrichment at the cleavage furrow, which plays pivotal roles in cytokinesis (Frémont and Echard 2018).

Overall targeted membrane secretion and accumulation of vesicles allow delivery of key proteins and lipids at the cleavage/abscission site and might participate in membrane surface increase during daughter cell formation. Of note, the endocytic pathway, shut down during mitosis, is reactivated as cleavage furrow formation starts and is spatially restricted to the poles of the nascent cells. Endocytosed vesicles are then trafficked to the midbody,

probably to move specific cargo molecules to the cleavage site. Endocytosis has also been observed at the intercellular bridge, potentially to balance membrane delivery and promote bridge stability (Schweitzer *et al.* 2005).

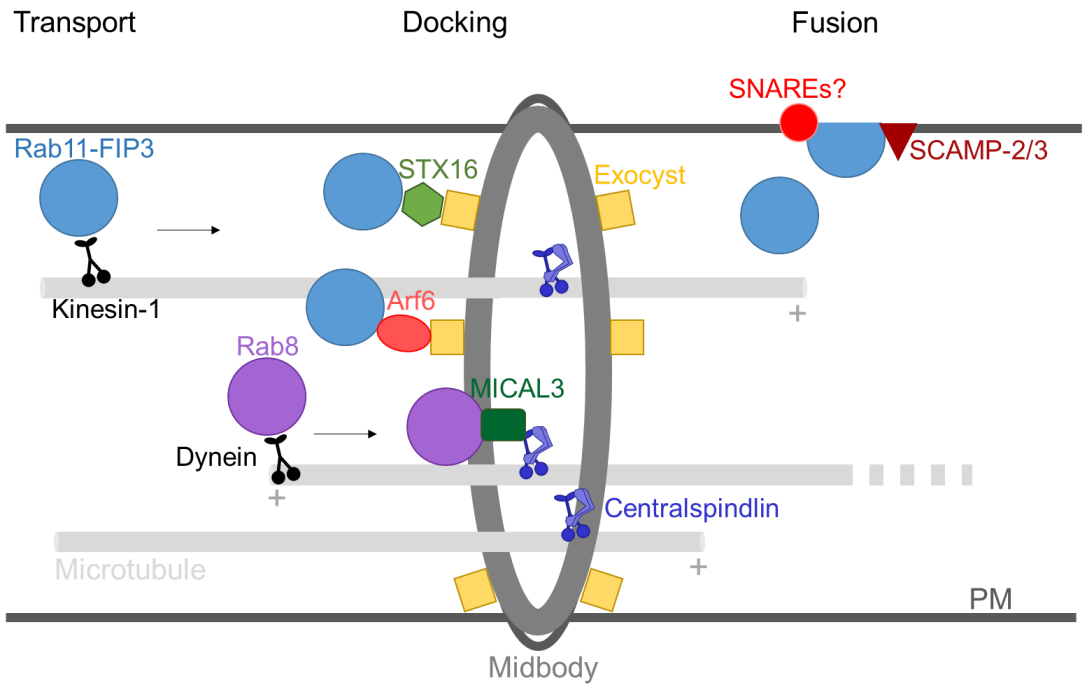

Diagram 1.10. Overview of the mechanisms of vesicle targeting, docking and fusion at the cytoplasmic intercellular bridge. Rab11-FIP3 endosomes (blue) are transported on microtubules via kinesin-1 towards the midbody where they interact with the exocyst (yellow) via syntaxin 16 (STX16, light green) or Arf6 (light red). Fusion with the PM is mediated by unknown SNAREs (red) and SCAMP-2/3 (dark red) near the future abscission site. Rab8-positive vesicles (purple) travel on the microtubules using Dynein. They associate with the midbody component centralspindlin (blue) though interaction with MICAL3 (dark green). Adapted from (Frémont and Echard 2018).

As described above, vesicle trafficking and fusion are required in the late stages of cell division. In addition, endocytic trafficking has been described as an important mechanism that regulates the drastic changes in PM area observed during mitosis. At the onset of mitosis the PM surface area decreases, leading to the rounding up of the cells; surface area recovery

occurs at the late stages of cell division. In their study of mitotic HeLa and BSC-1 cells, Boucrot and Kirchhausen (Boucrot and Kirchhausen 2007) proposed that whilst endocytosis remains unchanged throughout cell division, recycling of endocytosed material slows down substantially at the start of mitosis, concomitant with a decrease in cell surface area; despite fragmentation of the Golgi apparatus, the process resumes at anaphase and the PM surface area fully recovers before abscission. Interestingly, since the Golgi is disassembled during mitosis, the authors suggest a role of Ca^{2+}-regulated exocytosis involving the fusion of membrane-storing late endosomes and lysosomes with the PM (Boucrot and Kirchhausen 2007).

1.1.7.2. Roles of phosphoinositides in cytokinesis

Although representing a small fraction of total cellular lipids, phosphoinositides (PIs) are a class of phospholipids that play many pivotal roles in cells (Balla 2013). The hydrophilic head of PIs, which localise to membranes, faces the cytosol and is accessible for modification by phosphatases and kinases. Dynamic PI synthesis and degradation allows the creation of specific spatio-temporally controlled PI- subdomains on the PM and other organelles. Therefore PIs contribute to intracellular compartments identity (Di Paolo and De Camilli 2006). In addition, the differential distribution of PIs and their highly regulated modifications reflect the variety of signalling events and cellular functions they participate in (Di Paolo and De Camilli 2006). The role of PIs in cytokinesis was first revealed in a study on sea urchin embryos. Lithium-induced disruption of the PI cycle demonstrated a role of PI regulation in mitosis and cytokinesis completion (Forer and Sillers 1987). Since then several PIs and regulatory phosphatases and kinases have been found to participate in various stages of cytokinesis (Brill *et al.* 2011). Here the focus will be on phosphatidylinositol 4,5-bisphosphate ($PI(4,5)P_2$), phosphatidylinositol 4-phosphate (PI(4)P) and phosphatidylinositol 3-phosphate (PI(3)P) (**Diagram 1.11.**).

Cell elongation that occurs during anaphase is accompanied by membrane protrusions termed blebs at the cellular poles of the nascent cells (Sedzinski

et al. 2011). Bleb formation is caused by a dissociation of the cortical actin from the PM, whereas bleb retractions result from acto-myosin driven contractions (Charras 2008). A fine balance between the two processes is required for longitudinal expansion of the cell. Through their interaction with $PI(4,5)P_2$, the proteins ERM (Ezrin, Radixin, Moesin) promote cortical stiffness by inducing bleb retraction (Charras 2008; Roch *et al.* 2010). During cytokinesis, $PI(4,5)P_2$ accumulates at the cleavage furrow membrane partly due to the presence of phosphatase and tensin homolog (PTEN), the phosphatase responsible for its production from phosphatidylinositol 3,4,5-trisphosphate ($PI(3,4,5)P_3$) (**Diagram 1.11.**), and is absent from the rest of the cell membrane (Roubinet *et al.* 2011). Thus PI(4,5)P2-mediated ERM activation is restricted to the furrow area. ERM is inactivated in the cellular poles to allow the decrease in cortical stiffness necessary for cell growth and transiently reactivated to allow bleb retraction (Kunda *et al.* 2008; Roubinet *et al.* 2011). Consistent with this, excessive activation of ERM hampers cell elongation and ERM depletion causes abnormal blebs, hyper-relaxation at the poles and exaggerated cell expansion. Loss of $PI(4,5)P_2$ via PTEN inactivation or $PI(4,5)P_2$ depletion by a rapamycin-inducible $PI(4,5)P_2$ phosphatase construct induces similar defects (Roubinet *et al.* 2011).

Accumulation of $PI(4,5)P_2$ at the cleavage site from furrow ingression to cytokinesis completion was observed in many cell types including *Drosophila* (Roubinet *et al.* 2011), yeast (Zhang *et al.* 2000) and mammalian cells (Field *et al.* 2005b). The bulk production of $PI(4,5)P_2$ at the cleavage site comes from an enrichment in phosphatidylinositol 4-phosphate 5-kinase (PIP5K), which phosphorylates PI(4)P (Emoto *et al.* 2005) (**Diagram 1.11.**). Additional $PI(4,5)P_2$ production is ensured by concomitant dephosphorylation of $PI(3,4,5)P_3$ by PTEN (Janetopoulos *et al.* 2005).

In addition to its role in retraction of blebs and in the stimulation of actin polymerisation (Echard 2012), $PI(4,5)P_2$ was shown to contribute significantly to intercellular bridge stability after furrow ingression by binding to molecular factors essential for furrow stabilisation (Cauvin and Echard 2015). $PI(4,5)P_2$ has the ability to interact with RhoA (Yoshida *et al.* 2009) and Ect2 (Dambournet *et al.* 2011) *in vitro*, essential for cleavage specification, furrow

contraction and maintenance (D'Avino *et al.* 2015). Thus PI(4,5)P_2 participates in the correct localisation and accumulation of RhoA at the cleavage furrow. However, whilst depletion of PI(4,5)P_2 causes a decrease in RhoA at the furrow and cytokinesis defects (Abe *et al.* 2012), it does not prevent furrow ingression, suggesting that: 1) supplementary mechanisms of Ect2 and RhoA accumulation at the furrow take place and 2) PI(4,5)P_2 is likely to be directly involved in post-furrowing events, rather than furrow ingression *per se*. Indeed PI(4,5)P_2 interacts *in vitro* with the pleckstrin homology (PH) domain of anillin. Mutation of the anillin PH domain or depletion of PI(4,5)P_2 disrupts anillin localisation at the furrow, which in turn induces cytokinesis defects. These effects are rescued by ectopic expression of a modified version of anillin in which the PH domain was replaced by another PI(4,5)P_2 binding domain (Liu *et al.* 2012).

PI(4,5)P_2 can also bind to septins *in vitro* (Bertin *et al.* 2010), actin crosslinking and curved bundling components important for furrow stability after ingression (Kinoshita *et al.* 1997; Mavrakis *et al.* 2014). PI(4,5)P_2 depletion at the furrow delocalises septins from the cleavage site and the intercellular bridge and triggers furrow regression (Kouranti *et al.* 2006). Thus, by recruiting septins, PI(4,5)P_2 could contribute to bridge stability, potentially through septin-induced actin crosslinking into curved bundles (Mavrakis *et al.* 2014) that in turn could facilitate membrane curvature.

In addition to anillin and septins PI(4,5)P_2 binds to the GAP component of centralspindlin (Lekomtsev *et al.* 2012). Mutation in the PI(4,5)P_2-binding site of MgcRacGAP leads to furrow ingression followed by detachment of the PM at the intercellular bridge, furrow regression and cytokinesis abortion, further linking PI(4,5)P_2 to bridge stability (Lekomtsev *et al.* 2012).

Finally PI(4,5)P_2 is also involved in exocytosis and endocytosis (Mayinger 2012). Both processes are required for successful cytokinesis (Echard 2008), suggesting an additional layer of control of bridge stability by PI(4,5)P_2. Interestingly, PI(4,5)P_2 binds to Sec3 and Exo70 components of the exocyst, which allows the tethering of vesicles at the PM before exocytosis

(Archambault and Glover 2009). Whether these interactions play a role in cytokinesis remains to be fully investigated (Brill *et al.* 2011).

The role of PI(4)P in cytokinesis is less clear. In *Drosophila*, loss of four wheel drive (Fwd), the equivalent of mammalian PI4KIIIβ, the kinase that catalyses formation of PI(4)P from phosphatidyl inositol (PtdIns) (**Diagram 1.11.**), leads to actin ring defects and multinucleation (Brill *et al.* 2000). Fwd is involved in PI(4)P production at the Golgi, in the maintenance of the Golgi complex and in the formation of PI(4)P-positive vesicles targeted to the midzone (Polevoy *et al.* 2009). Thus the kinase could promote PI(4)P delivery at the furrow, which could then be converted in $PI(4,5)P_2$ necessary for bridge stability (Cauvin and Echard 2015). Additionally, Fwd possesses a non-enzymatic function responsible for the recruitment of vesicles decorated with Rab11 and accumulation of Rab11-PI(4)P vesicles at the midzone (Polevoy *et al.* 2009). Rab11 is essential in mammalian cytokinesis through actin remodelling at the intercellular bridge (Schiel *et al.* 2012). Therefore it would be interesting to investigate the role of PI(4)P and PI4KIIIβ in actin remodelling at the bridge and transport of Rab11 vesicles during mammalian cytokinesis. A recent study in *Drosophila* demonstrated that PI(4)P can exert a direct effect on cytokinesis through binding to the Golgi phosphoprotein 3 (GOLPH3), directing its localisation at the cleavage furrow and activating it (Sechi *et al.* 2014). GOLPH3 is responsible for the recruitment of Rab11-vesicles at the cleavage furrow, proper furrow ingression and interacts with components of the contractile rings (Sechi *et al.* 2014). Therefore the protein could provide a mechanistic link between furrow components and PI(4)P.

PI(3)P and its effectors are involved in endosomal fusion, motility and sorting and autophagy (Schink *et al.* 2013). Disruption of the class III phosphatidyl inositol 3-kinase (PI3K), which promotes PI(3)P biogenesis from PtdIns, interferes with both endosomal function and abscission (Sagona *et al.* 2010). In addition, the enzyme has been found to localise at the intercellular bridge (Sagona *et al.* 2010; Sagona *et al.* 2011). Interestingly, PI(3)P-vesicles carry the protein FYVE-CENT, which interacts with TCC19. In turn, TCC19 binds to the ESCRT-III subunit CHMP4 and depletion of either TCC19 or FYVE-CENT triggers abnormally late abscission and cell multi-nucleation (Sagona *et al.*

2010). Therefore PI(3)P might participate in the regulation of abscission through the recruitment of components essential in the process.

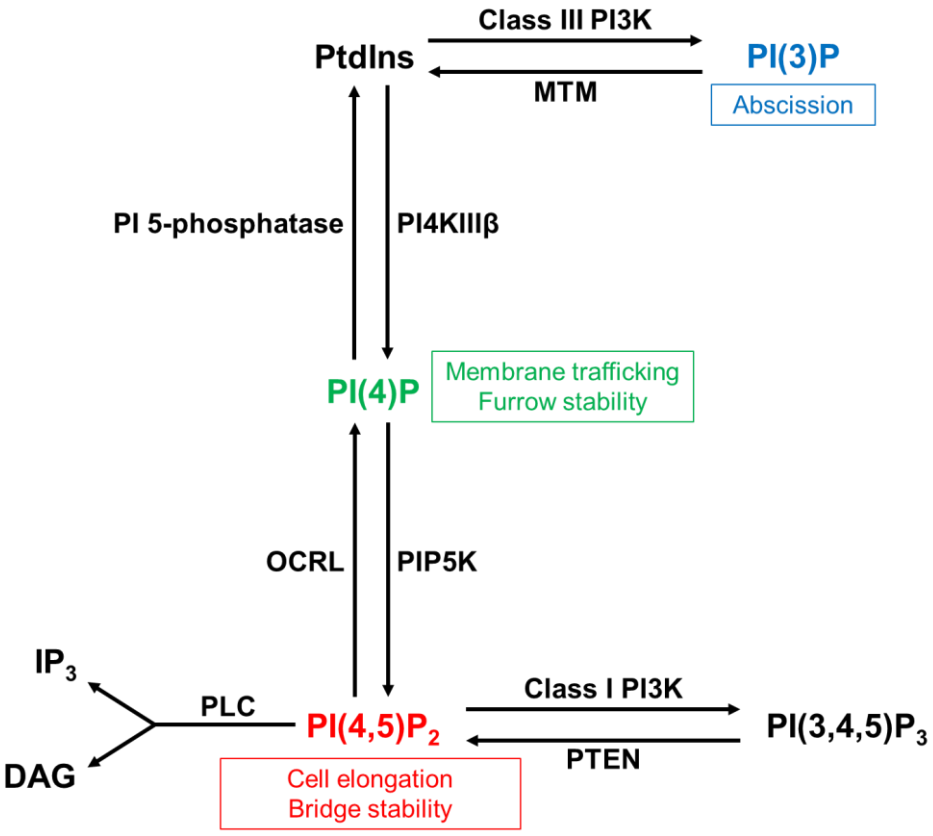

Diagram 1.11. Regulatory cycle of phosphoinositides and their known/potential contribution in cytokinesis. MTM: myotubularin. Of note, PI(3)P does not play a role in abscission *per se* but its production is required prior to abscission as PI(3)P-positive endosomes indirectly interact with ESCRT-III. Adapted from (Brill *et al.* 2011) and (Cauvin and Echard 2015).

1.1.8. Lysosomes and cytokinesis

In addition to endosomal and Golgi-derived vesicles, lysosomes, another type of intracellular compartment have been observed to cluster around the intercellular bridge during cytokinesis (Rajamanoharan *et al.* 2015). Interestingly, lysosomes were shown to be decorated with PI4KIIIβ, an enzyme that not only preserves the organelle identity (Sridhar *et al.* 2013) but also participates in the generation of PI4P essential for cytokinesis completion

(Brill *et al.* 2000). Rajamanoharan and co-workers also demonstrated that disrupting the lysosomal rearrangement and clustering around the intercellualr bridge during cytokinesis via a PI4KIIIβ-dependent pathway, compromised cytokinesis completion and induced division defects (Rajamanoharan *et al.* 2015). This novel observation suggests that lysosome positioning during cytokinesis, far from being fortuitous is functionally required as its disruption impacts cell division.

1.2. Lysosomes

Discovered and purified in the 1950s by Christian de Duve (Samie and Xu 2014), lysosomes did not occupy the most prestigious position among cellular organelles for many years. Poetically termed 'waste bags', lysosomes are acidic membrane-bound compartments primarily responsible for the catabolic functions of eukaryotic cells (Appelqvist *et al.* 2013). They contain more than 60 distinct hydrolases that degrade intracellular components derived from autophagy and extracellular substrates that have been internalised via endocytosis (Saftig and Klumperman 2009). The lysosomal hydrolases target a wide range of substrates including DNA, RNA, carbohydrates, lipids and proteins (Dielschneider *et al.* 2017). Additionally, lysosome-related compartments secrete proteins tailored for the function of specialised cells (Saftig and Klumperman 2009). Electron microscopy analyses demonstrated that lysosomes account for ~5% of the total intracellular volume (Klumperman and Raposo 2014) and come in a variety of shapes and sizes , with diameters ranging from 0.2 to 1.2 μm (De Duve and Wattiaux 1966; Klumperman and Raposo 2014). They can be distinguished from late endosomes, the compartment immediately upstream of the lysosome in the endocytic pathway, by their lack of mannos-6-phosphate receptors (M6PRs) (Brown *et al.* 1986). The 7-10 nm lysosome phospholipid bilayer contains more than 150 membrane proteins involved in the stability of the organelle and that are required for the transport of particles for degradation (Maxfield *et al.* 2016). More specific lysosomal membrane proteins such as GTPases and SNAREs are dedicated to the trafficking/tethering and fusion properties of the organelle,

respectively (Saftig and Klumperman 2009). A unique characteristic of lysosomes is the extensive glycosylation of their membrane proteins. Glycosylations of the luminal domains of lysosomal membrane proteins (LMPs) constitute the glycocalyx, a protective barrier of the lysosomal membrane against the lytic enzymes residing in the lumen (Granger *et al.* 1990). Among the LMPs identified, the most abundant are CD63, lysosomal integral membrane protein 2 (LIMP2) and lysosomal-associated membrane proteins (LAMP) 1 and 2 (Eskelinen *et al.* 2003). The lysosomal membrane is also associated with lipids such as phosphoinositides responsible for the reformation of lysosomes and the maintenance of their identity (Luzio *et al.* 2007; Sridhar *et al.* 2013). Remarkably, lysosomes possess an acidic lumen with a pH ranging from 4.5 to 5.0 (Saftig and Klumperman 2009). This is generated and maintained by the activity of the vacuolar ATPase (V-ATPase), a proton pump located on the lysosome limiting membrane. As the large influx of H^+ across the lysosomal membrane generates a net positive voltage and inhibits further pumping, counterion flux (anion influx and cation efflux) is required to neutralise the membrane potential and facilitate organellar acidification (Ishida *et al.* 2013). The high H^+ concentration not only contributes to lysosomal acidification but also creates a concentration gradient that can be used to transport Ca^{2+} into the lysosomal lumen, via calcium hydrogen exchangers (CAXs) (Patel and Docampo 2010). The luminal Ca^{2+} concentration of lysosomes is estimated at approximately 200-600 μM, a concentration not dissimilar to that found in the endoplasmic reticulum (ER) (Lloyd-Evans *et al.* 2008). Thus, unsurprisingly, lysosomes were also suggested to function as Ca^{2+} signalling platforms (Patel and Docampo 2010). In addition, the acidity of the lysosomes confers an optimal environment for the catalytic activity of most lysosome-resident hydrolases (Bainton 1981). Indeed, many of these specialised enzymes have a pH optima between 4.5 and 5.5 and a poor efficiency at neutral cytoplasmic pH, conferring the cell a highly evolved protective mechanism in the event of lysosomal damage and hydrolase leakage into the cytoplasm (De Duve and Wattiaux 1966; Mellman *et al.* 1986).

Although long viewed as the terminal degradative and recycling centre of the cell, lysosomes are now viewed as a highly dynamic and versatile organelle tasked with a wide variety of biological processes and considered major regulators of cellular homeostasis (Appelqvist *et al.* 2013). Notably, they can detect the nutrient status of the cell and act as signalling platforms that regulate the starvation response and control energy metabolism (Settembre *et al.* 2013). Additionally, they can undergo regulated exocytosis, a process of fusion with the PM known to play a pivotal role in secretion and PM repair (Chieregatti and Meldolesi 2005).

1.2.1. Lysosome biogenesis and delivery of lysosomal proteins

The biosynthesis of lysosomes is regulated by the transcription of a network of genes encoding lysosomal proteins transcribed in a coordinated fashion. The promoter region of many of the lysosomal genes is enriched with a palindromic 10-base pair (bp) GTCACGTGAC motif called coordinated lysosomal expression and regulation (CLEAR) element. The binding of the CLEAR element to transcription factor EB (TFEB) drives the transcription of lysosomal genes (Sardiello *et al.* 2009). TFEB activation/repression relies on cellular nutrient status. Under normal conditions, TFEB is maintained in a phosphorylated state by mammalian target of rapamycin complex 1 (mTORC1) on the surface of lysosomes, and is thus sequestered in the cytosol. Under conditions of starvation and insufficient nutrients, mTORC1 phosphorylation is abolished and TFEB translocates to the nucleus, where it drives the expression of lysosomal components (Settembre and Ballabio 2014).

Lysosomes constitute the terminal compartment of the degradative endocytic pathway, which forms a continuum that starts at the PM and progresses through a series of distinct intermediate compartments. A number of events such as fusion/fission of compartments, exchange of membranes and gradual acidification progressively reshape early endosomes (EE) into late endosomes (LE), a process called maturation. Of importance, the inner membrane of endosomes pinches off and intraluminal vesicles (ILVs) form in the endosomal

lumen. ILVs facilitate the sorting and delivery of cargo (Woodman and Futter 2008). As endosomes mature, the number of ILVs increases to eventually form LE intermediates, called multivesicular bodies (MVBs). MVBs fuse with preexisting lysosomal compartment forming a transient hybrid organelle, the endolysosome (Huotari and Helenius 2011). The lysosomes are eventually re-formed and turned into classical lysosomes, which store high levels of hydrolases and membrane proteins (Saftig and Klumperman 2009) (**Diagram 1.12.**). Thus there is a high degree of overlap between the LE and the lysosome, however the latter can be distinguished from LEs, as aforementioned, by the lack of M6PR (Appelqvist *et al.* 2013).

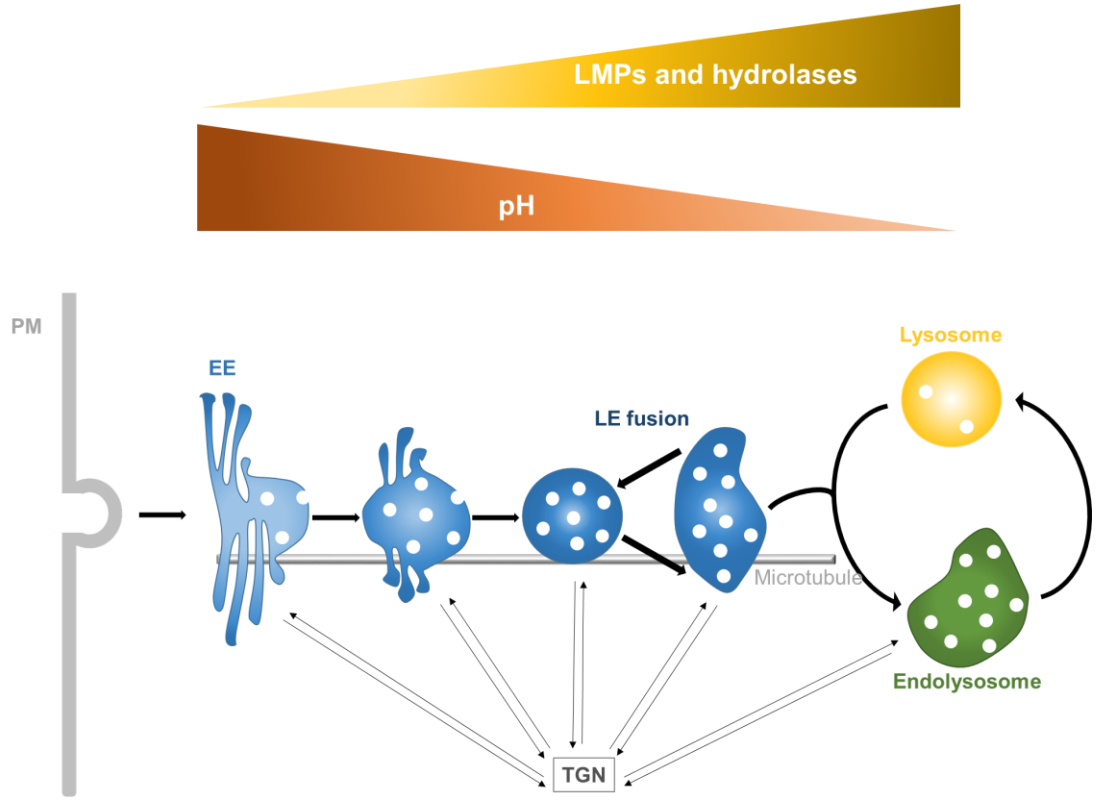

Diagram 1.12. The endocytic pathway and lysosome formation. Endocytic vesicles emerge from the PM (grey) and deliver their content to EEs (light blue) located in the vicinity of the PM. The incoming cargo is then either recycled back to the PM by recycling endosomes (not depicted) or further transported to the endocytic pathway. EEs form a clathrin-coated vacuole from which emanates a network of tubules. By a process of maturation, EEs are gradually converted into LEs (dark blue), globular vacuoles with very few tubules and lined with a bilayer of clathrin coat. This transition is marked by association with distinct GTPases, with LE exchanging Rab5 for Rab7. LEs subsequently fuse with other LEs, grow in size and form intermediates

called MVBs, which acquire more intraluminal vesicles (white circles) formed by inward budding of the limiting membrane. The maturation process of LEs prepares them to fuse with preexisting lysosomes, generating endolysosomes (green). Finally conversion into classical lysosomes (yellow), heterogeneously shaped globular structures, takes place. Throughout the endosomal maturation process, the TGN receives and delivers proteins from and to endosomes (double arrows). From EEs to lysosomes, a progressive acidification takes place (brown triangle showing a decrease in pH) and the levels of hydrolases and LMPs increase (yellow triangle). Adapted from (Huotari and Helenius 2011) and (Saftig and Klumperman 2009).

Lysosome delivery of lysosomal proteins results from the cooperation between the biosynthetic and endocytic pathways (**Diagrams 1.12.** and **1.13.**). There are broadly two classes of proteins that are critical to lysosomal function: lysosomal hydrolases and integral LMPs. As mentioned previously, lysosomal hydrolases, which reside in the lysosome lumen, are responsible for the catabolic properties of lysosomes (Saftig and Klumperman 2009). They are also essential in other cellular processes including apoptosis (Conus and Simon 2008), degradation of the extracellular matrix (Hämälistö and Jäättelä 2016), PM repair (Castro-Gomes *et al.* 2015) and antigen processing (Shibutani *et al.* 2015). LMPs, which mainly localise to the lysosomal limiting membrane mediate other important lysosomal functions such as luminal acidification, translocation of proteins into the lysosome lumen, release of catabolites into the cytosol, organellar homotypic and heterotypic fusion and exocytosis (Eskelinen *et al.* 2003).

The delivery of lysosomal proteins can take two possible routes: a direct pathway in which newly synthesised proteins travel from the *trans*-Golgi network (TGN) to the endolysosomal system, or an indirect pathway where proteins are first transported from the TGN to the PM, retrieved by endocytosis and subsequently carried to the endolysosomal system (Saftig and Klumperman 2009).

Most newly synthesised hydrolases are transported to lysosomes via a direct pathway mediated by M6PR, a well-characterised mode of protein delivery which relies on the recognition of M6P sugar residues on hydrolases by M6PR

(Luzio *et al.* 2014) (**Diagram 1.13.**). Newly synthesised soluble lysosomal hydrolases undergo signal sequence cleavage in the ER. Vesicle-mediated transport allows the transfer of lysosomal hydrolases to the Golgi where they acquire M6P residues (Braulke and Bonifacino 2009). Addition of M6P residues depends on the activity of *N*-acetylglucosaminyl-1-phosphotransferase. A second enzyme, the *N*-acetylglucosamine-1-phosphodiester α *N*-acetylglucosaminidase (uncovering enzyme) unmasks the M6P residues (Braulke and Bonifacino 2009). Upon reaching the TGN, the enzymes are recognised by M6PR. The cytosolic tail of the receptor also binds to adaptor protein 1 (AP1) and the Golgi-localised, γ-ear-containing, ADP ribosylation factor binding proteins (GGAs). This induces the formation of clathrin coated vesicles loaded with cargo-associated M6PRs which are subsequently transported to endosomes (Luzio *et al.* 2014). Entry into the mildly acidic endosome lumen induces dissociation of lysosomal hydrolases from the M6PR, which is subsequently recycled back to the TGN using the endosome-to-TGN retrieval retromer machinery for further rounds of hydrolase delivery (Attar and Cullen 2010). The hydrolases present in the endosome lumen travel further through the endolysosomal system to eventually reach the lysosome by the dynamic fusion/fission events described previously in this section (**Diagram 1.12.**). The majority of hydrolases are delivered to lysosomes via the M6PR route. However, previous studies suggest the existence of alternative pathways. Accordingly *N*-acetylglucosaminyl-1-phosphotransferase deficiency does not prevent hydrolases from reaching their lysosomal target in certain cell types of patients suffering from I-cell disease, despite the absence of the M6P tag on the hydrolases (Tsuji *et al.* 1988). Additionally, examples of M6PR-independent delivery of lysosomal enzymes exist such as the LIMP2-mediated pathway that uses the lysosomal integral membrane protein to transport β-glucocerebrosidase to the lysosome (Coutinho *et al.* 2012).

The delivery of LMPs is M6PR-independent and sorting of LMPs destined to lysosomes is based on the recognition of specific di-leucine- or tyrosine-based motifs located on the cytosolic tail of LMPs (Saftig and Klumperman 2009). Variants of both signals have also been demonstrated to target some proteins

to lysosomes (Braulke and Bonifacino 2009). Tyrosine and di-leucine motifs can interact with AP1, AP2, AP3 and AP4 complexes (Braulke and Bonifacino 2009). AP2 is responsible for rapid endocytosis at the PM, whereas AP1, AP3 and AP4 function at the TGN (Boehm and Bonifacino 2001). Of note, AP4 is distinct from AP1, AP2 and AP3 as it is part of a nonclathrin coat (Mattera *et al.* 2017). Following recognition of their motif, many LMPs, including LAMPs and LIMPs, can reach lysosomes via two possible routes (**Diagram1.13.**). LMPs can be transported to the endolysosomal system directly from the TGN. Alternatively, they can follow the constitutive secretory pathway from the TGN to the PM. Subsequent endocytosis allows them to reach the endolysosomal system (indirect pathway) (Saftig and Klumperman 2009). LMPs can traffic to the lysosome via both routes. However it is unclear what proportion of each LMP travels via either pathway (Braulke and Bonifacino 2009). In addition, the nature of the AP complex responsible for the sorting of LMPs other than LAMPs differs greatly but likely reflects the preferential mode of pathway (direct or indirect) adopted by LMPs. For example, knock-down of AP1 in mouse fibroblasts induced trafficking defects in the Mucolipin-1 member of the transient receptor potential (TRP) ion channel superfamily, whereas knock-down of AP2 had no effect, suggesting that delivery of the channel to lysosomes occurs preferentially via the direct pathway (Miedel *et al.* 2006).

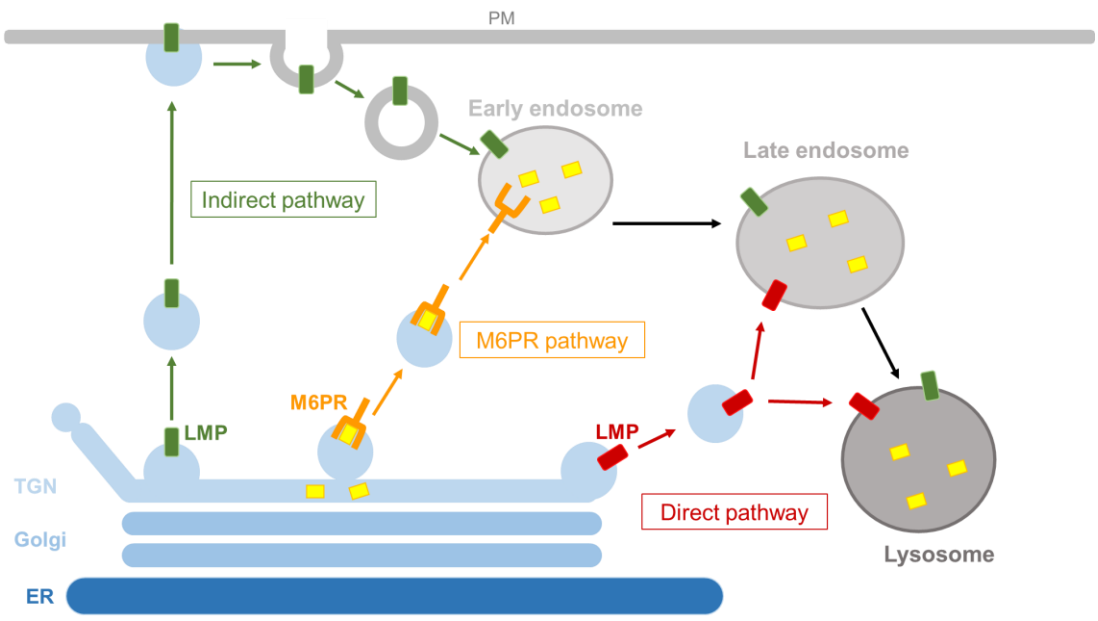

Diagram 1.13. Modes of delivery of lysosomal proteins. LMPs can enter lysosomes via a direct (red) or an indirect (green) pathway. In the direct pathway, LMPs enter the endolysosomal system directly from the TGN, whereas the indirect pathway involves an extra step of delivery to the PM and endocytosis prior to entry into the endolysosomal system. The delivery of most soluble lysosomal hydrolases to the endolysosomal system is mediated by the M6PR pathway which recognises the M6P tag (yellow squares) on these enzymes. Of note, the M6PR-mediated delivery of hydrolases tagged with M6P is a type of direct pathway. Subsequent fusions/fissions, transfer of cargo between endosomes and lysosomes allow an enrichment of hydrolases and LMPs in the lysosome. Adapted from (Saftig and Klumperman 2009).

1.2.2. Lysosomal functions

The term lysosome was coined from the Greek for “digestive body” as their function first appeared to be restricted to degradation and recycling of cellular components (Appelqvist *et al.* 2013). Accordingly, within a few years of their discovery, lysosomes were found to be central in the catabolism of intra- and extracellular particles. Further study revealed the complexity of lysosomes which are now considered as highly advanced, dynamic structures, functioning at the crossroads of different cellular pathways and critical in cellular homeostasis (Luzio *et al.* 2007). Broadly speaking, their functions are classified as catabolism, signalling and secretion (Settembre *et al.* 2013). However the versatility and critical functions of lysosomes come at a price. Defects in any of these lysosomal functions can have devastating consequences. Indeed, abnormal lysosomal activity is evident in various lipid storage disorders (LSDs), a set of inherited metabolic pathologies (Futerman and Van Meer 2004). It is also linked to neurodegenerative diseases (Menzies *et al.* 2015), and even has the potential to promote cancer (Hämälistö and Jäättelä 2016). Therefore the benefits of gaining a better understanding of lysosomal functions are clear.

1.2.2.1. The degradative function of lysosomes

Lysosomal degradative processes are mediated by the diverse set of lysosome resident enzymes, which collectively target all classes of macromolecules. Lysosomal hydrolases include proteases, peptidases, phosphatases, nucleases, glucosidases, lipases and sulfatases (Appelqvist *et al.* 2013). Among the proteases, cathepsins have been particularly well investigated. The characterisation of several cathepsins has led to the identification of three subgroups, namely serine (A and G), cysteine (B, C, F, H, K, L, O, S, V, W and X) and aspartic cathepsins (D and E), based upon the amino acid composition of their active site (Appelqvist *et al.* 2013). Cathepsins D, B, C, H and L are expressed constitutively and are present in all cell types. The expression levels of other enzymes such as the cysteine cathepsins K and S are adjusted according to the requirements of specific cell types (Mohamed and Sloane 2006). For example, the expression of cathepsin K is particularly regulated in osteoclasts, where bone remodelling is needed (Saftig *et al.* 1998). In addition, cathepsins B and L are known not only for their activity in extracellular matrix (ECM) proteolysis, but also for their role in PM repair (Castro-Gomes *et al.* 2015). Thus, whilst most lysosomal hydrolases require an acidic environment for optimum activity, some cathepsins retain their activity outside lysosomes and act as exopeptidases (Mohamed and Sloane 2006). This highlights a unique facet of lysosome physiology, an organelle with both intra- and extra-cellular functionality.

Extracellular components reach the lysosome via the endocytic pathway, whereas intracellular material destined for lysosomal degradation reach their final destination by various types of autophagy (Settembre and Ballabio 2014).

The endocytic pathway

The endocytic pathway begins with the process of endocytosis through which material is internalised at the PM. The modes of molecule uptake at the PM are varied. Internalisation can occur by clathrin- or caveolae-mediated or clathrin-independent endocytosis (Elkin *et al.* 2016) (**Diagram 1.14.**). In clathrin-mediated endocytosis, the PM forms clathrin-coated pits (CCPs) that

invaginate to form clathrin-coated vesicles (CCVs). CCPs are first generated by the AP2 complex targeted to the PM by $PI(4,5)P_2$ (Traub and Bonifacino 2013). Clathrin is subsequently mobilised by the AP2 complex and assembles around the pit (Kirchhausen 1999). Membrane curvature is induced by recruitment of proteins containing a Bin-Amphiphysin-Rvs (BAR) domain (Qualmann *et al.* 2011). The growth of the CCP is accompanied by an accumulation of cargo mediated by AP2 and other adaptor proteins (Elkin *et al.* 2016). Fission of the neck of the CCP is induced by the GTPase dynamin, recruited by BAR domain-containing proteins (Ferguson *et al.* 2009). The released CCV subsequently uncoats and fuses with early endosomes (Elkin *et al.* 2016). Clathrin-mediated endocytosis is responsible for the uptake of low-density lipoprotein (Carpentier *et al.* 1982) and transferrin (Neutra *et al.* 1985). The second type of material uptake is caveolae-mediated endocytosis. The structural subunit of caveolae is caveolin, present on the inner PM (Parton and Del Pozo 2013). Caveolin binds to cholesterol, forming cholesterol and sphingolipid-enriched membrane domains responsible for lipid metabolism, detection of surface tension and signalling, besides endocytosis (Murata *et al.* 1995; Harder and Simons 1997; Parton and Del Pozo 2013). The mechanisms of caveolae-mediated endocytosis are not fully elucidated but the budding process is thought to depend on kinase and phosphatase activity (Kiss 2012). Eventually the caveolin formed vesicle is detached from the PM by dynamin (Henley *et al.* 1998) and is free to fuse with recycling endosomes. The third mechanism of endocytosis, as its name suggests, does not rely on clathrin or caveolae. Clathrin- and caveolae-independent endocytosis is thought to be composed of a collection of at least four pathways involving different molecular players (Elkin *et al.* 2016). Its functional significance, contribution to overall endocytosis as well as the degree of overlap between its different pathways are not fully understood. Some studies propose its contribution is minimal to overall endocytic flux, compared to clathrin-mediated endocytosis (Bitsikas *et al.* 2014). However most recently, it was shown to be significantly altered in cancer, suggesting that non-canonical endocytosis is an important cellular process (Elkin *et al.* 2015). Once internalised by either type of endocytosis, cargo enters endosomes. Most cargo is recycled back to the PM through REs (Huotari and Helenius 2011), the remaining cargo is retained in

EE and is passed on to LEs through maturation of early into late endosomes (see section 1.2.1. of this chapter). As the number of ILVs increases in LEs, MVBs are generated (Appelqvist *et al.* 2013). Those which fuse with lysosomes form endolysosomes, where degradation takes place (Luzio *et al.* 2014).

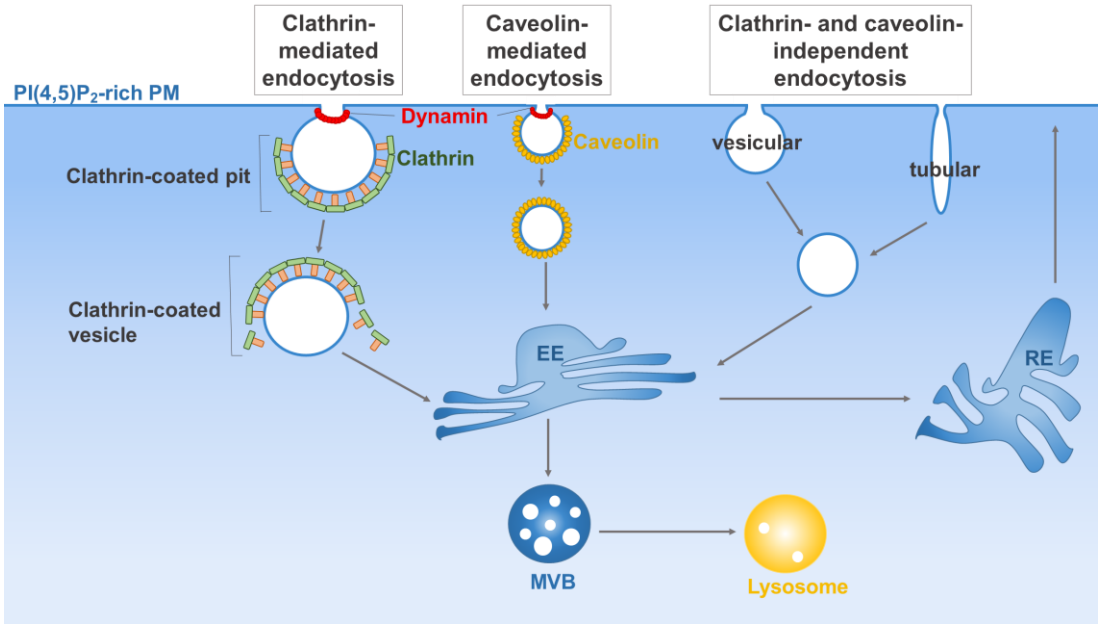

Diagram 1.14. The mechanisms of endocytic extracellular particle uptake. Three mode of endocytosis have been characterised: clathrin-mediated, caveolin-mediated and clathrin- and caveolin-independent. Internalised macromolecules are delivered to EEs and can either be trafficked back to the cell surface through a RE or travel further along the endolysosomal system to be degraded in lysosomes. Adapted from (McMahon and Boucrot 2011).

Fusion of LEs and lysosomes requires the cytosolic factors N-ethylmaleimide-sensitive factor (NSF), soluble NSF-attachment proteins, the GTPase Rab7 and homotypic fusion and vacuole protein sorting (HOPS) proteins (Luzio *et al.* 2014). In addition, Ca^{2+} release from both compartments and *trans*-SNARE complexes composed of syntaxin-7, Vti1b, syntaxin 8 and the vesicle-associated membrane protein 7 (VAMP7) are needed (Luzio *et al.* 2014) (**Diagram 1.15.**). Both organelles are subsequently recovered from the hybrid compartment by a mechanism involving content condensation depending on V-ATPase activity and luminal Ca^{2+} (Pryor *et al.* 2000). Re-formation of

organelles also requires removal of endosomal membrane proteins and recycling of SNAREs (Luzio *et al.* 2014).

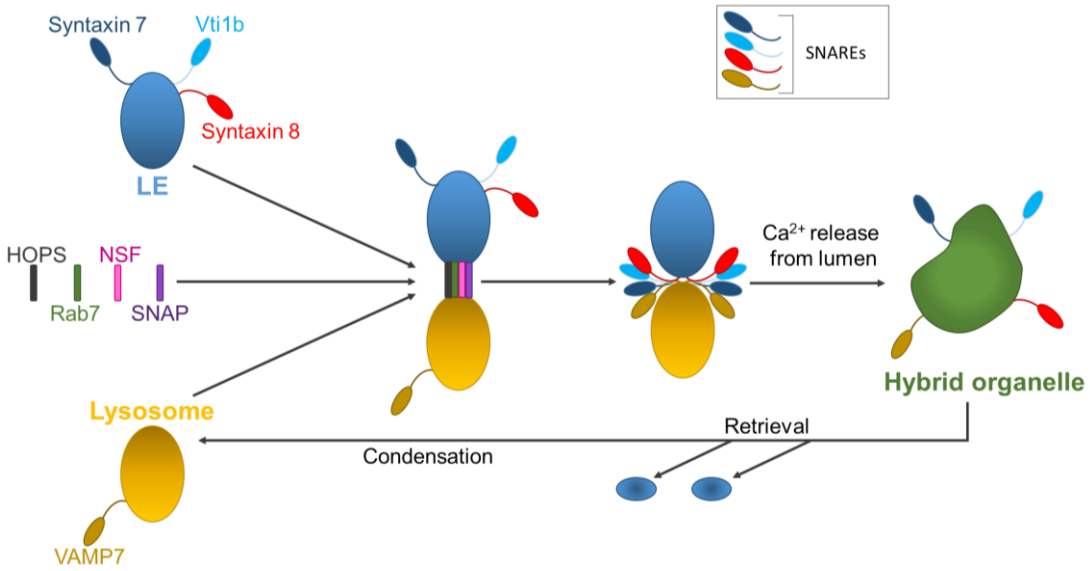

Diagram 1.15. Mechanisms of endosome-lysosome fusion. Rab7 together with HOPS allows tethering of endosome and lysosome. Soluble N-ethylmaleimide-sensitive factor (NSF) and soluble N-ethylmaleimide attachment protein (SNAP) are also recruited. Subsequently syntaxin 7, Vtib and syntaxin 8 permit formation of a *trans*-SNARE complex. VAMP7 located on the lysosomal membrane is also needed for the heterotypic fusion of organelles. Ca^{2+} is released from the lumen of both organelles and triggers fusion of membranes. Lysosomes are recovered by SNARE retrieval, loss of M6PR and condensation of its luminal compartment to generate a lysosome with a dense core. Adapted from (Luzio *et al.* 2007) and (Luzio *et al.* 2014).

Autophagy

Autophagy refers to the mechanism by which the cell degrades and recycles its own components. The process is initiated by cellular stress such as amino acid starvation, misfolding of proteins or viral attack (Saftig and Klumperman 2009). Autophagy mediates the degradation of a wide range of cytoplasmic components including oxidised lipids, damaged organelles, protein aggregates and intracellular pathogens (Settembre *et al.* 2013). In mammalian cells, autophagy comes in three forms: macroautophagy (MA), microautophagy and chaperone-mediated autophagy (CMA). They differ

predominantly by the mechanisms of material delivery into the lysosomal lumen (Settembre *et al.* 2013) (**Diagram 1.16.**).

Microautophagy is the non-selective, direct engulfment of cytoplasmic material by the lysosomal membrane itself (Li *et al.* 2012). It is a constitutive process that can also be triggered by conditions of starvation such as nitrogen deprivation. The main purpose of microautophagy is the maintenance of organellar membrane composition and membrane homeostasis. Through uptake of lipids located on the lysosomal membrane, it also participates in lipid degradation (Li *et al.* 2012).

During CMA, cytosolic proteins containing a pentapeptide recognition signal, namely the consensus motif KFERQ, are identified by the chaperone heat shock cognate protein of 70 kDa (hsc70) which subsequently directs the molecules to the lysosome for degradation (Kaushik and Cuervo 2012). All proteins contain the KFERQ motif thus degradation depends on whether the motif is accessible to the cytosolic chaperone. Protein-protein interactions, binding to membranes or sequestration in cellular compartments all mask the recognition domain of the protein. By contrast, fully or partially unfolded proteins can expose the motif to the chaperone (Kaushik and Cuervo 2012). Following recognition by the hsc70, proteins bind to the cytosolic tail of LAMP2A, located on the lysosomal membrane (Cuervo and Dice 1996). This interaction generates multimerisation of LAMP2A, which permits translocation and entry of the substrate into the lysosomal lumen for degradation by hydrolases (Bandyopadhyay *et al.* 2008). The free amino acids resulting from protein degradation are critical for metabolic balance as they can be re-used for the synthesis of other proteins or utilised as energy source. In addition, CMA provides a quality control functionality by selectively targeting damaged or misfolded proteins and proteins prone to aggregation (Kaushik and Cuervo 2012).

MA is the most well-documented type of autophagy and is thought to be the main pathway in autophagy (Mizushima and Komatsu 2011). The cytosolic substrate is isolated from the rest of the cytoplasm by a membrane known as the phagophore, which elongates to completely surround and sequester it,

forming an enclosed membranous structure, the autophagosome (Nikoletopoulou *et al.* 2015). Subsequent fusion of the autophagosome with the lysosome generates an autolysosome, inside which degradation takes place. Damaged organelles, cytosolic proteins and foreign microbes are all target substrates for MA-mediated degradation (Furuta *et al.* 2010; Nikoletopoulou *et al.* 2015). MA is a constitutive process occurring at basal levels in most cells, however it can be upregulated in certain conditions such as nutrient depletion and environmental stress (Singh and Cuervo 2011). The origin of the phagophore membrane remains highly controversial. Possible sources responsible for its formation include the ER (Axe *et al.* 2008), Golgi complex (Geng *et al.* 2010), PM (Ravikumar *et al.* 2010) and mitochondria (Hailey *et al.* 2010). Its generation (induction), growth, maturation and degradation are all governed by the products of many highly conserved autophagy genes (ATG) such as LC3 (Lee 2012; Lee and Lee 2016). The fusion of autophagosomes with lysosomes also involves additional non-ATG factors. Like the heterotypic fusion of lysosomes with endosomes, the formation of the autolysosome requires the participation of Rab GTPases (Nikoletopoulou *et al.* 2015), SNAP29 (Yu and Melia 2017) and SNAREs including VAMP7, VAMP8, Vti1b and Stx17 (Itakura *et al.* 2012).

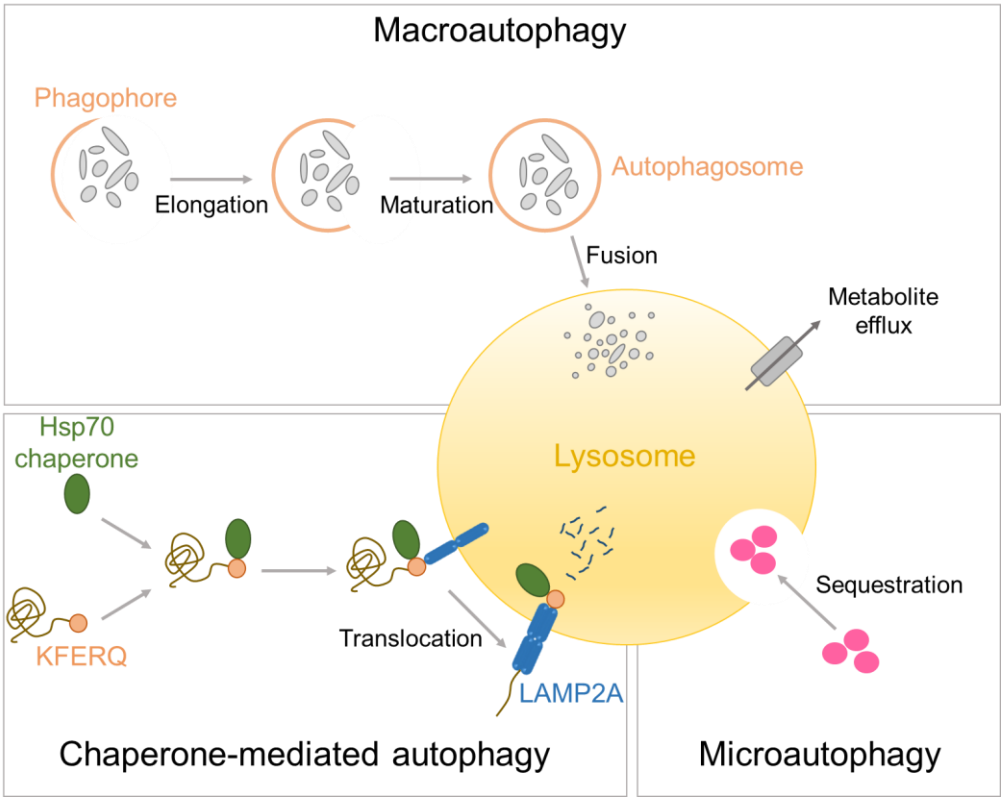

Diagram 1.16. Types of autophagy and their mechanisms of material delivery to lysosomes. MA involves elongation and maturation of the phagophore into an autophagososme that engulfs particles and subsequently fuses with the lysosome. CMA targets proteins exclusively. Hsp70 chaperone recognises the KFERQ motif on proteins and the complex interact with LAMP2A located on lysosomes. Multimerisation and translocation of LAMP2A allows the transfer of the protein in the lysosomal lumen. Microautophagy involves invagination of the lysosomal membrane and engulfment of particles for degradation. The resulting metabolites are extruded from lysosomes for re-use through specific exporters located on the lysosomal limiting membrane. Adapted from (Boya *et al.* 2013).

Lysosomes, nutrient sensors

The nutrient status is an important factor regulating autophagy. As described previously in this section, conditions of starvation trigger the autophagy pathway in which the lysosome is the terminal compartment. However lysosomes are also present at the top of this regulation. Through the lysosome nutrient sensing machinery (LYNUS), lysosomes monitor the nutrient availability and communicate with nutrient-sensitive signalling molecules, such

as the master regulator TFEB (Xu and Ren 2015) (see section 1.2.1.). During starvation, TFEB induces the expression of the lysosomal-autophagy pathway which in turn mediates lipophagy and fatty acid β-oxidation (Settembre *et al.* 2013).

1.2.2.2. Lysosomes and Ca^{2+} signalling

Ca^{2+} is fundamental in lysosomal activity. This cation is known to mediate trafficking of the organelle (Shen *et al.* 2012), fusion with other compartments (Xu and Ren 2015) and to control their regulated exocytosis (Andrews 2000). In addition, studies revealed that lysosomes constitute an important Ca^{2+} storage pool (Appelqvist *et al.* 2013). Accordingly, a large increase in cytosolic Ca^{2+} is observed upon treatment with glycyl-L-phenylalanine-naphthylamide (GPN), an agent that induces osmotic lysis of lysosomes and content release of the organelle (Haller *et al.* 1996). Although challenging to measure, lysosome Ca^{2+} concentration was estimated to be up to 600 μM, an appreciable amount and close to that found in the ER (Appelqvist *et al.* 2013). Although still highly debated, the mechanisms of lysosomal Ca^{2+} entry and release are being progressively unravelled and the importance of lysosomal Ca^{2+} in signalling is now beginning to be fully appreciated.

Unlike the ER, lysosomes harbour an acidic lumen provided by the V-ATPase. This feature is of a particular importance as the net H^+ concentration gradient across the lysosomal membrane constitutes an important energy source that can be used for the secondary active transport of Ca^{2+} (Patel and Docampo 2010; Raffaello *et al.* 2016). In accordance with this, dissipation of the H^+ gradient with membrane-permeant bases or pharmacological agents prevents lysosomal Ca^{2+} sequestration (Churchill *et al.* 2002). The primary active transport of H^+ driving acidification in the lysosomal lumen is mediated by the ubiquitously expressed V-ATPase, an electrogenic pump that by definition promotes positive membrane potential and a proton gradient (Cipriano *et al.* 2008). It is composed of 14 subunits arranged into a cytosolic ATP-hydrolysing (V_1) and membrane-embedded H^+-translocation (V_0) domains. ATP hydrolysis drives a rotary mechanism of the central stalk attached to V_0 that permits H^+

entry (Beyenbach and Wieczorek 2006; Stransky *et al.* 2016). As lysosome homeostasis greatly depends on the luminal pH and lysosomal membrane potential, the organelle has developed mechanisms to maintain a low pH. The membrane-positive potential generated by the V-ATPase activity prevents further H^+ uptake, thus charge neutralisation must take place. This is provided by anion influx via the antiporter Cl^- channel (ClC) coupled to H^+ (Jentsch 2007) and cation efflux through Na^+ and K^+ extrusion (Xu and Ren 2015). In addition, H^+ leak is reduced in lysosomes compared to the other compartments of the endolysosomal system, limiting potential impact on the H^+ concentration gradient (Morgan *et al.* 2011).

Little is known regarding the channel responsible for Ca^{2+} uptake into lysosomes. The calcium hydrogen exchanger (CAX) is a potential candidate of secondary active Ca^{2+} transport into the lysosome and this protein is conserved in primitive organisms such as yeasts (Cunningham and Fink 1996). Putative CAX genes were identified in vertebrates including reptiles and birds and most remarkably in non-placental mammals, suggesting for the first time the existence of mammalian CAXs responsible for lysosomal Ca^{2+} filling (Melchionda *et al.* 2016). Active transport of Ca^{2+} is another mechanism by which the lysosomal stores could be refilled. Although the identity of the pump remains unknown, some lines of evidence suggest the existence of a Ca^{2+}-ATPase, as shown by the monitoring of a Ca^{2+}-ATPase activity in rat liver cells (Ezaki *et al.* 1992).

Although it remains a debated field, major progress has been made in the study of lysosomal Ca^{2+} release. Two potential Ca^{2+} permeable channels have been identified on the lysosomal membrane, namely the two-pore channel (TPC) and the transient receptor potential-mucolipin (TRPML) families of proteins (Patel and Docampo 2010). The TPCs, which share sequence similarities with voltage-sensitive Na^+ and Ca^{2+} channels, belong to the 6 transmembrane ion channel superfamily (Horton *et al.* 2015). In plants, TPCs were shown to contain a potential voltage sensor and a Ca^{2+} binding domain, however the features of their animal counterparts remain largely unknown (Patel and Docampo 2010). All three members of the TPC family (TPC1-3) are present in the endolysosomal system in plants, with TPC3 being absent in

humans and TPC2 localising specifically on the LE/lysosome in humans (Galione 2011; Horton *et al.* 2015). Remarkably, TPC2 was shown to stimulate Ca^{2+}-induced Ca^{2+} release (CICR) channels at lysosome-ER contact microdomains (Galione 2011). Furthermore, inhibition of TPC2 in fibroblasts was found to lower the exaggerated Ca^{2+} signals triggered by the potent Ca^{2+}-mobilising agent nicotinic acid adenine dinucleotide phosphate (NAADP), suggesting TPC2 stimulation is potentially NAADP-dependent (Hockey *et al.* 2015). Whether NAADP also activates the lysosomal TRPML channels remains unclear (Raffaello *et al.* 2016). TRPMLs constitute the mucolipin family of transient receptor potential (TRP) superfamily of cation channels, activated by $PI(3,5)P_2$ (Wang *et al.* 2011). Among the mammalian TRPML channels, TRPML1, TRPML2 and TRPML3 localise to the lysosomal membrane, with TRPML1 colocalising exclusively with LE and lysosome markers (Puertollano and Kiselyov 2009).

Overall the high Ca^{2+} concentration in the lysosomal lumen, coupled with the presence of Ca^{2+} channels on the lysosomal membrane demonstrate that lysosomes have the potential to act as a Ca^{2+} signalling platform in the cell, by creating local messenger-evoked Ca^{2+} signals, potentially amplified by CICR through lysosome-ER contact sites.

1.2.2.3. Lysosome exocytosis

In addition to their major function as digestive organelle, lysosomes have the ability to fuse with the PM, a process known as exocytosis (Samie and Xu 2014). This process is part of the “unconventional secretory pathway”, as opposed to the “conventional secretory pathway” mediated by the ER-Golgi-born secretory vesicles (Nickel and Rabouille 2009). Fusion of the organelle with the PM was first observed in specialised cells containing secretory lysosomes also known as lysosome-related organelles. Exocytosis is extensive in cells derived from the haematopoietic lineage, whose function directly relies on the fusion of secretory lysosomes with the PM. For example, in osteoclasts, the release of lysosomal hydrolases in the extracellular space via exocytosis accommodates lacunae resorption (Baron *et al.* 1985).

Exocytosis of secretory lysosomes also serves important immune functions. For example, natural killer cells and cytotoxic T lymphocytes utilise exocytosis to release cytolytic proteins that target infectious agents and tumour cells (Peters *et al.* 1989; Peters *et al.* 1991). Secretory lysosomes are not restricted to cells originating from the haematopoietic lineage. Melanocytes, another specialised cell type derived from neural crest cells, contain lysosome-related organelles called melanosomes which release the pigment proteins melanins (Orlow 1995). It was initially thought that lysosome exocytosis was an exclusive function of the specialised secretory lysosomes present in certain professional secretory cell types (Samie and Xu 2014), until the process was observed with conventional lysosomes (Reddy *et al.* 2001). Exocytosis is now considered a universal property of conventional lysosomes, present in all cell types (Samie and Xu 2014). It constitutes the principal output pathway of lysosomes and serves two fundamental functions: secretion and membrane remodelling (Samie and Xu 2014). For example, lysosome exocytosis is fundamental in bone resorption (Baron *et al.* 1985) and ATP-induced migration of microglia (Dou *et al.* 2012), which fall into the former category; lysosome exocytosis also participates in PM repair (Reddy *et al.* 2001), which falls in the latter category. For the process of exocytosis, lysosomes are preferred to other intracellular compartments for three reasons. First, as the terminal station of the degradative pathway, their fusion with the PM prevents the build-up of toxic particles and cellular debris. Second, as a result of material exchange with the endosomal system, they contain the molecular machinery required for fusion. Thirdly, they constitute a large membrane reservoir that can be used to remodel the PM if needed (Blott and Griffiths 2002).

Molecular mechanisms of lysosome exocytosis

Exocytosis is a tightly orchestrated process that involves the cooperation of PM, cytosolic and lysosomal factors (Andrews 2017) (**Diagram 1.17.**). The process is not dissimilar from exocytosis of synaptic vesicles as it involves tethering/docking factors and fusion (Samie and Xu 2014). Both processes are stimulated by an elevation in cytosolic Ca^{2+} above 1 μM (Rodríguez *et al.*

1997). However the molecular machinery employed by conventional lysosomes differs from that involved in exocytosis at neurological synapses (Samie and Xu 2014). The process of exocytosis examined in this thesis refers to the fusion of conventional lysosomes with the PM, in non-specialised cells.

Upon stimulation, lysosomes translocate to the vicinity of the PM and docking of lysosomes at the PM occurs via the formation of SNARE complexes. Three families of proteins interact to generate the SNARE complex required for the lysosome fusion machinery: VAMP7 on the surface of the lysosome and two proteins located on the PM, STX4 and SNAP23 (Samie and Xu 2014). The three proteins interact to form a stable complex that draws opposite membranes toward one another (Cooper and McNeil 2015). The formation of a robust SNARE complex overcomes the natural repulsion created by the presence of negatively charged phosphate headgroups on both the PM and lysosomal membrane. In addition, neutralisation of negative charges occurs by local release of Ca^{2+}, at the site of fusion (Cooper and McNeil 2015). The source of Ca^{2+} is thought to be the lysosome itself, which releases the cation via the TRPML1 channel (Samie and Xu 2014; Cooper and McNeil 2015). Activation of the TRPML1 channel is thought to be mediated by interaction with $PI(3,5)P_2$ located on the lysosomal membrane. Accordingly, *in vitro* binding assays have shown a direct binding between TRPML1 and $PI(3,5)P_2$, and whole-lysosome patch-clamp analysis have demonstrated that this interaction results in channel activation (Dong *et al.* 2010). Additionally, $PI(3,5)P_2$ facilitates exocytosis by inducing membrane curvature (Di Paolo and De Camilli 2006). The Ca^{2+} elevation triggered by TRPML1 stimulation is subsequently detected by synaptotagmin (Syt) VII, located on the lysosomal membrane, through its two Ca^{2+}-binding C2 domains, which constitute the cytosolic face of the protein (Samie and Xu 2014). Although a reduction in lysosomal exocytosis is observed in Syt VII knock-out mouse cells treated with ionomycin (Czibener *et al.* 2006), the process is not fully blocked, suggesting that additional Ca^{2+} sensors are present. The mechanisms by which Syt VII promotes Ca^{2+}-regulated fusion remains under debate. In synaptic exocytosis, Ca^{2+} binding to Syts triggers the binding of their C2 domains with the vesicle, the PM and SNARE complexes (Tang *et al.* 2006). Whether a similar

mechanism operates in normal lysosome exocytosis remains to be determined but seems likely given the universality of SNARE protein function in organelle fusion events.

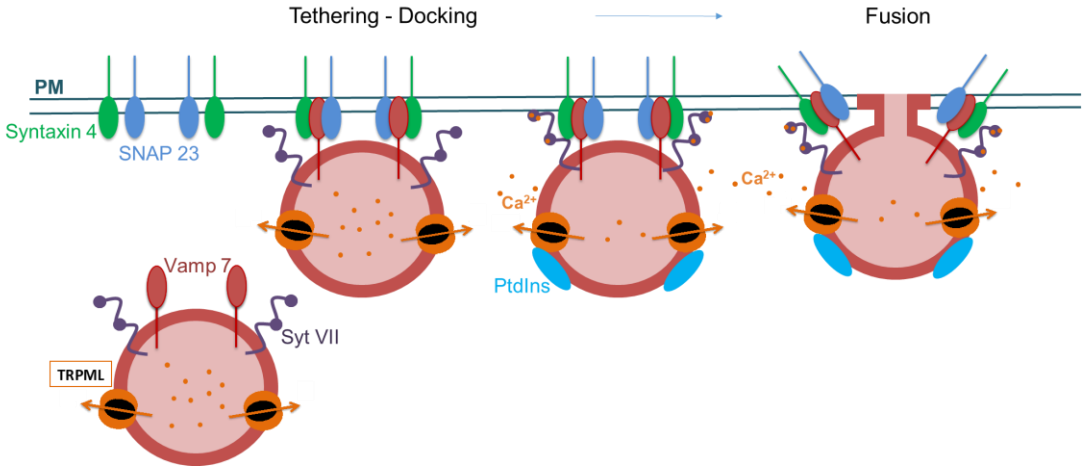

Diagram 1.17. Mechanisms of lysosome exocytosis. Upon stimulation, lysosomes are mobilised to the PM The protein Vamp7 on the lysosomal membrane forms a SNARE complex with Syntaxin 4 and SNAP23 located on the cytoplasmic face of the PM. A localised rise in intracellular Ca^{2+} is detected by the Ca^{2+} sensor Syt VII and induces membrane fusion. Phosphatidylinositols (PtIns, blue circles), $PI(3,5)P_2$, may trigger Ca^{2+} release from the TRPML channel and facilitate the fusion process. Adapted from (Samie and Xu 2014).

1.2.2.4. Lysosome motility, a functional requirement

With the discovery of additional lysosomal functions, the perception of lysosomes as static degradative compartments has been profoundly reshaped. Certain conditions such as starvation (Korolchuk *et al.* 2011) and cytosolic pH changes (Heuser 1989) directly induce a rearrangement of lysosomal distribution within cells, demonstrating that lysosomes are actually highly motile structures. They appear to patrol the cell and monitor the cytoplasmic nutrient status (Rosa-Ferreira and Munro 2011) and are able to translocate to the PM during exocytosis (Andrews 2017). Therefore their functional efficiency is dependent on their motility.

Lysosomes are widely distributed throughout the cell, with a population of lysosomes concentrating more particularly in the perinuclear region, towards the microtubule-organising centre (MTOC) in non-polarised cells (Pu *et al.* 2016). They undergo bidirectional movements along the microtubules between the MTOC and the cell periphery (Matteoni and Kreis 1987). Anterograde movements allow the translocation of lysosomes from the minus-end (MTOC) to the plus-end (cell periphery) of microtubules and depend on kinesin motor proteins (Hollenbeck and Swanson 1990). Retrograde movements pull lysosomes in the opposite direction and rely on dynein motors (Harada *et al.* 1998). Thus the microtubule-based transport of lysosomes powered by motor proteins mediates bidirectional movements that cover relatively long distances (from the cell centre to the cell periphery and *vice versa*). Lysosomes translocate to the actin-rich cell cortex during exocytosis, thus short-range actin-based movements responsible for lysosomal transport to the PM also take place (Raiborg and Stenmark 2016).

Mechanisms of long-range lysosomal movements

Anterograde movements of lysosomes along the microtubules are mediated by kinesin motor proteins, which comprise a globular domain attached to microtubules and a tail domain linked to specific adaptors (Pu *et al.* 2016). Lysosomes interact with a great variety of kinesins, including kinesin-1 (Nakata and Hirokawa 1995), kinesin-2 (Brown *et al.* 2005), kinesin-3 (Matsushita *et al.* 2004) and kinesin-13 (Santama *et al.* 1998) family members. The best characterised mode of lysosomal transport is that mediated by kinesin-1 (Pu *et al.* 2016). Recruitment of this motor protein results from the interaction of proteins which sequentially interact on the lysosomal membrane (**Diagram 1.18.**). First, the octameric BLOC-1-related complex (BORC) associates with the cytosolic face of the lysosomal membrane and recruits the Arf-like small GTPase Arl8 (Pu *et al.* 2015). In turn, Arl8 recruits its effector, the SifA and kinesin-interacting protein SKIP, which links the protein complex to kinesin-1 (Rosa-Ferreira and Munro 2011). ATP hydrolysis by the globular motor domain

of the kinesin subsequently drives the movement of lysosomes centrifugally, towards the minus-end of microtubules (Pu *et al.* 2016).

Alternatively, anterograde transport can be mediated by the ER-anchored adaptor protein protruding, which links lysosomal membrane to the ER. Subsequently, protruding allows Rab7 located on the lysosomal membrane to interact with its effector FYVE- and coiled-coil-domain-containing protein (FYCO1), which in turn binds to kinesin-1 and drives anterograde movement (Matsuzaki *et al.* 2011; Mrakovic *et al.* 2012).

Lysosomes move centripetally *i.e.* towards the minus-end of microtubules using dynactin-dependent association with dynein motor protein (Burkhardt *et al.* 1997; Pu *et al.* 2016) (**Diagram 1.18**). Dynein is formed by light, heavy and intermediate chains and dynactin constitutes a collection of 11 different proteins (Ishikawa 2012). Dynein-dynactin are recruited to the lysosome by the Rab7 effector, Rab7-interacting lysosomal protein (RILP) (Cantalupo *et al.* 2001; Pu *et al.* 2016). In addition to Rab7, other Rab proteins have been implicated in the positioning of lysosomes, including Rab9A (Ganley *et al.* 2004) and Rab34 (Wang and Hong 2002). Association of lysosomes with dynein-dynactin has also been demonstrated to be regulated by proteins other than Rabs. TRPML1 activity is required to induce Ca^{2+}-dependent retrograde movement of lysosomes, upon autophagy initiation (Li *et al.* 2016). Additionally, LAMP1 and LAMP2 have been found to promote association between lysosomes and dynein-dynactin (Huynh *et al.* 2007; Krzewski *et al.* 2013).

Mechanisms underlying short-range lysosomal movements

The molecular players involved in the short-range movements of lysosomes near the PM, were recently identified in the context of PM repair. The small GTPase Rab3a localised to peripheral lysosomes was the strongest hit in a systematic screening of the human Rab family performed to identify the small GTPases involved in lysosome exocytosis and PM repair (Encarnação *et al.* 2016). The model presented in this study stipulates that Rab3a located on the lysosome surface, interacts with the non-muscle myosin heavy chain IIA

(NMHC IIA), an actin-based motor protein, which links the Rab3a-lysosome complex to F-actin filaments, with the help of the Rab3a effector synaptotagmin-like protein 4a (Slp-4a) (Encarnação *et al.* 2016) (**Diagram 1.18.**). Silencing of Rab3a induces a juxtanuclear clustering of lysosomes, a decrease in lysosome exocytosis and blocks plasma membrane repair (Encarnação *et al.* 2016). Although identified in the context of PM injury and repair, this complex is now speculated to be involved more generally in the actin-based movement of Rab3a-lysosomes close to the PM (Raiborg and Stenmark 2016).

Lysosomal positioning and pH

Lysosomes are known to undergo minor morphological and functional changes within individual cells (Nilsson *et al.* 1997; Saftig and Klumperman 2009), however the functional significance of such changes is yet to be fully elucidated. Interestingly, recent work has highlighted that lysosomal positioning within cells influences the luminal pH of the organelle (Johnson *et al.* 2016). Using ratiometric fluorescence microscopy, the lysosomal pH was measured and correlated to the subcellular localisation of the organelle. Displacement of lysosomes towards the cell periphery or towards the MTOC by altering the components of the lysosomal motility machinery caused changes in the luminal pH, with peripheral lysosomes being more alkaline relative to lysosomes located in the perinuclear region (Johnson *et al.* 2016). In addition, the density of Rab7-positive lysosomes was found to be reduced in the cell periphery (Johnson *et al.* 2016). The Rab7 effector RILP is known to regulate the activity of the V-ATPase (De Luca *et al.* 2014), therefore the loss of Rab7 and RILP as the lysosomes move peripherally, coupled with proton leakage, could account for the increase in peripheral lysosome pH. The functional implication of lysosomal pH variations has not been established but pH changes are likely to account for the variety of lysosomal functions (Johnson *et al.* 2016).

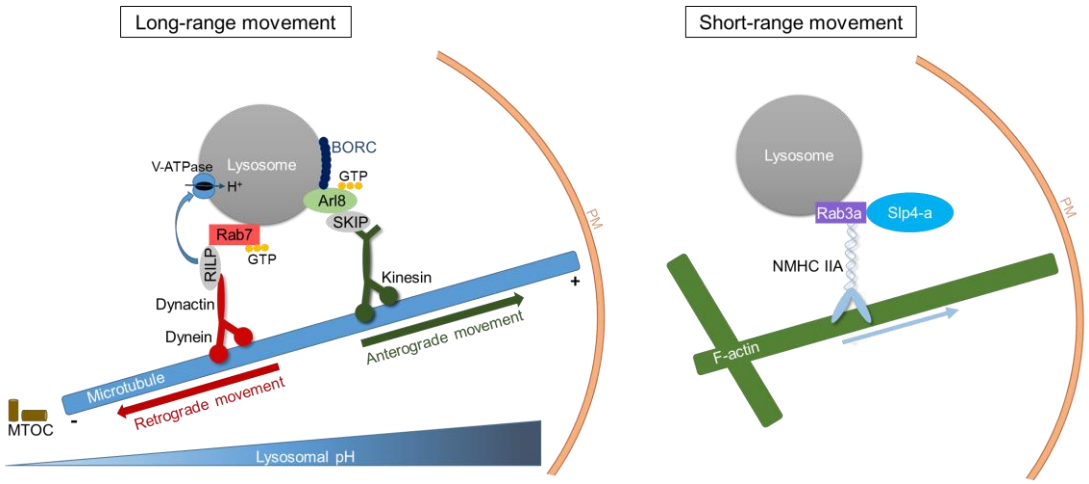

Diagram 1.18. Mechanisms and types of lysosome movement. The long-range transport of lysosomes towards the +end of microtubules is mediated by the small GTPase Arl8, recruited to lysosomes by BORC. In its GTP-bound form, Arl8 subsequently interacts with its effector SKIP, which in turn connects the complex lysosome-Arl8 with a kinesin motor. The small GTPase Rab7 regulates retrograde transport of lysosomes towards the microtubule organising centre (MTOC). In its active form (GTP-bound), the GTPase located on the lysosomal membrane, links the organelle to dynactin/dynein motor proteins via interaction with its effector RILP. An increase in lysosomal pH (represented by the graduated blue triangle) is observed from the centre to the periphery of the cell. The molecule RILP is thought to stabilise and activate the V-ATPase. As lysosomes move centrifugally, Rab7 dissociates from the lysosome and the RILP effect on the V-ATPase is abolished. This phenomenon, associated with proton leakage, induces an alkalinisation of lysosomes. Lysosome short-range transport directly underneath the plasma membrane is regulated by Rab3a which connects the organelle to F-actin via the NMHC IIA motor. The participation of Slp-4a is also required for movement to take place. Adapted from (Rosa-Ferreira and Munro 2011), (Pu *et al.* 2015) and (Encarnação *et al.* 2016).

1.2.3. The pathological lysosome

Dysfunction in lysosome activity underlies a number of severe pathologies including lipid storage disorders (LSDs), neurodegenerative diseases and cancer (Appelqvist *et al.* 2013).

LSDs are a type of inherited disease affecting on average 1 in 8000 live births worldwide (Poupětová *et al.* 2010). They are caused by a loss or reduction in

lysosomal protein activity, resulting in the accumulation of undigested substrates, which promote secondary lysosomal changes such as altered autophagy and impaired Ca^{2+} homeostasis (Appelqvist *et al.* 2013). Reduction of lysosomal Ca^{2+} has been observed in Niemann-Pick disease type C1 (Lloyd-Evans *et al.* 2008) a neurodegenerative LSD associated with gait ataxia, dysphagia, dysarthria and hepatosplenomegaly (Angelini 2014). Lysosomal Ca^{2+} release is also affected in mucolipidosis type IV in which mutation in the gene encoding the TRPML1 channel causes excessive release of the ion (Morgan *et al.* 2011). Patients affected by this diseases present psychomotor retardation and severe ophthalmological defects (Bach 2001). The clinical manifestations of LSDs are often neurological and the severity of the diseases relies on the type of cells and the altered proteins it affects as well as on the biochemical properties of the non-degraded molecules (Settembre *et al.* 2008).

Although not the primary cause, secondary changes associated with lysosomal dysfunction are also observed in more prevalent neurodegenerative disorders such as Parkinson's, Alzheimer's and Huntington's diseases. (Bellettato and Scarpa 2010). The autophagic process is particularly critical in neuronal cells as it promotes their survival in conditions where regeneration is limited (Hara *et al.* 2006). Therefore the development of treatments restoring lysosomal function is an important potential therapeutic target for tackling neurodegenerative disorders.

Lysosomal functions are also gaining increasing attention in the study of cancer. Transformation and cancer progression are favoured by effective lysosomal function. Oncogenic factors such as stimulation of angiogenesis, tumour growth and invasiveness are promoted by secretion of upregulated cathepsins into the extracellular space (Gocheva *et al.* 2006). Additionally, cancer progression is facilitated by the remodelling of the ECM through the release of the lysosome resident enzyme N-Acetyl-β-D-Glucosaminidase (Ramessur *et al.* 2010).

Interestingly, lysosomes also have anti-cancer properties as disruption of the organelle sensitises cells to cell death (Fehrenbacher *et al.* 2004). Cancer

resistance to treatment and cancer cell survival are linked to mutations in p53, a cell death-inducing agent. Since lysosomes have the ability to induce cell death through a p53-independent pathway, they represent promising targets for future cancer therapies (Erdal *et al.* 2005).

1.3. Summary

Cell division, the process by which a cell gives rise to two genetically identical daughter cells is a highly regulated process that governs fundamental biological events including proliferation, cell growth and the development, repair and ageing of all living organisms. Cell division is split into the temporally sequential processes of mitosis, where the duplicated chromosomes segregate equally between nascent cells and cytokinesis, which leads to the physical separation of cells. Vesicular transport and fusion near the transient intercellular bridge between the daughter cells, coupled to the cell cycle-dependent remodelling of phosphoinositides play an important role in the normal progression and completion of cytokinesis. Golgi-derived vesicles and endosomal compartments have been functionally implicated in cytokinesis. Lysosomes, versatile organelles known for their role in degradation, recycling and exocytosis, were observed to cluster at the intercellular bridge during cytokinesis. In addition, these organelles were found to be decorated with PI4KIIIβ responsible for the preservation of lysosomal identity and for the generation of PI4P, a phosphoinositide required for cytokinesis. Interestingly, disruption of lysosomal clustering near the intercellular bridge via a PI4KIIIβ-mediated pathway, leads to severe cytokinesis defects, suggesting that lysosomes are functionally involved in this process. This thesis is aimed at identifying the functional importance and exact role of lysosomes during cell division. More specifically, the studies reported here have addressed:

1. Lysosomal distribution and key properties during cytokinesis
2. The identification of the lysosomal function(s) involved in cell division
3. A detailed examination of lysosome exocytosis during mitosis/cytokinesis and a study of the role of PI4KIIIβ in both lysosome exocytosis and cytokinesis

Collectively, these investigations indicate that lysosome exocytosis is essential and significantly increased during cytokinesis. In addition PI4KIIIβ constitutes a positive factor in both cytokinesis and exocytosis regulation, suggesting the enzyme might provide a functional link between the two processes. This work provides novel insights into the regulation of cytokinesis by lysosomes and documents yet another fundamental role of these fascinating multifaceted organelles.

Chapter 2: Material and Methods

2.1. Suppliers and buffer recipes

2.1.1. Suppliers

All the reagents used in this thesis were of analytical grade. Suppliers along with their address are listed in the table below.

Table 2.1. List of suppliers

Supplier	Address
Abcam	Cambridge, UK
Addgene	Teddington, UK
ATCC	Virginia, USA
BD Biosciences	Oxford, UK
Bioline	London, UK
BioRad	California, USA
BMG LABTECH	Aylesbury, UK
Cayman chemicals	Utah, USA
Expedeon	Cambridge, UK
Formedium	Hunstanton, UK
Jasco	Dunmow, UK
MatTek Corporation	Massachussetts, USA
Millipore	Livingstone, UK
New England Biolabs (NEB)	Hertfordshire, UK
Promega	Southampton, UK
PromoCell	Staffordshire, UK
Roche	Hertfordshire, UK
Santa Cruz	Texas, USA
Sigma	Poole, UK
Takara	Saint-Germain-en-Laye, France
Thermo Fisher Scientific	Massachussetts, USA
Zeiss	Jena, Germany

2.1.2. Buffers recipes

The composition of the solutions used for experimental procedures are detailed below. Unless stated otherwise, all reagents used for recipes were provided by Sigma.

Table 2.2. Buffers description

Buffer	Recipe
Dissociation Buffer	10% (w/v) sucrose 10% (v/v) glycerol 4% (w/v) SDS 1% (v/v) β-mercaptoethanol 125 mM HEPES (pH 6.8) 2 mM EDTA 0.05 mg/ml bromophenol blue
IF Blocking Solution	PBS supplemented with 5% (w/v) Bovine Serum Albumin lyophilised powder (BSA)
LB Agar (Luria Broth Agar)	8.56 mM NaCl 1.5% (w/v) bacto-agar (BD Biosciences) 1% (w/v) tryptone (Formedium) 0.5% (w/v) yeast extract (Formedium)
LB Medium (Luria Broth Medium)	8.56 mM NaCl 1% (w/v) tryptone 0.5% (w/v) yeast extract
PBS (Phosphate Buffer Saline)	137 mM NaCl 2.7 mM KCl, 10 mM Na_2PO_4 2 mM NaH_2PO_4 pH 7.4
PBSL (PBS based solution for Lysis)	PBS supplemented with 0.1% (w/v) SDS, 1% (v/v) NP-40 and 1% (v/v) Proteoloc protease inhibitor cocktail (Expedeon)
PBST	PBS supplemented with 0.05% (v/v) Tween-20

(PBS Tween)	
SOC Media (Super Optimal broth with Catabolic repression Media)	2% (w/v) tryptone, 0.5% (w/v) yeast extract 8.56 mM NaCl, 2.5 mM KCl, 10 mM $MgCl_2$ 20 mM glucose
Surface Staining Solution	PBS supplemented with 1% (w/v) BSA
TAE Buffer (Tris base, Acetic acid and EDTA)	40 mM Tris base pH 8.0 20 mM acetic acid 1 mM EDTA
WB Blocking Solution (Western Blot Blocking Solution)	PBS supplemented with 3% (w/v) skimmed milk powder

2.2. Cell culture, synchronisation and transfection

Details about the cell lines used are listed in the following Table.

Table 2.3. Cell lines specifications

Name	Species	Tissue of origin	Cell type	Disease
BSC-1	*Cercopithecus aethiops,* Green Monkey	Kidney	Epithelial	Normal
HEK293T	*Homo Sapiens,* Human (fetus)	Kidney	Epithelial	Normal

HeLa	*Homo Sapiens,* Human	Cervix	Epithelial	Adenocarcinoma
NRK-49F	*Rattus norvegicus,* Rat	Kidney	Fibroblast	Normal
THP-1-derived macrophages	*Homo Sapiens,* Human (1 year infant)	Bone marrow	Monocytes differentiated into macrophages	Acute Monocytic Leukemia

2.2.1 Cell maintenance

Human THP-1 monocytes were kindly provided by Dr Bradley Meehan (University of Liverpool). The cells were cultured in THP Growth Media (TGM: RPMI 1640 containing 10% (v/v) FBS, 50 µM β-mercaptoethanol and 1% (v/v) penicillin/streptomycin (P/S). The monocytes were treated with 200 nM phorbol 12-myristate 13-acetate (PMA) for 3 days to induce cell differentiation into macrophages. The PMA-containing media was subsequently removed and THP-1-derived macrophages were incubated in fresh TGM for a further 1 to 3 days. HeLa, HEK293T and NRK-49F cells were maintained in DMEM supplemented with 10% (v/v) FBS, non-essential amino acids (1% v/v) and P/S (1% (v/v)). BSC-1 cells were maintained in EMEM supplemented with 10% (v/v) FBS, non-essential amino acids (1% v/v) and P/S (1% (v/v)). All cells were cultured at 37°C, 95% v/v air/5% v/v CO_2. Unless stated otherwise, all cells were obtained from ATCC.

2.2.2. Transfection

All transfections were performed using Promofectin reagent (PromoCell) according to manufacturer's instructions. Briefly, cells were cultured on 35 mm

Ø MatTek glass bottom dishes or 13 mm Ø coverslips until they reached 50% confluence. The plasmid DNA (3 µg in MatTek, 1 µg for coverslip) was mixed with 6 µl (MatTek) or 2 µl (coverslip) of Promofectin in serum-free RPMI. The DNA/Promofectin solution was incubated for 20 minutes at room temperature and added dropwise to the cells. Incubation with the transfection reagents was allowed for 24 to 48 hours at 37°C, 95% v/v air/5% v/v CO_2.

2.2.3. Cell synchronisation

Cells were grown onto 24-well or 6-well culture dishes until they attained 40% confluence. They were first arrested at interphase with growth media supplemented with 2 mM thymidine for a minimum of 20 hours, released from their block with growth media supplemented with 25 µM deoxycytidine for 3 to 6 hours and blocked again by incubation in growth media containing 2 mM thymidine (G1 block) or 35 ng/ml nocodazole (pro-metaphase block) for 12 to 24 hours. Subsequently cells were either maintained in their block or released with 25 µM deoxycytidine. Cells were released by washing 5x in fresh culture medium.

2.3. Molecular biology

2.3.1. Polymerase chain reaction (PCR)

In order to generate new expression plasmids, specific DNA coding sequences from existing plasmid constructs were amplified by PCR. Reactions were performed using oligonucleotide primers (Forward (Fwd) and Reverse (Rev)) that contained specific restriction endonuclease sites to permit subcloning into specific vector backbones. Briefly 10 µl of 5x Phusion® HF(NEB) was mixed to 200 µM dNTPs (NEB), 0.5 µM Fwd primer, 0.5 µM Rev primer, <250 ng DNA template and 1.0 U Phusion® DNA polymerase (NEB). Distilled water

was then added to bring the reaction to a final volume of 50 µl. The parameters used in PCR cycling reaction are detailed in **Table 2.4**.

Table 2.4. PCR parameters

	Process	**Temperature**	**Duration**	**Number of cycles**
Step 1	Initial Denaturation	98°C	1 min	1
Step 2	Denaturation Annealing Extension	98°C Primers T_m* 72°C	10 s 10 s 15 s/kb	30-35
Step 3	Final Extension	72°C	10 min	1
	Hold	4°C	∞	

*The annealing temperature was established according to the primers melting temperature (T_m or temperature at which 50% of the primer is duplexed with its complementary sequence and 50% is free in solution). Typically, an annealing temperature between 5-10^{o}C below the T_m of the primer with the lowest T_m was used although this was determined empirically for each individual PCR product generated.

2.3.2. Purification of PCR products

Purification of PCR products was performed using the Wizard ® SV Gel and PCR clean-up system (Promega) according to manufacturer's instructions. Briefly, each PCR reaction was added to an equal volume of membrane binding solution and incubated on a silica based spin minicolumn for 1 min at room temperature to allow binding of DNA to the column. The column was washed 2x with column wash solution (16000 x *g* for 5 min) and purified DNA eluted into 50 µl nuclease-free water by centrifugation (16000 x *g* for 1 min). Samples were stored at -20°C.

2.3.3. Restriction digests

Typically, 0.4 µg of insert or 0.4 µg of plasmid were added to 2 µl of 10x CutSmart® Buffer (NEB) and 1 µl of each specific restriction endonuclease (NEB). The final reaction volume was adjusted to 20 µl with double distilled water and restriction digest was allowed to proceed for 1 hour at 37°C.

2.3.4. Agarose gel electrophoresis and gel excision and purification of nucleic acid

2.3.4.1. Agarose gel preparation and electrophoresis

Low melting temperature high purity agarose powder (Bioline) was dissolved in 1x TAE buffer at a 1% (w/v) concentration by brief boiling in a microwave oven. The solution was allowed to cool at room temperature until it reached approximately 50°C. The nucleic acid staining reagent SYBR® Safe was added to the solution at a $1:10^4$ dilution. The mixture was gently swirled to permit complete mixing of the dye, transferred to prepared gel cast and allowed to solidify at room temperature. 5x loading dye (Bioline) was added to each DNA sample to a final 1x concentration and loaded onto the gel. 5 µl of Hyperladder™ I DNA molecular weight marker (Bioline) was also loaded onto the gel. Samples were resolved for 45 min at 80V.

2.3.4.2. Gel excision and purification of nucleic acids

DNA bands were visualised under LED UV illumination (Clare Chemical Research, Dark Reader®, Transilluminator) and the fragments excised with a clean scalpel into pre-weighed Eppendorf tubes. Nucleic acids were purified using the Wizard® SV Gel and PCR clean-up system (Promega) according to manufacturer's protocol. Briefly, following gel excision, 10 µl of membrane binding solution per 10 mg gel slice was added to each tube, vortexed and incubated at 65°C until the gel slice had completely dissolved. The solution was added to a silica based spin mini-column, DNA allowed to bind, then

washed and finally eluted in 50 µl nuclease-free water into a sterile Eppendorf tube.

2.3.5. Ligation of DNA fragments

Routinely, 2 µl of 10x T4 DNA Ligase Buffer concentrate (NEB) was added to 50 ng of vector DNA. The insert DNA was added at varying vector:insert molar ratios (1:3, 1:5 or 1:6) to 400U T4 DNA ligase (added last). The final reaction volume (20 µl) was achieved by addition of doubly distilled water and the ligation mix was incubated at room temperature for 30 min to 1 hour.

2.3.6. Transformation of chemically competent *E. coli*

The ligation mix (3 µl) or purified plasmid (0.5 µl) were added to 50 µl of competent *E. coli* bacteria (DH5α) for propagation and amplification of recombinant plasmid DNA. Samples was gently swirled to mix and incubated on ice for 30 min. Samples were heat-shocked for 45 seconds at 42 °C in a water bath, before incubation on ice for a further 2 minutes. Cells were then recovered with 950 µl SOC Media (**Table 2.2.**) for 1 hour at 37°C, 200 rpm with constant agitation. The resulting bacterial culture was plated onto a sterile 10 cm LB Agar plate (**Table 2.2.**) supplemented with appropriate antibiotic. Plates were inverted and incubated overnight at 37°C. Subsequently single colonies were picked using a pipette tip and incubated overnight in 5ml LB Medium supplemented with appropriate antibiotic for larger scale culture. The next day, cells were harvested by centrifugation (at 4200 x *g*, 4°C for 10 minutes) and the plasmid DNA was purified using a spin column mini prep kit (Promega) according to the manufacturer's instructions. Briefly bacteria were lysed in an alkaline solution supplemented with SDS and rapidly neutralised by addition of acetate to precipitate SDS. The solution was centrifuged for 5 min at 12000 x *g*. The DNA-containing supernatant was transferred to a silica gel based spin column to trap DNA. The DNA was washed and eventually recovered from the column into 50 µl elution buffer. The extracted DNA was

verified by test restriction digest and agarose gel electrophoresis and subsequent DNA sequencing of positive clones.

Following confirmation of the correct DNA sequence, the purified plasmid was re-transformed into DH5α *E. coli* for larger scale plasmid amplification. Single colonies were picked and inoculated into 100ml LB Medium supplemented with appropriate antibiotic for overnight growth at 37°C, 200 rpm. The next day, cells were harvested by centrifugation at 4000 × *g* for 10 minutes and plasmids purified using a PureLink HiPure Plasmid Midi/Maxi Kit (Thermo Fisher Scientific) according to the manufacturer's protocol. Briefly, harvested cells were lysed in a solution containing 0.2 M NaOH and 1% (w/v) sodium dodecyl sulfate for 5 min at room temperature and precipitated in 3.1 M Potassium acetate (pH 5.5). The precipitated lysate was transferred onto an anion exchange resin-based column and the DNA was recovered from the resin in a high salt solution (100 mM Tris-HCl, pH 8.5, 1.25 M NaCl). The eluted DNA was precipitated in isopropanol, centrifuged (at 12,000 × *g* for 5 minutes at 4°C), air-dried and re-suspended in 200 µl TE buffer. The concentration of extracted plasmid DNA was measured on a NanoDrop Lite Spectrophotometer (Thermo Fisher Scientific).

2.3.7. Plasmids

The plasmids used in this thesis, their source and antibiotic resistance are detailed in the table below.

Table 2.5. Plasmids description

Plasmid	Source	Resistance
LAMP1-EYFP	Dr Lee Haynes	Kanamycin
pCMV-Lyso-pHoenix	Christian Rosenmund (Addgene plasmid # 70112 ; http://n2t.net/addgene:70112 ; RRID:Addgene_70112)	Kanamycin

LysopHluorin-mCherry	Obtained by sub-cloning: Fwd: 5'CTGCTAGCATGGCGGTGGAAGGAGGAATG3' Rev: 5'CTGGATCCTTTTTGTATAGTTCATCCATGCCAT3' Template: pCMV-Lyso-pHoenix Restriction sites: NheI and BamHI	Kanamycin
HA-PI4KIIIβ	(Godi *et al*., 1999)	Ampicillin

For plasmid selection, ampicillin and kanamycin were used at a concentration of 100 µg/ml and 30 µg/ml, respectively.

2.3.8. In fusion cloning and generation of pHIV-LpH-mCh lentivirus and LpH-mCh stable cell lines

2.3.8.1. In-Fusion® cloning

pHIV-dTomato was kindly provided by Dr Mark Morgan (Institute of Translational Medicine, University of Liverpool). The vector was digested with XmaI and ClaI (NEB) to excise the dTomato fragment. The lpH-mCh coding sequence was amplified by PCR using primers designed for In-Fusion® HD Cloning (Takara), so that the resulting fragment shares 15-bp homology with the pHIV vector (forward primer: 5'-TTCTAGAGTACCCGGATGGCGGTGGAAGGAGGAATG-3'; reverse primer: 5'-AGGTCGACGGTATCGCTTGTACAGCTCGTCCATGCC-3'). The restriction digest and PCR product were resolved by horizontal agarose gel electrophoresis and stained with SYBR ® Safe DNA stain (Thermo Fisher Scientific). Gel purification of the linearised vector and PCR product was performed using the Wizard® SV Gel and PCR Clean-Up System (Promega) according to manufacturer's instructions and as described in section **2.3.2**. Digested pHIV-dTomato and LpH-mCh PCR product were combined using In-Fusion® HD enzyme (100ng linearised pHIV, 1µl PCR product, 2µl enzyme; reaction allowed for 15 min at 50°C). The resulting recombinant LpH-mCh

plasmid was subsequently transformed into competent *E. coli* bacteria (NEB) and amplified using standard techniques (section **2.3.6.**)

2.3.8.2. Generation of pHIV-LpH-mCh lentivirus and LpH-mCh stable cell lines

HEK293T cells were grown onto 10 cm diameter cell culture dishes to 80% confluence. Next the cells were transfected with lentiviral components and pHIV-lpH-mCh using Lipofectamine® 2000 (Thermo Fisher Scientific) according to manufacturer's instruction. Briefly, 20 µg pHIV-lpH-mCh, 10 µg pMDL g/RRE, 5 µg pRSV-Rev and 6 µg pVSVg env. were added to 100 µl Lipofectamine® 2000.Opti-MEM™ (Thermo Fisher Scientific) was added to the solution to a final volume of 2ml. The solution was incubated for 20 min at room temperature and added dropwise onto HEK293T cell medium. The virus-containing medium was collected 48 hours post-transfection and centrifuged for 15 min at 1,105 x *g*. The supernatant was filtered through a 0.45 µm filter membrane and mixed with fresh medium at a 1:1 dilution.

NRK cells were grown onto a 6-well cell culture plate. The incubation medium was replaced with virus-containing medium. Cells were infected for 48 hours at 37°C, 95% v/v air/5% v/v CO_2. Expression of the virus was verified by imaging and Western Blotting.

2.3.9. DNA sequencing

All newly generated constructs were verified by automated dideoxy sequencing in both 5' and 3' directions by Source Bioscience (UK).

2.4. Biotinylation of surface proteins

Synchronous (thymidine-nocodazole treated) and asynchronous (untreated) HeLa cells were grown on 10 cm circular cell culture dishes until they reached full confluence. Synchronised cells were washed 5x in 10 ml fresh DMEM to

release them from the last nocodazole block and incubated for 1 hour at 37°C in a tissue culture incubator. The media was removed from both cell populations and cells were washed with 10 ml of ice-cold PBS. The cells were gently detached from the dishes using a cell scraper and transferred to a 15 ml sterile falcon tube and centrifuged for 5 min at 2800 x *g*. The cell pellet was slowly resuspended in 1 ml ice-cold PBS supplemented with 0.5 mg/ml EZ-link Sulfo-NHS-SS-biotin (Thermo Fisher Scientific) and incubated on a rotator at 4°C for 30 min. Cells were pelleted by centrifugation and gently washed 1x in ice-cold PBS. Residual unreacted Sulfo-NHS-SS-biotin was quenched by incubation of cells with 1 ml PBS supplemented with 50 mM NH_4Cl for 30 min on ice. Cells were pelleted again and wahed 3x with ice-cold PBS. Following washes, cells were lysed in 1 ml ice-cold PBSL (**Table 2.2.**) for 1 hour on a rotator at 4°C. Cellular debris were discarded by centrifugation for 5 min at 4°C, 13000 rpm. The protein-containing supernatants were applied to 100 µl of Pierce Streptavidin Ultralink agarose resin (Thermo Fisher Scientific) that had been equilibrated by washing 3x in PBSL. Binding of biotinylated proteins to the resin was allowed for 1 hour at 4°C on a rotator. The Streptavidin resin was collected by centrifugation (refrigerated microfuge, 13000 rpm, 4°C for 1 min) and the unbound material in the supernatant collected into a clean Eppendorf tube (non-surface protein fraction). The resin was washed in 1 ml ice-cold PBS and the surface protein fraction liberated from the resin by boiling in 100 µl Dissociation Buffer (**Table 2.2.**).

2.5. SDS PAGE and Western blotting

Cells grown onto 6-well culture dishes were lysed in 100 µl of Dissociation buffer, scraped off the cell culture dishes using a cell scraper, passed through a syringe needle approximately 10x to reduce viscosity and boiled for 10 min at 95°C. Samples resulting from the biotinylation experiment were lysed as described in section **2.4**.

All samples were resolved on 4-12% (w/v) Novex NuPage™ Bis-Tris (Thermo Fisher Scientific) SDS-PAGE gels for 45 minutes at 200 V. Subsequently, proteins were transferred onto a nitrocellulose membrane (1 hour at 100 V)

using transverse electrophoresis. The nitrocellulose membrane was stained with Ponceau-S solution (Sigma) to verify successful protein transfer and to permit trimming of excess membrane material. Ponceau-S was removed by 2x 10 min washes with PBS and filters were then blocked with WB blocking solution (**Table 2.2.**) for 1 hour at room temperature. Next, membranes were incubated with primary antibody (**Table 2.6**) prepared at the appropriate dilution in WB blocking buffer for 1 hour at room temperature or overnight at 4°C with constant agitation. The membrane was then thoroughly washed in PBST and PBS and further incubated with HRP-conjugated secondary antibodies diluted in WB blocking solution for 1 hour at room temperature (**Table 2.6.**). The membrane was then washed 3x 5 minutes with PBST and further washed in PBS, before addition of equal volumes of ECL reagents (BioRad). The blot was subsequently developed and imaged using a ChemiDoc XRS gel-documentation system (BioRad).

Table 2.6. WB antibody description

Antibody	Species Origin	Source	Dilution
Anti-β-Actin	Mouse monoclonal	Sigma	1:500
Anti-EGFR	Rabbit monoclonal	Cell Signalling Technologies	1:1000
Anti-GFP	Mouse monoclonal	Roche	1:500
Anti-LAMP1	Mouse monoclonal	Santa Cruz	1:500
Anti-RFP	Rabbit polyclonal	Dr Ian Prior	1:500
Anti-RFP	Rabbit polyclonal	Roche	1:500
Anti-β-Tubulin	Rabbit polyclonal	Abcam	1:1000
Anti-Mouse IgG HRP	Goat polyclonal	Sigma	1:500
Anti-Rabbit IgG HRP	Goat polyclonal	Sigma	1:500

2.6. Pharmacological inhibition of lysosomal functions

Cell treatment was performed by incubating cells with selected drugs in a humidified cell incubator at 37°C, 95% v/v air/5% v/v CO_2. The pharmacological treatments used to impair lysosomal activity are listed in **Table 2.7**.

Table 2.7. Pharmacological drugs

Compound	Source	Optimal concentration	Treatment duration
Concanamycin	Abcam	100 mM	Overnight
E64	Santa Cruz	100 µM	Overnight
GPN	Cayman chemicals	50 µM	Overnight
NEM	Sigma	1mM	15 min
Pepstatin A1	Sigma	5 µM	Overnight
PIK93	Sigma	19 nM	40 min
Vacuolin-1	Millipore	1 µM	Overnight

2.7. Biochemical assays

2.7.1. Lucifer yellow (LY) assay

Cells were incubated in culture medium supplemented with 1 mg/ml Lucifer Yellow CH dipotassium salt (Santa Cruz) for 4 hours or overnight, at 37°C, 95% v/v air/5% v/v CO_2, washed 3x in PBS and chased in fresh culture medium for a minimum of 2 hours at 37°C, 5% CO_2. Cells were subsequently lysed and the incubation buffer was collected as described in section **2.7.2**. LY fluorescence was measured in the incubation buffer/cell lysate samples with

428 nm excitation /536 nm emission wavelengths using a Jasco FP-6300 spectrofluorimeter.

2.7.2. Cell lysis and media collection for biochemical assays

The incubation media were collected and kept on ice. All reagents and cells were maintained at 4°C throughout the lysis process. Cells were washed twice in PBS and incubated on ice on a rocking platform with RIPA buffer (Thermo Scientifc ^{TM}) for 5 min. Cells were removed from the culture dish with a sterile scraper and an equal volume of ice cold PBS added to the lysates. Insoluble cellular material was removed by centrifugation for 15 min at 13,000 x *g* and the clarified lysates transferred into fresh pre-chilled Eppendorf tubes.

2.7.3. N-Acetyl-β-D-Glucosaminidase (NAG) assay

Cell media were collected and cells were lysed as described in section **2.7.2**. Collected incubation buffers/cell lysates were incubated for 15 minutes to 1 hour at 37°C, 95% v/v air/5% v/v CO_2 with 3 mM 4-nitrophenyl N-acetyl-β-D-glucosaminide, a NAG substrate, dissolved in 0.09 M citrate buffer solution (pH 4.5). The pH of the solution was verified using Fisherbrand pH indicator paper sticks prior to the NAG reaction. The reaction was stopped by adding 0.4 M sodium carbonate (pH 11.5). The product of the NAG substrate hydrolysis, *p*-nitrophenol, ionised upon addition of stop solution, was measured colorimetrically at 405 nm using a FLUOstar Omega Microplate Reader (BMG LABTECH) in the collected incubation buffers and in the cell lysates. NAG secretion was expressed as % of total NAG (secreted+intracellular).

2.8. Immunostaining

2.8.1. Immunofluorescence (IF)

Cells were grown onto 13 mm Ø glass coverslips, washed 3x in PBS and fixed in 4% (w/v) formaldehyde (Sigma) in PBS for 6 min at room temperature. Cells were washed again in PBS and permeabilised with 0.5% (v/v) Triton-X-100 (Thermo Fisher Scientific) in PBS for 6 min at room temperature. Following permeabilisation, cells were washed again and blocked for 1 hour at room temperature in IF blocking solution (**Table 2.2.**). Next, cells were incubated in primary antibody diluted in IF blocking solution for 1 hour at room temperature (see **Table 2.8.** for antibody type, species and dilution). Subsequently cells were washed in PBS and further incubated in secondary antibody diluted in IF blocking solution (**Table 2.2.**) for 1 hour at room temperature (**Table 2.8.**). Cells were washed again in PBS, coverslips allowed to air-dry and then mounted onto glass slides using ProLong™ Gold Antifade reagent containing DAPI (Thermo Fisher Scientific).

Table 2.8. IF antibodies

Antibody	Species Origin	Source	Dilution
Anti-M6PR	Rabbit polyclonal	Abcam	1:125
Anti-RFP	Rabbit polyclonal	Dr Ian Prior	1:500
Anti-α-Tubulin	Mouse monoclonal	Abcam	1:500
Anti-Rabbit IgG Alexa Fluor 405	Goat polyclonal	Thermo Fisher Scientific	1:500
Anti-Mouse IgG Alexa Fluor 488	Goat polyclonal	Thermo Fisher Scientific	1:500

2.8.2. Surface staining

Cells were kept on ice and all reagents were maintained at 4°C throughout the entire procedure to inhibit endocytosis. LpH-mCh- stable NRK cells grown on 13 mm Ø glass coverslips were washed with PBS and incubated for 30 min with rabbit anti-RFP antibody, kindly provided by Dr Ian Prior (Institute of

Translational Medicine, University of Liverpool). Following incubation with primary antibody, cells were washed in PBS and further incubated for 30 min with goat anti-rabbit Alexa 405-conjugated antibody. After PBS washes, cells were fixed in 2% (w/v) formaldehyde in PBS for 6 min, coverslips air-dried and mounted onto glass slides using ProLong ™ Gold Antifade reagent (Thermo Fisher Scientific). All antibodies used in this procedure were diluted in surface staining solution (**Table 2.2.**).

2.9. Microscopy

The microscopy parameters used in the proceeding imaging techniques sections are described below. **Table 2.9.** details the properties of the fluorescent proteins (peak excitation and emission) and the specific laser lines utilised.

Table 2.9. Microscopy parameters used according to fluorescent proteins

Fluorescent proteins	***Laser line*** **Maximum excitation/Maximum emission**
Alexa Fluor 405	*405* 401/421
Alexa Fluor 488	*488* 490/525
GFP/pHluorin	*488* 488/510
mCherry	*561* 587/610
RFP	*561* 555/584
YFP	*515* 514/527

2.9.1. Fixed cell confocal microscopy

Confocal imaging of fixed samples was performed on a Zeiss LSM 800 Airyscan microscope equipped with a Zeiss AxioObserver Z1, a 63x/1.4 Plan-Apochromat oil immersion objective and diode laser as excitation light source. Emitted light was collected through Variable Secondary Dichroics (VSDs) onto a GaAsP-PMT detector. Exposure time to excitation light varied from 500 ms to 1s.

2.9.2. Live cell imaging and Total Internal Reflection Fluorescence (TIRF) microscopy

For live cell work, cells were maintained at 37°C, 5% CO_2 in an OKO lab incubation chamber for the duration of the experiment.

Live confocal fluorescence imaging was performed on a 3i Marianas spinning-disk microscope equipped with a Zeiss AxioObserver Z1 and 3i laser-stack as excitation light source. Emitted light was collected onto a CMOS camera (Hamamatsu, ORCA Flash 4.0) through a quadruple band-pass filter. Images were acquired at a rate of 1 frame every 2 to 5 min. Samples were exposed to excitation light for 200 ms to 500 ms.

Bright field live images were acquired on a Zeiss apotome widefield system.

TIRF microscopy (TIRFM) imaging was performed using the TIRF module of the same 3i Marianas system used for confocal imaging. Image acquisition was carried out at a rate of 1 frame every 0.5 to 2s. Exposure time to excitation light was set to 200 ms.

2.10. Image analysis

2.10.1. Cytokinesis and polynucleate cell count

For each treatment condition and respective vehicle control 5 to 10 non-overlapping fields of view were acquired. In each field of view Z-stacks were performed in order to image cells in all focal planes. The proportion of cells undergoing cytokinesis (i.e. connected by an intercellular bridge) and bi/tetranucleate cells were assessed as % of total cell number in each field. The cell count was performed in 3 to 12 independent experiments. The data was anonymised and scored independently by a second member of laboratory staff expert in analysis of immunofluorescence image data. The average of these two independent scores was used to account for confirmation bias in the counting method.

2.10.2. Plasma membrane fluorescence analysis with Fiji

NRK cells were transfected with LpH-mCh and the luminal part of the construct was detected by surface staining (section **2.8.2.**) using confocal microscopy (section **2.9.1.**). Different Z-stack planes were recorded in order to obtain sum projections of each channel. Data were exported as TIFF images and analysis was performed using Fiji software. One region of interest (ROI) was drawn around the plasma membrane in the sum image of the blue channel (405 nm, RFP tagged with Alexa 405 detection, surface labelling of lysosomal luminal epitopes); another ROI was selected around the cell cytoplasm just below the plasma membrane in the sum image of the red channel (561 nm, mCherry detection, cytosolic lysosomes) of the same cell. The fluorescence at the membrane was determined as % of total cell fluorescence in interphase and cytokinesis and calculated as follows:

$$\%F_{PM} = ((F_{405} - F_{background\ 405}) * 100) / ((F_{561} - F_{background\ 561}) + (F_{405} - F_{background\ 405}))$$

Where F_{405} is the sum fluorescence intensity in the ROI of the blue channel (405 nm), F_{561} the sum fluorescence in the ROI of the red channel (561 nm)

and $F_{background\ 405}$ and $F_{background\ 561}$ the background fluorescence subtracted to the blue and red channel measurements, respectively.

2.10.3. Fluorescence intensity and diffusion analysis in TIRF microscopy

Data acquired during TIRFM experiments were exported as TIFF images and analysed in Fiji.

2.10.3.1. Fluorescence intensity measurement

ROI's were drawn around single lysosomes in NRK cells stably expressing LpH-mCh. The fluorescence intensity at each ROI was measured frame by frame. Due to the high mobility of lysosomes and cellular movement during cell division, the ROI position was adjusted at each frame so that the centre of the ROI was aligned with the centre of the lysosome. The fluorescence values were normalised to background fluorescence in each frame and plotted against time. Only clearly visible lysosomes i.e. present in the evanescent field and exhibiting a sharp fluorescence signal were analysed.

2.10.3.2. Diffusion analysis

The interpretation of variations in fluorescence intensities over time of Lysotracker®-loaded lysosomes can be ambiguous. An increase/decrease of fluorescence intensity can account for exocytosis as well as for docking/undocking or random motion of an organelle. In order to avoid any confusion a diffusion analysis was developed whereby fluorescence intensity was measured over a defined distance. Exocytosis of fluorescently tagged lysosomes is accompanied by a spreading of fluorescence across the extra-cellular space that is measurable along the longitudinal axis of the PM (*x* or *y* axes) and is absent from docking/undocking events. In Fiji software a line was drawn across a Lysotracker®-loaded lysosome approaching the PM. The line was set so that its length was constant throughout measurements and approximately 1 µm longer than the lysosome diameter on either side of the organelle. The position of the line was adjusted frame by frame so that its midpoint was aligned with the lysosome centre for all measurements.

Fluorescence intensity values were normalised to background fluorescence and plotted against the distance of the line.

2.10.4. Measurement of fluorescence intensity of clustered lysosomes during cytokinesis under bromophenol blue treatment

Image acquisition was performed on a spinning disk confocal microscope and exported as TIFF. Using Fiji, a circular ROI was drawn around each set of lysosomes clustered at either side of the intercellular bridge and fluorescence intensity of mCherry (561 nm, red channel) and pHluorin (488 nm, green channel) measured frame by frame. The ROI was adjusted frame by frame so that it coincided with the clustered lysosomes. The fluorescence measurements were normalised to background and plotted against imaging time.

2.11. Statistical analysis

Unless stated otherwise experiments were performed in triplicate (N = 3) and results are expressed as mean ± S.E.M. Where applicable, the number of cells (n) is stated in the figure legends. All statistical analyses were performed on GraphPad Prism 6 software. Students' unpaired *t*-tests were used for statistical comparison between groups, as indicated and p values in the figures are represented by stars (*$p < 0.05$, **$p < 0,01$ and ***$p < 0.0001$).

Chapter 3: Investigating lysosomal distribution and physiological properties during cell division

3.1. Introduction

3.1.1 Lysosomes, versatile organelles

Lysosomes are acidic intracellular organelles found in all eukaryotic cells. Typically they are 100-500 nm in diameter but their size, shape, number and distribution vary according to the cell type and its metabolic status. Lysosomes are the terminal compartment of the endocytic pathway and are distinguished from all earlier compartments, including late endosomes, by the absence of mannose-6-phosphate receptor (Luzio *et al.* 2007). More than 50 proteins decorate their membrane, the most abundant being LAMP1, LAMP2 and CD63 (Appelqvist *et al.* 2013; Samie and Xu 2014). A single phospholipid bilayer delimits them and ensures physical separation between the cytosol and their acidic lumen which provides the optimal functional environment for more than 60 distinct types of hydrolytic enzymes including proteases, lipases and nucleases which digest a vast array of cellular substrates (Bainton 1981; Saftig *et al.* 2010). Luminal acidity (pH between 4.5 and 5.5) is initiated and maintained by the action of V-ATPase which pumps protons into the lysosome lumen (Luzio *et al.* 2007; Samie and Xu 2014). Due to their involvement in the catabolic degradation of intra-cellular particles via autophagy and extra-cellular particles arising from the phagocytic-endocytic pathway, they are best known as the cell's "waste bag" (Samie and Xu 2014). They were long thought to be solely the final degradative centre for macromolecules in the endocytic pathway (Rodríguez *et al.* 1997). However, recent findings have profoundly reshaped the view of lysosomes as a one-dimensional degradative organelle. They are now viewed as dynamic and multifaceted structures able to undergo regulated exocytosis and to detect and adapt to the nutrient status of the cell, thereby contributing to cellular homeostasis (Samie and Xu 2014). Indeed, lysosomes should be more accurately regarded as the cells recycling centre as they are responsible for catabolising a number of classes of macromolecule and returning the building blocks to the cytosol to fuel on-going anabolic processes. They are additionally involved in plasma membrane (PM) repair (Reddy *et al.* 2001), cell migration and adhesion (Nguyen *et al.* 2018), cholesterol transport (Basant *et al.* 2015), pathogen sensing (Vieira *et al.* 2003) and participate in calcium signalling events (Morgan *et al.* 2011). The

Ca^{2+} concentration in the lysosomal lumen ranges from 400 to 600 µM, a concentration similar to that in the endoplasmic reticulum (ER), the major cellular Ca^{2+} store (Appelqvist *et al.* 2013). High lysosomal Ca^{2+} levels are generated by entry of Ca^{2+} via the H^+/Ca^{2+} exchanger, whose potential energy is provided by the V-ATPase (Raffaello *et al.* 2016). Therefore, luminal Ca^{2+} levels and pH are interconnected (Christensen *et al.* 2002). In order to act as true Ca^{2+} signalling platforms lysosomes also have to release Ca^{2+} in response to specific stimuli. It has been known for many years that the most potent intracellular Ca^{2+} mobilising second messenger, Nicotinic acid adenine dinucleotide phosphate (NAADP) acts on lysosomes and it has since been discovered that there are specific lysosomal Ca^{2+} release channels. Two classes of lysosomal membrane protein mediate the release of Ca^{2+}, the two-pore channel (TPC) and the mucolipin family of transient receptor potential (TRPML) channels (Raffaello *et al.* 2016). TPC2 channel responds to NAADP and the evidence for lysosomes as true Ca^{2+} signalling organelles is now unequivocal. Interestingly, lysosomes form membrane contact sites with the ER at which Ca^{2+} microdomains exist that permit crosstalk between the two organelles (Penny *et al.* 2015). It has been speculated that lysosomes operate as 'trigger' factors in this system to initiate larger Ca^{2+} release events from the ER (Kilpatrick *et al.* 2013) and thus the complexity of possible Ca^{2+} signals available to the cell has increased markedly in light of these findings. In addition, dysfunction in lysosomal trafficking and Ca^{2+} release has been associated with lipid storage disorders (Shen *et al.* 2012). Collectively, these recent studies demonstrate further the functional complexity of lysosomes and reinforce the importance of lysosomes in physiological and pathological conditions.

3.1.2. Lysosome motility

Lysosomes are motile structures within cells. This property is essential since they monitor the cytoplasmic nutrient content and maintain cellular homeostasis (Rosa-Ferreira and Munro 2011). Indeed, the cellular levels of nutrients directly modify the subcellular location of lysosomes (Appelqvist *et*

al. 2013) and influence the interaction between the organelle and the mammalian target of rapamycin mTOR, which regulates autophagic flux (Roczniak-Ferguson *et al.* 2012). Lysosomes are able to move bi-directionally i.e. towards the microtubule organising centre (centripetal or retrograde movement) or to the cell periphery (centrifugal or anterograde movement) (Bento *et al.* 2013). Lysosomes move centripetally and centrifugally along microtubules via their connection with dynein (Harada *et al.* 1998) and kinesin (Hollenbeck and Swanson 1990) motor proteins, respectively. These interactions are in turn mediated by the small GTPases Arl8 (centrifugal movement), an Arf-like GTPase and Rab7 (centripetal movement) which alternately decorate the surface of the organelle (Mrakovic *et al.* 2012). These GTPases, linked to their appropriate motor proteins via their effectors, govern lysosomal identity, trafficking properties and ultimately sub-cellular localisation (Bucci *et al.* 2000; Bagshaw *et al.* 2006). It is the balance between Rab7 and Arl8 activity that determines the subcellular positioning of the organelle. Expression of RILP, a Rab7 effector protein, drives the lysosomes towards the minus end of microtubules and the microtubule organising centre (Jordens *et al.* 2001); on the other hand, ectopic expression of Arl8, induces a peripheral accumulation of lysosomes (Johnson *et al.* 2016). Interestingly, in turn, the subcellular location of lysosomes seems to influence their luminal pH. The acidity of the organelle tends to decrease as it moves from the juxtanuclear to the peripheral region of the cell; this loss of acidity is attributed to an increase in proton leak combined with a decreased V-ATPase activity (Johnson *et al.* 2016). Indeed, RILP is associated preferentially with juxtanuclear lysosomes, recruits the V-ATPase subunit V1G1 at the lysosomal membrane and stabilises the proton pump (De Luca *et al.* 2014). As lysosomes move further from the cell centre toward the periphery, Rab7/RILP association declines leading to decreased V-ATPase activity and luminal alkalinisation (Figure 2). The functional significance of lysosomal pH variations has not been established but these variations appear linked to the functional versatility of lysosomes (Johnson *et al.* 2016).

3.1.3. Emerging role of lysosomes in cell division

Mitosis is the process by which a cell divides to give rise to two daughter cells bearing the same genetic material; it involves segregation of the chromosomes and nuclear division. Cell division is accompanied by cytokinesis, the phase during which the cytoplasm constricts and divides (Zheng *et al.* 2014). Cytokinesis is a highly orchestrated mechanism that can be subdivided into different stages. First a cleavage furrow is specified and undergoes an ingression that generates a transient intercellular bridge. Next a dense structure, the midbody is formed. Eventually the process terminates when the cytoplasm connecting the two nascent cells is severed during abscission (Normand and King 2010).

A recent study has shown that, during cytokinesis, lysosomes exhibit a highly specific re-distribution to either side of the intercellular bridge. In addition, the clustered organelles are decorated with CaBP7, a calcium-binding protein related to calmodulin (Rajamanoharan *et al.* 2015). This protein, also referred to as Calneuron II (McCue *et al.* 2010), belongs to the calmodulin related family of EF-hand containing small Ca^{2+}-binding proteins (CaBPs). CaBP7 was first identified as a trans-Golgi network (TGN) associated protein that is involved in regulation of TGN-to-PM trafficking; it targets PI4KIIIβ (Mikhaylova *et al.* 2009), an enzyme that generates PI4P required for biogenesis of secretory vesicles. In addition to the CaBP7-decorated lysosome pool, an independent group of lysosomes associates with PI4KIIIβ (Sridhar *et al.* 2013). However the functional significance of these associations remains unclear in cell division. Interestingly, suppression of CaBP7 expression by gene silencing has been shown to induce cytokinesis failure (Neumann *et al.* 2010). These findings, combined with the fact that CaBP7 associates with lysosomes during cell division, raises the intriguing possibility of a potential involvement of phosphoinositide metabolism on lysosomes in mitosis.

This chapter focuses on characterising lysosome distribution and physiological properties during cell division, in particular, during cytokinesis.

3.2. Results

3.2.1. Lysosomes are present at the site of cytoplasmic constriction and cluster at either side of the intercellular bridge during the late stages of cell division

Lysosomal positioning and motility are driven by the functional requirements of the cell, particularly in response to nutrient status. Almost all studies to date have examined lysosome localisation under cellular conditions at interphase and virtually nothing is known regarding their dynamics during cell division (Pu *et al.* 2016). Using a combination of fixed and live cell imaging, the positioning of lysosomes throughout cell division was examined. First HeLa cells were transfected with LAMP1-EYFP, a construct that targets to the lysosomal membrane. Subsequent tubulin immunostaining allowed clear identification of cell at cytokinesis. Consistent with a study performed in our laboratory (Rajamanoharan *et al.* 2015), lysosomes displayed a highly organised and coordinated clustering at either side of the intercellular cytoplasmic bridge separating nascent cells during cytokinesis. In addition, LAMP1 punctae were detected to a lesser extent on the intercellular bridge, suggesting the presence of lysosomes at the site of cytoplasmic separation between daughter cells (**Figure 3.1.**).

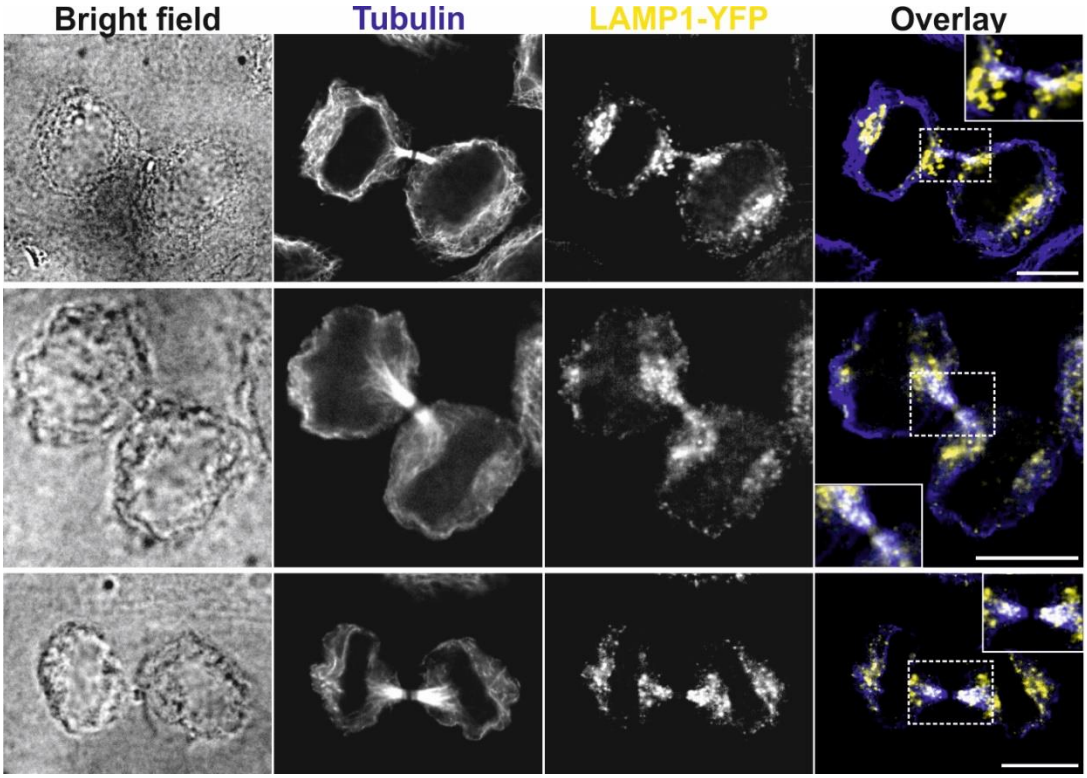

Figure 3.1. Lysosomes cluster at either side of the cytoplasmic intercellular bridge during cytokinesis in HeLa cells. HeLa cells were transfected with LAMP1-EYFP construct, fixed, permeabilised and immunostained with anti-tubulin tagged with Alexa Fluor 405. Cells were imaged on a confocal spinning disk microscope. Scale bars 10 μm.

In order to follow the course of lysosomal positioning in close proximity to the PM during the entirety of mitosis, Total Internal Reflection Fluorescence Microscopy (TIRFM) time lapse imaging of Lysotracker® - loaded lysosomes was performed. HeLa cells lose their attachment to the substratum during mitosis as they exhibit characteristic and extensive rounding and therefore visualisation of mitotic HeLa cells in the evanescent field is problematic. Thus cell lines that adopt a flatter morphology during mitosis (NRK and BSC-1) were employed for these studies (Goss and Toomre 2008) (**Figure 3.2.**). The lysosomal clustering observed in HeLa cells at cytokinesis was recapitulated in these cell lines, suggesting that it is not a phenomenon specific to HeLa cells but rather a more general feature of lysosome behaviour during mitosis (**Figure 3.2.B**). Time lapse images demonstrated that lysosomes are initially randomly dispersed in the cytoplasm at early stages of cell division and

progressively accumulate at the site of the cleavage furrow during early telophase. Additionally these organelles were clearly observed at the intercellular bridge, consistent with the positioning of lysosomes in LAMP1 transfected cells as shown in **Figure 3.1** (**Figure 3.2.A**).

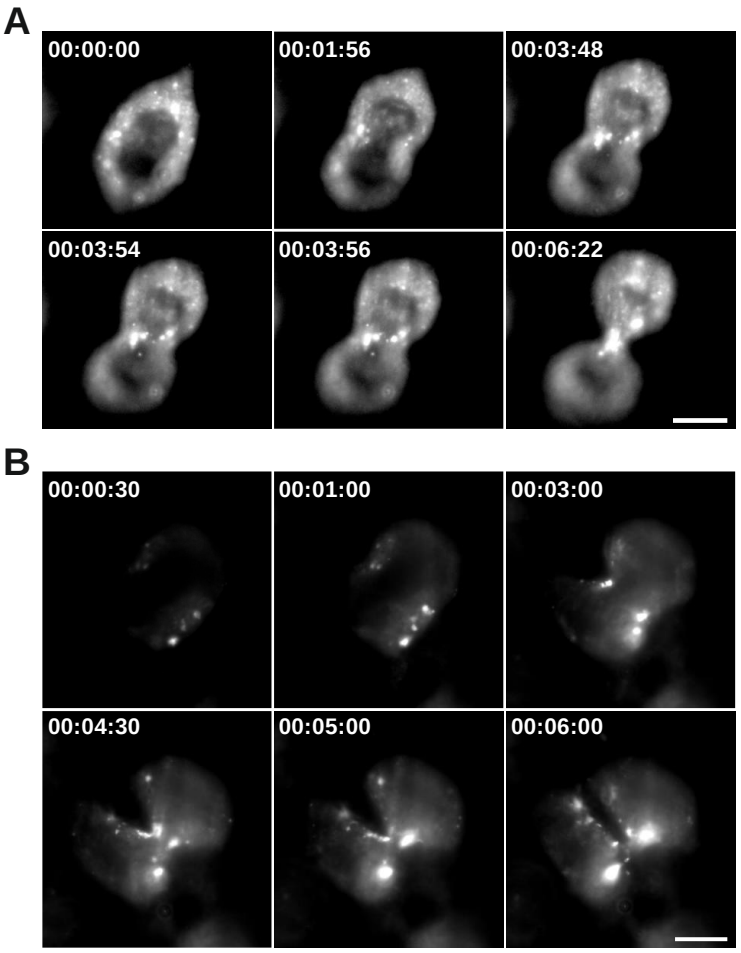

Figure 3.2. Lysosomes are present at the site of cytoplasmic constriction during cell division. Cells were loaded with 50 nM Lysotracker ® red for 30 minutes and imaged at a rate of 1 frame every 2 seconds (NRK cells; **A**) or every 30 seconds (BSC-1 cells; **B**). Time lapse experiments were performed on a TIRFM system. Time indicated as h:min:s. Scale bars: 10 µm.

3.2.2. Development of a genetically encoded, lysosomally targeted tool to study the luminal pH and exocytosis of lysosomes during cell division

One of the characteristics of lysosomes that distinguishes them from other intracellular compartments is their low luminal pH (4.5-5.5) (Wang *et al.* 2015). In order to examine potential fluctuations in lysosomal pH during cell division a pH-sensitive lysosomally targeted probe was engineered. The construct called LysopHluorin-mCherry (LpH-mCh) is derived from a previously described LysopHoenix probe (Rost *et al.* 2015). It contains the targeting information from the lysosomal tetraspannin membrane protein CD63 followed by a super-ecliptic pHluorin GFP variant and finally mCherry. The pHluorin protein acts as a pH sensor as it is quenched in the normally acidic lysosomal lumen and its fluorescence output increases as a function of increasing pH which permits detection of luminal alkalinisation as might occur when a lysosome exocytoses at the cell PM (**Figure 3.3**).

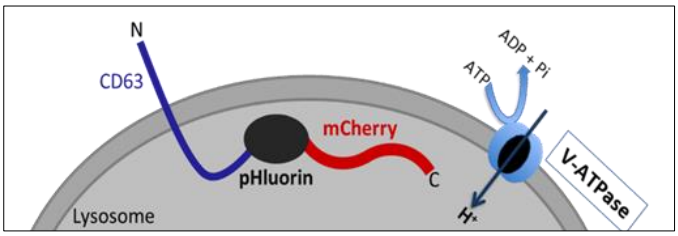

Figure 3.3. Architecture of LysopHluorin-mCherry. The CD63 targeting sequence efficiently trafficks the construct to lysosomes. Fluorescence of pHluorin (pKa 6.9) (Martinière *et al.* 2013) is quenched inside the lysosome due to the activity of the V-ATPase that maintains low luminal pH (lysosomal pH 4.5-5.5). The mCherry tag located in the lysosomal lumen is pH insensitive in the same acidic environment (pKa ≤4.5) (Costantini *et al.* 2015) therefore allowing visualisation of the construct at all times.

LpH-mCh was originally designed for transient exogenous expression in HeLa cells. The cloning steps and verification of expression are illustrated in **Figure 3.4**.

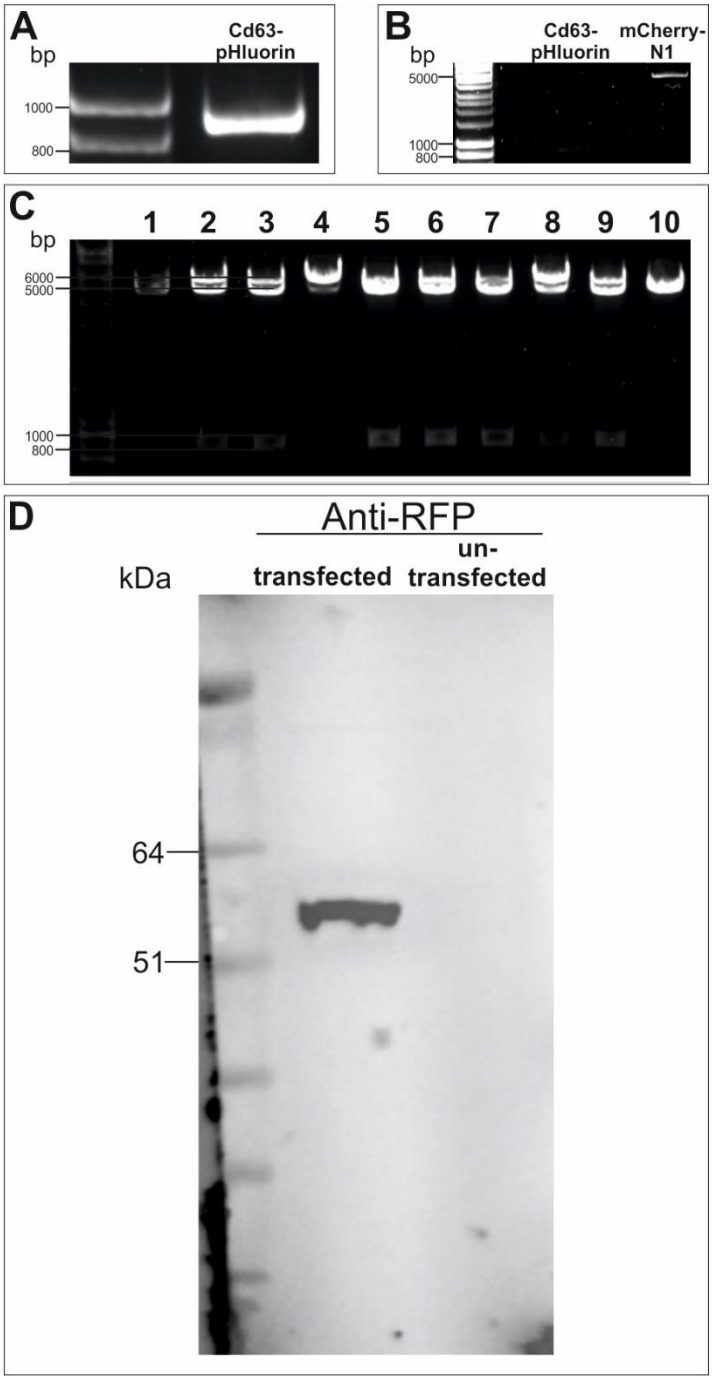

Figure 3.4. Cloning and verification of expression of LpH-mCh in HeLa cells. A. PCR amplification of CD63-pHluorin fragment from LysopHoenix. **B.** Agarose gel electrophoresis showing mCherry N1 vector and CD63-pHluorin after incubation with restriction endonucleases and gel purification, prior to ligation. **C.** Screening of 10 minipreps purified from single bacterial colonies. Miniprep in lane 5 was used to re-transform DH5α *E. coli* for larger scale culture and maxiprep. CD63-pHluorin size: 879 bp; mCherry N1 size: 4722 bp. **D.** Western blot of LpH-mCh-transfected and un-transfected HeLa lysates with anti-RFP specific antibody. The predicted size of the expressed protein is 59 kDa and the calculated molecular weight 58.7 kDa.

Transient transfection of chemically synchronised cells with standard lipophilic reagents elicits significant levels of cell death and to circumvent this issue, LpH-mCh was sub-cloned into a pHIV expression vector for lentivirus production and subsequent generation of stably expressing LpH-mCh cell lines. For this the In-Fusion® cloning technique was employed. The cloning stages and expression in virally infected cells are highlighted in **Figure 3.5**.

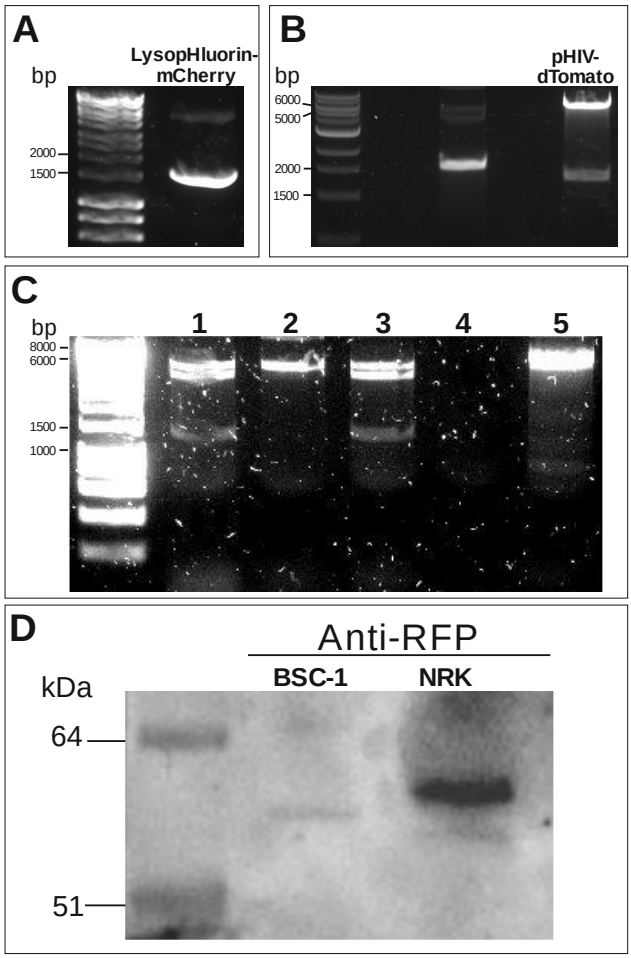

Figure 3.5. Cloning of LysopHluorin-mCherry into pHIV for lentivirus generation and verification of pHIV-LpH-mCh expression in NRK and BSC-1 cells. A. Amplification of LpH-mCh by PCR for addition of 15 bp overhangs. LpH-mCh size: 1560 bp. **B.** Linearisation of pHIV-dTomato vector prior to gel purification of the empty pHIV vector. Empty pHIV size: 5600 bp; dTomato size: 2000 bp. Linearisation was performed using XmaI-ClaI restriction endonucleases. **C.** Single bacterial colony screening from minipreps. The screening was achieved using XhoI-ApaI enzymes to generate two fragments of 1100 bp and 6000 bp. Sequencing results showed that the miniprep from colony 5 was positive for the construct. **D.** Western blot analysis of BSC-1 and NRK cells infected with the pHIV-LpH-mCh lentivirus. Verification of

expression was performed using anti-RFP antibody. Note that the level of expression in BSC-1 cells was low and so only NRK stable cell lines were used in subsequent imaging experiments. LpH-mCh predicted size: 59 kDa.

In order to confirm correct localisation of LpH-mCh cells were imaged with confocal microscopy. This construct would be expected to co-localise with Lysotracker®, an acidotropic dye that accumulates in acidic sub-cellular compartments. As organelles like late endosomes are also relatively acidic Lysotracker® will accumulate here also. To truly distinguish lysosomes from other endocytic compartments Mannose-6-phosphate receptor (M6PR) immunostaining was therefore performed. Unlike late endsosomes, lysosomes are devoid of M6PRs and this is the only definite way to distinguish these organelles. (**Figure 3.6.**).

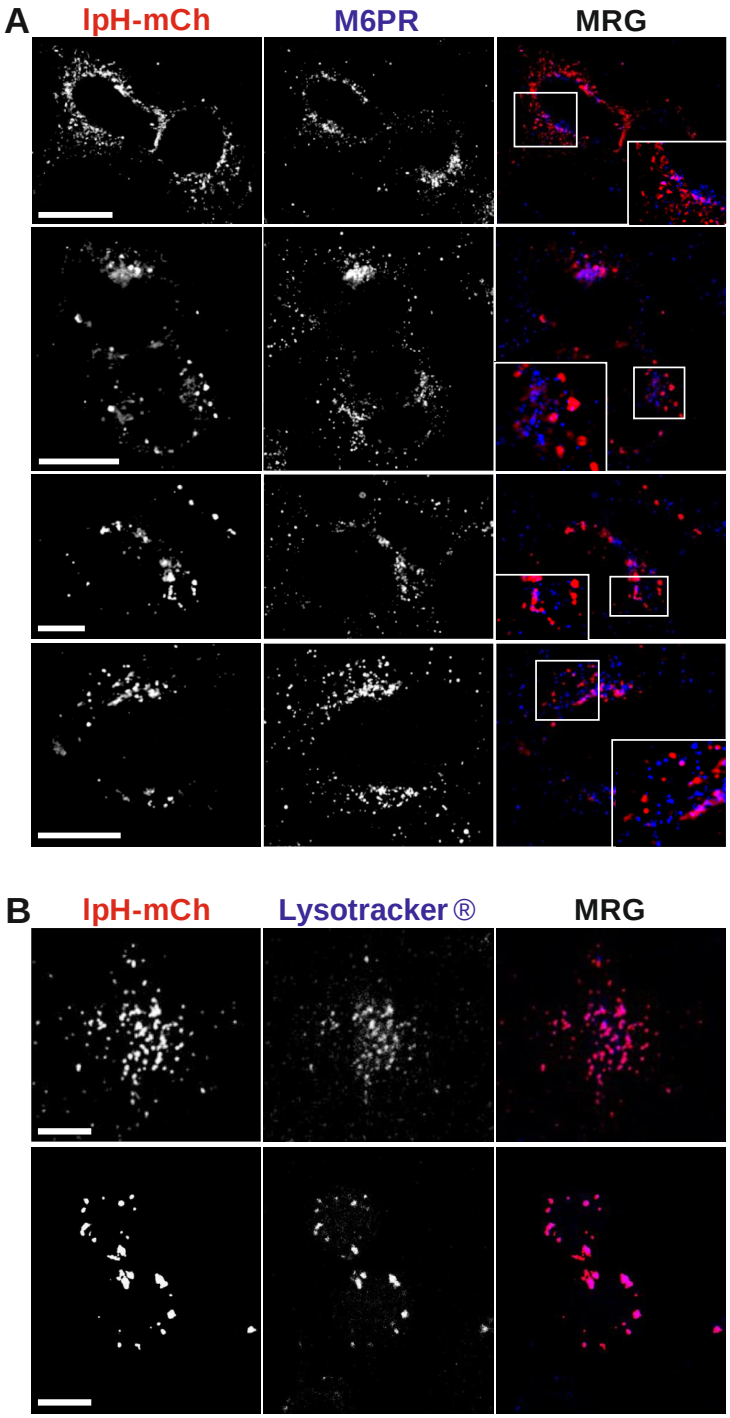

Figure 3.6. LysopHluorin-mCherry expression is restricted to lysosomes in mammalian cells. A. Endogenous expression of M6PR in HeLa cells transfected with lpH-mCh. Limited co-localisation between M6PR and lpH-mCh was observed and this was restricted to regions close to the nucleus. Imaging was performed on a Zeiss LSM880 confocal system with Airyscan. **B.** LpH-mCh co-localised with Lysotracker® in NRK cells stably expressing the LpH-mCh construct. Images were collected on a 3i Marianas spinning disk confocal microscope. Note that only mCherry (red channel) was recorded to show expression of LpH-mCh. Scale bars 10 µm.

3.2.3. Lysosomes undergo de-acidification during cell division

Expression of LpH-mCh in mammalian cells revealed an unexpected and potentially novel property of lysosomes during cell division. Whilst pHluorin remained largely quenched at interphase, a progressive de-quenching from the onset of mitosis through to cytokinesis occurred, suggesting an alkalinisation of the lysosome lumen. Time lapse live imaging demonstrated that the increase in luminal pH was most marked at cytokinesis, when lysosomes were clustered at either side of the intercellular bridge. Interestingly lysosome alkalinisation was detected in LpH-mCh-transfected HeLa- (**Figure 3.7.**) as well as in Lph-mCh-stable NRK-cells (**Figure 3.8.**), indicating that the process is conserved in different mammalian cell lines.

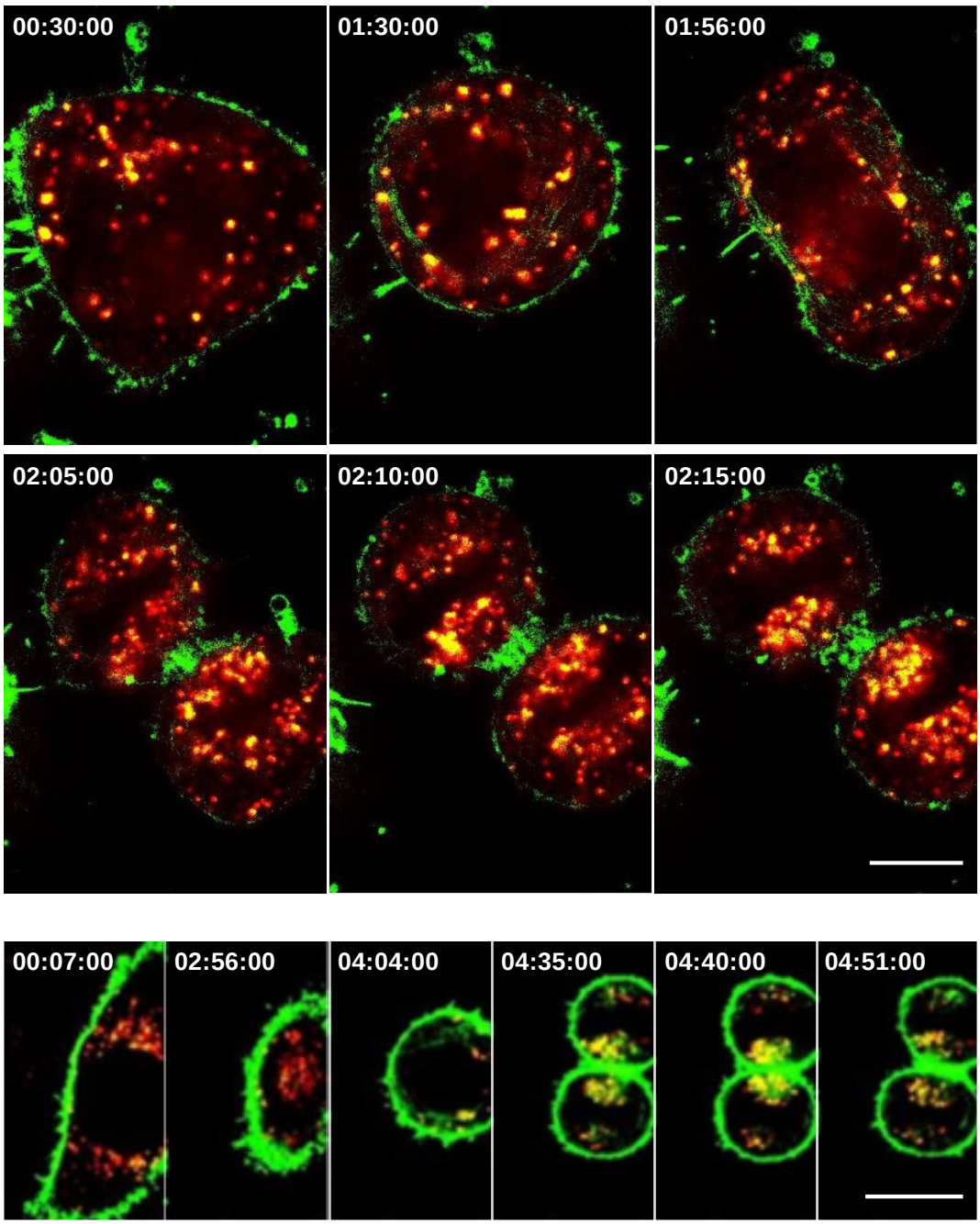

Figure 3.7. The luminal pH of lysosomes increases during HeLa cell division. HeLa cells were transfected with LpH-mCh and imaged overnight on a spinning disk confocal microscope at a rate of 1 frame every 2 minutes. Scale bars: 10 µm (top panel) and 5 µm (bottom panel). Time shown as hr:min:s.

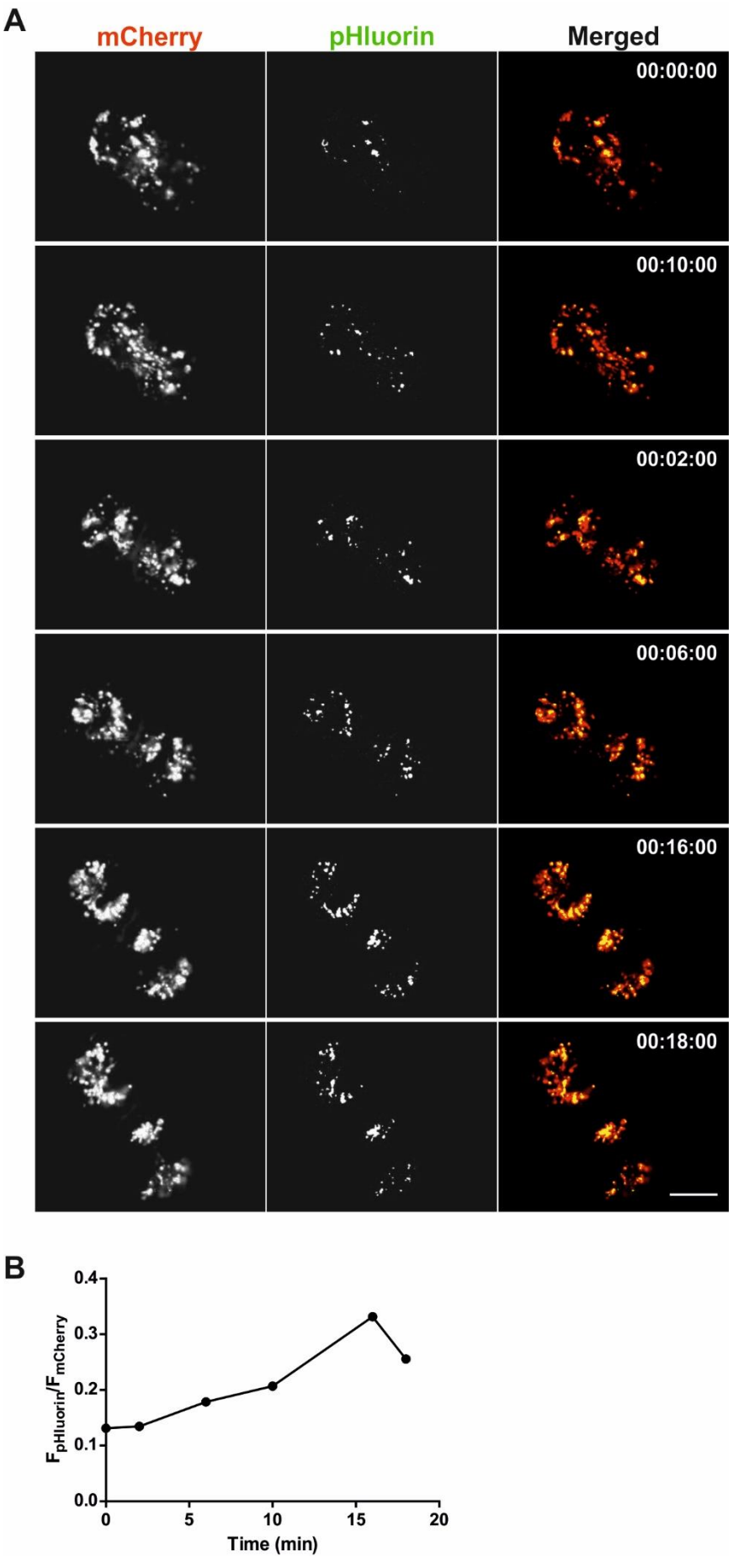
A
mCherry
pHluorin
Merged
00:00:00
00:10:00
00:02:00
00:06:00
00:16:00
00:18:00
B
0.4
0.3
0.2
0.1
0.0
$F_{pHluorin}/F_{mCherry}$
0
5
10
15
20
Time (min)

Figure 3.8. Lysosomes undergo luminal alkalinisation during NRK cell division. **A.** LpH-mCherry-stable NRK cells were imaged overnight on a spinning disk confocal microscope at a rate of 1 frame every 2 minutes. Panels show mCherry (561 nm) and pHluorin (488 nm) expression and merged view. Scale bars: 10 µm. Time shown as hr:min:s. **B.** Graph depicts ratio of fluorescence intensity between pHluorin ($F_{pHluorin}$) mCherry fluorescence ($F_{mCherry}$) during imaging shown in **A**.

3.3. Discussion

3.3.1. Lysosomal clustering at cytokinesis: stochastic distribution or coordinated and active process?

This chapter aimed at examining lysosomal positioning and properties during cell division. Fixed cell imaging and TIRFM first confirmed what has been previously observed in our laboratory: lysosomes re-distribute in clusters at either side of the intercellular bridge separating the nascent cells at cytokinesis (Rajamanoharan *et al.* 2015). Immunofluorescence imaging of fluorescently labelled lysosomes also demonstrated the presence of lysosome clusters on the opposite side of the nucleus. Since lysosomes mostly gather in the perinuclear region in non-polarised cells at interphase (Jongsma *et al.* 2016), one could argue that the particular positioning and clustering of the organelle during mitosis is a simple mechanical consequence of the deep cellular (Pu *et al.* 2016) partitioning that pushes lysosomes towards the cell periphery, resulting in their clustering at either side of the nucleus and either side of the cytoplasmic bridge. However this hypothesis is invalidated by two observations. First lysosome clustering in mitosis was observed in cell lines bearing different morphologies and sizes (NRK, BSC-1 and HeLa cells). Second, TIRFM and fixed cell imaging uncovered that prior to lysosomal clustering, a bulk of lysosomes was present at the site of furrow ingression and on the intercellular bridge, cellular locations subjected to the greatest force constraint. Consequently it seems likely that lysosomes are actively repositioned during cell division. Identification of the motor proteins involved in lysosomal movement along the microtubules during cell division by

immunostaining would confirm that lysosomal positioning results from an active process.

Previous studies have shown that lysosome active positioning and movement inside the cell are strongly linked to their cellular function (Pu *et al.* 2016). Therefore it is reasonable to assume that the active clustering of the organelle during cytokinesis is not trivial and that a particular lysosomal function is required during mitosis. Indeed previous work illustrated that antagonism of lysosomal clustering through a PI4KIIIβ dependent pathway correlated with significant mitotic failure (Rajamanoharan *et al.* 2015). This reinforces the functional requirement of lysosomes during mitosis but also highlights the fact that whatever specific function they provide can only be delivered through their specific spatial distribution.

3.3.2. Mechanisms of lysosomal de-acidification

Live imaging of cells expressing the pH-sensitive lysosomally targeted probe LpH-mCh uncovered an astonishing property of lysosomes during mitosis. The organelles undergo a transient luminal alkalinisation. This pH increase illustrated by pHluorin de-quenching and its subsequent rise in fluorescence intensity seems to climax when lysosomes are clustered at either side of PM constriction in mitotic cells. The alkalinisation process is unlikely to be an isolated event since it was observed in independent cell types (NRK and HeLa cells).

As aforementioned, different factors can affect lysosomal pH. A pH increase could result from a downregulation of the lysosomal V-ATPase as a result of lysosome subcellular distribution. Indeed, as lysosomes move peripherally, Rab7 density is reduced, resulting in decreased recruitment of its effector RILP, which normally modulates the recruitment and stability of components of the V-ATPase (Johnson *et al.* 2016). Due to the profound reshaping of the cell during mitosis, it is difficult to assess here whether lysosome clustering occurs peripherally or in the perinuclear region. Immunofluorescence staining to reveal the position of the small GTPases and their effectors in relation with lysosomal markers at different stages of cell division would therefore provide

valuable information on exact lysosomal localisation and on potential factors affecting luminal pH. RILP staining was attempted as part of this thesis in order to provide evidence of a potential molecular mechanism for lysosomal alkalinisation during mitosis; however the antibody proved unreliable.

Lysosome alkalinisation could also arise from fusion of lysosomes with organelles bearing a higher luminal pH, such as endosomes. However M6PR immunostaining of cells expressing LpH-mCh indicated that the vast majority of lysosomes are not hybrid organelles. In addition, previous time lapse imaging of fluorescently labelled endosomes and lysosomes demonstrated that the two compartments remain distinct from each other throughout mitosis (Bergeland *et al.* 2001).

3.3.3. Functional significance of lysosomal positioning and alkalinisation during cytokinesis

As opposed to a passive consequence of lysosomal positioning, an active process of luminal alkalinisation that triggers a lysosomal function required near the site of cytoplasmic constriction during cell division could take place. In interphase, peripherally dispersed lysosomes are typically more alkaline than lysosomes clustered in the perinuclear regions (Johnson *et al.* 2016). The study performed here demonstrated that clustered lysosomes are more alkaline, suggesting a novel mechanism of de-acidification might take place in the late stages of cell division, distinct from lysosomal alkalinisation in interphase.

Lysosomes are best known as terminal degradative centres within cells. Since lysosomal hydrolases require an acidic environment to be active, a luminal pH increase of lysosomes during cell division implies that the preservation of the enzyme activity is not essential for mitosis completion. However this remains highly hypothetical and requires further investigation.

Spatially and temporally coordinated Ca^{2+} signals play a pivotal role in cell proliferation (Machaca 2011), therefore the Ca^{2+} handling function of lysosomes is relevant in the context of cell division. The V-ATPase creates a

proton concentration gradient which provides energy for Ca^{2+} entry through the H^+/Ca^{2+} exchanger; therefore low lysosomal pH correlates with high lysosomal Ca^{2+} content (Raffaello *et al.* 2016). Conversely, lysosome alkalinisation has been shown to be accompanied by a reduction in lysosomal calcium and an increase in cytosolic Ca^{2+} concentration (Christensen *et al.* 2002). In zebrafish embryos, Ca^{2+} elevations during cytokinesis were shown to precede furrow ingression and subsequent cleavage (Webb *et al.* 2008) but the origin of Ca^{2+} signals remains obscure (Atilla-Gokcumen *et al.* 2010). Given the high Ca^{2+} content of lysosomes and their strategic repositioning near the site of cytoplasmic constriction, one could argue that the organelles act as Ca^{2+} suppliers during cytokinesis. However this is highly unlikely since lysosome alkalinisation is accompanied by a low lysosomal Ca^{2+} content.

De-acidification of lysosomes could also reflect the requirement of fusion events at a particular location in cytokinesis. Indeed, lysosomal alkalinisation has been shown to increase the organelle exocytic properties (Sundler 1997; Carnell *et al.* 2011). In *Dictyostelium discoideum,* the neutralisation of lysosomes by the WASP and SCAR homologue (WASH) promotes exocytosis of the organelles. WASH is recruited to acidic lysosomes causing local actin polymerisation and the sorting of V-ATPase from the lysosomal surface. The loss of V-ATPase induces organelle neutralisation which leads to maturation into post-lysosomes primed for exocytosis (Carnell *et al.* 2011). In addition to serving secretory purposes, lysosome exocytosis confers the cell with a molecular mechanism for PM repair. Under conditions of PM injury, lysosome exocytosis is thought to alleviate PM tension and favour spontaneous repair of the wounded lipid bilayer. However this is only applicable in circumstances where the extent of membrane damage is limited. A second hypothesis proposes that lysosomes give rise to larger structures by homotypic fusion and form a “patch” over the injured area (Idone *et al.* 2008). The fusogenic properties of lysosomes are relevant in the context of cell division. By acting as membrane donors during exocytosis, lysosomes also offer the cell the possibility to increase their surface area. This property is of particular interest in the late stages of mitosis, since the formation of the nascent daughter cells requires addition PM expansion. Boucrot and co-workers demonstrated that

the onset of mitosis is marked by a rounding up of cells that is necessary for appropriate spindle formation, accompanied by membrane endocytosis and a decrease in secretory traffic; conversely, they suggested that from anaphase to cytokinesis, new membrane, stored in intracellular compartments was added to the cell surface via Ca^{2+}-mediated exocytosis (Boucrot and Kirchhausen 2007). Lysosomes would therefore be an obvious candidate in the deposition of extra membrane during the late steps of cellular division based on their well-documented exocytic behaviour.

In order to understand the functional significance of lysosome alkalinisation, attempts to re-acidify the lysosomal lumen were made during these studies using LysopHoenix, the originial construct from which LpH-mCh was derived. The probe bears similarities with LpH-mCh; it contains a CD63 trafficking domain and pHluorin. An mKate2 fluorescent marker oriented on the cytosolic face of the lysosome allows permanent visualisation of the construct. In addition, light-driven activation of the bacterial proton pump Arch3 located next to the pHluorin protein permits optogenetic acidification of the lysosomal lumen. Due to technical difficulties such as permanent proton leaks that instantly re-alkalinised lysosomes coupled with time constraints the experiment could not be fully optimised. However the manipulation of lysosomal pH has the potential to unravel the functional significance of lysosome alkalinisation during cell division with important implications for furthering our understanding of the molecular basis of mitosis.

It is however important to take into account the limitations of the use of pHluorin as a pH indicator in lysosomes. First of all, the probe can only serve as a qualitative indicator of pH increase, since its pKa does not match the acidic pH of the lysosomal compartment. Second only changes in lysosomal pH above the pKa of pHluorin (6.9) can be monitored. Thus slight de-acidification of lysosomes from pH 5.5 to 6.9 would remain unnoticed. Ratiometric measurements of lysosomal pH, using probes such as LysoSensor™ whose fluorescence undergoes an emission shit from acidic to alkaline environment would therefore constitute a more reliable and quantifiable way to assess lysosomal alkalinisation.

3.4. Summary

In this chapter, lysosomes were shown to undergo a spatially and temporally regulated clustering near the site of cytoplasmic constriction during the late stages of cell division. In addition, they were found to accumulate at the site of furrow ingression and be present at the cytoplasmic bridge using time resolved TIRFM. These observations coupled with a transient lysosomal alkalinisation prompted us to further investigate the potential functional implication of the organelle in mitosis and the next chapter assesses the importance of lysosomes in mitosis completion and examines organelle function in greater detail.

Chapter 4: Investigating lysosomal function during mitosis

4.1. Introduction

4.1.1. Cell division

Mammalian cell division consists of a highly orchestrated mitotic phase integrated in the larger cell cycle. Mitosis encompasses a series of events leading to nuclear (mitosis) and subsequent cytoplasmic (cytokinesis) divisions, which permit the formation of two genetically identical daughter cells (Rattner 1992; Zheng *et al.* 2014). Mitosis can be subdivided into 5 main stages – prophase, prometaphase, metaphase, anaphase and telophase each with distinct spatiotemporal rearrangements of chromosomes and cytoskeleton (Jongsma *et al.* 2015). At cytokinesis a contractile ring assembles at the location of the cleavage furrow. Progressive ingression of the cleavage site induces cytoplasmic constriction and formation of a transient tubulin-rich intercellular bridge between nascent cells that is eventually physically severed at abscission (Atilla-Gokcumen *et al.* 2010).

Mitosis is involved in fundamental biological processes such as normal growth, development, ageing and tissue repair. Dysregulation of mitosis can lead to aneuploidy and genomic instabilities characteristic of tumour cells and therefore it is subject to multiple levels of regulation (Dominguez-Brauer *et al.* 2015). Understanding the regulatory mechanisms governing cell division is therefore essential in informing our ability to implement effective therapeutic strategies to combat a number of human pathologies.

Over the years, many studies have focused on the regulatory mechanisms controlling mitosis, the cytoskeleton rearrangement that accompanies it and the chromosome segregation that results from it. However little is known about the fate and potential role of intracellular compartments in cell division, notably lysosomes.

4.1.2. Lysosomal catabolic role

Lysosomes are highly dynamic and remarkably versatile intracellular organelles tasked with a vast array of cellular functions (Luzio *et al.* 2007). They primarily act as the recycling centre of cells by degrading extracellular

particles arising from endocytosis and phagocytosis and intracellular particles resulting from autophagy. Ultimately the products of lysosomal catabolism (e.g. free amino acids) are returned to the cytoplasm to participate in new anabolic processes. The catabolic function of lysosomes is fulfilled by more than 60 lysosomal hydrolases which target a broad range of molecules for degradation (Saftig and Klumperman 2009). Most hydrolases usually require an acidic environment for optimal activity. This is provided by the low luminal pH of lysosomes via the action of the V-ATPase (pH 4.5-5.5) (Luzio *et al.* 2007; Samie and Xu 2014). However a family of lysosomal proteases known as cathepsins remain fully functional outside of the acidic lysosome. In addition to their catabolic role, they accomplish other degradative functions, distinct from cellular metabolism, such as induction of apoptosis, antigen processing and degradation of the ECM (Conus and Simon 2008; Saftig and Klumperman 2009). They have been shown more recently to act as key extracellular factors in plasma membrane repair upon lysosome exocytosis (Castro-Gomes *et al.* 2016). Therefore, lysosomal hydrolases confer multifunctionality to this organelle and it is therefore no surprise that these enzymes are implicated in numerous human diseases. Indeed when released extracellularly by lysosomes, cysteine cathepsins can act as pro-oncogenic factors that facilitate the breakdown of the extracellular matrix, activate angiogenesis and favour migration of tumour cells (Kirkegaard and Jäättelä 2009).

4.1.3. Ca^{2+} handling function of lysosomes

There is growing evidence that, due to their high luminal Ca^{2+} content (similar to levels found in the ER), lysosomes have important roles in cellular Ca^{2+} signaling (Appelqvist *et al.* 2013; Kilpatrick *et al.* 2013). Ca^{2+} entry into lysosomes relies upon the proton gradient created by the V-ATPase across the lysosomal membrane and Ca^{2+} uptake by the lysosomes is potentially mediated by a Ca^{2+}/H^{+} exchanger or indirectly via a Ca^{2+}/Na^{+} exchanger (López-Sanjurjo *et al.* 2013). The mechanisms of lysosomal Ca^{2+} release are better characterised. TRPML1, which belongs to a family of evolutionarily conserved channels activated by the specific phosphoinositide $PI(3,5)P_2$

(Dong *et al.* 2010), mediates Ca^{2+} release by the lysosomes. The channel has been shown to participate in the biogenesis and trafficking of intracellular vesicles and in the ionic homeostasis of organelles (Venkatachalam *et al.* 2015). The lysosomal membrane is also decorated with TPC2, which shares sequence similarities with the superfamily of voltage-gated ion channels and localises to acidic organelles. Although still matter of controversy, the channel is thought to be activated by NAADP the most potent intracellular Ca^{2+}-mobilizing second messenger (Patel 2015).

4.1.4. Lysosome exocytosis

Soluble cytoplasmic proteins are sequestered in the lysosome lumen and subsequently delivered to the extracellular space via lysosome fusion with the PM, a process known as exocytosis (Nickel and Rabouille 2009). Evidence for lysosomal exocytosis was first observed in specialised cells containing lysosome-related organelles or secretory lysosomes (Burgoyne and Morgan 2003) such as cells of the hemopoietic lineage (Stinchcombe and Griffiths 1999), macrophages, monocytes, dendritic cells (Eder 2009), osteoclasts, hepatocytes and pancreatic acinar cells (Rodríguez *et al.* 1997). In addition to serving secretory purposes, fusion of lysosomes with the PM is also involved in other important biological functions such as the repair of mechanical (Reddy *et al.* 2001) and toxin-mediated injury (Castro-Gomes *et al.* 2016) of the PM, neurite outgrowth, material uptake from immune cells (Samie and Xu 2014) and ATP release for microglia-mediated repair of damaged neural tissue (Dou *et al.* 2012). As lysosome exocytosis fulfils a wide variety of biological tasks, some of which are homeostatic in nature, the process is now, unsurprisingly, thought to operate in most cell types (Tardieux *et al.* 1992; Bi *et al.* 1995; Jaiswal *et al.* 2002) and the exocytosis of conventional lysosomes is an active field of study (Reddy *et al.* 2001).

4.1.5. Lysosome: a key player in cell division?

A recent study analysing the role of a small Ca^{2+} binding protein, CaBP7 and phosphatidylinositol 4-kinaseIIIβ (PI4K) revealed a potential role for lysosomes

during mitosis in mammalian cells (Rajamanoharan *et al.* 2015). Lysosomes spatially and temporally re-organised as clusters at either side of the intercellular cytoplasmic bridge at cytokinesis and disruption of this spatial distribution via a PI4K-dependent pathway induced a significant increase in division defects. This indicates that the spatial arrangement of lysosomes had a potentially important functional impact on mitosis completion. To date, evidence of the functional requirement for lysosomes during mitosis remains limited, however, further proof of this would open new potential ways of controlling cellular proliferation. Determining the precise role of lysosomes during mitosis is therefore a worthwhile scientific endeavour that has wide potential impact for both cell biology research and human health. With this in mind, this chapter focuses on investigating, in greater detail, the functional role of lysosomes in mammalian cell division.

4.2. Results

In this chapter pharmacological inhibitors known to target specific lysosomal functions were employed. In order to assess the impact of these agents on cell division, a quantitative analysis based on the quantification of bi/tetranucleate cells and cells linked by an intercellular bridge established by a previous study was implemented (Rajamanoharan *et al.* 2015). Division failure can cause the collapse of nascent daughter cells, without physical separation, initially into a binucleate cell and, if another failed round of mitosis occurs with the same fate, then into a tetranucleate structure, producing a state of polyploidy. Likewise, a significantly increased number of cells linked by a cytoplasmic bridge reflects abnormality in intercellular bridge stability or the inability of the cells to successfully complete abscission. The quantification was made on cells immunolabelled with tubulin antibody and co-stained with DAPI (**Figure 4.1.**). Where more applicable, the effect of certain drugs on mitosis was additionally examined using time lapse bright field imaging of treated and untreated cells.

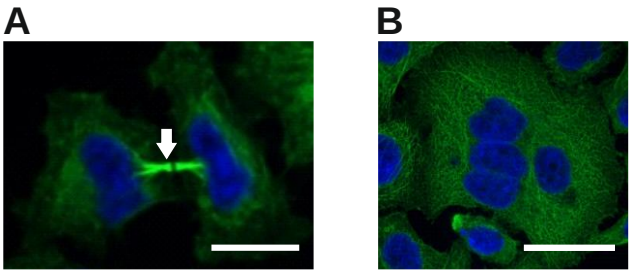

Figure 4.1. Representative confocal middle sections of HeLa cells used for analysis of mitosis failure. Following treatment, cells were fixed, permeabilised, and stained with DAPI and anti-tubulin antibody labelled with Alexa Fluor 488. The labelling of DNA and tubulin enabled the visualisation of tubulin-enriched intercellular cytoplasmic bridges during cytokinesis along with cells harbouring >1 nucleus (**A**, arrow) and allowed the detection of multinucleate cells (**B**). Z-stack imaging was performed on a spinning disk confocal microscope. Scale bars: 10 µm.

4.2.1. Inhibition of lysosomal hydrolase activity does not impair cell division

Degradation of extra- and intracellular particles is a widely studied function of lysosomes. Cathepsins are the most abundant class of lysosome-resident protein hydrolases, able to retain activity outside the acidic lysosome lumen (Appelqvist *et al.* 2013; Davidson and Vander Heiden 2017). In this section, the functional requirement of cathepsins during mitosis was examined. Cells were first treated with E64, a potent cell-permeable irreversible cysteine protease inhibitor which directly binds to cathepsins B and L (Li *et al.* 2013). NRK and HeLa cells treated with E64 did not display any failure in mitosis completion, detectable using the analysis outlined above, compared to the vehicle control (**Figure 4.2.**).

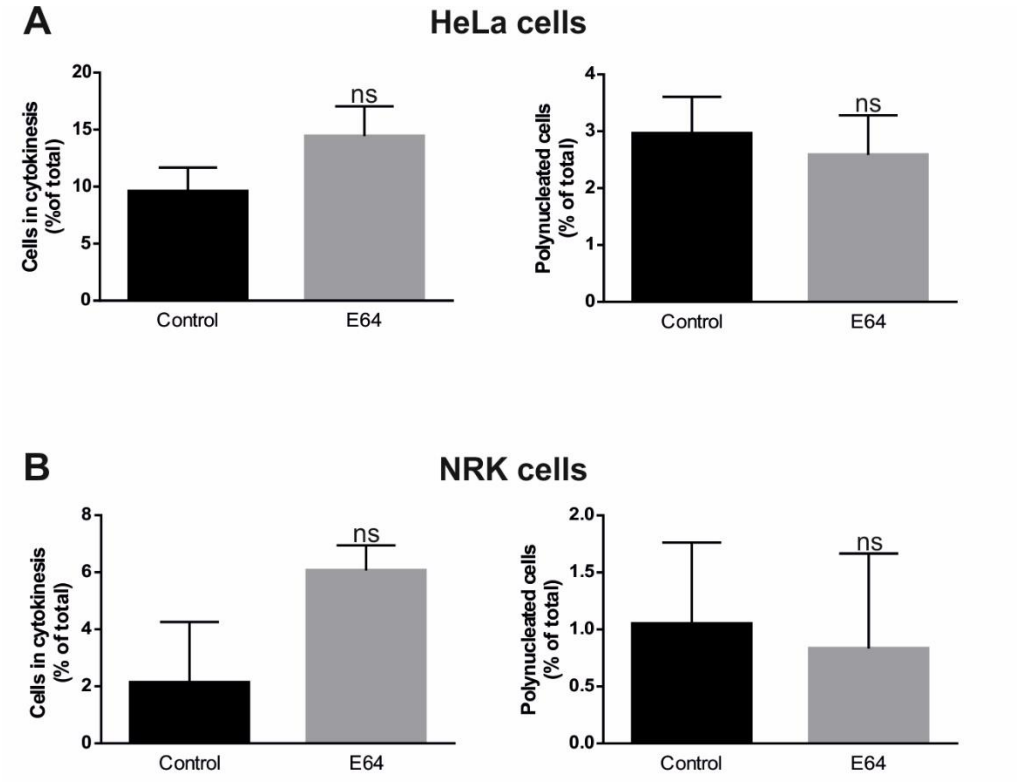

Figure 4.2. Inhibition of lysosomal cathepsins B and L by E64 has no negative impact on mammalian cell mitosis. Cells were treated overnight with 100 µM E64 (or untreated, control). The proportion of cells linked by an intercellular bridge during cytokinesis and the number of bi/tetranucleate cells were assessed. Unpaired student t-tests were performed, results shown as ± S.E.M, ns: not significant. **A.** HeLa cells; $n_{control}$ = 960 cells, n_{E64} = 909 cells, N = 6 independent experiments. **B.** NRK cells; $n_{control}$ = 521 cells, n_{E64} = 619 cells, N = 6 independent experiments.

Similarly cells incubated with pepstatin A, an inhibitor of the aspartic proteases cathepsins E and D (Fusek *et al.* 2013; Li *et al.* 2013; Zaidi and Kalbacher 2013) did not exhibit any detectable defects in cell division. The number of cells linked by an intercellular bridge and the proportion of bi/tetranucleated cells were not significantly raised under treatment with the inhibitor (**Figure 4.3.A**). In addition, the clustering of LAMP1-YFP positive lysosomes at either side of the cytoplasmic bridge during cytokinesis was not affected by pepstatin A treatment, showing that inhibition of cathepsins E and D does not alter the mitotic-specific positioning of the organelle (**Figure 4.3.B**).

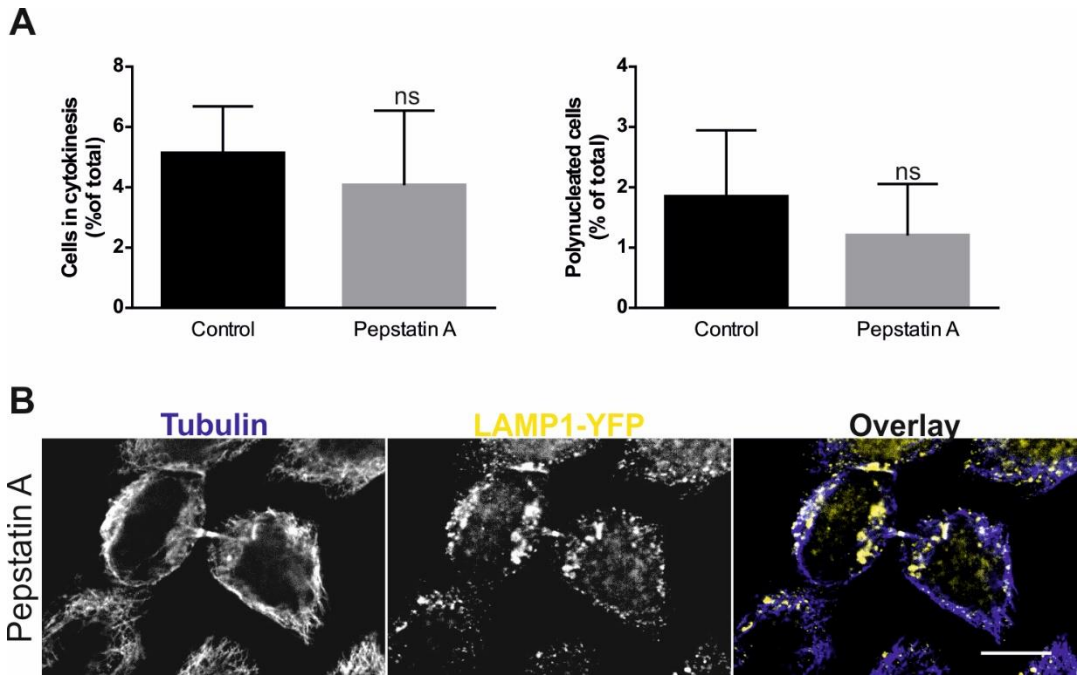

Figure 4.3. Inhibition of lysosomal cathepsins E and D by pepstatin A does not impair HeLa cell division and does not affect lysosome clustering during cytokinesis. A. Cells were treated overnight with 5 μM pepstatin A (or 0.1% DMSO, control), fixed, permeabilised and immunostained with anti-tubulin and DAPI. Cells in cytokinesis and bi/tetranucleated were quantified and presented in the graphs as % of total cell number. Unpaired student t-test was performed to determine statistical significance, results shown as ± S.E.M, ns: not significant; n_{DMSO}= 334 cells, $n_{Pepstatin}$ = 171 cells, N = 10. **B.** HeLa cells were transfected with LAMP1-YFP construct (yellow) targeting lysosomes and treated overnight with 5 μM pepstatin A. Following treatment, cells were fixed, permeabilised and immunostained with anti-tubulin tagged with Alexa Fluor 405 (blue). Cells were imaged on a confocal spinning disk microscope. Scale bars 10 μm.

4.2.2. The activity of the V-ATPase is not required for mitosis completion

Concanamycin-A (folimycin) was used to specifically inhibit the V-ATPase (Dröse and Altendorf 1997). Inhibition of the proton pump results in the dissipation of the lysosomal H^+ gradient, which in turn blocks Ca^{2+} uptake by the lysosomal H^+/Ca^{2+} exchanger (López-Sanjurjo *et al.* 2013). Alkalinisation of the organelle under concanamycin-A treatment was confirmed by time lapse imaging of HeLa cells transfected with LpH-mCh. Treatment with the drug proved reliable as it induced the progressive de-quenching of pHluorin

(marked by an increase in green fluorescence) (**Figure 4.4.**). Next analysis of concanamycin-A treated cells demonstrated that the number of cells in cytokinesis and the proportion of polynucleated cells were not significantly different from the control, untreated condition (**Figure 4.5.A**). This indicates that Ca^{2+} uptake by the lysosome and the V-ATPase activity are not essential requirements for mitosis completion. Furthermore imaging of fixed cells transfected with LAMP1-YFP revealed that lysosomes remained clustered near the cytoplasmic bridge during cytokinesis under treatment with the V-ATPase inhibitor (**Figure 4.5.B**).

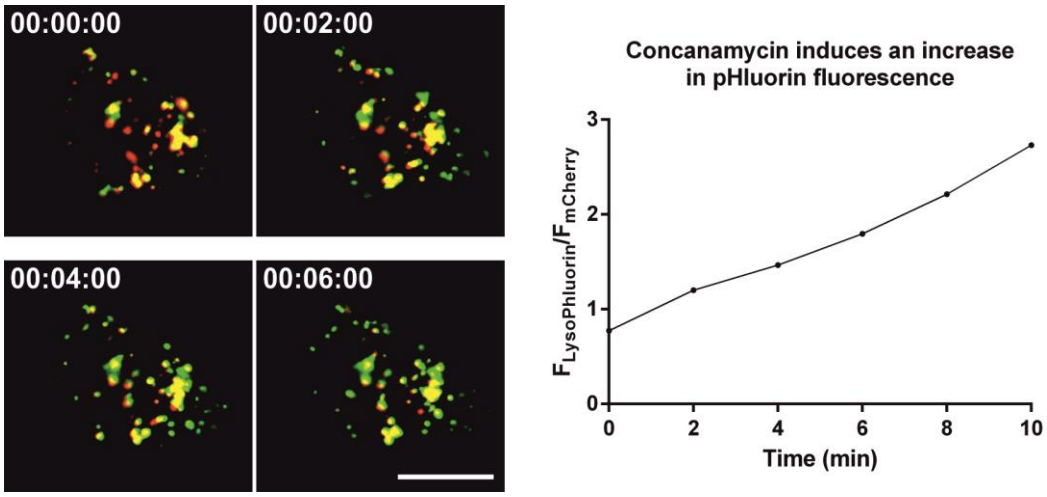

Figure 4.4. Concanamycin-A induces the collapse of the pH gradient in lysosomes. HeLa cells transfected with LpH-mCh were incubated with 25 nM concanamycin-A and imaged on a spinning disk confocal microscope at a rate of one frame every 2 min. Time shown as hr:min:s, scale bar: 10 µm. The graph depicts the LysopHluorin fluorescence ($F_{LysopHluorin}$) mCherry fluorescence ($F_{mCherry}$) ratio over imaging time.

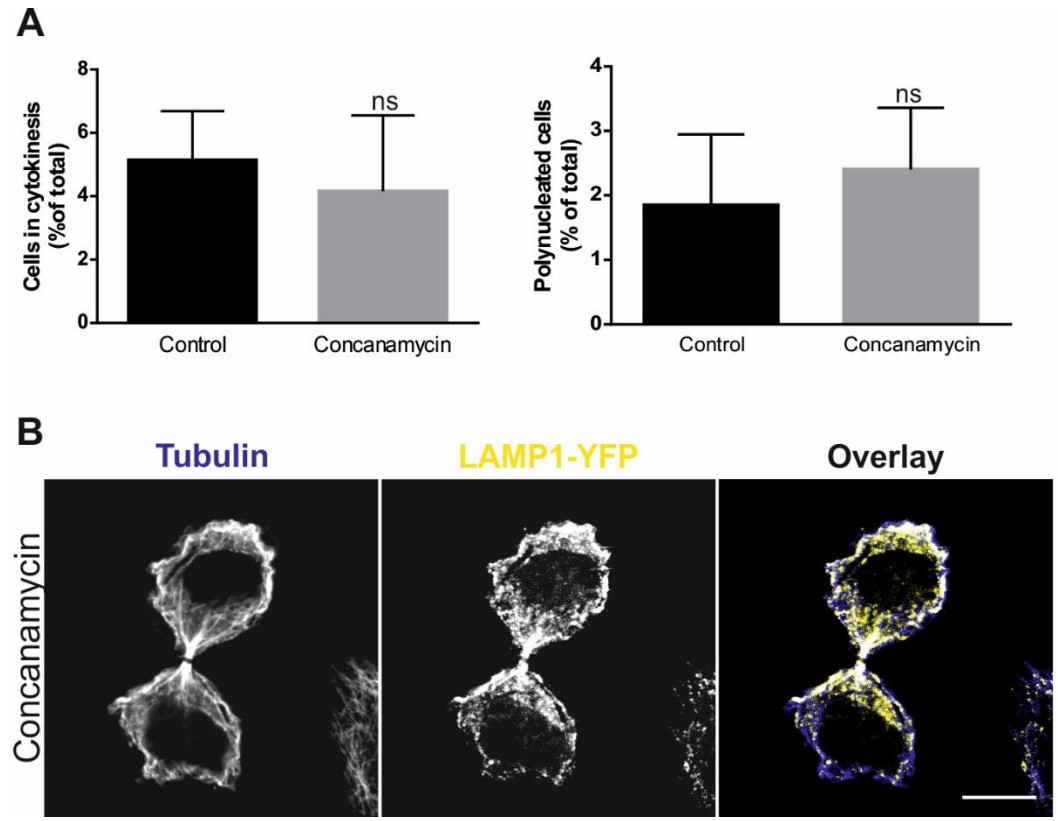

Figure 4.5. Concanamycin-A treatment has no significant impact on cytokinesis and does not disrupt lysosomal positioning in HeLa cells. A. Overnight treatment of cells with 25 nM concanamycin-A (or 0.1% DMSO, control) was followed by fixing permeabilisation and immunolabelling with anti-tubulin and DAPI. The proportion of cells in cytokinesis and polynucleated cells were calculated as % of total cell number and illustrated in the graphs. Statistical significance was calculated using unpaired student t-test, results shown as ± S.E.M, ns: not significant; n_{DMSO} = 334 cells, $n_{concanamycin}$ = 222 cells, N = 10. **B.** HeLa cells were transfected with LAMP1-YFP construct (yellow) and treated overnight with 25 nM concanamycin-A. Cells were subsequently fixed, permeabilised and immunolabelled with anti-tubulin tagged with Alexa Fluor 405 (blue). Imaging was performed on a confocal spinning disk microscope. Scale bars 10 µm.

4.2.3. Disruption of lysosomal membrane integrity impairs mitosis

Since neither the degradative nor calcium signalling functions of lysosomes appeared essential for mitosis completion, the exocytic properties of the organelle were scrutinised. Two pharmacological agents were employed here to alter the physical properties of lysosomes: Vacuolin-1 (Vacuolin) and glycyl-

L-phenylalanine 2-naphthylamide (GPN). Vacuolin affects membrane traffic and induces the formation of enlarged vesicles resulting from the homotypic fusion of lysosomes and endosomes (Jadot *et al.* 1984; Cerny *et al.* 2004). GPN is a substrate of the lysosomal hydrolase cathepsin C. The resulting hydrolysis product is insoluble in the lysosome lumen and causes osmotic swelling and lysis of the organelle (Berg *et al.* 1994). Cytokinesis failure was only observed under GPN treatment; this drug significantly increased the number of cells linked by a cytoplasmic intercellular bridge as well as the proportion of bi/tetranucleate cells (**Figure 4.6.A**). Cell incubation with vacuolin on the other hand slightly decreased the number of cells in cytokinesis but had no significant impact on the proportion of polynucleated cells (**Figure 4.6.A**). Note that vacuolin treatment induced the formation of enlarged vacuolar structures, suggesting the drug worked effectively. Interestingly, whilst vacuolin did not impair division completion, it slightly affected lysosomal distribution during cytokinesis. Some LAMP1-YFP tagged structures examined by confocal microscopy concentrated near the cytoplasmic bridge whereas others appeared scattered in the cytosol and in areas surrounding enlarged vesicles (**Figure 4.6.B**, top panels). Under GPN treatment, lysosome clustering remained unaffected at cytokinesis (**Figure 4.6.B**, bottom panels).

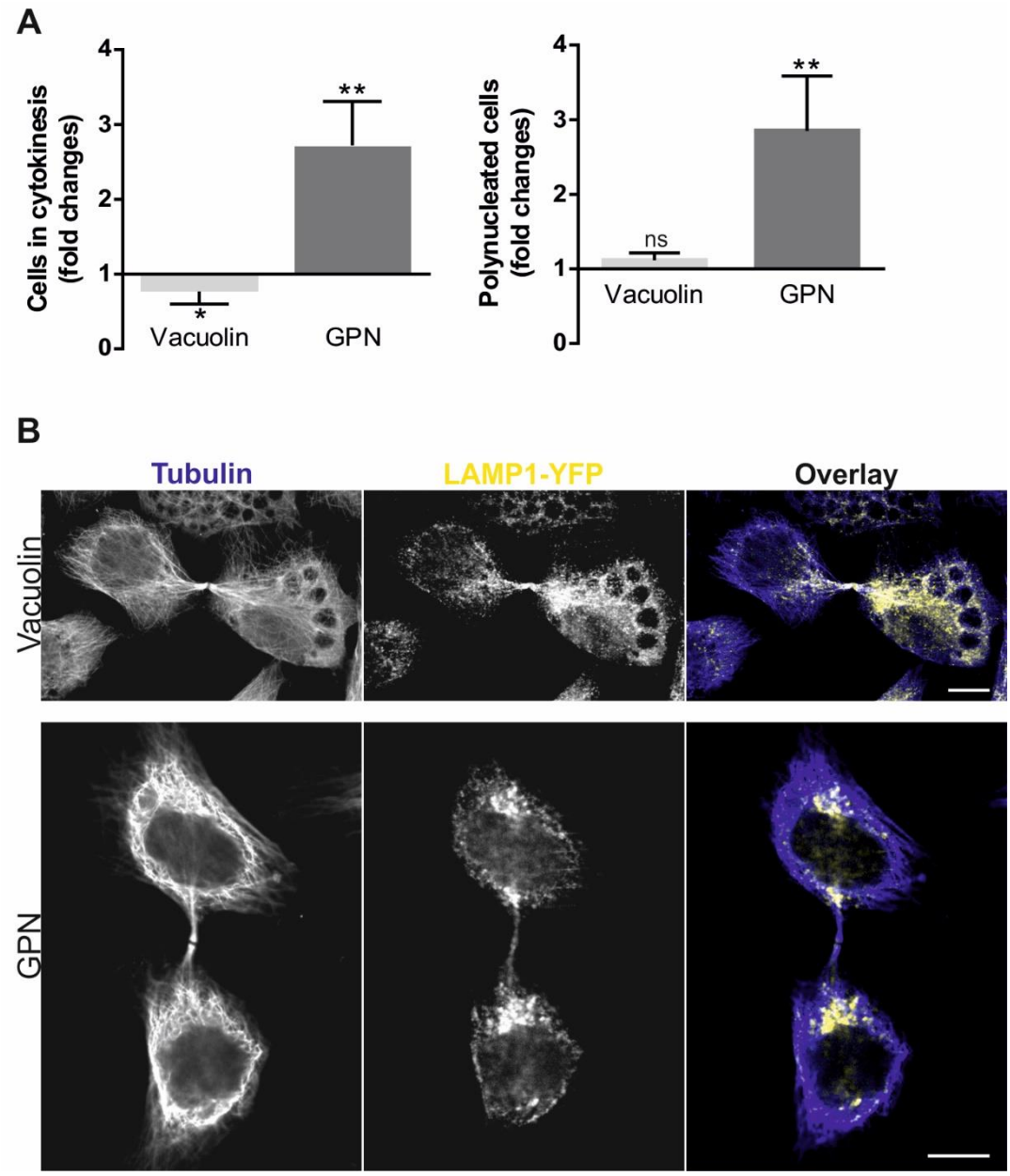

Figure 4.6. GPN but not Vacuolin triggers significant division defects in HeLa cells. A. Cells were treated overnight with 1 µM Vacuolin (or 0.1% DMSO, control) or with 50 µM GPN (or 0.1% DMF, control), fixed, permeabilised and tubulin and Dapi stained. Fold changes in the number of cells in cytokinesis (N = 12 independent experiments, *p = 0.0298 and **p = 0.006) and polynucleated cells (N = 8 independent experiments, **p = 0.001, ns = not significant) under treatment with the drugs compared to their respective vehicle control are represented. Unpaired student t-tests were performed (drug versus respective vehicle control) and results shown as mean ± S.E.M. n_{DMSO} = 1250 cells, $n_{Vacuolin}$ = 1560 cells, n_{DMF} = 1322 cells, n_{GPN} = 1648 cells. **B.** Following transfection with LAMP1-YFP construct, HeLa cells were treated overnight with either 1 µM Vacuolin or with 50 µM GPN. Cells were then fixed,

permeabilised and immunostained with anti-tubulin tagged with Alexa Fluor 405. Imaging was carried out on a confocal spinning disk microscope. Scale bars 10 μm.

4.2.4. Lysosome exocytosis is essential in cell division

In order to examine in more detail the importance of lysosome membrane fusion in cell division, cells were treated with N-ethylmaleimide (NEM). This compound is known to inhibit the hexameric ATPase NEM-sensitive factor (NSF), a component of the membrane fusion machinery responsible for most vesicular fusion events (Block *et al.* 1988; Band *et al.* 2001; Sivaramakrishnan *et al.* 2012). The inhibitory effect of NEM on lysosome fusion was first verified in lucifer yellow-loaded BSC-1 cells. Under NEM treatment, cells exhibited significantly reduced lysosome exocytosis (**Figure 4.7.A**). Next the effect of NEM on mitosis in synchronised cells was examined by bright field time lapse imaging. NEM abolished cell division, a result that was statistically significant, compared to synchronised untreated cells (**Figure 4.7.B**). Under NEM treatment some cells became pre-mitotic (spherical appearance, time = 00:00:00) but remained trapped at that stage throughout the duration of imaging (time = 02:20:00), whereas most of the control cells that rounded up at the start of imaging fully divided over the same time period (**Figure 4.7.C**).

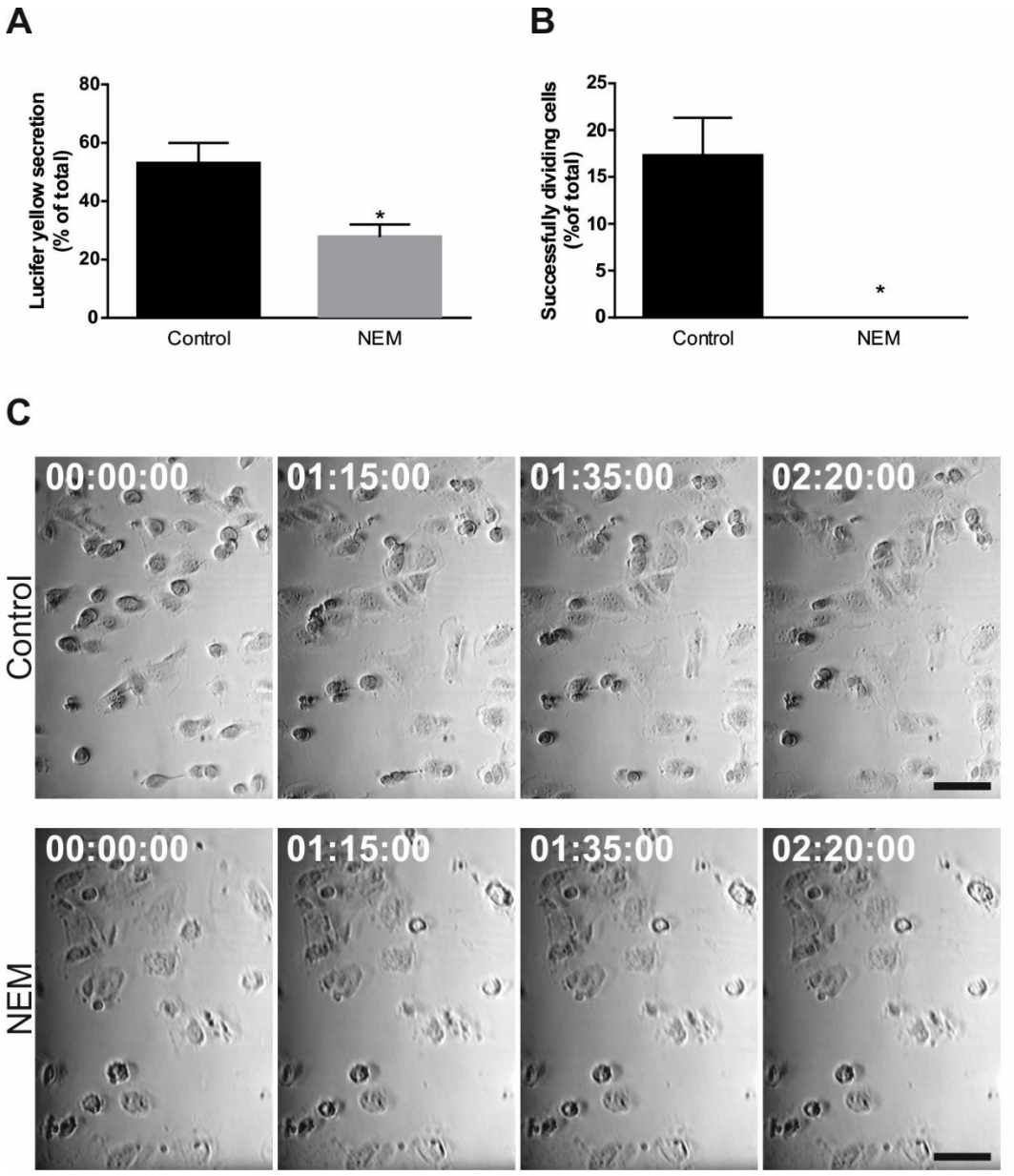

Figure 4.7. NEM blocks BSC-1 cell division. A. Cells were incubated with 1 mg/ml lucifer yellow (LY) for 4 hours (pulse) and further incubated in fresh, LY-free, medium for 2 hours (chase). Subsequently cells were treated with 1 mM NEM (or 0.1% (v/v) Ethanol, control) for 15 min and LY secretion was assessed as % of total (% $LY_{secreted}$ = (LY_{medium}*100)/($LY_{intracellular}$ + LY_{medium})). Statistical significance was calculated using unpaired student t-test, results shown as mean ± S.E.M. (*p = 0.0370, N = 3). **B.** BSC-1 cells were synchronised using thymidine-nocodazole block. Cells were then released from the last block and treated with 1 mM NEM (or 0.1% Ethanol, control) for 15 min. Straight after treatment, cells were imaged and the % of cells successfully completing mitosis was determined. Unpaired student t-test was performed between treated and untreated conditions, results are represented as mean ± S.E.M. (*p = 0.0130, N = 3, $n_{Ethanol}$ = 247 cells, n_{NEM} = 217 cells). **C.** Representative time lapse

bright field images of synchronised NEM-treated (or treated with 0.1% Ethanol, control) BSC-1 cells before (00:00:00), during (01:15:00 and 01:35.00) and after (02:20:00) cell division. Bright field imaging was performed on a spinning disk confocal microscope at a rate of 1 frame every 5 min for 2.3 hours. Time shown as hr:min:sec, scale bars: 100 µm.

4.3. Discussion

In this work the function of lysosomes during mitosis was examined. Initially, lysosomal proteolytic activity was investigated with rationale being that cathepsins are known to play roles outside of the degradation of extracellular particles from endocytosis and of intracellular components from autophagy. These enzymes have the ability to remodel the extracellular matrix (ECM), a process involved in the facilitation of plasma membrane repair (Castro-Gomes *et al.* 2016), proliferation, regulation of cell morphogenesis, migration and differentiation (Bonnans *et al.* 2014). Pepstatin A and E64 target the most abundant lysosomal proteases, namely cathepsins E, D, B and L. The proteolytic activity of these enzymes appeared to be dispensable for mitosis completion as their irreversible inhibition did not induce mitotic defects. However the potential role of other lysosomal hydrolases in cell division cannot be ruled out based on the results shown here; an exhaustive study on lysosomal enzymes would constitute a more rigorous approach towards elucidating the potential catalytic requirement of lysosomes in mitosis. What these data certainly do highlight however is that whatever function of lysosomes is required during mitosis, this is distinct from their role during PM wound repair which requires activity of cathepsins B,D and L (Castro-Gomes *et al.* 2015). It is important to note that the absence of negative impact on cytokinesis under pepstatin A and E64 treatment could also result from drugs inefficiency. Future experiments should involve parallel measurement of cathepsins E, D, B and L enzymatic activity in order to confirm the efficacy of both inhibitory drugs.

Imaging of cells expressing LAMP1-YFP and treated with pepstatin A demonstrated that lysosomal positioning and clustering at either side of the

cytoplasmic bridge during cytokinesis was retained, suggesting that lysosomal trafficking and re-distribution during the late stages of cell division is also independent of activity of cathepsins D and E.

The effect of changing lysosome luminal pH on cell division were next tested. Disruption of V-ATPase activity by concanamycin-A leads to various degrees of alkalinisation of the organelle (Xu and Ren 2015), depending on the proton leak conductance of the organelle (Galione *et al.* 2010). In this study, inhibition by concanamycin-A did not affect mitosis completion, suggesting that lysosome acidification and Ca^{2+} function are unlikely to be involved in cell division. In addition, it further reinforces the idea that some lysosomal enzymes, which normally require an acidic environment for optimal function, are not required for mitosis completion.

In addition to alkalinising the organelle, inhibition of the V-ATPase dissipates the proton gradient necessary for Ca^{2+} uptake by the lysosome (López-Sanjurjo *et al.* 2013). Here, data is presented where concanamycin-A was used uninterruptedly over a prolonged period of time, which should prevent lysosome Ca^{2+} refilling. Previous studies demonstrated that pre-treatment with bafilomycin A1, an inhibitor of the V-ATPase analogous to concanamycin-A, abolished both NAADP-stimulated Ca^{2+} release (Galione *et al.* 2010) and ML-SA1-induced Ca^{2+} response (Shen *et al.* 2012). As a consequence of lysosomal Ca^{2+} depletion, concanamycin-A should therefore prevent Ca^{2+} release by TPC2 and TRPML1. Ca^{2+} has been shown to be necessary in some mitotic steps such as nuclear envelope breakdown in fibroblasts (Kao *et al.* 1990) and chromatin condensation in sea urchin embryos (Twigg *et al.* 1988). No mitotic defect was observed under chronic concanamycin-A treatment, suggesting that lysosomes do not act as a Ca^{2+} source during mitosis. However, in a previously published study, a Ca^{2+}-ATPase activity has been monitored on lysosomes, thus the use of the proton gradient might not be the sole route of Ca^{2+} entry into lysosomes (Patel and Docampo 2010). To date the nature of the Ca^{2+}-ATPase remains elusive. If it were to be identified, complementary inhibition of the Ca^{2+} pump should therefore be performed in conjunction with concanamycin-A treatment in order to draw more rigorous conclusions. Alternatively, Ca^{2+} release by lysosomes could be targeted in this

cell division study using Ned19, a compound that blocks NAADP-dependent Ca^{2+} release (Rah *et al.* 2017).

Although still controversial and in conflict with previous studies (Churchill *et al.* 2002), Ca^{2+} refilling of lysosomes is thought to be permitted by membrane contact sites with the ER, even under pharmacological alteration of their proton gradient (Garrity *et al.* 2016). Due to the tight clustering and accumulation of lysosomes at cytokinesis, close contact sites between the ER and lysosomes would be difficult to identify using confocal microscopy. Higher resolution imaging such as electron microscopy of cells at cytokinesis would greatly help determine the existence of such contact microdomains. Aditionally, engineering a Ca^{2+} indicator targeted to the lysosomal lumen would help identify fluctuations in lysosomal Ca^{2+}. This coupled to correlative live imaging of ER and lysosomal markers would greatly enhance our knowledge of lysosomal Ca^{2+} changes in regards to the ER-lysosome microdomains. However Ca^{2+} imaging in acidic compartments remains challenging since low pH affects the Ca^{2+} binding affinity of Ca^{2+} indicators (Christensen *et al.* 2002).

Whilst inhibition of cathepsins and V-ATPase activity had no apparent impact on mitosis completion, impairment of lysosomal membrane properties by GPN had demonstrable effects. Treatment of HeLa cells with GPN, a pharmacological agent that induces osmotic swelling of lysosomes and subsequent membrane perforation of the organelle (Jadot *et al.* 1984; Berg *et al.* 1994) significantly increased the frequency of cells connected by an intercellular bridge and cells with 2n copies of the nucleus, suggesting that integrity of the lysosome membrane is likely to play a role in normal cytokinesis completion. As shown by immunofluorescence imaging, the lysosomal clustering at either side of the cytoplasmic bridge during cytokinesis remained unaffected in cells expressing LAMP1-YFP and treated with GPN. Thus the compound alters lysosomal membrane properties essential for mitosis completion, without affecting the organelle trafficking and re-positioning near the site of cytoplasmic constriction.

Due to its osmotic properties, GPN was used in previous studies as a Ca^{2+}-mobilising agent acting at the lysosome (Shen *et al.* 2012). Thus here

overnight treatment with the compound should chronically deplete lysosomes of Ca^{2+}. Given that previous concanamycin-A treatment did not affect division, it is reasonable to assume that the defects in cell division under GPN treatment do not arise from a lysosomal Ca^{2+} depletion but rather from the alterations of the lysosomal membrane *per se*.

Lysosomal properties were modified using a second pharmacological agent, vacuolin. The drug induces the homotypic fusion of lysosomes, giving rise to enlarged intracellular vesicles (Jadot *et al.* 1984; Cerny *et al.* 2004). The functional impairment of lysosomes by vacuolin is still controversial. The compound was first thought to inhibit Ca^{2+}-stimulated exocytosis (Cerny *et al.* 2004) however a later study showed that despite affecting lysosome morphology, the molecule does not alter the ability of lysosomes to undergo fusion with the PM (Huynh and Andrews 2005). Here, overnight treatment did not have a detectable negative effect on mitosis, suggesting that the vacuolin-induced morphological changes of lysosomes are not sufficient to interfere with this specific process.

Deciphering the way in which GPN and vacuolin affect lysosomal behaviour and identity would greatly improve our knowledge of lysosomal function in mitosis. Overall, treatment with vacuolin and GPN demonstrated that lysosomal membrane integrity is key to successful cell division.

These observations logically led to an examination of a known lysosomal function requiring lysosomal membrane integrity, exocytosis. In order to impair lysosome exocytosis, NEM was used. This compound inhibits vesicular fusion events dependent upon the hexameric ATPase NSF (Block *et al.* 1988; Band *et al.* 2001; Sivaramakrishnan *et al.* 2012) and significantly reduced lysosome exocytosis at the PM. In addition, this reduction of exocytosis was accompanied by a complete blockade of BSC-1 cell division, suggesting that vesicular fusion events are key to cytokinesis completion. Whether the sole inhibition of lysosome exocytosis is enough to induce cytokinesis defects remains to be fully investigated. A more thorough study should be carried out by inhibiting the specific components responsible for lysosome exocytosis,

such as Syt VII, since NEM inhibition is not restricted specifically to lysosome fusion and affects all vesicular fusion events.

Lysosome exocytosis has many purposes including secretion of specific factors (Nickel and Rabouille 2009) and repair of the PM (Reddy *et al.* 2001; Castro-Gomes *et al.* 2016). Under conditions of plasma membrane injury, lysosome exocytosis is thought to alleviate plasma membrane tension and favour spontaneous repair of the wounded lipid bilayer (Reddy *et al.* 2001). In Streptolysin-O-induced plasma membrane injury, lysosomes exocytose at the site of injury leading to the release of lysosomal cysteine proteases which act extracellularly to promote PM remodelling and subsequent wound repair (Castro-Gomes *et al.* 2015). However this is only applicable in circumstances where the extent of membrane damage is limited. A second hypothesis proposes that lysosomes give rise to larger structures by homotypic fusion and form a “patch” over the injured area (Idone *et al.* 2008). In addition to conferring the cell the ability to reseal its membrane, lysosomes, by acting as membrane donors during exocytosis, also offer the cell the possibility to increase cell surface area. This property is of particular interest during the late stages of mitosis, since the formation of the nascent daughter cells requires addition of extra membrane. Boucrot and Kirchhausen (Boucrot and Kirchhausen 2007) have demonstrated that the onset of mitosis was marked by a rounding up of the cells necessary for appropriate spindle formation, accompanied by membrane endocytosis and decrease in secretory traffic; conversely, they suggested that from anaphase to cytokinesis, new membrane, stored in intracellular compartments, speculated to be endosomes, was added to the cell surface via Ca^{2+}-mediated exocytosis. Lysosomes exhibit all of the functionality required to be considered a candidate organelle in the deposition of extra membrane during the late steps of cellular division and the evidence provided in this chapter are fully consistent with this hypothesis.

4.4. Summary

In this chapter, the functional significance of lysosomes during cell division was examined using a pharmacological approach. Results suggest that the

catalytic activity of the most abundant lysosomal cathepsins, required for PM wound repair, is not required during mitosis. Importantly this further indicates that exocytosis during wound repair is mechanistically distinct from the exocytosis that occurs during mitosis. Likewise V-ATPase function and potentially lysosomal Ca^{2+} are not essential in mammalian cell division. Lysosome exocytosis was identified as a potential key function involved in normal mitosis completion, since inhibition of the organelles fusogenic properties was accompanied by mitosis defects. Lysosome exocytosis in the context of cell division is therefore the focus of the next chapter.

Chapter 5: Investigating lysosome exocytosis in cell division

5.1. Introduction

5.1.1. Cell reshaping during cell division

Cell division/mitosis is the fundamental process by which a single cell produces two genetically identical daughter cells. The mitotic M phase, which encompasses a nuclear (mitosis) and a cytoplasmic (cytokinesis) division (Zheng *et al.* 2014) is essential for normal cell growth and development and replacement of any impaired, dying or senescent cells (Sancar *et al.* 2004). Therefore the incorrect orchestration of this crucial process may have catastrophic consequences and lead to various diseases including cancer (Dominguez-Brauer *et al.* 2015).

Division of adherent cells necessitates a high degree of cellular reshaping driven by the interplay of local formation of protein complexes, remodelling of the cytoskeleton, changes in lipid composition and membrane trafficking (Cauvin and Echard 2015). The drastic changes in cell morphology are particularly well illustrated in the late stages of cell division where the cytoplasm elongates and the cleavage furrow ingresses to form an intercellular cytoplasmic bridge eventually severed at abscission (D'Avino *et al.* 2015) (**Diagram 5.1.**). The plasma membrane must therefore develop mechanisms to accommodate the surface area increase that drives daughter cell formation. A process of folding and unfolding of the plasma membrane was observed in some cell types (Porter *et al.* 1973; Erickson and Trinkaus 1976). However there is growing evidence that cellular organelles donate the additional membrane needed to increase cell surface area (Drechsel *et al.* 1997) and endosomes and Golgi-derived vesicles were identified as potential mediators for membrane expansion (Boucrot and Kirchhausen 2007; Goss and Toomre 2008).

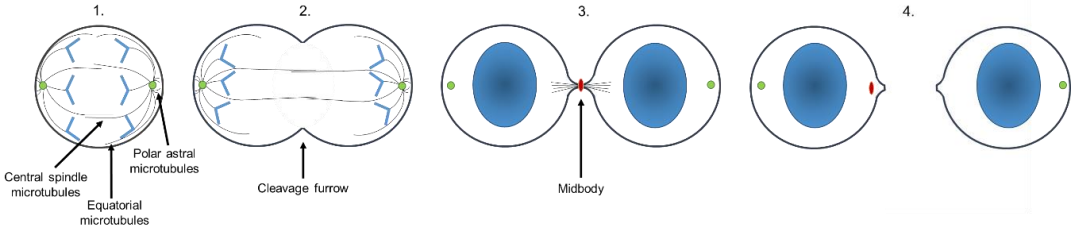

Diagram 5.1. The stages of cytokinesis. 1. The site of cytoplasmic separation is defined by the three types of microtubules highlighted which activate the small GTPase RhoA at the site of the future furrow. 2. An actomyosin ring forms around the cleavage zone and ingression starts. 3. The microtubule-containing midzone is compacted, giving rise to a tubulin-rich intercellular bridge. A dense structure, the midbody, forms by accumulation of kinesin-like motor proteins and chromosomal passenger proteins. 4. The cytoplasmic bridge narrows and abscission completely separates the two daughter cells. Proteins implicated in trafficking and fusion processes are required during abscission. Adapted from (Normand and King 2010).

5.1.2. Lysosomes

Lysosomes are multifaceted intracellular compartments responsible for a wide variety of complex cellular tasks ranging from cellular metabolism, catabolism of cellular debris, autophagy and Ca^{2+} signalling (Luzio *et al.* 2007; Kilpatrick *et al.* 2013; Wartosch *et al.* 2015). In addition, the organelle can undergo Ca^{2+}-dependent exocytosis (Rodríguez *et al.* 1997), which contributes to the repair of mechanical (Reddy *et al.* 2001) and toxin-mediated injury (Castro-Gomes *et al.* 2016) of the plasma membrane.

5.1.3. Mechanisms of lysosome exocytosis

Once tethered in close proximity to the PM, the docking of lysosomes proceeds with the formation of a trans-SNARE complex between Vamp7 on the lysosome surface, syntaxin4 and SNAP23, two SNARE proteins on the PM (Samie and Xu 2014). The formation of this complex, which stably attaches lysosomes to the plasma membrane, is regulated by a rise in intracellular Ca^{2+}. This Ca^{2+} elevation is detected by the C2A domain of lysosomally associated

synaptotagmin VII, which subsequently interacts with SNAP23, via Syntaxin4, to further dock the lysosomes at the plasma membrane (Rao *et al.* 2004). As investigated by Rodriguez and co-workers, an intracellular Ca^{2+} concentration of between 1 and 5 µM is sufficient to induce lysosome exocytosis in cells permeabilised with the toxin streptolysin O (Rodríguez *et al.* 1997). During plasma membrane injury, the intracellular rise in Ca^{2+} is likely to be due to a Ca^{2+} influx from the extracellular space through the wounded area (Samie *et al.* 2013). In intact cells where lysosomal exocytosis is potentially required, the source of Ca^{2+} has been proposed to be the lysosome itself. Although controversial, the release of Ca^{2+} from the lysosome is thought to be mediated by the TRPML channel (Samie and Xu 2014). Indeed lysosome exocytosis increases significantly in macrophages treated with the pharmacological agent ML-SA1, a TRPML synthetic agonist. Therefore TRPML-regulated Ca^{2+} release is sufficient to induce exocytosis in professional secretory cells (Samie *et al.* 2013). Whether TRPML activation is essential for the exocytosis of conventional lysosomes remains to be investigated, as Ca^{2+} release from the TRPML channel is supposedly bypassed in ionomycin-mediated and in plasma membrane wound-induced exocytosis. Docked lysosomes subsequently fuse with the PM, releasing their luminal content into the extracellular space and exposing the luminal domains of trans-membrane proteins to the cell surface (Pu *et al.* 2016).

The fusogenic properties of lysosomes are thought, in part, to be regulated by phosphoinositides, a relatively rare class of cellular phospholipids found on various cellular organelles and which exert important signalling and cell biological functions (Samie and Xu 2014). The reversible phosphorylation of the inositol ring of phosphatidylinositol can give rise to seven unique types of phosphoinositide (Tan *et al.* 2015). Among them, $PI(3,5)P_2$ localises to the lysosomal membrane and is thought to aid fusion by facilitating the mixing of lipid bilayers and activating the TRPML channel (Shen *et al.* 2011; Samie and Xu 2014).

5.1.4. Mechanical properties and relevance of lysosome exocytosis in cell division

Through the process of exocytosis, lysosomes release the tension caused by plasma membrane injury and facilitate plasma membrane repair (Castro-Gomes *et al.* 2015).

Interestingly recent work has demonstrated that during the late stages of cell division, lysosomes behave in a highly organised and temporally coordinated manner by accumulating at either side of the intercellular cytoplasmic bridge. Additionally inhibition of this clustering via a PI4KIIIβ-dependent pathway caused mitotic failure, suggesting that the organelle is functionally and locally required in the late phases of division (Rajamanoharan *et al.* 2015). Cells undergo drastic changes in morphology and size during cell division, and similar to conditions of injury, are subjected to mechanical deformation. Lysosomes, by acting as a membrane donor could therefore contribute to the dynamic adjustment of plasma membrane surface area as cells approach cytokinesis. This hypothesis is investigated in this chapter using a combination of biochemical, immunofluorescence and higher resolution imaging techniques. Furthermore, the role of PI4KIIIβ in exocytosis and mitosis is explored in further detail.

5.2. Results

5.2.1. Lysosomal proteins are detected at the cell surface during mitosis

Upon exocytosis, lysosomes expose the luminal domains of their integral membrane proteins to the cell surface (Pu *et al.* 2016). A biotinylation assay utilising a cell impermeant biotinylation reagent followed by resin affinity purification allowed the separation of the membrane-(surface) and cytosolic-protein fractions of HeLa cells. The assay was first verified by Western blot analysis of the two cell fractions using anti-actin (cytosolic marker) and anti-EGFR (membrane marker) antibodies. The results showed that the surface fraction was enriched with EGFR whereas actin expression was largely

confined, as expected, in the cytosolic cell fraction (**Figure 5.1.A**). Having validated the assay, two populations of HeLa cells were prepared: a synchronous sample mainly composed of mitotic cells and an asynchronous sample comprising predominantly interphase cells. Western blot analysis of the biotinylated membrane fraction and non-biotinylated cytosolic protein from the two cell populations revealed that when total LAMP1 levels were quantified by normalisation to internal tubulin loading controls within respective sample sets, LAMP1 expression was increased ~7-fold in mitotic cells. It further highlighted the presence of LAMP1 at the surface of mitotic cells which, in contrast, was undetectable in the biotinylated membrane fraction of asynchronous cells (**Figure 5.1.B**).

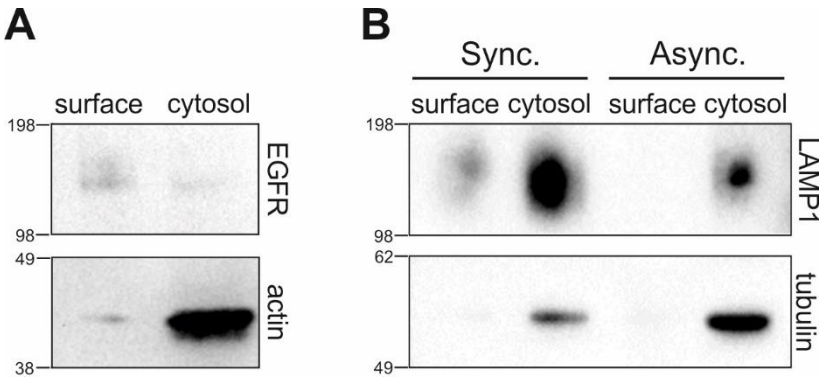

Figure 5.1. LAMP1 expression is increased and detected at the cell surface during cell division. A. Verification of HeLa cell surface labelling. Following biotinylation of surface proteins with the cell impermeant cross-linker sulfo-NHS-SS-biotin, cells were lysed, incubated with and subsequently eluted from streptavidin agarose affinity resin. The biotinylated surface proteins and the non-biotinylated cytosolic fraction were blotted with antibodies directed against a cytoplasmic protein, β-actin (predicted size: 42 kDa), and a cell surface receptor, EGFR (predicted size: 175 kDa). **B.** HeLa cells were treated with a thymidine-nocodazole block (Synchronous, Sync.). Cells were released from the last block and monitored by light microscopy to determine entry into mitosis. Asynchronous HeLa cells (Async.) were also analysed for comparison purposes. The surface accessible protein fraction of synchronous and asynchronous cells was captured by surface biotinylation and streptavidin affinity purification as previously described. Post-streptavidin cell lysates

(non-surface, cytosol) were also prepared. Surface and cytosol fractions were analysed by Western blot using anti-LAMP1 and anti-β-tubulin antibodies. Predicted sizes: 120 kDa (LAMP1), 50 kDa (β-tubulin).

As a complimentary method to detect lysosomal proteins at the PM, surface immunofluorescence was performed. HeLa cells were transfected with LysopHluorin-mCherry (LpH-mCh), a construct targeted to the lysosomal membrane and composed of a luminal mCherry tag. mCherry fluorescence was used here to determine LpH-mCh localisation throughout the cell and anti-RFP antibody staining was performed in non-permeabilised cells to detect surface-accessible mCherry in interphase cells and in cells at cytokinesis (**Figure 5.2.A**). The surface LpH-mCh signal was then normalised to total cellular LpH-mCh signal. Consistent with the previous biotinylation data, the surface LpH-mCh signal was significantly increased in cells undergoing cytokinesis compared to interphase cells (**Figure 5.2.B**).

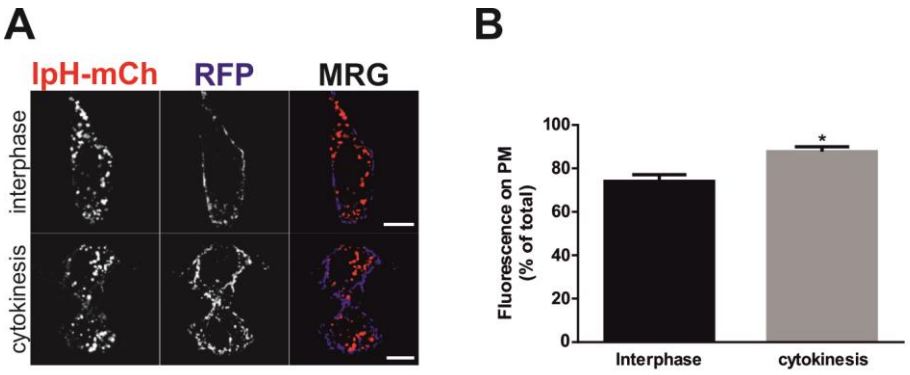

Figure 5.2. LpH-mCh fluorescence is detected and increased at the PM of HeLa cells during late telophase/cytokinesis. A. HeLa cells were transfected with LpH-mCh. Surface exposure of the luminal part of the construct (mCherry, red, proxy for lysosome exocytosis) was detected using rabbit anti-RFP (blue) and goat anti-rabbit Alexa 405 conjugated antibodies, prior to cell fixation without cell permeabilisation. Confocal images show deconvoluted middle sections at interphase and cytokinesis. Scale bars: 10 µm. **B.** Quantification of data from (**A**). The fluorescence of RFP at the membrane is expressed as % of total cellular fluorescence. Statistical significance

was determined using unpaired student t-test, results shown as mean ± S.E.M., p = 0.0115, n = 5 cells in interphase, n = 4 cells in late telophase/cytokinesis.

5.2.2. Lysosome exocytosis is stimulated by Ca^{2+}

In addition to exposing luminal domains of integral membrane proteins to the cell surface, lysosomes secrete their soluble content into the extracellular space upon exocytosis. Thus one way of assessing the extent of lysosome exocytosis is to quantify release of soluble luminal contents into the extra cellular space. N-Acetyl-β-D-glucosaminidase (NAG) is a lysosomal enzyme that catalyses the degradation of glycoproteins and glycolipids in mammalian cells. During lysosome exocytosis, the enzyme is released into the extracellular space. Thus the secreted enzyme activity can be used as a direct index of lysosome fusion with the plasma membrane (Samie and Xu 2014). As lysosomes in HeLa cells are not subjected to marked changes in exocytosis under stimulatory conditions, the enzymatic assay was performed on THP-1-derived macrophages (professional secretory cells) and NRK cells, previously characterised as having measurable levels of both basal and stimulated lysosome exocytosis (Bourbouze *et al.* 1991; Rodríguez *et al.* 1997; Sundler 1997). Under ionomycin treatment, both cell lines exhibited robust lysosome exocytosis, demonstrating that they are well suited to the NAG assay (**Figure 5.3.A** and **B**). In parallel, ionomycin treatment was optimised by using different incubation times with 10 µM ionomycin. The graph depicted in **Figure 5.3.C** shows that the maximal response to ionomycin was achieved after 5 min treatment with the drug following which a plateau was reached.

In conjunction with the enzymatic assay, a lucifer yellow (LY) pulse-chase experiment was also developed. The fluorescent dye, loaded into lysosomes via the endocytic pathway, has the advantage of being independent of anterograde protein trafficking towards the plasma membrane and is therefore less subject to bias (introduced from NAG synthesis and trafficking) compared to the NAG assay (Rodríguez *et al.* 1997). The assay proved reliable as a significant increase in LY was measured in cells treated with ionomycin (**Figure 5.3.D**).

Overall, these results confirmed the reliability of both NAG and LY biochemical assays and that lysosome exocytosis can be stimulated by increases in cytoplasmic Ca^{2+} concentration.

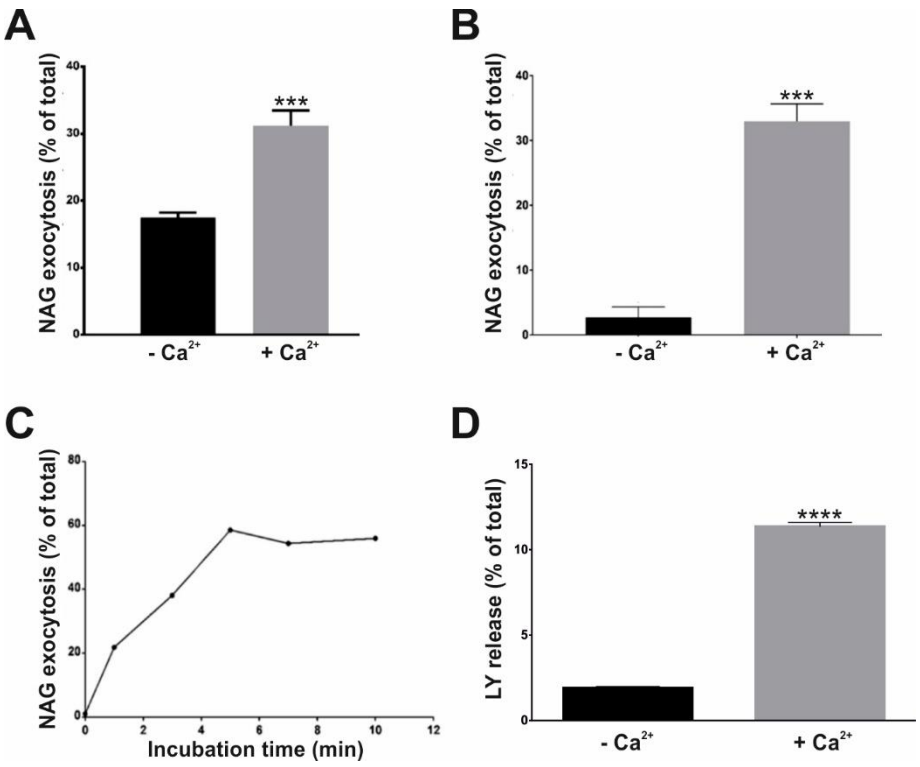

Figure 5.3. Validation and optimisation of NAG and lucifer yellow (LY) assays in mammalian cell lines. Macrophages (**A**) and NRK cells (**B**) were treated with 0.1% v/v DMSO + 0.1% v/v ethanol in PBS supplemented with 1 mM $CaCl_2$ (-Ca^{2+} condition) or 10 µM ionomycin in PBS containing 1 mM $CaCl_2$ (+Ca^{2+} condition) for 5 min (NRK) or 10 min (macrophages). The incubation buffer was harvested and cells were lysed. The NAG reaction was allowed for 15 min and absorbance was measured at 405 nm. The enzyme secretion was assessed as a percentage of total enzyme ((extracellular NAG*100)/(extracellular NAG + intracellular NAG)). Statistical analysis was carried out using an unpaired students t-test (THP-1: N = 6; NRK: N= 3) and the results are shown as mean ± S.E.M (***p=0.0001 in macrophages; ***p=0.0006 in NRK). **C.** NRK cells were treated with 10 µM ionomycin; cells were lysed and incubation buffers harvested at various time points. NAG secretion assay was performed as for (**A**) and (**B**). **D.** Macrophages were incubated with 1 mg/ml lucifer yellow for 4 hours (pulse) and further incubated in lucifer yellow-free culture medium for 2 hours (chase). They were subsequently bathed in a solution of 0.1 % ethanol in PBS (-Ca^{2+} condition) or with 10 µM ionomycin (+Ca^{2+} condition). Incubation buffers

were collected and cells were lysed. The fluorescence intensity of lucifer yellow was measured at 536 nm (excitation wavelength: 428 nm) and lucifer yellow release calculated as percentage of total ((extracellular LY*100)/(extracellular LY + intracellular LY)). Student unpaired t-test (N = 6); results shown as mean ± S.E.M, ****p<0.0001.

5.2.3. Lysosome exocytosis increases during cell division

In order to differentiate the levels of mitotic-specific LY release from LY exocytosis in interphase, LY was allowed to accumulate in lysosomes of cells either trapped in interphase with a double thymidine block or released to undergo division. Exocytosed LY was assessed at different time points: immediately (directly following the release from the second thymidine block in mitotic cells (t = 0 hour) or at 20 hours following the release (t = 20 hours) to allow synchronised cells to undergo a complete round of division. Cells arrested in interphase were processed at precisely the same time points, however they were maintained incubated in thymidine throughout the experiment. Mitosis- and interphase-specific LY releases were then calculated as fold changes between the t = 0 hour and t = 20 hour time points in each condition (mitosis and interphase). NRK cells demonstrated a significant increase in exocytosis during mitosis (**Figure 5.4**).

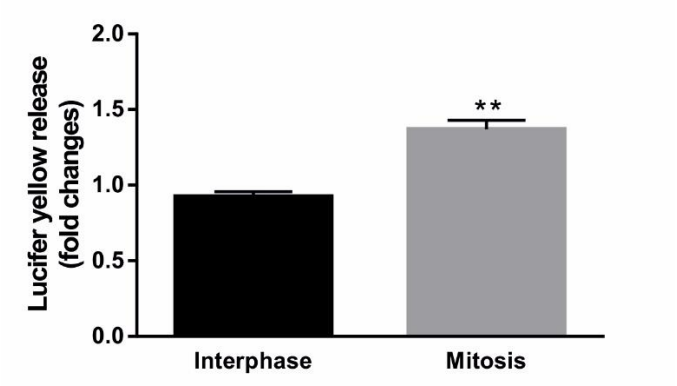

Figure 5.4. Lucifer yellow (LY) secretion increases during NRK cell division. All cells were synchronised using a double thymidine block and loaded with 1mg/ml LY

(12-hour pulse and 2-hour chase). After the second thymidine treatment, cells were maintained in thymidine (interphase) or released from the block (mitosis). LY secretion was measured immediately after the start of second release (time = 0 hour) and 20 hours post-release in both mitotic and interphase cell populations. The results are depicted as LY fold changes, from 0 to 20 hours after the second release. Results are shown as mean ± S.E.M., an unpaired student's t-test was performed for statistical significance, **p = 0.0029, N = 3.

In order to examine the reproducibility of LY increase during mitosis in other cell types, the assay was repeated in BSC-1 cells. BSC-1 cells proved less resilient than NRK cells in culture and more prone to cellular death under treatment. Since cellular death can be accompanied by a membrane rupture and the release of intracellular content in the extracellular space (Pérez-Garijo and Steller 2015), it can cause additional LY release and create false positive LY exocytosis. Therefore an examination of cell death using bright field imaging of thymidine blocked and released BSC-1 cells was performed in conjunction with the LY assay (**Figure 5.5.A** and **B**). No significant changes in cell death were observed between interphase and mitosis (**Figure 5.5.B**). Cell death data were subsequently subtracted from LY release values and consistent with the previous LY assay in NRK cells, BSC-1 cells exhibited a significant rise in lysosome exocytosis during mitosis, compared to the interphase control population (**Figure 5.5.C**).

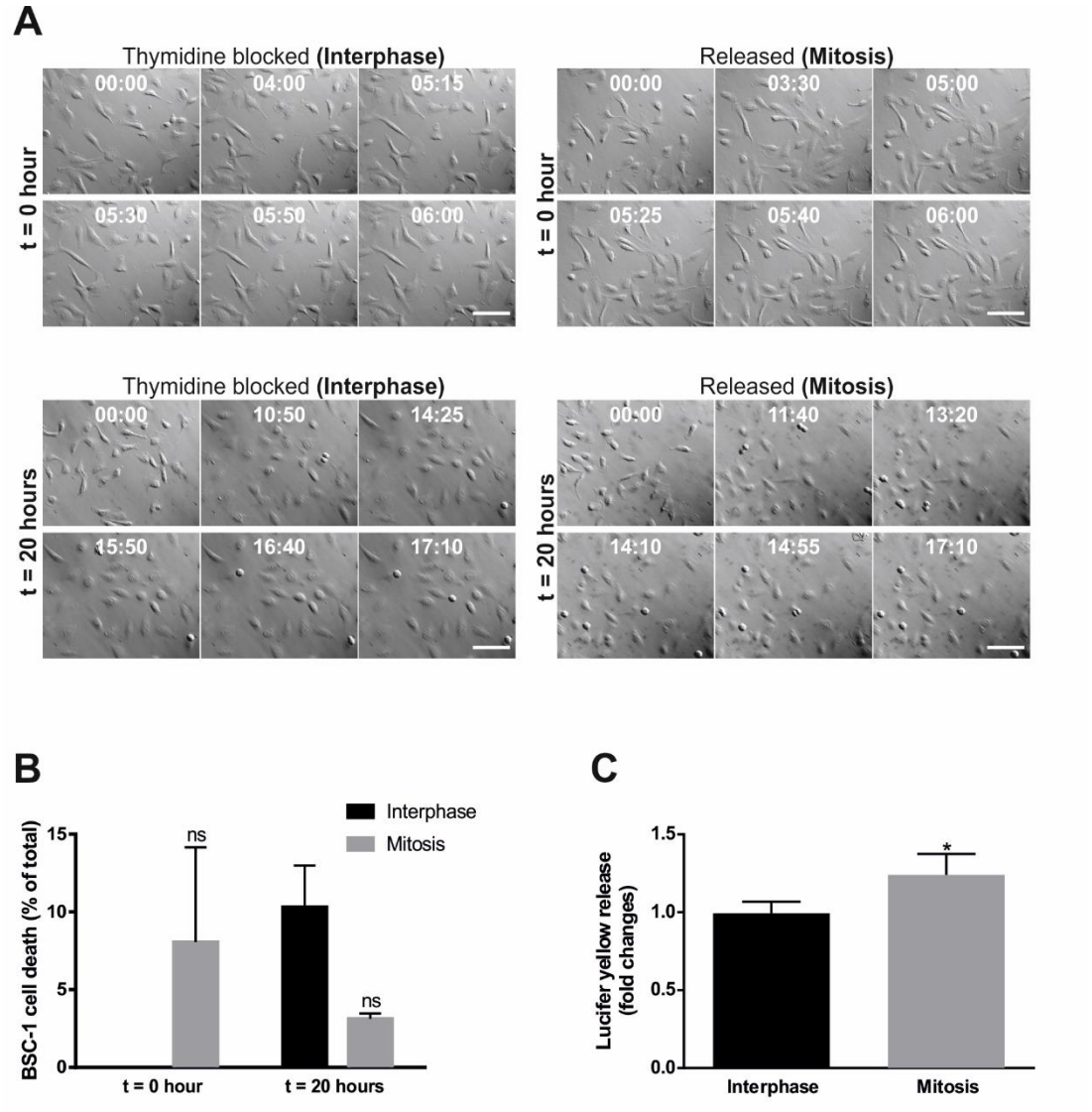

Figure 5.5. Lucifer yellow (LY) release is enhanced in mitotic BSC-1 cells, compared to interphase. A. Representative bright field images from each condition indicated in one triplicate for assessment of cell death. The time between the start of release from the last block in mitotic cells/the end of thymidine block in interphase cells and the start of the lucifer yellow assay is indicated at the left side of each panel. Time lapse imaging was carried out on a Zeiss apotome widefield system at a rate of 1 frame every 5 min. Imaging time is shown as hr:min, scale bars: 50 µm. **B.** Cell death quantified using bright field images was plotted as % of total cell number in all conditions and subtracted from LY secretion data. Data shown as mean cell death ± S.E.M. Unpaired student t-test was used to compare mitosis and interphase at t = 0 hour and t = 20 hours. N = 3, ns: not significant. **C.** LY release in mitotic and interphase BSC-1 cells after cell death subtraction. An unpaired student's t-test was used for analysis of statistical significance. Data represent mean fold changes ±

S.E.M. from t = 0 hour to t = 20 hours in interphase and in mitotic BSC-1 cells, N = 3, *p = 0.0494.

5.2.4. Lysosome exocytosis is detected in TIRF microscopy during late telophase/cytokinesis

Having acquired data indicating that lysosome exocytosis is increased as cells progress through mitosis, the process was next examined directly at the level of individual exocytic events in live cells using TIRF microscopy. The objective of this approach was twofold: 1. To visualise exocytosis and confirm its occurrence during mitosis and 2. To identify the precise mitotic stage at which exocytosis takes place.

TIRF microscopy (TIRFM) is a high resolution imaging technique based on the generation of an evanescent wave that excites fluorophores located in a narrow volume near the portion of PM that adheres to the glass interface (Axelrod 2003). Therefore the efficiency of sample illumination relies heavily on the cell adherence to the coverslip. Since NRK cells adopt a more adherent phenotype upon entry into mitosis, they were preferentially used for TIRFM analysis.

Lysosome exocytosis was first characterised in cells loaded with Lysotracker® using a previously described diffusion analysis (Goss and Toomre 2008). This technique is based on the measurement of the diffusion of a lysosomal fluorophore along a line drawn across the lysosome. It permits the distinction between true exocytosis and docking-undocking events without exocytosis. Upon lysosome fusion with the PM, the fluorescence of the dye (here Lysotracker®) first increased due to its close proximity with the PM and then decreased due to diffusion of the dye into the extracellular space, which was also marked by a spreading and widening of fluorescence across the line in subsequent imaging frames (**Figure 5.6.A**). In the case of docking/undocking the fluorescence of Lysotracker® increased upon movement of the lysosome towards the PM however subsequent decrease in fluorescence was accompanied by a narrowing of the dye fluorescence across the line due to lysosomal movement away from the PM and absence of fusion (**Figure 5.6.B**).

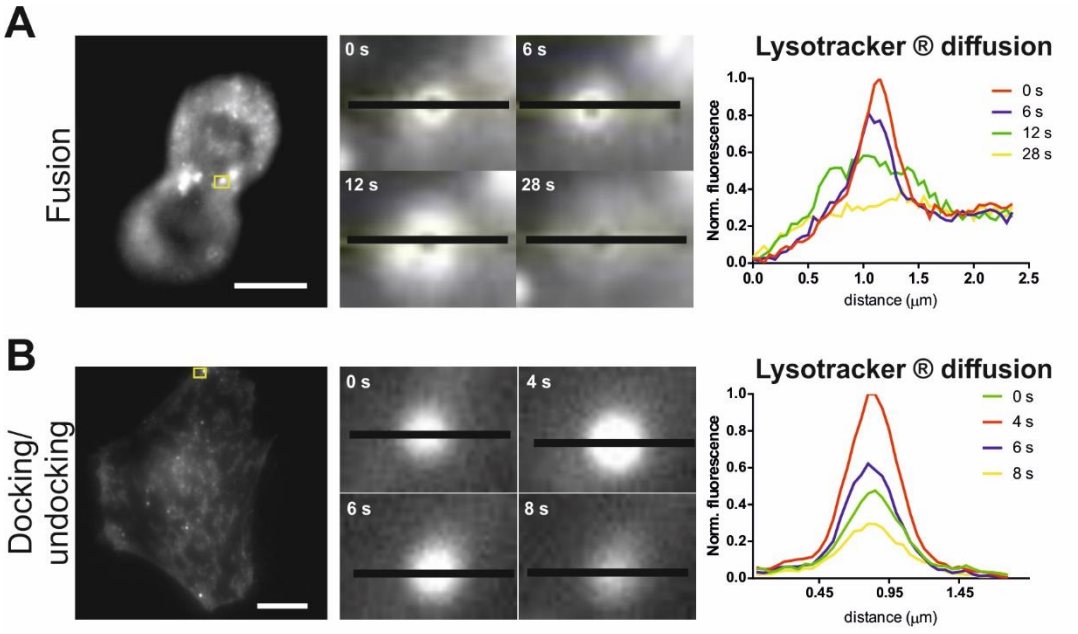

Figure 5.6. Distinction between fusion and docking/undocking events using Lysotracker® diffusion analysis. NRK cells were loaded with 50 nM Lysotracker red® for 30 min and imaged at a rate of 1 frame every 2s on a TIRFM system. A line was drawn across a lysosome and the fluorescence intensity and spreading across the line was measured frame by frame. Scale bars: 10 µm. **A.** Zoomed view of a lysosome loaded with Lysotracker red® (highlighted by the yellow square in the first image) undergoing fusion with the PM. The time indicates that taken for the lysosome to dock, fuse with the PM and for Lysotracker® fluorescence diffusion across the black line. The graph shows the diffusion analysis of Lysotracker® fluorescence across the line (black) upon exocytosis. **B.** Diffusion analysis of a Lysotracker®-loaded lysosome moving in close proximity to the cytoplasmic face of the PM (docking-undocking) during interphase. The lysosome analysed frame by frame is highlighted by the yellow square in the first image and the fluorescence analysis along the line (black) depicted in the accompanying graph.

In order to maximise the efficiency of lysosome exocytosis detection, diffusion analysis was completed by fluorescence intensity analysis of LpH-mCh-expressing lysosomes. LpH-mCh is a lysosomally targeted construct that allows visualisation of lysosomes at all times via a luminal mCherry tag. The probe also contains a pH-sensitive fluorescent protein, super-ecliptic pHluorin, which permits detection of pH changes. Upon lysosome fusion with the PM, the continuity between the lysosome content and the extracellular space

causes a loss in lysosomal acidity which can be detected by the de-quenching of pHluorin. Using ionomycin-elicited exocytosis, the de-quenching of pHluorin was characterised in LpH-mCh-stable NRK cells (**Figure 5.7**). Exocytosis was marked by a sharp increase in pHluorin fluorescence intensity, coincident with an increase in mCherry fluorescence (graph of normalised fluorescence intensity versus time and picture at frame t = 14.5s where a yellow signal is visible due to fluorescence in both mCherry and pHluorin channels). Diffusion of lysosomal membrane content in the plane of the PM was rapid and the yellow fluorescence signal was lost within 4s of exocytosis (t = 18.5s).

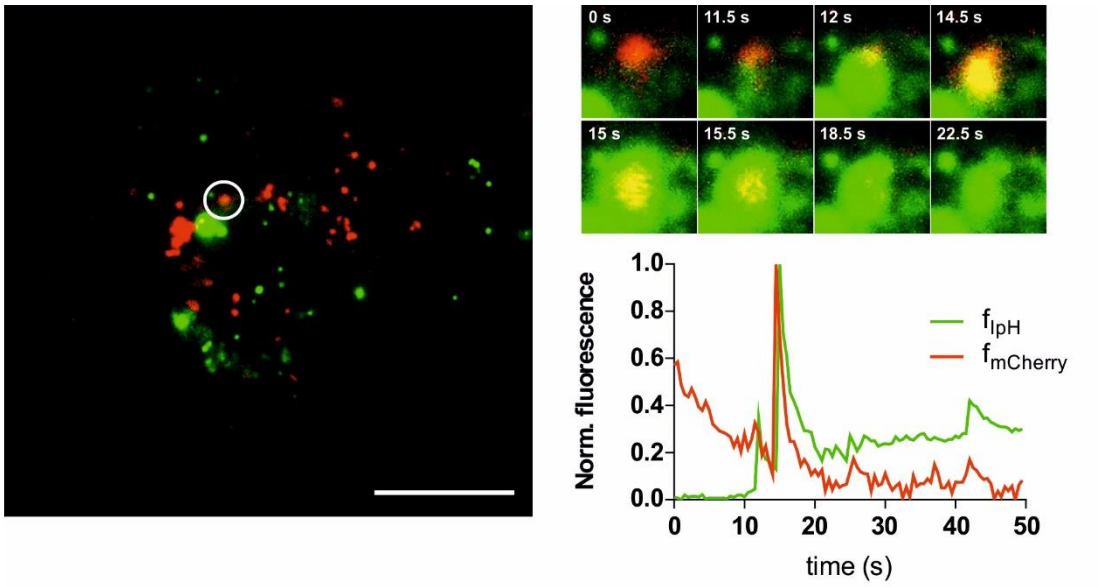

Figure 5.7. Characterisation of lysosome exocytosis using ionomycin-treated LpH-mCh-stable cells. Representative TIRF data from an LpH-mCh-stable NRK cell treated with 10 µM ionomycin and immediately imaged at a rate of 1 frame every 0.5s. A ROI at the site of lysosome exocytosis was selected (white circle in the left panel and expanded ROI in the top right panel) and the fluorescence intensity of mCherry ($f_{mCherry}$, red trace) and pHluorin (f_{lpH}, green trace) was measured (graph). The time on the zoomed pictures indicates the elapsed imaging time in sec. Scale bars: 10 µm.

Using both diffusion and pHluorin de-quenching analyses, lysosome exocytosis was examined in LpH-mCh-stable NRK cells undergoing mitosis.

During the late stages of cell division a yellow signal emanating from a lysosome located near the site of cytoplasmic constriction was first monitored in TIRFM live imaging (**Figure 5.8.A**). Subsequent diffusion analysis revealed an increase followed by a decrease and spreading of mCherry fluorescence along a line drawn across the examined lysosome (**Figure 5.8.B**). Finally, a rise in mCherry signal concomitant with an increase and the de-quenching of pHluorin fluorescence was observed (**Figure 5.8.C**). Overall the different analytical approaches undertaken here demonstrated that lysosome exocytosis occurs during the late stages of mitosis. Note that no exocytic events were detected before cytoplasmic constriction in mitotic cells and only docking/undocking events similar to the one depicted in **Figure 5.6.B** were observed in LpH-mCh-stable NRK cells in interphase.

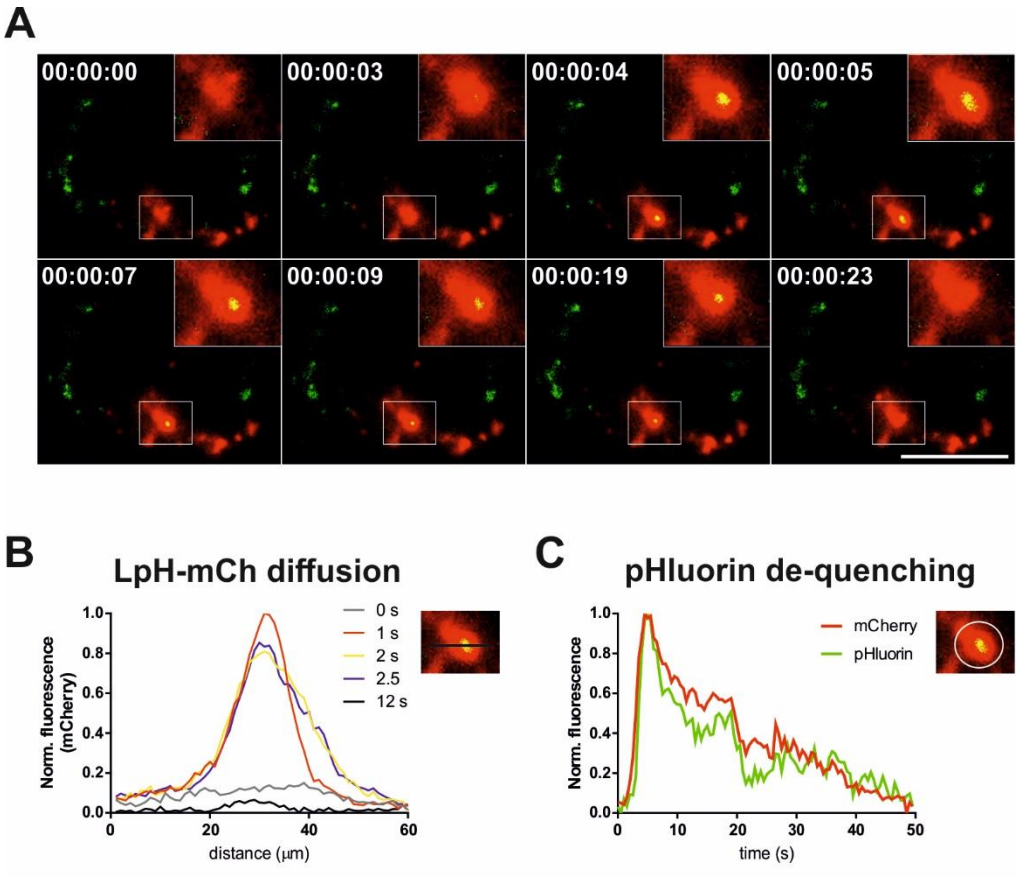

Figure 5.8. Detection of lysosome exocytosis in the late stages of cell division. **A.** Representative TIRF images of lysosome exocytosis during late telophase/cytokinesis in an LpH-mCh-stable NRK cell. The white square (and expanded view) represents the exocytosing lysosome analysed in (**B**) and (**C**). LpH-

mCh-stable NRK cell was imaged every 0.5s. Time indicated as hr:min:s, scale bar: 10 µm. **B.** Diffusion analysis along a line (black) drawn across the lysosome. **C.** Fluorescence intensity analysis of mCherry (red trace) and pHluorin (green trace) in a ROI (white circle) drawn around the lysosome.

5.2.5. Lysosome exocytosis is likely to occur near the intercellular bridge at cytokinesis

Spinning disk confocal microscopy was used to further examine exocytosis of lysosomes in LpH-mCh-stable NRK cells. In the first results chapter of this thesis, lysosomes were found to undergo alkalinisation during the late stages of cell division however the origin of the pH increase was unknown. Bromophenol blue (BPB), a membrane impermeable, fast-acting pHluorin quencher (Eckenstaler *et al.* 2016), was employed here to discriminate content release from lysosomes upon exocytosis from active de-acidification of the organelle in the absence of fusion. Time lapse imaging of LpH-mCh-stable NRK cells bathed in a solution containing BPB uncovered a fluorescence loss in both pHluorin fluorescence and mCherry fluorescence in lysosomes clustered near the intercellular bridge (white arrows in **Figure 5.9.A** and graph in **Figure 5.9.B**). The fluorescence of both dyes remained visible in the other subset of clustered lysosomes throughout time lapse imaging (blue arrows in **Figure 5.9.A**), suggesting that the lumen of this subset of lysosomes was not in direct contact with the extracellular space.

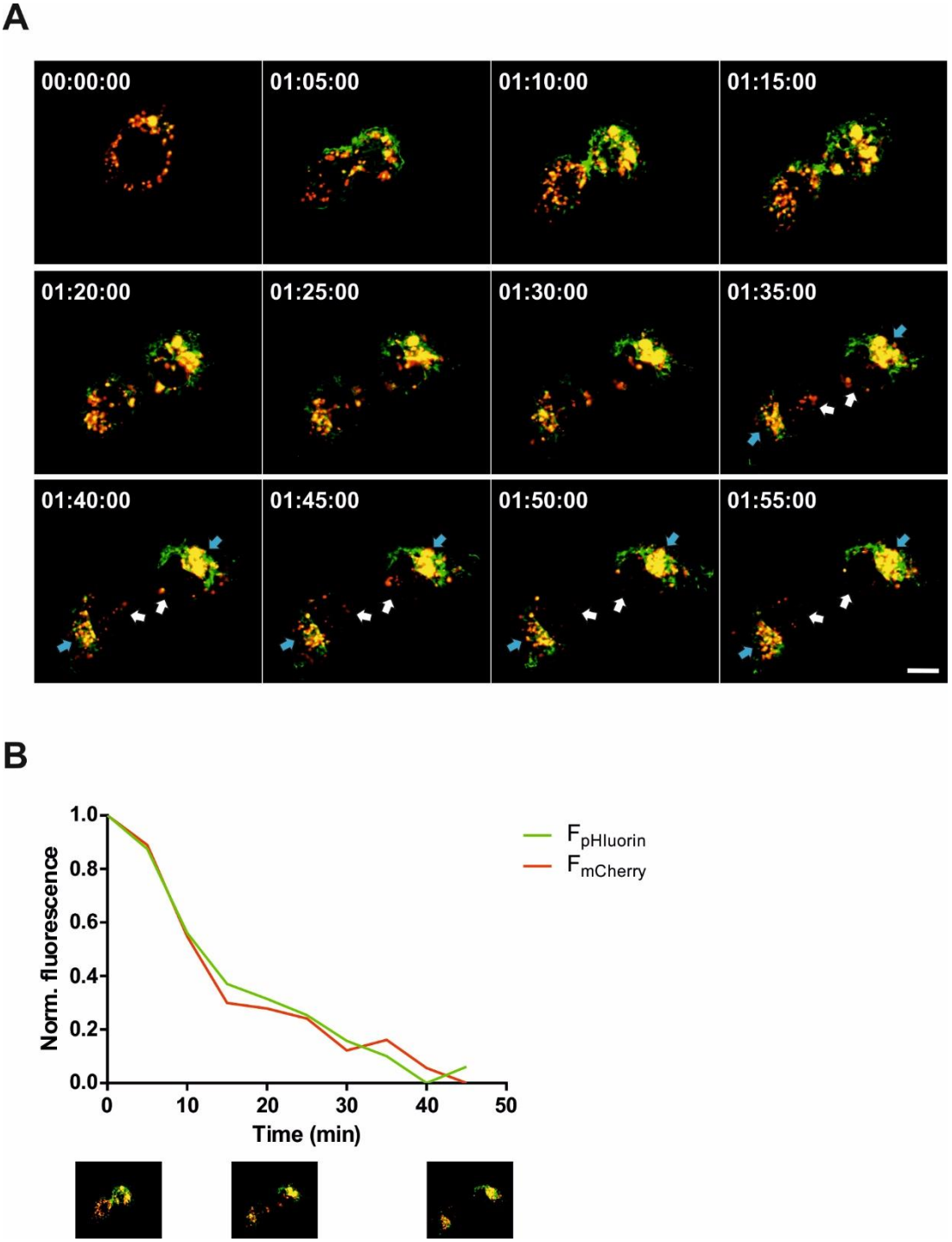

Figure 5.9. LpH-mCh-stable NRK cells bathed in bromophenol blue (BPB) undergo a loss of fluorescence at the site of lysosome clustering at either side of the intercellular bridge during cytokinesis. A. Immediately before imaging, the culture medium of LpH-mCh-stable NRK cells was replaced by culture medium supplemented with 0.3 mM BPB. Time lapse imaging was performed on a spinning disk confocal microscope at a rate of 1 frame every 5 min. The white arrows indicate the loss in LpH-mCh fluorescence near the intercellular bridge at cytokinesis; the persistence of LpH-mCh fluorescence is shown by the blue arrows. Time shown as

hr:min:s; scale bar: 10 µm. **B.** Quantification of pHluorin ($F_{pHluorin}$) and mCherry ($F_{mCherry}$) fluorescence at the site of lysosome clustering near the intercellular bridge during the late stages of cell division (indicated by the white arrows in **A.**). A circular region of interest was drawn around the clustered lysosomes and fluorescence measurements were performed from cytokinesis until division completion, as indicated by the corresponding images below the graph.

5.2.6 PI4KIIIβ enhances lysosome exocytosis and is essential for mitosis completion in mammalian cells

In a previous study clustered lysosomes at cytokinesis were found to be decorated with PI4KIIIβ and disruption of lysosome clustering via a PI4KIIIβ-dependent pathway led to mitotic defects (Rajamanoharan *et al.* 2015). PIK93 is a drug originally designed as a PI3K inhibitor but it was shown to have a highly selective activity against PI4KIIIβ when used at the published IC_{50} of 19 nM, which is considerably below the inhibitory concentration for other kinases (Knight *et al.* 2006). NRK cells were treated with the drug, fixed, permeabilised, immunostained with anti-tubulin antibody and nuclei were visualised with DAPI. The proportion of cells in cytokinesis and number of bi/tetranucleated cells were then determined as indices of mitotic failure. Although PIK93 treatment had no significant impact on the number of cells in cytokinesis (**Figure 5.10.A**), it significantly raised the proportion of polynucleated cells (**Figure 5.10.B**), consistent with a role of PI4KIIIβ in cell division.

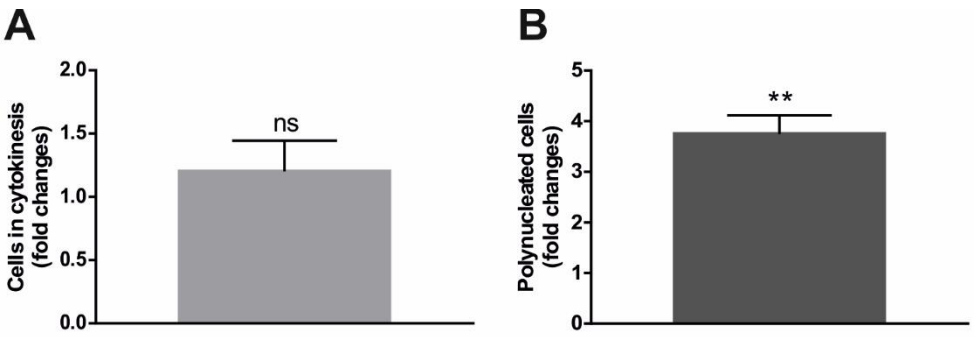

Figure 5.10. PIK93 treatment induces division defects in NRK cells. NRK cells were treated for 40 min with 19 nM PIK93 (or 0.1% (v/v) DMSO, control), fixed, permeabilised and immunostained with anti-tubuliln antibody and DAPI. The

proportion of cells at cytokinesis (**A**) and bi/tetranucleate cells (**B**) were counted in each condition. Results represent fold changes under treatment with the drug compared to the vehicle control. The proportion of bi/tetranucleate NRK cells is significantly raised under treatment with PIK93. Statistical significance was calculated using unpaired student's t-test and all results are shown as mean ± S.E.M.; **p = 0.0031, $n_{Control}$ = 942 cells, n_{PIK93} = 1310 cells, N = 6, ns: not significant.

Since previous data demonstrated a role for PI4KIIIβ in lysosome physiology (Rajamanoharan *et al.* 2015), the effect of enzyme overexpression on lysosome exocytosis was next scrutinised. As aforementioned, HeLa cells typically exhibit low levels of both basal and stimulated lysosome exocytosis however cells transfected with HA-PI4K exhibited a surprisingly significant increase in NAG release (**Figure 5.11.A**).

Conversely PIK93 treatment of NRK cells abolished Ca^{2+}-dependent exocytosis, bringing the levels of NAG release back to the basal levels measured in the control condition and in the absence of Ca^{2+} stimulation (**Figure 5.11.B**).

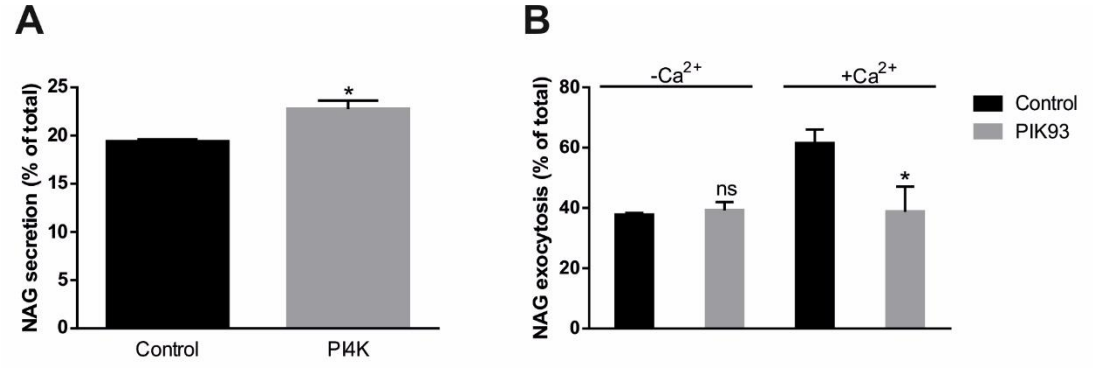

Figure 5.11. PI4K stimulates lysosome exocytosis and inhibition of the enzyme by PIK93 decreases Ca^{2+}-dependent exocytosis. A. HeLa cells were transfected with HA-PI4K or transfected with transfection reagents only (control) and NAG secretions were measured as % of total NAG (% secreted NAG = (extracellular NAG *100)/(extracellular NAG + intracellular NAG)). Statistical analysis was performed using an unpaired student's t-test, results shown as mean ± S.E.M., *p = 0.0356, N = 6. **B.** NRK cells were incubated with 19 nM PIK93 (or 0.1% (v/v) DMSO, control) for

40 min in the presence (+Ca^{2+}) or absence (-Ca^{2+}) of 10 µm ionomycin for 10 min. NAG lysosomal enzyme secretion was measured in the incubation media and in the cell lysates and calculated as % of total cellular NAG. Unpaired student's t-test, results shown as mean ± S.E.M., ns: not significant, *p = 0.0149, N = 3.

5.3. Discussion

Biochemical separation of surface accessible and cytosolic protein fractions by biotinylation and affinity resin purification in mitotic and interphase cells demonstrated that LAMP1 expression is increased in the cytosol of mitotic cells. This could reflect a higher demand for lysosomal proteins during cell division and highlight a potential role of the organelle in this biological process. In addition, LAMP1 expression was detected at the surface of mitotic cells. Since protein trafficking to the PM is downregulated during mitosis (Yeong 2013), the appearance of LAMP1 at the cell surface could be attributed to mitotic-specific lysosome exocytosis. However the experiment was only performed twice and should be repeated and LAMP1 expression quantified more reliably in order to draw precise conclusions. The biotinylation experiment is supported by complimentary surface immunofluorescence imaging. This experiment allowed detection of the luminal part of the lysosomally targeted construct LpH-mCh at the surface of interphase and mitotic cells, and suggested that lysosome exocytosis increases during the process of cell division. The absence of detectable LAMP1 at the surface of interphase cells in the biotinylation experiment on the other hand is subject to more varied and challenging interpretations. It conflicts with the LpH-mCh fluorescence detection at the surface of interphase cells, which demonstrates the presence of a lysosome-specific membrane protein at the PM. The efficiency of the antibody used in Western blotting cannot be questioned since LAMP1 was detected at the surface of mitotic cells. The absence of LAMP1 detection could therefore result from a smaller loading of detectable proteins during protein migration and the Western blot analysis could benefit from the use of a loading control specific to the PM such as an antibody that targets the Na^{+}/Ca^{2+} exchangers (Strehler 1990). Alternatively, the presence of LpH-mCh fluorescence at the cell surface could reflect an overload of the biosynthetic

pathway and abnormal trafficking of ectopic proteins to the plasma membrane. The biotinylation assay constitutes a more reliable way to assess the presence of lysosomal proteins at the surface since it examines the expression of endogenous proteins. For more accuracy, the surface staining should be performed using antibodies that target the luminal epitope of endogenous lysosomal proteins.

Quantification of surface immunofluorescence revealed that the fluorescence of the LpH-mCh construct was significantly increased at the PM during cytokinesis compared to interphase, highlighting a potential increase in lysosome exocytosis during the late stages of mitosis. This observation was corroborated by the LY-based assays in NRK and BSC-1 cells which demonstrated a significant increase in LY release during mitosis, unequivocally attributed to enhanced lysosome exocytosis. Indeed the LY assay offered the added advantage of measuring the release of lysosomal content independently of protein synthesis and trafficking.

It is important to note that during the optimisation and validation of the NAG- and LY-based assays performed on NRK and macrophages discrepancies in basal release between cell lines were observed. It could be argued that only a particular subset of lysosomes per cell line is competent for secretion. However this hypothesis is discredited by the fact that under ionophore-induced secretion, a drastic increase in lysosome exocytosis is observed in both macrophages and NRK cells. These variations in lysosomal exocytosis have been discussed in previous studies where lysosomal secretion in NRK cells (epithelial cells) was found to be much lower than those of haemopoietic lineage. Inhibition of actin polymerisation drastically increased lysosomal secretions, demonstrating that the variations in secretion observed from one cell line to another are likely to be the result of cytoskeleton architecture (Vitale *et al.* 1995; Andrews 2000). Variations in the basal release of lysosomal content within the same cell line were also observed. Lysosomes monitor the cellular nutrient status and, in turn, this has an important influence on the subcellular distribution of this organelle. For example, in nutrient-rich conditions, lysosomes re-locate peripherally (Appelqvist *et al.* 2013). Thus, assuming that peripheral lysosomes undergo fusion with the plasma

membrane more readily than perinuclear ones, the discrepancies in basal release observed could potentially reflect the nutrient status of the cell. In addition, macrophages are specialised secretory cells thus more likely to undergo higher basal exocytosis. Overall, the secretion assays proved to be reliable and reproducible in macrophages and NRK cells as both cell lines demonstrated robust responses in stimulatory conditions, confirming that exocytosis is favoured in the presence of Ca^{2+}.

The use of TIRFM enabled the detection of single exocytic events in cells undergoing cell division. However the technical difficulties that arise from the use of highly motile mitotic cells that easily escape the evanescent field prevented the generation of quantitative data. Fusion events were observed in 3 dividing cells, and at equal imaging duration no exocytosis was detected in interphase cells. All fusion events occurred at the late stages of cell division, usually following cytoplasmic ingression or intercellular bridge formation. The detected exocytic events were also sporadic. This was surprising given the extent of exocytosis increase monitored in the LY biochemical assays. First it seems highly probable that many fusion events remained unnoticed, given the focus instability inherent in TIRFM. Second, TIRF microscopy allows the examination of a restricted PM area, i.e., the PM in close contact with the glass interface. This area is particularly restricted during mitosis when cells adopt a more spherical morphology. Thus the possibility that other fusogenic events occur at parts of the PM that are not in the evanescent field cannot be ruled out. Third, similar to the process of PM repair (Idone *et al.* 2008), lysosomes could undergo homotypic fusion prior to exocytosis leading to fewer but quantitatively larger exocytic events. This would explain why only a few exocytic events were observed, whilst a significant increase of lysosomal release was monitored during cell division. Further investigation measuring the diameter and/or volume of exocytic vesicles is essential to clarify this issue. Finally, the initial detection of fusion events was based on the de-quenching of pHluorin visualised by a shift from red to yellow fluorescence. As depicted in the figure characterising fusion in ionomycin-treated LpH-mCh-stable NRK cell (and supplemental video), most fusing vesicles appeared green. A potential explanation lies in the quantum yield (φ) of each fluorophore.

pHluorin has a higher quantum yield than mCherry (φEGFP = 0.60 and φmCherry = 0.22) (Shaner *et al.* 2008). Since the brightness is proportional to the quantum yield (Wu *et al.* 2009) pHluorin brightness could potentially mask mCherry brightness upon fusion, making the shift from red to yellow fluorescence characteristic to fusion events more challenging to detect in TIRFM experiments.

In the first results chapter, lysosomes expressing LpH-mCh were shown to undergo alkalinisation during the late stages of cytokinesis. In order to assess whether the alkalinisation was a consequence of fusion, cell impermeable BPB was used to quench extracellular pHluorin. The preliminary imaging performed here demonstrated that alkalinisation preceded a loss of fluorescence. This suggests that the observed lysosomal pH increases arose from an intracellular mechanism and is not the result of organelle exocytosis. Subsequent loss in pHluorin and mCherry fluorescence might result from different factors. First it could be ascribed to a loss of focus. However, this seems unlikely since the other subpopulations of LpH-mCh-expressing lysosomes were still visible in the same cells. This implies that cells did not significantly move out of the focal plane. Second it could be due to fusion of lysosomes with the PM which then resulted in a decrease in both pHluorin and mCherry fluorescence intensities. It is unclear whether BPB quenched pHluorin since time lapse recording was performed at an imaging rate potentially slower than BPB quenching. For more accuracy, faster imaging acquisition should be performed in future experiments.

The persistence of pHluorin and mCherry fluorescence in the other subset of clustered lysosomes located on the other side of the nucleus and away from the intercellular bridge of nascent cells indicated that the lysosomal lumen remained separated from the extracellular space. This suggests that the bulk of exocytosis is unlikely to take place at this particular location and occurs preferentially near the intercellular bridge.

Inhibition of PI4KIIIβ activity induced significant mitotic defects, demonstrating the importance of the enzyme in mitosis. Consistent with this result, a previous study showed that the loss of four-wheel drive (Fwd), the type IIIβ PI4K

homologue in *Drosophila* induced furrow regression after contraction and bridge instability in spermatocytes (Polevoy *et al.* 2009). The localisation of phosphatidylinositol 4-phosphate (PI4P), the product of PI4KIIIβ, at the site of furrow ingression is thought to contribute to the formation and enrichment of $PI(4,5)P_2$, which in turn interacts with proteins essential for furrow stability after ingression (Polevoy *et al.* 2009; Cauvin and Echard 2015). PI4P also associates with Golgi phosphoprotein 3 (GOLPH 3) which interacts with Rab11, cytoskeletal and motor proteins, thereby promoting furrow contraction to completion during cytokinesis (Sechi *et al.* 2014). Thus the significant increase in the number of polynucleate cells under treatment with the PI4KIIIβ inhibitor PIK93 reported in this chapter, could reflect the cells inability to maintain furrow ingression, thereby inducing the collapse of nascent cells back into polynucleated structures. PI4KIIIβ is predominantly associated with the trans-Golgi network but a pool of the enzyme, with unique biochemical characteristics, has additionally been found to decorate lysosomes (Sridhar *et al.* 2013). Given the strategic clustering and re-positioning of lysosomes at cytokinesis, the organelle could potentially participate in PI4P delivery and enrichment at the cleavage furrow.

Interestingly, PI4KIIIβ inhibition by PIK93 significantly decreased Ca^{2+}-stimulated exocytosis of lysosomes; conversely overexpression of the enzyme enhanced lysosome fusion with the plasma membrane. This is consistent with previous studies that showed that PI4KIIIβ inhibition suppresses exocytosis of secretory granules in PC12 cells (de Barry *et al.* 2006) and pancreatic β cells (Olsen *et al.* 2003). However here we show for the first time the negative impact of enzyme inhibition in non-secretory cells. The enzyme catalyses the formation of phosphatidylinositol 4-phosphate (PI4P) (Balla and Balla 2006) which participates in Golgi to lysosome trafficking and preserves lysosomal identity during fast dynamic events such as fusion and fission (Sridhar *et al.* 2013). This lipid has also been shown to promote curvature of biological membranes (Furse *et al.* 2012). Thus PI4P could mediate lysosome exocytosis at the plasma membrane by facilitating membrane mixing, whilst preserving lysosomal identity and allowing the organelle to re-form if needed. Since the product of PI4KIIIβ is involved in protein interactions essential for

successful cell division, it is difficult to assess whether PIK93 impairs division via its specific action on lysosome exocytosis. A more reliable way to examine the effect of PI4P would be to focally deplete or over-produce the lipid pool at the lysosomes using a rapamycin-inducible construct such as the one developed by Balla and co-workers (Hammond *et al.* 2014). Nonetheless the experiments on PI4KIIIβ carried out in this chapter provide a novel mechanistic insight into the importance of the enzyme in the process of lysosome exocytosis in non-specialised cells.

Overall, all the data presented in this chapter highlight an increase in lysosome exocytosis at the late stages of cell division and near the site of furrow ingression/intercellular bridge. The process is relevant in the context of mitosis where daughter cell formation requires expansion of the PM. By a process of exocytosis, facilitated by PI4KIIIβ, lysosomes could act as membrane providers and accommodate PM surface increase. Additionally lysosomes could contribute to PI4P delivery and enrichment at the cleavage furrow.

The set of experiments presented in this chapter however present some limitations that should be addressed. First of all, not all experiments were performed on the same cell line. Since the approaches undertaken here were complementary to each other, it would have been more accurate to use one mammalian cell type and repeat all the experiments on another cell line. Second, the biotinylation experiments and surface staining should have been repeated at least three times in order to generate solid and reliable results. Third, the quantification of lysosome exocytosis using NAG and LY assays should have been performed in a timely manner and correlated to immunofluorescence analysis of dividing cells in order to identify the precise stage of cell division at which lysosomal exocytosis increases. Finally, TIRF was used here as a qualitative indicator of lysosome exocytosis during cell division. For more accuracy, TIRF imaging should be repeated and exocytic events during mitosis quantified and compared to those in interphase.

5.4. Summary

In this chapter the fusogenic properties of lysosomes with the PM were examined in the context of cell division. Biotinylation and surface immunofluorescence experiments first revealed the appearance and increase of lysosomal membrane proteins at the PM surface during mitosis. The biochemical assays allowed the quantification of lysosomal content release and demonstrated that lysosome exocytosis is enhanced during cell division, compared to interphase. TIRFM confirmed that exocytic events take place during cell division and that lysosome fusion with the PM most likely occurs during late telophase/cytokinesis. Spinning disk confocal imaging combined with BPB treatment next showed that lysosome exocytosis is likely to arise from the subset of clustered lysosomes located at either side of the intercellular bridge at cytokinesis, as opposed to the group of lysosomes present at the other side of the nascent cells' nuclei. Finally the study of PI4KIIIβ unfolded an unexpected role of the enzyme in lysosome exocytosis, in addition to confirming its function in cell division completion.

Chapter 6: Main Discussion

Lysosomes are incredibly versatile acidic organelles involved in a wide range of cellular functions including: nutrient sensing, macromolecule degradation/recycling, Ca^{2+}-signaling and PM repair (Xu and Ren 2015). Recent work on the characterisation of the small EF-hand Ca^{2+}-binding protein (CaBP)-7 and its effector PI4KIIIβ, further expanded the palette of lysosomal roles by highlighting a potential function of the organelle during cytokinesis (Rajamanoharan *et al.* 2015). Cytokinesis represents the final stage of mitotic cell division. It is characterised by the cytoplasmic constriction between nascent daughter cells, followed by the formation of a transient cytoplasmic intercellular bridge, and abscission, the process by which the separation of the two daughter cells is finalised (D'Avino *et al.* 2015). The recent study examining CaBP7 demonstrated that lysosomes re-distribute in a highly coordinated fashion during cytokinesis and that disruption of their clustering near the cytoplasmic intercellular bridge through manipulation of PI4KIIIβ activity induced significant cytokinesis defects (Rajamanoharan *et al.* 2015). Trafficking of intracellular compartments into and out of the intercellular bridge is known to be crucial in the different steps of cytokinesis, however, so far only endosomal and Golgi-derived compartments have been implicated in the process (Frémont and Echard 2018). In addition, enzymes such as Fwd, the *Drosophila* homologue of mammalian PI4KIIIβ was shown to be essential for cytokinesis in the fly (Frémont and Echard 2018). The observation that lysosomal clustering near the intercellular bridge is important in cytokinesis (Rajamanoharan *et al.* 2015), coupled to the knowledge that a pool of lysosomes are decorated with PI4KIIIβ (Sridhar *et al.* 2013), constitute the roots of the work presented here.

The purpose of this thesis was to first characterise lysosome positioning and biochemical properties during cytokinesis and second to assess the functional role of lysosomes in cell division and pinpoint their requirement during cytokinesis.

The data presented in this work first confirmed that lysosomes do cluster near the intercellular bridge at cytokinesis, consistent with a previous study (Rajamanoharan *et al.* 2015). Live cell imaging also clearly showed that lysosomes initiate their re-distribution in early cytokinesis, as they position

near the site of furrow ingression. In late cytokinesis, they localise as distinctive and organised clusters at either side of the intercellular bridge and even appear as motile structures within the bridge. As discussed previously, the lysosomal spatial re-arrangement during cytokinesis is unlikely to be due to the mechanical constraints that stochastically partition the lysosome pools between the nascent cells for two reasons. First, they are present at the site of cytoplasmic constriction, where the force constraints are the highest. In other words, they should be pushed outside of the constriction zone and not be present within it. Second, the active positioning of lysosomes within cells is related to their functions (Pu *et al.* 2016), suggesting a functional requirement of the organelle during cytokinesis. In addition, trafficking of recycling endosomes and Golgi-derived vesicles to and from the cleavage site/intercellular bridge is known to be functionally important in furrow stability before and after ingression (Frémont and Echard 2018). Therefore, similar to other intracellular organelles, the strategic positioning of lysosomal compartments during cytokinesis could explain functional requirements.

Although the disruption of lysosomal positioning and clustering is enough to impair mitosis (Rajamanoharan *et al.* 2015), the importance of organelle integrity had never been assessed until now. Here, GPN-induced disruption of lysosome activity demonstrated for the first time the importance of lysosomal membrane integrity during cytokinesis. Thus, both lysosomal positioning and lysosomal membrane integrity must be preserved during cytokinesis, suggesting the organelle is functionally involved in the process.

These findings prompted a more detailed investigation as to the exact role played by lysosomes during cytokinesis. In order to do this, the proteolytic, Ca^{2+}-handling and exocytic functions of lysosomes were systematically assessed by pharmacological inhibition. Cathepsins are among the most abundant lysosomal hydrolases (Appelqvist *et al.* 2013). In addition to their luminal activity, they were found to have extracellular roles including the degradation of the ECM (Mohamed and Sloane 2006) and the repair of the PM (Castro-Gomes *et al.* 2016). Therefore a potential role of lysosomal hydrolases in cytokinesis was investigated. According to the results presented here, cathepsins E, D, B and L are dispensable for cytokinesis. It is however

possible that other hydrolases are needed in the process of cell division and a more exhaustive study of all lysosome hydrolases should shed light onto their possible functions in cell division. Nonetheless, based on the present study, it appears that the most abundant hydrolases and those that possess documented extra-lysosomal activity are not needed in the process of cytokinesis.

Since Ca^{2+} signals were previously shown to mediate mitotic events such as nuclear breakdown in fibroblasts (Kao *et al.* 1990) and chromatin condensation in sea urchin embryos (Twigg *et al.* 1988), the role of lysosome Ca^{2+} in cytokinesis was next examined. Chronic treatment of cells with bafilomycin A1 prevents lysosomal Ca^{2+} refilling, through dissipation of the H^+ gradient, which abolishes the force required for Ca^{2+} transport into the lysosomal lumen via the calcium hydrogen exchanger. In addition the drug also abolishes NAADP-stimulated (Galione *et al.* 2010) and MLSA1-induced Ca^{2+} response (Shen *et al.* 2012), suggesting that the drug affects the Ca^{2+} release mediated by both TPC and TRPML1. Perturbation of the organelle's ability to store and release Ca^{2+} had no significant impact on cytokinesis, suggesting that if Ca^{2+} is required during cytokinesis, lysosomes do not act as the cation provider. Nonetheless, recent work highlighted that lysosome-ER contact sites allow pH-independent Ca^{2+} refilling of lysosomes (Garrity *et al.* 2016). Despite being in conflict with previous studies (Churchill *et al.* 2002), this alternative mode of Ca^{2+} uptake by lysosomes cannot be ruled out and further investigations should be carried out. For example, the position of lysosomes in respect to the ER could be monitored throughout cell division to identify the potential existence of such microdomains. Another route of Ca^{2+} entry could be provided by a lysosomal Ca^{2+}-ATPase. Indeed a Ca^{2+}-ATPase activity was recorded on lysosomes, however its identity is still unknown. If such Ca^{2+} pump were to be rigorously identified, its inhibition should be used in complement to bafilomycin A1 treatment coupled with lysosomal Ca^{2+} measurement to fully assess the implication of lysosomal Ca^{2+} in cytokinesis.

Overall these results suggest that neither the proteolytic nor the Ca^{2+} sequestering activities of lysosomes are critical for cytokinesis.

The fusogenic properties of the organelle were next scrutinised. Inhibition of exocytic events was performed using NEM, a non-specific alkylating agent that prevents vesicular fusion by irreversibly inhibiting the key trafficking ATPase NSF (Block *et al.* 1988; Band *et al.* 2001; Sivaramakrishnan *et al.* 2012). Interestingly, NEM was shown to induce significant reductions in lysosomal exocytosis in parallel with a substantial increase in cytokinesis failure. NEM affects any fusion events requiring NSF, therefore the compound not only disrupts exocytosis of lysosomes but also interferes with the fusion (exocytic, homotypic, heterotypic) of other secretory pathway compartments. The cytokinesis defects observed under NEM treatment could thus result from the combinatory inhibition of other organelle fusion processes. However lysosome membrane integrity was also shown to be essential for cytokinesis completion, since GPN treatment induced significant division defects. This combined to the effect of NEM on cytokinesis suggests that lysosomal exocytosis plays a role in cytokinesis. In the future, a more specific inhibition of lysosomal exocytosis could be performed by silencing Synaptotagmin VII, the lysosomal Ca^{2+} sensor involved specifically in lysosome exocytosis (Martinez *et al.* 2000).

The cytokinesis defects monitored under GPN and NEM treatments, led to the study and quantitation of lysosomal exocytosis during cytokinesis, the focus of the final results chapter. The different experimental approaches undertaken, including surface biotinylation and immunofluorescence assays, all converged to reveal an increase in lysosome exocytosis during cell division. This increase was quantitatively assessed using a LY-based biochemical assay and was shown to be significant in two unspecialised (non-secretory) cell types (NRK and BSC-1). The novel observation that lysosome exocytosis rises during cell division is not only consistent with the idea that lysosomes are important in cell division but also suggests that the process is likely to be conserved throughout cell types and mammalian species. In order to identify the division stage at which lysosomes fuse with the PM, TIRF microscopy was used. Using fluorophore diffusion analysis combined with pHluorin de-quenching, a rigorous method of exocytosis detection was carried out which permitted the identification of fusion events between lysosomes and the PM before, during and after furrow ingression. Since no other exocytic events were detected in

the early stages of mitosis, lysosome exocytosis is likely to occur preferentially at later stages, during cytokinesis. This is consistent with the fact that treatment with drugs that either impair lysosome integrity (GPN) or inhibit lysosome exocytosis (NEM) promotes cytokinesis defects such as polynucleation. In addition, lysosome exocytosis was exclusively detected near the intercellular bridge in TIRF microscopy and no fluorescence quenching was monitored from the lysosomes residing near the centrosomes, as confirmed by the live imaging of cells expressing LpH-mCh and bathed in a BPB solution. This suggests that lysosome exocytosis occurs during the late stages of cell division, and that the pool of lysosomes located near the intercellular bridge is likely to participate in the majority of exocytosis required during cell division. The other cluster of lysosomes located near the centrosomes might participate in the maintenance of an intact lysosomal pool throughout cell division. The purpose of lysosomal exocytosis in cytokinesis cannot be directly inferred from these observations and requires further thorough investigation including the identification of lysosomal cargo and potential association of the organelle with Rab and Arf proteins. One possibility is that lysosomal exocytosis promotes the release of enzymes extracellularly and allows them to perform functions outside of their expected catalytic scope. However based on the work presented here, this is unlikely since inhibition of cathepsins did not induce division defects, demonstrating that lysosomal fusion with the PM serves other purposes than the delivery of these hydrolases into the extracellular space during cytokinesis. Alternatively, lysosomes, which are large potential membrane reservoirs (Blott and Griffiths 2002) could contribute to cell expansion by adding membrane through their exocytosis, facilitating the formation of daughter cells. Another hypothesis is that they might participate in bridge stability by balancing the endocytic process resuming during late cytokinesis (Schweitzer *et al.* 2005). Finally they could also participate in the delivery of important cargos that take part in subsequent cytokinesis events such as maintenance of furrow ingression and/or abscission. These hypotheses are not mutually exclusive and since lysosome exocytosis was observed at various stages of cytokinesis, the process could serve multiple purposes.

In addition to their clustering at cytokinesis, lysosomes were shown to be intimately linked to PI4KIIIβ. This enzyme, one of four mammalian PI4Ks responsible for the production of PI4P from PI (Balla and Balla 2006), was shown to maintain lysosomal identity during fusion and fission with other compartments (Sridhar *et al.* 2013) and participate in bridge stability during cytokinesis in *Drosophila* (Polevoy *et al.* 2009). The data presented here confirm the importance of the enzyme in the process of cell division, since inhibition of PI4KIIIβ by PIK93 induced severe cytokinesis defects. However whether these defects result from depletion of lysosomal PI4KIIIβ remains to be fully investigated. Indeed, the product of PI4KIIIβ, PI4P, was identified on other compartments such as Rab11-positive recycling endosomes and was shown to form a complex with key cytoskeletal and motor proteins via the effector protein GOLPH3 at the site of the ingression furrow, promoting completion of furrow contraction (Frémont and Echard 2018). Therefore future work should involve: 1. Identification of PI4P-positive lysosomes at cytokinesis by PI4P and LAMP1 co-immunostaining and 2. Acute focal depletion of lysosomal PI4P during cytokinesis using a rapamycin-inducible construct (Hammond *et al.* 2014). This way, the functional role of PI4P-posisitve lysosomes in cytokinesis could be directly assessed.

In addition to causing significant cytokinesis failure, inhibition of PI4KIIIβ was shown for the first time to significantly decrease lysosome exocytosis in non-specialised cells. Conversely, overexpression of the enzyme induced a significant increase in lysosome exocytosis. Although a direct causal effect on cytokinesis cannot be inferred from these observations, it is interesting to observe that the enzyme is not only essential for cytokinesis but also favours a process that, based on this thesis, is essential in cytokinesis, *i.e.* fusion of lysosomes with the PM. The purpose of the enzyme could potentially be double. First it could promote PI4P production on lysosomes whose clustering would contribute to PI4P delivery to the site of the cleavage furrow. Similar to Rab11-positive endosomes, lysosomes harbouring PI4P could interact with furrow contractile proteins and favour bridge stability. Alternatively PI4P-positive lysosomes could participate in PI(4,5)P_2 enrichment at the furrow, via conversion of PI4P into PI(4,5)P_2. Second, since this lipid has been shown to

induce membrane curvature (Furse *et al.* 2012), PI4P production by PI4KIIIβ on the lysosomal surface could facilitate mixing of lipid bilayers and promote lysosome exocytosis at the site of furrow ingression/intercellular bridge. Once again focal depletion of lysosomal PI4P could provide deeper insights into the work performed in this thesis. It would not only give precious information on the role of lysosomal PI4P in cytokinesis but also establish whether or not PI4KIIIβ-stimulated exocytosis of lysosomes is required in cytokinesis.

The study of lysosomes during cytokinesis revealed an unexpected phenomenon. Not only do lysosomes re-distribute near the cleavage site between nascent cells, but they also undergo a parallel increase in pH, as demonstrated by the de-quenching of pHluorin in LpH-mCh-transfected/stable cells. The luminal pH increase was observed in cells dividing normally. This suggests that the process does not interfere with division completion and reinforces the idea that lysosomal hydrolases and lysosomal Ca^{2+} storage, which both require high luminal H^{+} concentration, are not needed in cytokinesis. As for the mechanisms underlying lysosomal pH increase during cytokinesis, the question remains whether lysosomal alkalinisation results from a directed reduction in V-ATPase activity, is a consequence of lysosomal proton leak during trafficking and positioning of the organelle, or both. It has been established that lysosomal positioning influences the organelle pH, with anterograde transport promoting pH increase and retrograde transport inducing pH decrease (Johnson *et al.* 2016). Anterograde movement of lysosomes is mediated by Arl8 GTPase and its effector SKIP coupled to kinesin motor and is accompanied by proton leak. Conversely, lysosome centripetal transport is regulated by Rab7 and its effector RILP, which links the organelle to dynein/dynactin motor and stabilises the V-ATPase (Johnson *et al.* 2016). During cytokinesis, microtubules re-organise in an anti-parallel fashion, so that their plus-end faces the cleavage site (Frémont and Echard 2018). Thus it is reasonable to assume that lysosomal clustering near the cleavage site/intercellular bridge results from an anterograde transport of the organelle along microtubules (from minus- to plus-end). Lysosomal pH increase during cytokinesis could therefore arise from a loss of Rab7-RILP, subsequent decrease in V-ATPase stability and proton leak.

The functional significance of lysosomal pH increase remains elusive. In addition to being a consequence of lysosomal positioning, the process could potentially be required for lysosomal function in cytokinesis. Intriguingly, lysosomal pH increase through WASH-mediated V-ATPase retrieval at the lysosome was observed in *Dictyostelium discoideum.* The process was shown to be required for lysosome maturation and subsequent exocytosis (Carnell *et al.* 2011). Thus, by extrapolation, the lysosome neutralisation observed during cytokinesis in mammalian cells might be a maturation step priming the organelle for exocytosis. Further investigation on the V-ATPase/WASH localisation in regards to lysosomes during cytokinesis would help elucidate the mechanisms of lysosome pH increase. In addition, manipulation of lysosomal pH using an optogenetic tool such as LysopHoenix (Rost *et al.* 2015) would provide a functional assessment of lysosomal de-acidification during cytokinesis. In addition to being part of organellar maturation, lysosomal neutralisation prior to exocytosis could potentially constitute a protective mechanism that prevents release of acidic content in the extracellular space and damage to neighbouring cells.

The most interesting question arising from this thesis is why would lysosomes, out of all the other membranous organelles, be relevant in cytokinesis? The answer potentially lies in the nature of the organelle itself. Through multiple fusion and fission events in the endocytic pathway, lysosomes acquire the machinery necessary for exocytosis (Blott and Griffiths 2002). Additionally, they contain an extraordinarily large pool of membrane that can be donated via exocytosis (Blott and Griffiths 2002), permitting the overall membrane rearrangement required for the various steps of cytokinesis and daughter cell formation. Finally, lysosome interplay with PI4KIIIβ an enzyme involved in cytokinesis as well as exocytosis, provides an additional reason as to why lysosomes could be the organelle of choice in cytokinesis.

Conclusion

This thesis aimed to investigate lysosomal characteristics and function during mammalian cell division. The varied imaging approaches undertaken allowed

the identification of a pool of lysosomes clustered near the cytoplasmic constriction site in early cytokinesis and at either side and within the intercellular bridge during late cytokinesis. Among lysosomal functions, exocytosis was identified as being increased and important during cell division. This observation is completely novel and provides a new insight into lysosome function and requirement during cell division. A second novel finding is that lysosomes undergo de-acidification, a process that has been previously observed to precede exocytosis. Finally, PI4KIIIβ was demonstrated for the first time to be essential during cytokinesis in non-specialised mammalian cells and to positively regulate lysosomal exocytosis. Collectively this work highlights a new and fundamental role for lysosomes during mammalian cell cytokinesis which may have significant implications for the future targeting of various human diseases that derive from aberrant cell division (**Diagram 6.1.**).

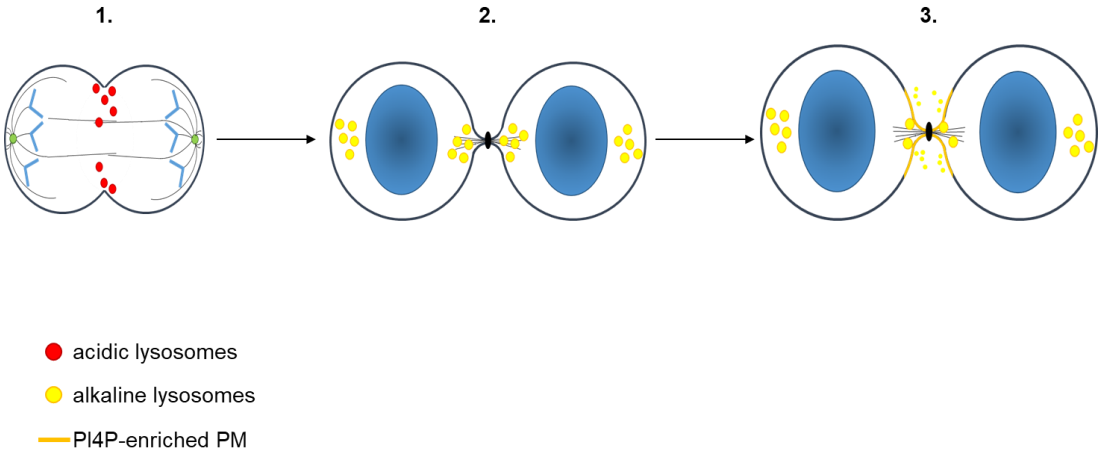

Diagram 6.1. Diagrammatic model of lysosome exocytosis in cytokinesis. 1. Lysosomes cluster at the site of cytoplasmic constriction during late telophase/early cytokinesis. **2.** The organelle undergoes alkalinisation either as a consequence of its peripheral position in the cell or to actively inactivate its hydrolases and avoid harm to the neighbouring cells before release of its content in the extracellular space. **3.** Lysosomes undergo fusion with the PM towards the end of cell division, prior to abscission. The aim of lysosome exocytosis can be dual: it could participate to PI4P enrichment at the PM later converted into PI(4,5)P_2 and/or allow addition of extra membrane for expansion of the two nascent daughter cells.

Bibliography

Abe, M., A. Makino, F. Hullin-Matsuda, K. Kamijo, Y. Ohno-Iwashita, K. Hanada, H. Mizuno, A. Miyawaki and T. Kobayashi (2012) A role for sphingomyelin-rich lipid domains in the accumulation of PIP2 to the cleavage furrow during cytokinesis. *Molecular and cellular biology*, MCB. 06113-11.

Alberts, B., A. Johnson, J. Lewis, M. Raff, K. Roberts and P. Walter (2002) An overview of the cell cycle.

Andrews, N. W. (2000) Regulated secretion of conventional lysosomes. *Trends in cell biology*. **10**, 316-321.

Andrews, N. W. (2017) Detection of Lysosomal Exocytosis by Surface Exposure of Lamp1 Luminal Epitopes. *Lysosomes: Methods and Protocols*, 205-211.

Angelini, C. (2014) Niemann-Pick Disease Type C1. *Genetic Neuromuscular Disorders*, pp 289-291, Springer

Appelqvist, H., P. Wäster, K. Kågedal and K. Öllinger (2013) The lysosome: from waste bag to potential therapeutic target. *Journal of molecular cell biology*. **5**, 214-226.

Archambault, V. and D. M. Glover (2009) Polo-like kinases: conservation and divergence in their functions and regulation. *Nature reviews Molecular cell biology*. **10**, 265.

Atilla-Gokcumen, G. E., A. B. Castoreno, S. Sasse and U. S. Eggert (2010) Making the cut: the chemical biology of cytokinesis. *ACS chemical biology*. **5**, 79-90.

Attar, N. and P. J. Cullen (2010) The retromer complex. *Advances in enzyme regulation*. **50**, 216-236.

Axe, E. L., S. A. Walker, M. Manifava, P. Chandra, H. L. Roderick, A. Habermann, G. Griffiths and N. T. Ktistakis (2008) Autophagosome formation from membrane compartments enriched in phosphatidylinositol 3-phosphate and dynamically connected to the endoplasmic reticulum. *The Journal of cell biology*. **182**, 685-701.

Axelrod, D. (2003) [1] Total internal reflection fluorescence microscopy in cell biology. *Methods in enzymology*, pp 1-33, Elsevier

Bach, G. (2001) Mucolipidosis type IV. *Molecular genetics and metabolism*. **73**, 197-203.

Bagshaw, R. D., J. W. Callahan and D. J. Mahuran (2006) The Arf-family protein, Arl8b, is involved in the spatial distribution of lysosomes. *Biochemical and biophysical research communications*. **344**, 1186-1191.

Bai, J., Y. Li and G. Zhang (2017) Cell cycle regulation and anticancer drug discovery. *Cancer biology & medicine*. **14**, 348.

Bainton, D. F. (1981) The discovery of lysosomes. *The Journal of cell biology*. **91**, 66s-76s.

Balla, A. and T. Balla (2006) Phosphatidylinositol 4-kinases: old enzymes with emerging functions. *Trends in cell biology*. **16**, 351-361.

Balla, T. (2013) Phosphoinositides: tiny lipids with giant impact on cell regulation. *Physiological reviews*. **93**, 1019-1137.

Baluška, F., D. Menzel and P. W. Barlow (2006) Cytokinesis in plant and animal cells: endosomes 'shut the door'. *Developmental biology*. **294**, 1-10.

Ban, R., Y. Irino, K. Fukami and H. Tanaka (2004) Human mitotic spindle-associated protein PRC1 inhibits MgcRacGAP activity toward Cdc42 during the metaphase. *Journal of Biological Chemistry*. **279**, 16394-16402.

Band, A. M., J. Määttä, L. Kääriäinen and E. Kuismanen (2001) Inhibition of the membrane fusion machinery prevents exit from the TGN and proteolytic processing by furin. *FEBS letters*. **505**, 118-124.

Bandyopadhyay, U., S. Kaushik, L. Varticovski and A. M. Cuervo (2008) The chaperone-mediated autophagy receptor organizes in dynamic protein complexes at the lysosomal membrane. *Molecular and cellular biology*. **28**, 5747-5763.

Baron, R., L. Neff, D. Louvard and P. J. Courtoy (1985) Cell-mediated extracellular acidification and bone resorption: evidence for a low pH in resorbing lacunae and localization of a 100-kD lysosomal membrane protein at the osteoclast ruffled border. *The Journal of cell biology*. **101**, 2210-2222.

Barr, A. R. and F. Gergely (2007) Aurora-A: the maker and breaker of spindle poles. *Journal of cell science*. **120**, 2987-2996.

Basant, A. and M. Glotzer (2018) Spatiotemporal Regulation of RhoA during Cytokinesis. *Current Biology*. **28**, R570-R580.

Basant, A., S. Lekomtsev, Y. C. Tse, D. Zhang, K. M. Longhini, M. Petronczki and M. Glotzer (2015) Aurora B kinase promotes cytokinesis by inducing centralspindlin oligomers that associate with the plasma membrane. *Developmental cell*. **33**, 204-215.

Bassi, Z. I., M. Audusseau, M. G. Riparbelli, G. Callaini and P. P. D'Avino (2013) Citron kinase controls a molecular network required for midbody formation in cytokinesis. *Proceedings of the National Academy of Sciences*. **110**, 9782-9787.

Bassi, Z. I., K. J. Verbrugghe, L. Capalbo, S. Gregory, E. Montembault, D. M. Glover and P. P. D'Avino (2011) Sticky/Citron kinase maintains proper RhoA localization at the cleavage site during cytokinesis. *J Cell Biol*. **195**, 595-603.

Bastos, R. N., S. R. Gandhi, R. D. Baron, U. Gruneberg, E. A. Nigg and F. A. Barr (2013) Aurora B suppresses microtubule dynamics and limits central spindle size by locally activating KIF4A. *J Cell Biol*. **202**, 605-621.

Bellettato, C. M. and M. Scarpa (2010) Pathophysiology of neuropathic lysosomal storage disorders. *Journal of inherited metabolic disease*. **33**, 347-362.

Bento, C. F., C. Puri, K. Moreau and D. C. Rubinsztein (2013) The role of membrane-trafficking small GTPases in the regulation of autophagy. *J Cell Sci*. **126**, 1059-1069.

Berg, T., P. Strømhaug, T. Løvdal, P. Seglen and T. Berg (1994) Use of glycyl-L-phenylalanine 2-naphthylamide, a lysosome-disrupting cathepsin C substrate, to distinguish between lysosomes and prelysosomal endocytic vacuoles. *Biochemical Journal*. **300**, 229-236.

Bergeland, T., J. Widerberg, O. Bakke and T. W. Nordeng (2001) Mitotic partitioning of endosomes and lysosomes. *Current Biology*. **11**, 644-651.

Bertin, A., M. A. McMurray, L. Thai, G. Garcia, V. Votin, P. Grob, T. Allyn, J. Thorner and E. Nogales (2010) Phosphatidylinositol-4, 5-bisphosphate

promotes budding yeast septin filament assembly and organization. *Journal of molecular biology*. **404**, 711-731.

Beyenbach, K. W. and H. Wieczorek (2006) The V-type H+ ATPase: molecular structure and function, physiological roles and regulation. *Journal of Experimental Biology*. **209**, 577-589.

Bi, G.-Q., J. M. Alderton and R. A. Steinhardt (1995) Calcium-regulated exocytosis is required for cell membrane resealing. *The Journal of cell biology*. **131**, 1747-1758.

Bitsikas, V., I. R. Corrêa Jr and B. J. Nichols (2014) Clathrin-independent pathways do not contribute significantly to endocytic flux. *Elife*. **3**, e03970.

Block, M. R., B. S. Glick, C. A. Wilcox, F. T. Wieland and J. E. Rothman (1988) Purification of an N-ethylmaleimide-sensitive protein catalyzing vesicular transport. *Proceedings of the national academy of sciences*. **85**, 7852-7856.

Blott, E. J. and G. M. Griffiths (2002) Secretory lysosomes. *Nature reviews Molecular cell biology*. **3**, 122.

Bluemink, J. G. and S. W. De Laat (1973) New membrane formation during cytokinesis in normal and cytochalasin B-treated eggs of Xenopus laevis: I. Electron microscope observations. *The Journal of cell biology*. **59**, 89-108.

Boehm, M. and J. S. Bonifacino (2001) Adaptins: the final recount. *Molecular biology of the cell*. **12**, 2907-2920.

Bonnans, C., J. Chou and Z. Werb (2014) Remodelling the extracellular matrix in development and disease. *Nature reviews Molecular cell biology*. **15**, 786.

Boucrot, E. and T. Kirchhausen (2007) Endosomal recycling controls plasma membrane area during mitosis. *Proceedings of the National Academy of Sciences*. **104**, 7939-7944.

Bourbouze, R., F. Raffi, G. Dameron, H. Hali-Miraftab, F. Loko and J.-L. Vilde (1991) N-acetyl-β-D-Glucosaminidase (NAG) isoenzymes release from human monocyte-derived macrophages in response to zymosan and human recombinant interferon-γ. *Clinica chimica acta*. **199**, 185-194.

Boya, P., F. Reggiori and P. Codogno (2013) Emerging regulation and functions of autophagy. *Nature cell biology*. **15**, 713.

Braulke, T. and J. S. Bonifacino (2009) Sorting of lysosomal proteins. *Biochimica et Biophysica Acta (BBA)-Molecular Cell Research*. **1793**, 605-614.

Brill, J. A., G. R. Hime, M. Scharer-Schuksz and M. T. Fuller (2000) A phospholipid kinase regulates actin organization and intercellular bridge formation during germline cytokinesis. *Development*. **127**, 3855-3864.

Brill, J. A., R. Wong and A. Wilde (2011) Phosphoinositide function in cytokinesis. *Current biology*. **21**, R930-R934.

Brown, C. L., K. C. Maier, T. Stauber, L. M. Ginkel, L. Wordeman, I. Vernos and T. A. Schroer (2005) Kinesin-2 is a motor for late endosomes and lysosomes. *Traffic*. **6**, 1114-1124.

Brown, W. J., J. Goodhouse and M. G. Farquhar (1986) Mannose-6-phosphate receptors for lysosomal enzymes cycle between the Golgi complex and endosomes. *The Journal of cell biology*. **103**, 1235-1247.

Bucci, C., P. Thomsen, P. Nicoziani, J. McCarthy and B. van Deurs (2000) Rab7: a key to lysosome biogenesis. *Molecular biology of the cell*. **11**, 467-480.

Burgoyne, R. D. and A. Morgan (2003) Secretory granule exocytosis. *Physiological reviews*. **83**, 581-632.

Burkhardt, J. K., C. J. Echeverri, T. Nilsson and R. B. Vallee (1997) Overexpression of the dynamitin (p50) subunit of the dynactin complex disrupts dynein-dependent maintenance of membrane organelle distribution. *The Journal of cell biology*. **139**, 469-484.

Caldwell, C. M., R. A. Green and K. B. Kaplan (2007) APC mutations lead to cytokinetic failures in vitro and tetraploid genotypes in Min mice. *J Cell Biol*. **178**, 1109-1120.

Cantalupo, G., P. Alifano, V. Roberti, C. B. Bruni and C. Bucci (2001) Rab-interacting lysosomal protein (RILP): the Rab7 effector required for transport to lysosomes. *The EMBO journal*. **20**, 683-693.

Carmena, M. (2012) Abscission checkpoint control: stuck in the middle with Aurora B. *Open biology*. **2**, 120095.

Carmena, M., M. Wheelock, H. Funabiki and W. C. Earnshaw (2012) The chromosomal passenger complex (CPC): from easy rider to the godfather of mitosis. *Nature reviews Molecular cell biology*. **13**, 789.

Carnell, M., T. Zech, S. D. Calaminus, S. Ura, M. Hagedorn, S. A. Johnston, R. C. May, T. Soldati, L. M. Machesky and R. H. Insall (2011) Actin polymerization driven by WASH causes V-ATPase retrieval and vesicle neutralization before exocytosis. *The Journal of cell biology*, jcb. 201009119.

Carpentier, J.-L., P. Gorden, R. Anderson, J. L. Goldstein, M. S. Brown, S. Cohen and L. Orci (1982) Co-localization of 125I-epidermal growth factor and ferritin-low density lipoprotein in coated pits: a quantitative electron microscopic study in normal and mutant human fibroblasts. *The Journal of Cell Biology*. **95**, 73-77.

Castro-Gomes, T., M. Corrotte, C. Tam and N. Andrews (2015) Plasma-membrane Repair is Regulated Extracellularly by Proteases Released from Lysosomes. *The FASEB Journal*. **29**, 884.42.

Castro-Gomes, T., M. Corrotte, C. Tam and N. W. Andrews (2016) Plasma membrane repair is regulated extracellularly by proteases released from lysosomes. *PloS one*. **11**, e0152583.

Cauvin, C. and A. Echard (2015) Phosphoinositides: Lipids with informative heads and mastermind functions in cell division. *Biochimica et Biophysica Acta (BBA)-Molecular and Cell Biology of Lipids*. **1851**, 832-843.

Cerny, J., Y. Feng, A. Yu, K. Miyake, B. Borgonovo, J. Klumperman, J. Meldolesi, P. L. McNeil and T. Kirchhausen (2004) The small chemical vacuolin-1 inhibits Ca2+-dependent lysosomal exocytosis but not cell resealing. *EMBO reports*. **5**, 883-888.

Charras, G. (2008) A short history of blebbing. *Journal of microscopy*. **231**, 466-478.

Chieregatti, E. and J. Meldolesi (2005) Regulated exocytosis: new organelles for non-secretory purposes. *Nature reviews Molecular cell biology*. **6**, 181.

Chin, C. F. and F. M. Yeong (2010) Safeguarding entry into mitosis: the antephase checkpoint. *Molecular and cellular biology*. **30**, 22-32.

Christensen, K. A., J. T. Myers and J. A. Swanson (2002) pH-dependent regulation of lysosomal calcium in macrophages. *Journal of cell science*. **115**, 599-607.

Churchill, G. C., Y. Okada, J. M. Thomas, A. A. Genazzani, S. Patel and A. Galione (2002) NAADP mobilizes Ca2+ from reserve granules, lysosome-related organelles, in sea urchin eggs. *Cell*. **111**, 703-708.

Cipriano, D. J., Y. Wang, S. Bond, A. Hinton, K. C. Jefferies, J. Qi and M. Forgac (2008) Structure and regulation of the vacuolar ATPases. *Biochimica et Biophysica Acta (BBA)-Bioenergetics*. **1777**, 599-604.

Conus, S. and H.-U. Simon (2008) Cathepsins: key modulators of cell death and inflammatory responses. *Biochemical pharmacology*. **76**, 1374-1382.

Cooper, S. T. and P. L. McNeil (2015) Membrane repair: mechanisms and pathophysiology. *Physiological reviews*. **95**, 1205-1240.

Costantini, L. M., M. Baloban, M. L. Markwardt, M. Rizzo, F. Guo, V. V. Verkhusha and E. L. Snapp (2015) A palette of fluorescent proteins optimized for diverse cellular environments. *Nature communications*. **6**, 7670.

Coutinho, M. F., M. J. Prata and S. Alves (2012) A shortcut to the lysosome: the mannose-6-phosphate-independent pathway. *Molecular genetics and metabolism*. **107**, 257-266.

Cuervo, A. M. and J. F. Dice (1996) A receptor for the selective uptake and degradation of proteins by lysosomes. *Science*. **273**, 501-503.

Cunningham, K. W. and G. R. Fink (1996) Calcineurin inhibits VCX1-dependent H+/Ca2+ exchange and induces Ca2+ ATPases in Saccharomyces cerevisiae. *Molecular and Cellular Biology*. **16**, 2226-2237.

Czibener, C., N. M. Sherer, S. M. Becker, M. Pypaert, E. Hui, E. R. Chapman, W. Mothes and N. W. Andrews (2006) Ca2+ and synaptotagmin VII–dependent delivery of lysosomal membrane to nascent phagosomes. *The Journal of cell biology*. **174**, 997-1007.

D'Avino, P. P., T. Takeda, L. Capalbo, W. Zhang, K. S. Lilley, E. D. Laue and D. M. Glover (2008) Interaction between Anillin and RacGAP50C

connects the actomyosin contractile ring with spindle microtubules at the cell division site. *Journal of cell science*. **121**, 1151-1158.

D'Avino, P. P., M. G. Giansanti and M. Petronczki (2015) Cytokinesis in animal cells. *Cold Spring Harbor perspectives in biology*, a015834.

Dambournet, D., M. Machicoane, L. Chesneau, M. Sachse, M. Rocancourt, A. El Marjou, E. Formstecher, R. Salomon, B. Goud and A. Echard (2011) Rab35 GTPase and OCRL phosphatase remodel lipids and F-actin for successful cytokinesis. *Nature cell biology*. **13**, 981.

Davidson, S. M. and M. G. Vander Heiden (2017) Critical functions of the lysosome in cancer biology. *Annual review of pharmacology and toxicology*. **57**, 481-507.

de Barry, J., A. Janoshazi, J. L. Dupont, O. Procksch, S. Chasserot-Golaz, A. Jeromin and N. Vitale (2006) Functional implication of neuronal calcium sensor-1 and phosphoinositol 4-kinase-β interaction in regulated exocytosis of PC12 cells. *Journal of Biological Chemistry*. **281**, 18098-18111.

De Duve, C. and R. Wattiaux (1966) Functions of lysosomes. *Annual review of physiology*. **28**, 435-492.

De Luca, M., L. Cogli, C. Progida, V. Nisi, R. Pascolutti, S. Sigismund, P. P. Di Fiore and C. Bucci (2014) RILP regulates vacuolar ATPase through interaction with the V1G1 subunit. *J Cell Sci*. **127**, 2697-2708.

Di Paolo, G. and P. De Camilli (2006) Phosphoinositides in cell regulation and membrane dynamics. *Nature*. **443**, 651.

Dielschneider, R. F., E. S. Henson and S. B. Gibson (2017) Lysosomes as oxidative targets for cancer therapy. *Oxidative medicine and cellular longevity*. **2017**.

Dominguez-Brauer, C., K. L. Thu, J. M. Mason, H. Blaser, M. R. Bray and T. W. Mak (2015) Targeting mitosis in cancer: emerging strategies. *Molecular cell*. **60**, 524-536.

Dong, X.-p., D. Shen, X. Wang, T. Dawson, X. Li, Q. Zhang, X. Cheng, Y. Zhang, L. S. Weisman and M. Delling (2010) PI (3, 5) P 2 controls membrane trafficking by direct activation of mucolipin Ca 2+ release channels in the endolysosome. *Nature communications*. **1**, 38.

Dou, Y., H.-j. Wu, H.-q. Li, S. Qin, Y.-e. Wang, J. Li, H.-f. Lou, Z. Chen, X.-m. Li and Q.-m. Luo (2012) Microglial migration mediated by ATP-induced ATP release from lysosomes. *Cell research*. **22**, 1022.

Dröse, S. and K. Altendorf (1997) Bafilomycins and concanamycins as inhibitors of V-ATPases and P-ATPases. *Journal of experimental biology*. **200**, 1-8.

Echard, A. (2008) Membrane traffic and polarization of lipid domains during cytokinesis, Portland Press Limited

Echard, A. (2012) Phosphoinositides and cytokinesis: the “PIP” of the iceberg. *Cytoskeleton*. **69**, 893-912.

Eckenstaler, R., V. Lessmann and T. Brigadski (2016) CAPS1 effects on intragranular pH and regulation of BDNF release from secretory granules in hippocampal neurons. *J Cell Sci*, jcs. 178251.

Eder, C. (2009) Mechanisms of interleukin-1β release. *Immunobiology*. **214**, 543-553.

Elkin, S. R., N. Bendris, C. Reis, Y. Zhou, Y. Xie, K. E. Huffman, J. D. Minna and S. L. Schmid (2015) A systematic analysis reveals heterogeneous changes in the endocytic activities of cancer cells. *Cancer research*, canres. 0939.2015.

Elkin, S. R., A. M. Lakoduk and S. L. Schmid (2016) Endocytic pathways and endosomal trafficking: a primer. *Wiener Medizinische Wochenschrift*. **166**, 196-204.

Emoto, K., H. Inadome, Y. Kanaho, S. Narumiya and M. Umeda (2005) Local change in phospholipid composition at the cleavage furrow is essential for completion of cytokinesis. *Journal of biological chemistry*. **280**, 37901-37907.

Encarnação, M., L. Espada, C. Escrevente, D. Mateus, J. Ramalho, X. Michelet, I. Santarino, V. W. Hsu, M. B. Brenner and D. C. Barral (2016) A Rab3a-dependent complex essential for lysosome positioning and plasma membrane repair. *J Cell Biol*. **213**, 631-640.

Erdal, H., M. Berndtsson, J. Castro, U. Brunk, M. C. Shoshan and S. Linder (2005) Induction of lysosomal membrane permeabilization by compounds that activate p53-independent apoptosis. *Proceedings of the National Academy of Sciences*. **102**, 192-197.

Erickson, C. and J. Trinkaus (1976) Microvilli and blebs as sources of reserve surface membrane during cell spreading. *Experimental cell research*. **99**, 375-384.

Eskelinen, E.-L., Y. Tanaka and P. Saftig (2003) At the acidic edge: emerging functions for lysosomal membrane proteins. *Trends in cell biology*. **13**, 137-145.

Ezaki, J., M. Himeno and K. Kato (1992) Purification and characterization of (Ca2+-Mg2+)-ATPase in rat liver lysosomal membranes. *The Journal of Biochemistry*. **112**, 33-39.

Fededa, J. P. and D. W. Gerlich (2012) Molecular control of animal cell cytokinesis. *Nature cell biology*. **14**, 440.

Fehrenbacher, N., M. Gyrd-Hansen, B. Poulsen, U. Felbor, T. Kallunki, M. Boes, E. Weber, M. Leist and M. Jäättelä (2004) Sensitization to the lysosomal cell death pathway upon immortalization and transformation. *Cancer research*. **64**, 5301-5310.

Ferguson, S., A. Raimondi, S. Paradise, H. Shen, K. Mesaki, A. Ferguson, O. Destaing, G. Ko, J. Takasaki and O. Cremona (2009) Coordinated actions of actin and BAR proteins upstream of dynamin at endocytic clathrin-coated pits. *Developmental cell*. **17**, 811-822.

Field, C. M., M. Coughlin, S. Doberstein, T. Marty and W. Sullivan (2005a) Characterization of anillin mutants reveals essential roles in septin localization and plasma membrane integrity. *Development*. **132**, 2849-2860.

Field, S. J., N. Madson, M. L. Kerr, K. A. Galbraith, C. E. Kennedy, M. Tahiliani, A. Wilkins and L. C. Cantley (2005b) PtdIns (4, 5) P2 functions at the cleavage furrow during cytokinesis. *Current biology*. **15**, 1407-1412.

Fischer, M., C. V. Dang and J. A. DeCaprio (2018) Control of Cell Division. *Hematology (Seventh Edition)*, pp 176-185, Elsevier

Fishkind, D. J. and Y.-l. Wang (1993) Orientation and three-dimensional organization of actin filaments in dividing cultured cells. *The Journal of Cell Biology*. **123**, 837-848.

Flemming, W. (1965) Contributions to the knowledge of the cell and its vital processes. *The Journal of cell biology*. **25**, 3.

Forer, A. and P. J. Sillers (1987) The role of the phosphatidylinositol cycle in mitosis in sea urchin zygotes: Lithium inhibition is overcome by myo-inositol but not by other cyclitols or sugars. *Experimental cell research*. **170**, 42-55.

Frémont, S. and A. Echard (2018) Membrane Traffic in the Late Steps of Cytokinesis. *Current Biology*. **28**, R458-R470.

Frémont, S., H. Hammich, J. Bai, H. Wioland, K. Klinkert, M. Rocancourt, C. Kikuti, D. Stroebel, G. Romet-Lemonne and O. Pylypenko (2017) Oxidation of F-actin controls the terminal steps of cytokinesis. *Nature communications*. **8**, 14528.

Fujiwara, T., M. Bandi, M. Nitta, E. V. Ivanova, R. T. Bronson and D. Pellman (2005) Cytokinesis failure generating tetraploids promotes tumorigenesis in p53-null cells. *Nature*. **437**, 1043.

Furse, S., N. J. Brooks, A. M. Seddon, R. Woscholski, R. H. Templer, E. W. Tate, P. R. Gaffney and O. Ces (2012) Lipid membrane curvature induced by distearoyl phosphatidylinositol 4-phosphate. *Soft Matter*. **8**, 3090-3093.

Furuta, N., T. Yoshimori and A. Amano (2010) Mediatory molecules that fuse autophagosomes and lysosomes. *Autophagy*. **6**, 417-418.

Fusek, M., M. Mares and V. Vetvicka (2013) Cathepsin D. *Handbook of Proteolytic Enzymes (Third Edition)*, pp 54-63, Elsevier

Futerman, A. H. and G. Van Meer (2004) The cell biology of lysosomal storage disorders. *Nature reviews Molecular cell biology*. **5**, 554.

Galione, A. (2011) NAADP receptors. *Cold Spring Harbor perspectives in biology*. **3**, a004036.

Galione, A., A. J. Morgan, A. Arredouani, L. C. Davis, K. Rietdorf, M. Ruas and J. Parrington (2010) NAADP as an intracellular messenger regulating lysosomal calcium-release channels, Portland Press Limited

Ganem, N. J., S. A. Godinho and D. Pellman (2009) A mechanism linking extra centrosomes to chromosomal instability. *Nature*. **460**, 278.

Ganley, I. G., K. Carroll, L. Bittova and S. Pfeffer (2004) Rab9 GTPase regulates late endosome size and requires effector interaction for its stability. *Molecular biology of the cell*. **15**, 5420-5430.

Garrity, A. G., W. Wang, C. M. Collier, S. A. Levey, Q. Gao and H. Xu (2016) The endoplasmic reticulum, not the pH gradient, drives calcium refilling of lysosomes. *Elife*. **5**, e15887.

Geng, J., U. Nair, K. Yasumura-Yorimitsu and D. J. Klionsky (2010) Post-Golgi Sec proteins are required for autophagy in Saccharomyces cerevisiae. *Molecular biology of the cell*. **21**, 2257-2269.

Gocheva, V., W. Zeng, D. Ke, D. Klimstra, T. Reinheckel, C. Peters, D. Hanahan and J. A. Joyce (2006) Distinct roles for cysteine cathepsin genes in multistage tumorigenesis. *Genes & development*. **20**, 543-556.

Goss, J. W. and D. K. Toomre (2008) Both daughter cells traffic and exocytose membrane at the cleavage furrow during mammalian cytokinesis. *The Journal of cell biology*. **181**, 1047-1054.

Granger, B., S. Green, C. Gabel, C. L. Howe, I. Mellman and A. Helenius (1990) Characterization and cloning of lgp110, a lysosomal membrane glycoprotein from mouse and rat cells. *Journal of Biological Chemistry*. **265**, 12036-12043.

Green, R. A., E. Paluch and K. Oegema (2012) Cytokinesis in animal cells. *Annual review of cell and developmental biology*. **28**, 29-58.

Gregory, S. L., S. Ebrahimi, J. Milverton, W. M. Jones, A. Bejsovec and R. Saint (2008) Cell division requires a direct link between microtubule-bound RacGAP and Anillin in the contractile ring. *Current biology*. **18**, 25-29.

Gromley, A., C. Yeaman, J. Rosa, S. Redick, C.-T. Chen, S. Mirabelle, M. Guha, J. Sillibourne and S. J. Doxsey (2005) Centriolin anchoring of exocyst and SNARE complexes at the midbody is required for secretory-vesicle-mediated abscission. *Cell*. **123**, 75-87.

Gruneberg, U., R. Neef, R. Honda, E. A. Nigg and F. A. Barr (2004) Relocation of Aurora B from centromeres to the central spindle at the metaphase to anaphase transition requires MKlp2. *The Journal of cell biology*. **166**, 167-172.

Gruneberg, U., R. Neef, X. Li, E. H. Chan, R. B. Chalamalasetty, E. A. Nigg and F. A. Barr (2006) KIF14 and citron kinase act together to promote efficient cytokinesis. *The Journal of cell biology*. **172**, 363-372.

Guse, A., M. Mishima and M. Glotzer (2005) Phosphorylation of ZEN-4/MKLP1 by aurora B regulates completion of cytokinesis. *Current biology*. **15**, 778-786.

Hailey, D. W., A. S. Rambold, P. Satpute-Krishnan, K. Mitra, R. Sougrat, P. K. Kim and J. Lippincott-Schwartz (2010) Mitochondria supply membranes for autophagosome biogenesis during starvation. *Cell*. **141**, 656-667.

Hakem, R. (2008) DNA-damage repair; the good, the bad, and the ugly. *The EMBO journal*. **27**, 589-605.

Haller, T., P. Dietl, P. Deetjen and H. Völkl (1996) The lysosomal compartment as intracellular calcium store in MDCK cells: a possible involvement in InsP3-mediated Ca2+ release. *Cell calcium*. **19**, 157-165.

Hämälistö, S. and M. Jäättelä (2016) Lysosomes in cancer—living on the edge (of the cell). *Current opinion in cell biology*. **39**, 69-76.

Hammond, G. R., M. P. Machner and T. Balla (2014) A novel probe for phosphatidylinositol 4-phosphate reveals multiple pools beyond the Golgi. *The Journal of cell biology*. **205**, 113-126.

Hara, T., K. Nakamura, M. Matsui, A. Yamamoto, Y. Nakahara, R. Suzuki-Migishima, M. Yokoyama, K. Mishima, I. Saito and H. Okano (2006) Suppression of basal autophagy in neural cells causes neurodegenerative disease in mice. *Nature*. **441**, 885.

Harada, A., Y. Takei, Y. Kanai, Y. Tanaka, S. Nonaka and N. Hirokawa (1998) Golgi vesiculation and lysosome dispersion in cells lacking cytoplasmic dynein. *The Journal of cell biology*. **141**, 51-59.

Harder, T. and K. Simons (1997) Caveolae, DIGs, and the dynamics of sphingolipid—cholesterol microdomains. *Current opinion in cell biology*. **9**, 534-542.

Henley, J. R., E. W. Krueger, B. J. Oswald and M. A. McNiven (1998) Dynamin-mediated internalization of caveolae. *The Journal of cell biology*. **141**, 85-99.

Heuser, J. (1989) Changes in lysosome shape and distribution correlated with changes in cytoplasmic pH. *The Journal of cell biology*. **108**, 855-864.

Higgins, J., C. Midgley, A.-M. Bergh, S. M. Bell, J. M. Askham, E. Roberts, R. K. Binns, S. M. Sharif, C. Bennett and D. M. Glover (2010) Human

ASPM participates in spindle organisation, spindle orientation and cytokinesis. *BMC cell biology*. **11**, 85.

Hochegger, H., S. Takeda and T. Hunt (2008) Cyclin-dependent kinases and cell-cycle transitions: does one fit all? *Nature reviews Molecular cell biology*. **9**, 910.

Hockey, L. N., B. S. Kilpatrick, E. R. Eden, Y. Lin-Moshier, G. C. Brailoiu, E. Brailoiu, C. E. Futter, A. H. Schapira, J. S. Marchant and S. Patel (2015) Dysregulation of lysosomal morphology by pathogenic LRRK2 is corrected by TPC2 inhibition. *J Cell Sci*. **128**, 232-238.

Högnäs, G., S. Tuomi, S. Veltel, E. Mattila, A. Murumägi, H. Edgren, O. Kallioniemi and J. Ivaska (2012) Cytokinesis failure due to derailed integrin traffic induces aneuploidy and oncogenic transformation in vitro and in vivo. *Oncogene*. **31**, 3597.

Hollenbeck, P. J. and J. A. Swanson (1990) Radial extension of macrophage tubular lysosomes supported by kinesin. *Nature*. **346**, 864.

Horton, J. S., C. T. Wakano, M. Speck and A. J. Stokes (2015) Two-pore channel 1 interacts with citron kinase, regulating completion of cytokinesis. *Channels*. **9**, 21-29.

Huotari, J. and A. Helenius (2011) Endosome maturation. *The EMBO journal*. **30**, 3481-3500.

Huynh, C. and N. W. Andrews (2005) The small chemical vacuolin-1 alters the morphology of lysosomes without inhibiting Ca2+-regulated exocytosis. *EMBO Rep*. **6**, 843-7.

Huynh, K. K., E. L. Eskelinen, C. C. Scott, A. Malevanets, P. Saftig and S. Grinstein (2007) LAMP proteins are required for fusion of lysosomes with phagosomes. *The EMBO journal*. **26**, 313-324.

Idone, V., C. Tam and N. W. Andrews (2008) Two-way traffic on the road to plasma membrane repair. *Trends in cell biology*. **18**, 552-559.

Inoue, Y. H., M. S. Savoian, T. Suzuki, E. Máthé, M.-T. Yamamoto and D. M. Glover (2004) Mutations in orbit/mast reveal that the central spindle is comprised of two microtubule populations, those that initiate cleavage and those that propagate furrow ingression. *J Cell Biol*. **166**, 49-60.

Ishida, Y., S. Nayak, J. A. Mindell and M. Grabe (2013) A model of lysosomal pH regulation. *The Journal of general physiology*. **141**, 705-720.

Ishikawa, T. (2012) Structural biology of cytoplasmic and axonemal dyneins. *Journal of structural biology*. **179**, 229-234.

Itakura, E., C. Kishi-Itakura and N. Mizushima (2012) The hairpin-type tail-anchored SNARE syntaxin 17 targets to autophagosomes for fusion with endosomes/lysosomes. *Cell*. **151**, 1256-1269.

Ito, M. (2000) Factors controlling cyclin B expression. *The Plant Cell Cycle*, pp 133-146, Springer

Jadot, M., C. Colmant, S. Wattiaux-De Coninck and R. Wattiaux (1984) Intralysosomal hydrolysis of glycyl-L-phenylalanine 2-naphthylamide. *Biochemical Journal*. **219**, 965-970.

Jaiswal, J. K., N. W. Andrews and S. M. Simon (2002) Membrane proximal lysosomes are the major vesicles responsible for calcium-dependent exocytosis in nonsecretory cells. *The Journal of cell biology*. **159**, 625-635.

Janetopoulos, C., J. Borleis, F. Vazquez, M. Iijima and P. Devreotes (2005) Temporal and spatial regulation of phosphoinositide signaling mediates cytokinesis. *Developmental cell*. **8**, 467-477.

Jentsch, T. J. (2007) Chloride and the endosomal–lysosomal pathway: emerging roles of CLC chloride transporters. *The Journal of physiology*. **578**, 633-640.

Johnson, D. E., P. Ostrowski, V. Jaumouillé and S. Grinstein (2016) The position of lysosomes within the cell determines their luminal pH. *The Journal of cell biology*. **212**, 677-692.

Jongsma, M. L., I. Berlin and J. Neefjes (2015) On the move: organelle dynamics during mitosis. *Trends in cell biology*. **25**, 112-124.

Jongsma, M. L., I. Berlin, R. H. Wijdeven, L. Janssen, G. M. Janssen, M. A. Garstka, H. Janssen, M. Mensink, P. A. van Veelen and R. M. Spaapen (2016) An ER-associated pathway defines endosomal architecture for controlled cargo transport. *Cell*. **166**, 152-166.

Jordens, I., M. Fernandez-Borja, M. Marsman, S. Dusseljee, L. Janssen, J. Calafat, H. Janssen, R. Wubbolts and J. Neefjes (2001) The Rab7 effector protein RILP controls lysosomal transport by inducing the recruitment of dynein-dynactin motors. *Current Biology*. **11**, 1680-1685.

Kao, J., J. M. Alderton, R. Y. Tsien and R. A. Steinhardt (1990) Active involvement of Ca2+ in mitotic progression of Swiss 3T3 fibroblasts. *The Journal of Cell Biology*. **111**, 183-196.

Kaplan, A. and O. Reiner (2011) Linking cytoplasmic dynein and transport of Rab8 vesicles to the midbody during cytokinesis by the doublecortin domain-containing 5 protein. *J Cell Sci*, jcs. 085407.

Kaushik, S. and A. M. Cuervo (2012) Chaperone-mediated autophagy: a unique way to enter the lysosome world. *Trends in cell biology*. **22**, 407-417.

Kechad, A., S. Jananji, Y. Ruella and G. R. Hickson (2012) Anillin acts as a bifunctional linker coordinating midbody ring biogenesis during cytokinesis. *Current biology*. **22**, 197-203.

Kilpatrick, B. S., E. R. Eden, A. H. Schapira, C. E. Futter and S. Patel (2013) Direct mobilisation of lysosomal Ca2+ triggers complex Ca2+ signals. *J Cell Sci*. **126**, 60-66.

Kim, H., F. Guo, S. Brahma, Y. Xing and M. E. Burkard (2014) Centralspindlin assembly and 2 phosphorylations on MgcRacGAP by Polo-like kinase 1 initiate Ect2 binding in early cytokinesis. *Cell Cycle*. **13**, 2952-2961.

Kim, J.-E., D. D. Billadeau and J. Chen (2005) The tandem BRCT domains of Ect2 are required for both negative and positive regulation of Ect2 in cytokinesis. *Journal of biological chemistry*. **280**, 5733-5739.

Kinoshita, M., S. Kumar, A. Mizoguchi, C. Ide, A. Kinoshita, T. Haraguchi, Y. Hiraoka and M. Noda (1997) Nedd5, a mammalian septin, is a novel cytoskeletal component interacting with actin-based structures. *Genes & development*. **11**, 1535-1547.

Kirchhausen, T. (1999) Adaptors for clathrin-mediated traffic. *Annual review of cell and developmental biology*. **15**, 705-732.

Kirkegaard, T. and M. Jäättelä (2009) Lysosomal involvement in cell death and cancer. *Biochimica et Biophysica Acta (BBA)-Molecular Cell Research*. **1793**, 746-754.

Kiss, A. L. (2012) Caveolae and the regulation of endocytosis. *Caveolins and Caveolae*, pp 14-28, Springer

Klumperman, J. and G. Raposo (2014) The complex ultrastructure of the endolysosomal system. *Cold Spring Harbor perspectives in biology*, a016857.

Knight, Z. A., B. Gonzalez, M. E. Feldman, E. R. Zunder, D. D. Goldenberg, O. Williams, R. Loewith, D. Stokoe, A. Balla and B. Toth (2006) A pharmacological map of the PI3-K family defines a role for p110α in insulin signaling. *Cell*. **125**, 733-747.

Kops, G. J., B. A. Weaver and D. W. Cleveland (2004) On the road to cancer: aneuploidy and the mitotic checkpoint. *Nature Reviews Cancer*. **5**, 773.

Korolchuk, V. I., S. Saiki, M. Lichtenberg, F. H. Siddiqi, E. A. Roberts, S. Imarisio, L. Jahreiss, S. Sarkar, M. Futter and F. M. Menzies (2011) Lysosomal positioning coordinates cellular nutrient responses. *Nature cell biology*. **13**, 453.

Kosako, H., T. Yoshida, F. Matsumura, T. Ishizaki, S. Narumiya and M. Inagaki (2000) Rho-kinase/ROCK is involved in cytokinesis through the phosphorylation of myosin light chain and not ezrin/radixin/moesin proteins at the cleavage furrow. *Oncogene*. **19**, 6059.

Kotýnková, K., K.-C. Su, S. C. West and M. Petronczki (2016) Plasma membrane association but not midzone recruitment of RhoGEF ECT2 is essential for cytokinesis. *Cell reports*. **17**, 2672-2686.

Kouranti, I., M. Sachse, N. Arouche, B. Goud and A. Echard (2006) Rab35 regulates an endocytic recycling pathway essential for the terminal steps of cytokinesis. *Current biology*. **16**, 1719-1725.

Krzewski, K., A. Gil-Krzewska, V. Nguyen, G. Peruzzi and J. E. Coligan (2013) LAMP1/CD107a is required for efficient perforin delivery to lytic granules and NK cell cytotoxicity. *Blood*, blood-2012-08-453738.

Kunda, P., A. E. Pelling, T. Liu and B. Baum (2008) Moesin controls cortical rigidity, cell rounding, and spindle morphogenesis during mitosis. *Current Biology*. **18**, 91-101.

Kurasawa, Y., W. C. Earnshaw, Y. Mochizuki, N. Dohmae and K. Todokoro (2004) Essential roles of KIF4 and its binding partner PRC1 in organized central spindle midzone formation. *The EMBO journal*. **23**, 3237-3248.

Lapenna, S. and A. Giordano (2009) Cell cycle kinases as therapeutic targets for cancer. *Nature reviews Drug discovery*. **8**, 547.

Lee, J.-A. (2012) Neuronal autophagy: a housekeeper or a fighter in neuronal cell survival? *Experimental neurobiology*. **21**, 1-8.

Lee, Y.-K. and J.-A. Lee (2016) Role of the mammalian ATG8/LC3 family in autophagy: differential and compensatory roles in the spatiotemporal regulation of autophagy. *BMB reports*. **49**, 424.

Lekomtsev, S., K.-C. Su, V. E. Pye, K. Blight, S. Sundaramoorthy, T. Takaki, L. M. Collinson, P. Cherepanov, N. Divecha and M. Petronczki (2012) Centralspindlin links the mitotic spindle to the plasma membrane during cytokinesis. *Nature*. **492**, 276.

Li, M., B. Khambu, H. Zhang, J.-H. Kang, X. Chen, D. Chen, L. Vollmer, P.-Q. Liu, A. Vogt and X.-M. Yin (2013) Suppression of lysosome function induces autophagy via a feedback downregulation of MTORC1 activity. *Journal of Biological Chemistry*, jbc. M113. 511212.

Li, R. (2007) Cytokinesis in development and disease: variations on a common theme. *Cellular and molecular life sciences*. **64**, 3044-3058.

Li, W.-w., J. Li and J.-k. Bao (2012) Microautophagy: lesser-known self-eating. *Cellular and Molecular Life Sciences*. **69**, 1125-1136.

Li, X., N. Rydzewski, A. Hider, X. Zhang, J. Yang, W. Wang, Q. Gao, X. Cheng and H. Xu (2016) A molecular mechanism to regulate lysosome motility for lysosome positioning and tubulation. *Nature cell biology*. **18**, 404.

Lingle, W. L., S. L. Barrett, V. C. Negron, A. B. D'Assoro, K. Boeneman, W. Liu, C. M. Whitehead, C. Reynolds and J. L. Salisbury (2002) Centrosome amplification drives chromosomal instability in breast tumor development. *Proceedings of the National Academy of Sciences*. **99**, 1978-1983.

Lingle, W. L., W. H. Lutz, J. N. Ingle, N. J. Maihle and J. L. Salisbury (1998) Centrosome hypertrophy in human breast tumors: implications for genomic stability and cell polarity. *Proceedings of the National Academy of Sciences*. **95**, 2950-2955.

Liu, J., G. D. Fairn, D. F. Ceccarelli, F. Sicheri and A. Wilde (2012) Cleavage furrow organization requires PIP2-mediated recruitment of anillin. *Current biology*. **22**, 64-69.

Liu, L., H. Liao, A. Castle, J. Zhang, J. Casanova, G. Szabo and D. Castle (2005) SCAMP2 interacts with Arf6 and phospholipase D1 and links their function to exocytotic fusion pore formation in PC12 cells. *Molecular biology of the cell*. **16**, 4463-4472.

Liu, Q., F. Liu, K. L. Yu, R. Tas, I. Grigoriev, S. Remmelzwaal, A. Serra-Marques, L. C. Kapitein, A. J. Heck and A. Akhmanova (2016) MICAL3 flavoprotein monooxygenase forms a complex with centralspindlin and regulates cytokinesis. *Journal of Biological Chemistry*, jbc. M116. 748186.

Lloyd-Evans, E., A. J. Morgan, X. He, D. A. Smith, E. Elliot-Smith, D. J. Sillence, G. C. Churchill, E. H. Schuchman, A. Galione and F. M. Platt (2008) Niemann-Pick disease type C1 is a sphingosine storage disease that causes deregulation of lysosomal calcium. *Nature medicine*. **14**, 1247.

López-Sanjurjo, C. I., S. C. Tovey, D. L. Prole and C. W. Taylor (2013) Lysosomes shape Ins (1, 4, 5) P3-evoked Ca2+ signals by selectively sequestering Ca2+ released from the endoplasmic reticulum. *J Cell Sci*. **126**, 289-300.

Luzio, J. P., Y. Hackmann, N. M. Dieckmann and G. M. Griffiths (2014) The biogenesis of lysosomes and lysosome-related organelles. *Cold Spring Harbor perspectives in biology*. **6**, a016840.

Luzio, J. P., P. R. Pryor and N. A. Bright (2007) Lysosomes: fusion and function. *Nature reviews Molecular cell biology*. **8**, 622.

Machaca, K. (2011) Ca2+ signaling, genes and the cell cycle. *Cell calcium*. **49**, 323-330.

Mark Gustafson, L., L. L. Gleich, K. Fukasawa, J. Chadwell, M. Ann Miller, P. J. Stambrook and J. L. Gluckman (2000) Centrosome hyperamplification in head and neck squamous cell carcinoma: a potential phenotypic marker of tumor aggressiveness. *The Laryngoscope*. **110**, 1798-1801.

Martinez, I., S. Chakrabarti, T. Hellevik, J. Morehead, K. Fowler and N. W. Andrews (2000) Synaptotagmin VII regulates Ca2+-dependent exocytosis of lysosomes in fibroblasts. *The Journal of cell biology*. **148**, 1141-1150.

Martinière, A., G. Desbrosses, H. Sentenac and N. Paris (2013) Development and properties of genetically encoded pH sensors in plants. *Frontiers in plant science*. **4**, 523.

Matsumura, F. (2005) Regulation of myosin II during cytokinesis in higher eukaryotes. *Trends in cell biology*. **15**, 371-377.

Matsushita, M., S. Tanaka, N. Nakamura, H. Inoue and H. Kanazawa (2004) A novel kinesin-like protein, KIF1Bβ3 is involved in the movement of lysosomes to the cell periphery in non-neuronal cells. *Traffic*. **5**, 140-151.

Matsuzaki, F., M. Shirane, M. Matsumoto and K. I. Nakayama (2011) Protrudin serves as an adaptor molecule that connects KIF5 and its cargoes in vesicular transport during process formation. *Molecular biology of the cell*. **22**, 4602-4620.

Matteoni, R. and T. E. Kreis (1987) Translocation and clustering of endosomes and lysosomes depends on microtubules. *The Journal of cell biology*. **105**, 1253-1265.

Mattera, R., S. Y. Park, R. De Pace, C. M. Guardia and J. S. Bonifacino (2017) AP-4 mediates export of ATG9A from the trans-Golgi network to promote autophagosome formation. *Proceedings of the National Academy of Sciences*, 201717327.

Mavrakis, M., Y. Azou-Gros, F.-C. Tsai, J. Alvarado, A. Bertin, F. Iv, A. Kress, S. Brasselet, G. H. Koenderink and T. Lecuit (2014) Septins promote F-actin ring formation by crosslinking actin filaments into curved bundles. *Nature cell biology*. **16**, 322.

Maxfield, F. R., J. M. Willard and S. Lu (2016) *Lysosomes: Biology, Diseases, and Therapeutics*, John Wiley & Sons

Mayinger, P. (2012) Phosphoinositides and vesicular membrane traffic. *Biochimica et Biophysica Acta (BBA)-Molecular and Cell Biology of Lipids*. **1821**, 1104-1113.

McCue, H. V., L. P. Haynes and R. D. Burgoyne (2010) Bioinformatic analysis of CaBP/calneuron proteins reveals a family of highly conserved vertebrate Ca 2+-binding proteins. *BMC research notes*. **3**, 1.

McMahon, H. T. and E. Boucrot (2011) Molecular mechanism and physiological functions of clathrin-mediated endocytosis. *Nature reviews Molecular cell biology*. **12**, 517.

Melchionda, M., J. K. Pittman, R. Mayor and S. Patel (2016) Ca2+/H+ exchange by acidic organelles regulates cell migration in vivo. *J Cell Biol*, jcb. 201510019.

Mellman, I., R. Fuchs and A. Helenius (1986) Acidification of the endocytic and exocytic pathways. *Annual review of biochemistry*. **55**, 663-700.

Menzies, F. M., A. Fleming and D. C. Rubinsztein (2015) Compromised autophagy and neurodegenerative diseases. *Nature Reviews Neuroscience*. **16**, 345.

Miedel, M. T., K. M. Weixel, J. R. Bruns, L. M. Traub and O. A. Weisz (2006) Posttranslational cleavage and adaptor protein complex-dependent trafficking of mucolipin-1. *Journal of Biological Chemistry*.

Mierzwa, B. and D. W. Gerlich (2014) Cytokinetic abscission: molecular mechanisms and temporal control. *Developmental cell*. **31**, 525-538.

Mikhaylova, M., P. P. Reddy, T. Munsch, P. Landgraf, S. K. Suman, K.-H. Smalla, E. D. Gundelfinger, Y. Sharma and M. R. Kreutz (2009) Calneurons provide a calcium threshold for trans-Golgi network to plasma membrane trafficking. *Proceedings of the National Academy of Sciences*. **106**, 9093-9098.

Mishima, M., S. Kaitna and M. Glotzer (2002) Central spindle assembly and cytokinesis require a kinesin-like protein/RhoGAP complex with microtubule bundling activity. *Developmental cell*. **2**, 41-54.

Mizushima, N. and M. Komatsu (2011) Autophagy: renovation of cells and tissues. *Cell*. **147**, 728-741.

Mohamed, M. M. and B. F. Sloane (2006) Cysteine cathepsins: multifunctional enzymes in cancer. *Nature Reviews Cancer*. **6**, 764.

Montagnac, G., J.-B. Sibarita, S. Loubéry, L. Daviet, M. Romao, G. Raposo and P. Chavrier (2009) ARF6 Interacts with JIP4 to control a motor switch mechanism regulating endosome traffic in cytokinesis. *Current Biology*. **19**, 184-195.

Morgan, A. J., F. M. Platt, E. Lloyd-Evans and A. Galione (2011) Molecular mechanisms of endolysosomal Ca2+ signalling in health and disease. *Biochemical Journal*. **439**, 349-378.

Mrakovic, A., J. G. Kay, W. Furuya, J. H. Brumell and R. J. Botelho (2012) Rab7 and Arl8 GTPases are necessary for lysosome tubulation in macrophages. *Traffic*. **13**, 1667-1679.

Murata, M., J. Peränen, R. Schreiner, F. Wieland, T. V. Kurzchalia and K. Simons (1995) VIP21/caveolin is a cholesterol-binding protein. *Proceedings of the National Academy of Sciences*. **92**, 10339-10343.

Nakata, T. and N. Hirokawa (1995) Point mutation of adenosine triphosphate-binding motif generated rigor kinesin that selectively blocks anterograde lysosome membrane transport. *The Journal of cell biology*. **131**, 1039-1053.

Neto, H., A. Kaupisch, L. L. Collins and G. W. Gould (2013) Syntaxin 16 is a master recruitment factor for cytokinesis. *Molecular biology of the cell*. **24**, 3663-3674.

Neumann, B., T. Walter, J.-K. Hériché, J. Bulkescher, H. Erfle, C. Conrad, P. Rogers, I. Poser, M. Held and U. Liebel (2010) Phenotypic profiling of the human genome by time-lapse microscopy reveals cell division genes. *Nature*. **464**, 721-727.

Neutra, M. R., A. Ciechanover, L. S. Owen and H. F. Lodish (1985) Intracellular transport of transferrin-and asialoorosomucoid-colloidal gold conjugates to lysosomes after receptor-mediated endocytosis. *Journal of Histochemistry & Cytochemistry*. **33**, 1134-1144.

Nguyen, J. T., C. Ray, A. L. Fox, D. B. Mendonça, J. K. Kim and P. H. Krebsbach (2018) Mammalian EAK-7 activates alternative mTOR signaling to regulate cell proliferation and migration. *Science advances*. **4**, eaao5838.

Nickel, W. and C. Rabouille (2009) Mechanisms of regulated unconventional protein secretion. *Nature Reviews Molecular Cell Biology*. **10**, 148-155.

Nikoletopoulou, V., M. Papandreou and N. Tavernarakis (2015) Autophagy in the physiology and pathology of the central nervous system. *Cell death and differentiation*. **22**, 398.

Nilsson, E., R. Ghassemifar and U. T. Brunk (1997) Lysosomal heterogeneity between and within cells with respect to resistance against oxidative stress. *The Histochemical journal*. **29**, 857-865.

Norbury, C. and P. Nurse (1992) Animal cell cycles and their control. *Annual review of biochemistry*. **61**, 441-468.

Normand, G. and R. W. King (2010) Understanding cytokinesis failure. *Polyploidization and cancer*, pp 27-55, Springer

Nurse, P. (2000) A long twentieth century of the cell cycle and beyond. *Cell*. **100**, 71-78.

Olsen, H. L., M. Høy, W. Zhang, A. M. Bertorello, K. Bokvist, K. Capito, A. M. Efanov, B. Meister, P. Thams and S.-N. Yang (2003) Phosphatidylinositol 4-kinase serves as a metabolic sensor and regulates priming of secretory granules in pancreatic β cells. *Proceedings of the National Academy of Sciences*. **100**, 5187-5192.

Orlow, S. J. (1995) Melanosomes are specialized members of the lysosomal lineage of organelles. *Journal of Investigative Dermatology*. **105**, 3-7.

Parton, R. G. and M. A. Del Pozo (2013) Caveolae as plasma membrane sensors, protectors and organizers. *Nature reviews Molecular cell biology*. **14**, 98.

Patel, S. (2015) Function and dysfunction of two-pore channels. *Sci. Signal.* **8**, re7-re7.

Patel, S. and R. Docampo (2010) Acidic calcium stores open for business: expanding the potential for intracellular Ca2+ signaling. *Trends in cell biology*. **20**, 277-286.

Pavicic-Kaltenbrunner, V., M. Mishima and M. Glotzer (2007) Cooperative assembly of CYK-4/MgcRacGAP and ZEN-4/MKLP1 to form the centralspindlin complex. *Molecular biology of the cell*. **18**, 4992-5003.

Penny, C. J., B. S. Kilpatrick, E. R. Eden and S. Patel (2015) Coupling acidic organelles with the ER through Ca 2+ microdomains at membrane contact sites. *Cell calcium*. **58**, 387-396.

Pérez-Garijo, A. and H. Steller (2015) Spreading the word: non-autonomous effects of apoptosis during development, regeneration and disease. *Development*. **142**, 3253-3262.

Peters, P. J., J. Borst, V. Oorschot, M. Fukuda, O. Krähenbühl, J. Tschopp, J. W. Slot and H. J. Geuze (1991) Cytotoxic T lymphocyte granules are secretory lysosomes, containing both perforin and granzymes. *Journal of Experimental Medicine*. **173**, 1099-1109.

Peters, P. J., H. J. Geuze, H. A. D. Van Donk, J. W. Slot, J. M. Griffith, N. J. Stam, H. C. Clevers and J. Borst (1989) Molecules relevant for T cell-target cell interaction are present in cytolytic granules of human T lymphocytes. *European journal of immunology*. **19**, 1469-1475.

Piekny, A. J. and M. Glotzer (2008) Anillin is a scaffold protein that links RhoA, actin, and myosin during cytokinesis. *Current biology*. **18**, 30-36.

Pihan, G. A., A. Purohit, J. Wallace, R. Malhotra, L. Liotta and S. J. Doxsey (2001) Centrosome defects can account for cellular and genetic changes that characterize prostate cancer progression. *Cancer research*. **61**, 2212-2219.

Polevoy, G., H.-C. Wei, R. Wong, Z. Szentpetery, Y. J. Kim, P. Goldbach, S. K. Steinbach, T. Balla and J. A. Brill (2009) Dual roles for the Drosophila PI 4-kinase four wheel drive in localizing Rab11 during cytokinesis. *The Journal of cell biology*. **187**, 847-858.

Pollard, T. D. (2017) Nine unanswered questions about cytokinesis. *J Cell Biol*, jcb. 201612068.

Porter, K., D. Prescott and J. Frye (1973) Changes in surface morphology of Chinese hamster ovary cells during the cell cycle. *The Journal of cell biology*. **57**, 815-836.

Poupětová, H., J. Ledvinová, L. Berná, L. Dvořáková, V. Kožich and M. Elleder (2010) The birth prevalence of lysosomal storage disorders in the Czech Republic: comparison with data in different populations. *Journal of inherited metabolic disease*. **33**, 387-396.

Pryor, P. R., B. M. Mullock, N. A. Bright, S. R. Gray and J. P. Luzio (2000) The role of intraorganellar Ca2+ in late endosome–lysosome heterotypic fusion and in the reformation of lysosomes from hybrid organelles. *The Journal of cell biology*. **149**, 1053-1062.

Pu, J., C. M. Guardia, T. Keren-Kaplan and J. S. Bonifacino (2016) Mechanisms and functions of lysosome positioning. *J Cell Sci*. **129**, 4329-4339.

Pu, J., C. Schindler, R. Jia, M. Jarnik, P. Backlund and J. S. Bonifacino (2015) BORC, a multisubunit complex that regulates lysosome positioning. *Developmental cell*. **33**, 176-188.

Puertollano, R. and K. Kiselyov (2009) TRPMLs: in sickness and in health. *American Journal of Physiology-Renal Physiology*. **296**, F1245-F1254.

Qi, G., I. Ogawa, Y. Kudo, M. Miyauchi, B. Siriwardena, F. Shimamoto, M. Tatsuka and T. Takata (2007) Aurora-B expression and its correlation with cell proliferation and metastasis in oral cancer. *Virchows Archiv*. **450**, 297-302.

Qualmann, B., D. Koch and M. M. Kessels (2011) Let's go bananas: revisiting the endocytic BAR code. *The EMBO journal*. **30**, 3501-3515.

Raffaello, A., C. Mammucari, G. Gherardi and R. Rizzuto (2016) Calcium at the Center of Cell Signaling: Interplay between Endoplasmic Reticulum, Mitochondria, and Lysosomes. *Trends in Biochemical Sciences*.

Rah, S.-Y., Y.-H. Lee and U.-H. Kim (2017) NAADP-mediated Ca2+ signaling promotes autophagy and protects against LPS-induced liver injury. *The FASEB Journal*. **31**, 3126-3137.

Raiborg, C. and H. Stenmark (2016) Plasma membrane repairs by small GTPase Rab3a. *J Cell Biol*. **213**, 613-615.

Rajamanoharan, D., H. V. McCue, R. D. Burgoyne and L. P. Haynes (2015) Modulation of phosphatidylinositol 4-phosphate levels by CaBP7 controls cytokinesis in mammalian cells. *Molecular biology of the cell*. **26**, 1428-1439.

Ramessur, K., P. Greenwell, R. Nash and M. Dwek (2010) Breast cancer invasion is mediated by β-N-acetylglucosaminidase (β-NAG) and associated with a dysregulation in the secretory pathway of cancer cells. *British journal of biomedical science*. **67**, 189-196.

Rao, S. K., C. Huynh, V. Proux-Gillardeaux, T. Galli and N. W. Andrews (2004) Identification of SNAREs involved in synaptotagmin VII-regulated lysosomal exocytosis. *Journal of Biological Chemistry*. **279**, 20471-20479.

Rappaport, R. and B. Rappaport (1974) Establishment of cleavage furrows by the mitotic spindle. *Journal of Experimental Zoology*. **189**, 189-196.

Rattner, J. (1992) Mapping the mammalian intercellular bridge. *Cell motility and the cytoskeleton*. **23**, 231-235.

Ravikumar, B., K. Moreau and D. C. Rubinsztein (2010) Plasma membrane helps autophagosomes grow. *Autophagy*. **6**, 1184-1186.

Reddy, A., E. V. Caler and N. W. Andrews (2001) Plasma membrane repair is mediated by Ca2+-regulated exocytosis of lysosomes. *Cell*. **106**, 157-169.

Riparbelli, M. G., G. Callaini, D. M. Glover and M. do Carmo Avides (2002) A requirement for the Abnormal Spindle protein to organise microtubules of the central spindle for cytokinesis in Drosophila. *Journal of cell science*. **115**, 913-922.

Roch, F., C. Polesello, C. Roubinet, M. Martin, C. Roy, P. Valenti, S. Carreno, P. Mangeat and F. Payre (2010) Differential roles of PtdIns (4, 5) P2 and phosphorylation in moesin activation during Drosophila development. *J Cell Sci*. **123**, 2058-2067.

Roczniak-Ferguson, A., C. S. Petit, F. Froehlich, S. Qian, J. Ky, B. Angarola, T. C. Walther and S. M. Ferguson (2012) The transcription factor TFEB links mTORC1 signaling to transcriptional control of lysosome homeostasis. *Science signaling*. **5**, ra42.

Rodríguez, A., P. Webster, J. Ortego and N. W. Andrews (1997) Lysosomes behave as Ca2+-regulated exocytic vesicles in fibroblasts and epithelial cells. *The Journal of cell biology*. **137**, 93-104.

Rosa-Ferreira, C. and S. Munro (2011) Arl8 and SKIP act together to link lysosomes to kinesin-1. *Developmental cell*. **21**, 1171-1178.

Rosario, C. O., M. A. Ko, Y. Z. Haffani, R. A. Gladdy, J. Paderova, A. Pollett, J. A. Squire, J. W. Dennis and C. J. Swallow (2010) Plk4 is required for cytokinesis and maintenance of chromosomal stability. *Proceedings of the National Academy of Sciences*, 200910941.

Rost, B. R., F. Schneider, M. K. Grauel, C. Wozny, C. G. Bentz, A. Blessing, T. Rosenmund, T. J. Jentsch, D. Schmitz and P. Hegemann (2015) Optogenetic acidification of synaptic vesicles and lysosomes. *Nature neuroscience*. **18**, 1845.

Roubinet, C., B. Decelle, G. Chicanne, J. F. Dorn, B. Payrastre, F. Payre and S. Carreno (2011) Molecular networks linked by Moesin drive remodeling of the cell cortex during mitosis. *J Cell Biol*. **195**, 99-112.

Saftig, P., E. Hunziker, O. Wehmeyer, S. Jones, A. Boyde, W. Rommerskirch, J. D. Moritz, P. Schu and K. Von Figura (1998) Impaired osteoclastic bone resorption leads to osteopetrosis in cathepsin-K-deficient mice. *Proceedings of the National Academy of Sciences*. **95**, 13453-13458.

Saftig, P. and J. Klumperman (2009) Lysosome biogenesis and lysosomal membrane proteins: trafficking meets function. *Nature reviews Molecular cell biology*. **10**, 623.

Saftig, P., B. Schröder and J. Blanz (2010) Lysosomal membrane proteins: life between acid and neutral conditions. *Biochemical Society Transactions*. **38**, 1420-1423.

Sagona, A. P., I. P. Nezis, K. G. Bache, K. Haglund, A. C. Bakken, R. I. Skotheim and H. Stenmark (2011) A tumor-associated mutation of FYVE-CENT prevents its interaction with Beclin 1 and interferes with cytokinesis. *PloS one*. **6**, e17086.

Sagona, A. P., I. P. Nezis, N. M. Pedersen, K. Liestøl, J. Poulton, T. E. Rusten, R. I. Skotheim, C. Raiborg and H. Stenmark (2010) PtdIns (3) P controls cytokinesis through KIF13A-mediated recruitment of FYVE-CENT to the midbody. *Nature cell biology*. **12**, 362.

Samie, M., X. Wang, X. Zhang, A. Goschka, X. Li, X. Cheng, E. Gregg, M. Azar, Y. Zhuo and A. G. Garrity (2013) A TRP channel in the lysosome regulates large particle phagocytosis via focal exocytosis. *Developmental cell*. **26**, 511-524.

Samie, M. A. and H. Xu (2014) Lysosomal exocytosis and lipid storage disorders. *Journal of lipid research*. **55**, 995-1009.

Sancar, A., L. A. Lindsey-Boltz, K. Ünsal-Kaçmaz and S. Linn (2004) Molecular mechanisms of mammalian DNA repair and the DNA damage checkpoints. *Annual review of biochemistry*. **73**, 39-85.

Santama, N., J. Krijnse-Locker, G. Griffiths, Y. Noda, N. Hirokawa and C. G. Dotti (1998) KIF2β, a new kinesin superfamily protein in non-neuronal cells, is associated with lysosomes and may be implicated in their centrifugal translocation. *The EMBO Journal*. **17**, 5855-5867.

Sardiello, M., M. Palmieri, A. di Ronza, D. L. Medina, M. Valenza, V. A. Gennarino, C. Di Malta, F. Donaudy, V. Embrione and R. S. Polishchuk (2009) A gene network regulating lysosomal biogenesis and function. *Science*. **325**, 473-477.

Sato, N., K. Mizumoto, M. Nakamura, K. Nakamura, M. Kusumoto, H. Niiyama, T. Ogawa and M. Tanaka (1999) Centrosome abnormalities in pancreatic ductal carcinoma. *Clinical Cancer Research*. **5**, 963-970.

Schafer, K. (1998) The cell cycle: a review. *Veterinary pathology*. **35**, 461-478.

Schiel, J. A., C. Childs and R. Prekeris (2013) Endocytic transport and cytokinesis: from regulation of the cytoskeleton to midbody inheritance. *Trends in cell biology*. **23**, 319-327.

Schiel, J. A., K. Park, M. K. Morphew, E. Reid, A. Hoenger and R. Prekeris (2011) Endocytic membrane fusion and buckling-induced microtubule severing mediate cell abscission. *Journal of cell science*, jcs. 081448.

Schiel, J. A., G. C. Simon, C. Zaharris, J. Weisz, D. Castle, C. C. Wu and R. Prekeris (2012) FIP3-endosome-dependent formation of the secondary ingression mediates ESCRT-III recruitment during cytokinesis. *Nature cell biology*. **14**, 1068.

Schink, K. O., C. Raiborg and H. Stenmark (2013) Phosphatidylinositol 3-phosphate, a lipid that regulates membrane dynamics, protein sorting and cell signalling. *BioEssays*. **35**, 900-912.

Schmidt, O. and D. Teis (2012) The ESCRT machinery. *Current Biology*. **22**, R116-R120.

Schwann, T. (1847) *Microscopical Researches into the Accordance in the Structure and Growth of Animals and Plants*, Рипол Классик

Schweitzer, J. K., E. E. Burke, H. V. Goodson and C. D'Souza-Schorey (2005) Endocytosis resumes during late mitosis and is required for cytokinesis. *Journal of Biological Chemistry*.

Sechi, S., G. Colotti, G. Belloni, V. Mattei, A. Frappaolo, G. D. Raffa, M. T. Fuller and M. G. Giansanti (2014) GOLPH3 is essential for contractile ring formation and Rab11 localization to the cleavage site during cytokinesis in Drosophila melanogaster. *PLoS genetics*. **10**, e1004305.

Sedzinski, J., M. Biro, A. Oswald, J.-Y. Tinevez, G. Salbreux and E. Paluch (2011) Polar actomyosin contractility destabilizes the position of the cytokinetic furrow. *Nature*. **476**, 462.

Settembre, C. and A. Ballabio (2014) Lysosomal adaptation: how the lysosome responds to external cues. *Cold Spring Harbor perspectives in biology*, a016907.

Settembre, C., A. Fraldi, D. L. Medina and A. Ballabio (2013) Signals from the lysosome: a control centre for cellular clearance and energy metabolism. *Nature reviews Molecular cell biology*. **14**, 283.

Settembre, C., A. Fraldi, D. C. Rubinsztein and A. Ballabio (2008) Lysosomal storage diseases as disorders of autophagy. *Autophagy*. **4**, 113-114.

Shaner, N. C., M. Z. Lin, M. R. McKeown, P. A. Steinbach, K. L. Hazelwood, M. W. Davidson and R. Y. Tsien (2008) Improving the photostability of bright monomeric orange and red fluorescent proteins. *Nature methods*. **5**, 545.

Shen, D., X. Wang, X. Li, X. Zhang, Z. Yao, S. Dibble, X.-p. Dong, T. Yu, A. P. Lieberman and H. D. Showalter (2012) Lipid storage disorders block lysosomal trafficking by inhibiting a TRP channel and lysosomal calcium release. *Nature communications*. **3**, 731.

Shen, D., X. Wang and H. Xu (2011) Pairing phosphoinositides with calcium ions in endolysosomal dynamics. *Bioessays*. **33**, 448-457.

Sherr, C. J. and J. M. Roberts (2004) Living with or without cyclins and cyclin-dependent kinases. *Genes & development*. **18**, 2699-2711.

Shibutani, S. T., T. Saitoh, H. Nowag, C. Münz and T. Yoshimori (2015) Autophagy and autophagy-related proteins in the immune system. *Nature Immunology*. **16**, 1014.

Shuster, C. and D. Burgess (2002) Targeted new membrane addition in the cleavage furrow is a late, separate event in cytokinesis. *Proceedings of the National Academy of Sciences*. **99**, 3633-3638.

Simon, G. C., E. Schonteich, C. C. Wu, A. Piekny, D. Ekiert, X. Yu, G. W. Gould, M. Glotzer and R. Prekeris (2008) Sequential Cyk-4 binding to ECT2 and FIP3 regulates cleavage furrow ingression and abscission during cytokinesis. *The EMBO journal*. **27**, 1791-1803.

Singh, R. and A. M. Cuervo (2011) Autophagy in the cellular energetic balance. *Cell metabolism*. **13**, 495-504.

Sivaramakrishnan, V., S. Bidula, H. Campwala, D. Katikaneni and S. J. Fountain (2012) Constitutive lysosome exocytosis releases ATP and engages P2Y receptors in human monocytes. *J Cell Sci*, jcs. 107318.

Somers, W. G. and R. Saint (2003) A RhoGEF and Rho family GTPase-activating protein complex links the contractile ring to cortical microtubules at the onset of cytokinesis. *Developmental cell*. **4**, 29-39.

Sridhar, S., B. Patel, D. Aphkhazava, F. Macian, L. Santambrogio, D. Shields and A. M. Cuervo (2013) The lipid kinase PI4KIIIβ preserves lysosomal identity. *The EMBO journal*. **32**, 324-339.

Stinchcombe, J. C. and G. M. Griffiths (1999) Regulated secretion from hemopoietic cells. *The Journal of cell biology*. **147**, 1-5.

Stransky, L., K. Cotter and M. Forgac (2016) The function of V-ATPases in cancer. *Physiological reviews*. **96**, 1071-1091.

Strehler, E. (1990) Plasma membrane Ca2+ pumps and Na+/Ca2+ exchangers. *Seminars in cell biology*, pp 283-295

Su, K.-C., W. M. Bement, M. Petronczki and G. von Dassow (2014) An astral simulacrum of the central spindle accounts for normal, spindle-less, and anucleate cytokinesis in echinoderm embryos. *Molecular biology of the cell*. **25**, 4049-4062.

Subramanian, R., E. M. Wilson-Kubalek, C. P. Arthur, M. J. Bick, E. A. Campbell, S. A. Darst, R. A. Milligan and T. M. Kapoor (2010) Insights into antiparallel microtubule crosslinking by PRC1, a conserved nonmotor microtubule binding protein. *Cell*. **142**, 433-443.

Sullivan, M. and D. O. Morgan (2007) Finishing mitosis, one step at a time. *Nature reviews Molecular cell biology*. **8**, 894.

Sundler, R. (1997) Lysosomal and cytosolic pH as regulators of exocytosis in mouse macrophages. *Acta physiologica scandinavica*. **161**, 553-556.

Tan, X., N. Thapa, S. Choi and R. A. Anderson (2015) Emerging roles of PtdIns (4, 5) P2–beyond the plasma membrane. *J Cell Sci*. **128**, 4047-4056.

Tang, J., A. Maximov, O.-H. Shin, H. Dai, J. Rizo and T. C. Südhof (2006) A complexin/synaptotagmin 1 switch controls fast synaptic vesicle exocytosis. *Cell*. **126**, 1175-1187.

Tardieux, I., P. Webster, J. Ravesloot, W. Boron, J. A. Lunn, J. E. Heuser and N. W. Andrews (1992) Lysosome recruitment and fusion are early events required for trypanosome invasion of mammalian cells. *Cell*. **71**, 1117-1130.

Traub, L. M. and J. S. Bonifacino (2013) Cargo recognition in clathrin-mediated endocytosis. *Cold Spring Harbor Perspectives in Biology*. **5**, a016790.

Tsuji, A., K. Omura and Y. Suzuki (1988) I-cell disease: evidence for a mannose 6-phosphate independent pathway for translocation of lysosomal enzymes in lymphoblastoid cells. *Clinica chimica acta*. **176**, 115-121.

Twigg, J., R. Patel and M. Whitaker (1988) Translational control of InsP3-induced chromatin condensation during the early cell cycles of sea urchin embryos. *Nature*. **332**, 366.

Uehara, R. and G. Goshima (2010) Functional central spindle assembly requires de novo microtubule generation in the interchromosomal region during anaphase. *The Journal of cell biology*. **191**, 259-267.

Venkatachalam, K., C.-O. Wong and M. X. Zhu (2015) The role of TRPMLs in endolysosomal trafficking and function. *Cell calcium*. **58**, 48-56.

Vermeulen, K., D. R. Van Bockstaele and Z. N. Berneman (2003) The cell cycle: a review of regulation, deregulation and therapeutic targets in cancer. *Cell proliferation*. **36**, 131-149.

Vieira, O. V., C. Bucci, R. E. Harrison, W. S. Trimble, L. Lanzetti, J. Gruenberg, A. D. Schreiber, P. D. Stahl and S. Grinstein (2003) Modulation of Rab5 and Rab7 recruitment to phagosomes by phosphatidylinositol 3-kinase. *Molecular and cellular biology*. **23**, 2501-2514.

Vinciguerra, P., S. A. Godinho, K. Parmar, D. Pellman and A. D. D'Andrea (2010) Cytokinesis failure occurs in Fanconi anemia pathway–deficient murine and human bone marrow hematopoietic cells. *The Journal of clinical investigation*. **120**, 3834-3842.

Virchow, R. and F. Chance (1860) *Cellular Pathology as based upon physiological and pathological histology. Twenty lectures delivered in... 1858. Translated from the second edition of the original by F. Chance. With notes and numerous emendations principally from MS. notes of the author, and illustrated by... engravings on wood*

Vitale, M., E. Seward and J.-M. Trifaro (1995) Chromaffin cell cortical actin network dynamics control the size of the release-ready vesicle pool and the initial rate of exocytosis. *Neuron*. **14**, 353-363.

von Dassow, G. (2009) Concurrent cues for cytokinetic furrow induction in animal cells. *Trends in cell biology*. **19**, 165-173.

Wagner, E. and M. Glotzer (2016) Local RhoA activation induces cytokinetic furrows independent of spindle position and cell cycle stage. *J Cell Biol*, jcb. 201603025.

Wang, Q., L. Zhou, L. Qiu, D. Lu, Y. Wu and X. B. Zhang (2015) An efficient ratiometric fluorescent probe for tracking dynamic changes in lysosomal pH. *Analyst*. **140**, 5563-9.

Wang, T. and W. Hong (2002) Interorganellar regulation of lysosome positioning by the Golgi apparatus through Rab34 interaction with Rab-interacting lysosomal protein. *Molecular biology of the cell*. **13**, 4317-4332.

Wang, X., X. Dong, D. Shen, T. Dawson, X. Li, Q. Zhang, X. Cheng, Y. Zhang, L. S. Weisman and M. Delling (2011) PI (3, 5) P2 Controls Membrane Trafficking by Direct Activation of Mucolipin Ca2+ Release Channels in the Endolysosome. *Biophysical Journal*. **100**, 109a.

Wang, Y.-l. (2005) The mechanism of cortical ingression during early cytokinesis: thinking beyond the contractile ring hypothesis. *Trends in cell biology*. **15**, 581-588.

Wartosch, L., N. A. Bright and J. P. Luzio (2015) Lysosomes. *Current Biology*. **25**, R315-R316.

Webb, S. E., W. M. Li and A. L. Miller (2008) Calcium signalling during the cleavage period of zebrafish development. *Philosophical Transactions of the Royal Society of London B: Biological Sciences*. **363**, 1363-1369.

Weinberg, R. A. (1995) The retinoblastoma protein and cell cycle control. *Cell*. **81**, 323-330.

Whitaker, M. (1997) Calcium and mitosis. *Progress in cell cycle research*, pp 261-269, Springer

Wolfe, B. A., T. Takaki, M. Petronczki and M. Glotzer (2009) Polo-like kinase 1 directs assembly of the HsCyk-4 RhoGAP/Ect2 RhoGEF complex to initiate cleavage furrow formation. *PLoS biology*. **7**, e1000110.

Woodman, P. G. and C. E. Futter (2008) Multivesicular bodies: co-ordinated progression to maturity. *Current opinion in cell biology*. **20**, 408-414.

Wu, B., Y. Chen and J. D. Müller (2009) Fluorescence fluctuation spectroscopy of mCherry in living cells. *Biophysical journal*. **96**, 2391-2404.

Xu, H. and D. Ren (2015) Lysosomal physiology. *Annual review of physiology*. **77**, 57-80.

Yamamoto, Y., S. Eguchi, A. Junpei, K. Nagao, S. Sakano, T. Furuya, A. Oga, S. Kawauchi, K. Sasaki and H. Matsuyama (2009) Intercellular centrosome number is correlated with the copy number of chromosomes in bladder cancer. *Cancer genetics and cytogenetics*. **191**, 38-42.

Yang, X., K. Yu, Y. Hao, D.-m. Li, R. Stewart, K. L. Insogna and T. Xu (2004) LATS1 tumour suppressor affects cytokinesis by inhibiting LIMK1. *Nature cell biology*. **6**, 609.

Yeong, F. M. (2013) Multi-step down-regulation of the secretory pathway in mitosis: A fresh perspective on protein trafficking. *Bioessays*. **35**, 462-471.

Yoshida, S., S. Bartolini and D. Pellman (2009) Mechanisms for concentrating Rho1 during cytokinesis. *Genes & Development*. **23**, 810-823.

Yu, S. and T. J. Melia (2017) The coordination of membrane fission and fusion at the end of autophagosome maturation. *Current opinion in cell biology*. **47**, 92-98.

Yüce, Ö., A. Piekny and M. Glotzer (2005) An ECT2–centralspindlin complex regulates the localization and function of RhoA. *The Journal of cell biology*. **170**, 571-582.

Zaidi, N. and H. Kalbacher (2013) Cathepsin E. *Handbook of Proteolytic Enzymes (Third Edition)*, pp 42-49, Elsevier

Zhang, D. and M. Glotzer (2015) The RhoGAP activity of CYK-4/MgcRacGAP functions non-canonically by promoting RhoA activation during cytokinesis. *Elife*. **4**, e08898.

Zhang, Y., R. Sugiura, Y. Lu, M. Asami, T. Maeda, T. Itoh, T. Takenawa, H. Shuntoh and T. Kuno (2000) Phosphatidylinositol 4-phosphate 5-kinase Its3 and calcineurin Ppb1 coordinately regulate cytokinesis in fission yeast. *Journal of Biological Chemistry*. **275**, 35600-35606.

Zheng, Y., J. Guo, X. Li, Y. Xie, M. Hou, X. Fu, S. Dai, R. Diao, Y. Miao and J. Ren (2014) An integrated overview of spatiotemporal organization and regulation in mitosis in terms of the proteins in the functional supercomplexes. *Frontiers in Microbiology*. **5**, 573.

Zhu, C., E. Lau, R. Schwarzenbacher, E. Bossy-Wetzel and W. Jiang (2006) Spatiotemporal control of spindle midzone formation by PRC1 in human cells. *Proceedings of the National Academy of Sciences*. **103**, 6196-6201.